Absorption of Carbon Dioxide into Novel Single and Blended Amine Solvents

Bisweswar Das

Absorption of Carbon Dioxide into Novel Single and Blended Amine Solvents

Thesis

submitted in partial fulfilment of the

requirements for the degree of

DOCTOR OF PHILOSOPHY

by

Bisweswar Das

Department of Chemical Engineering
Indian Institute of Technology Guwahati
Guwahati – 781039, Assam, India

October 2017

Dedicated

To

My parents and my mentor

Department of Chemical Engineering
Indian Institute of Technology Guwahati
Guwahati 781039, Assam, India

CERTIFICATE

It is certified that the work contained in this thesis entitled **"Absorption of Carbon Dioxide into Novel Single and Blended Amine Solvents"** submitted by **Mr. Biswesswar Das** for the award of the degree of Doctor of Philosophy has been carried out in the Department of Chemical Engineering, Indian Institute of Technology Guwahati under my supervision and this work has not been submitted elsewhere for the award of any other degree or diploma.

This thesis in my opinion, has reached the standard fulfilling the requirements for the award of the degree of Doctor of Philosophy in accordance with the regulations of the institute.

(**Dr. Bishnupada Mandal**)
Professor and Head
Department of Chemical Engineering
Indian Institute of Technology Guwahati
Guwahati 781039, India

ACKNOWLEDGEMENTS

I express my sincere gratitude to all those people that in several ways have helped me with my work on this doctoral thesis. I take this opportunity to express my sense of respect and sincere gratitude to my supervisors, **Prof. Bishnupada Mandal,** for giving me the opportunity to do this work.

I would like to thank **Prof. Bishnupada Mandal** for providing inspiring and valuable guidance, and giving me freedom in choosing how to approach with different issues. I am grateful very much for his flexibility and openness in dealing with the specific and general needs of this present thesis. His expertise in heterogeneous mass transfer processes and gas treating given me new insights towards my work, which has provided a good basis for this research work. I am also indebted to Professor Mandal for instilling in me a craving for perfection. I believe, it will always remain with me in my future life. It has really been a notable experience working with him.

I would like to express my sincere gratitude to **Prof. Prabirkumar Saha** for his knowledge and enthusiasm have proven an invaluable contribution to this research. The numerous brain storming sessions during the meetings with him were very useful in enriching my analytical power.

I must also thank my doctoral committee members, **Prof. Sasidhar Gumma, Prof. Mihir Kumar Purkait, Prof. G. Pugazhenthi,** Department of Chemical Engineering and **Dr. Lal Mohan Kundu,** Department of Chemistry, for their valuable suggestions and effort which made my thesis successful.

I am thankful to the faculty members of the Department of Chemical Engineering for their kind cooperation during my stay here and in particular, **Dr. Tapas Kumar Mandal** and **Dr. Animes Kumar Golder** for their help and constant encouragement.

I must thank the Central Instruments Facility of IIT Guwahati for providing me to carry out NMR experiments which has been very important in my research work. I acknowledge with thanks to **Mr. Suranjan De**, research scholar, Department of Chemistry for his aid in the NMR analysis. He spent a lot of valuable time for me in NMR measurements of 1D and 2D study.

I am thankful all the **technical staffs** of my department for their sincere help and support during this work. I would also like to thank all the **staffs** specially **Mr. Sailen Das, Mr. Deep Jyoti Sinha** and **Mr. Bhagya Boro,** for their support in various forms. I also enjoyed lively discussions with these fellows on the several aspects of local cultures.

I was fortunate enough to get excellent lab members specially research lab II and III of my department whose cooperation and friendly behavior comforted me in many ways. I am also thankful to my friends **Arun kumar, Binay Deogam** for their friendly assistance in the experimental run. I also thanks my lab juniors **Babul Prasad, Rajashree Borgohain, Mridusmita Barooah** for their friendly cooperation during my work**.** Among the PhD. students I extend my special thanks to **Sanjib Da** for his cooperation and guidance during his stay in IITG and also after leaving the place. I also want to mention the name of another senior, **Arejit Da.** I enjoyed a lot of encouraging discussions with him.

I am also thankful to my friends **Debasis, Sahu, pawan, arya** in the Bramhaputra Hostel and all my **seniors**, **juniors**, **friends,** other **well-wishers** whoever making my stay in IITG memorable. A big thank to all of you and my apologies to those I may have forgotten.

Most of all, I express my gratitude to my beloved **parents, brother, sisters** and other family members. Their love, care, sacrifices and encouragement have made it possible for me to come so far.

BISWESWAR

VITAE

Bisweswar Das

Date of Birth September 04, 1987

Email: bisho87@gmail.com
bisho87@yahoo.com

Permanent address Vill+Po-Hatkrishnanagar
P.S-Patrasayer, Dist-Bankura
West Bengal, India.
Pin No: 722206
Phone: (Res)09434513815
(M) 07896767016

Education

- PhD student
  Department of Chemical Engineering
  Indian Institute of Technology Guwahati
  Guwahati, Assam, India

- M.E (Chemical Engineering) (First Class)
  Department of Chemical Engineering
  Jadavpur University, West Bengal, India
  (2009-2011)

- B.Tech (Chemical Engineering) (First Class)
  Department of Chemical Engineering
  Heritage Institute of Technology, West Bengal, India
  (2005-2009)

Achievements

- *Qualified in GATE 2009*

VITAE

Publications

Journal Papers

1. Das, B., Deogam, B., Mandal, B., 2017. Experimental and theoretical studies on efficient carbon dioxide capture using novel bis(3-minopropyl)amine (APA)-activated aqueous2-amino-2-methyl-1-propanol (AMP) solutions. RSC Advances., 7, 21518–21530.

2. Das, B., Deogam, B., Mandal, B., 2017. Absorption of CO_2 into novel aqueous bis(3-aminopropyl)amine and enhancement of CO_2 absorption into its blends with N-methyldiethanolamine. International Journal of Greenhouse Gas Control 60, 172-185.

3. Das, B., Deogam, B., Agrawal, Y and Mandal, B., 2016. Measurement and Correlation of the Physicochemical Properties of Novel Aqueous Bis(3-aminopropyl)amine and Its Blend with N Methyldiethanolamine for CO_2 Capture. Journal of Chemical & Engineering Data. 61, 2226-2235.

4. Gupta, N., Mondal, A., Das, B., Deogam, B., Barma, S and Mandal, B. 2015. Modeling and Simulation for Post-Combustion Carbon Dioxide Capture from Power Plant Flue Gas with Economic Analysis. Separation Science and Technology 50, 1952–1963.

VITAE

Papers in Conferences

1. Das, B., Hembram, K.., Sontti, S.G. and Mandal, B. "Absorption of Carbon dioxide into Blended Amines: Diffusion Reaction Based Modelling". The Indian Chemical Engineering Congress (CHEMCON 2012), Dec 27-30, Jalandhar, INDIA (2012). [**BEST PRESENTATION award on this session**].

2. Deogam, B., Das, B. and Mandal, B. "CO_2 Absorption by Blended Amine solvents in Flat Sheet Membrane Contactor: Modeling and Simulation". The Indian Chemical Engineering Congress (CHEMCON 2012), Dec 27-30, Jalandhar, INDIA (2012).

3. Sontti, S.G., Das, B., Hembram, K. and Mandal, B. "Gas Phase overall volumetric transfer coefficient for CO_2 into Aqueous Blends of 2-Amino-2-Methyl-Propanol and Monoethanolamine". The Indian Chemical Engineering Congress (CHEMCON 2012), Dec 27-30, Jalandhar, INDIA (2012).

4. Deogam, B., Kumar. R., Das, B.and Mandal. B. "Absorption of carbon dioxide in aqueous blends of 2-amino-2-methyl-1-propanol+monoethanolamine and 2-amino-2-methyl-1-propanol+ diethanolamine". The Indian Chemical Engineering Congress (CHEMCON 2013), Dec 27-30, Mumbai, INDIA (2013).

5. Deogam, B., Das, B., Mondal, A., Barma, S. and Mandal, B. "Absorption of Carbon Dioxide into Piperazine Activated Aqueous Diethanolamine". The Energy System Modeling and Optimization Conference (ESMOC 2013), Dec 9-11, Durgapur, INDIA (2013).

6. Kumar, R., Deogam, B., Das, B. and Mandal, B. "Density and Viscosity of Aqueous Solutions of 2-(1-Piperazinyl)-ethylamine Activated 2-Amino-2-methyl-1-propanol". The Indian Chemical Engineering Congress (CHEMCON 2013), Dec 27-30, Mumbai, INDIA (2013).

7. Gupta, N., Das, B., Deogam, B., Mondal, A., Barma, S. and Mandal, B. "Modelling and simulation for post-combustion carbon dioxide capture from power plant flue gas with economic analysis". The Energy System Modeling and Optimization Conference (ESMOC 2013), Dec 9-11, Durgapur, INDIA (2013).

8. Das, B., Deogam, B., Kumar, A. and Mandal, B. "Absorption Rates of Carbon Dioxide into Novel Amine Solvent". Sustainable Development of Environment Systems (IIT GUWAHATI 2014), June 20-21, INDIA (2014).

9. Das, B., Deogam, B., and Mandal, B. "Rates of absorption of carbon dioxide into aqueous solutions of bis(3-aminopropyl)amine". The Indian Chemical Engineering Congress (CHEMCON 2014), Dec 27-30, Chandigarh, INDIA (2014).

10. Das, B., Deogam, B., and Mandal, B. "Carbon Dioxide Absorption into Novel Amine Solvent". 64th Canadian Chemical Engineering Conference (CCEC 2014), CANADA (2014).

11. Das, B., Agrawal, Y., Singh, A and Mandal, B. "Solubility and diffusivity of N_2O and CO_2 into novel ternary alkanolamine solution and simulate them with different models". The Indian Chemical Engineering Congress (CHEMCON 2015), Dec 27-30, Guwahati, INDIA (2015).

ABSTRACT

Absorption of Carbon Dioxide into Novel Single and Blended Amine Solvents

By

Bisweswar Das

Over the last few decades, the increasing concentration of carbon dioxide (CO_2) in the atmosphere has contributed adversely to the environment and has been a subject of worldwide attention. The capture of CO_2, which is one of the main greenhouse gas (GHG), currently represents an essential step in the performance of electric power stations, petroleum refineries, chemical fertilizer plants, coal gasifiers, cement factories, and the steel industries. In the recent days, gas scrubbing using activated aqueous alkanolamine solutions is the most reliable retrofit option for post combustion CO_2 capture. The present study investigates a novel activator, bis(3-aminopropyl)amine (APA), which can be an effective mode of eliminating CO_2 from flue gas. The kinetics of CO_2 absorption into chosen aqueous solution of APA was carried out at 303, 308, 313 and 323 K over a concentration range of 0.1-0.5 kmol m^{-3} and at different CO_2 partial pressure. A wetted-wall column absorber was used for the kinetics measurement. The reaction mechanism of CO_2 with primary and secondary amines (zwitterionic mechanism) is described and accordingly the experimentally obtained kinetic data are interpreted. A qualitative nuclear magnetic resonance [NMR (1D and 2D)] spectroscopy method has been applied to develop the reaction scheme for novel aqueous APA with CO_2. The kinetic rate parameters were investigated according to the pseudo-first-order condition for CO_2 absorption at each experimental condition. The values of second-order rate constant, $k_{2\text{-APA}}$ and reaction rate with CO_2 reported in this

study were higher than many existing amine activators like ethylenediamine (EDA), N-(2-aminoethyl) ethanolamine (AEEA), piperazine (PZ), 2-(1-piperazinl)-ethylamine (PZEA), etc. Two blended solvents such as aqueous blend of APA with N-Methyldiethanolamine (MDEA) and 2-Amino-2-methyl-1-propanol (AMP) were considered for potential use in CO_2 capture. It was observed that the enhancement factor increases significantly in comparison to single amine (aqueous MDEA) solutions when the APA concentrations increased in the blends with MDEA. Based on the pseudo-first-order condition for the CO_2 absorption, kinetic data for amine blend measurement are reported. Furthermore, the absorption of CO_2 into (APA + MDEA +H_2O) solutions using the same absorber was investigated over the range of temperature and CO_2 partial pressure. The molar concentration of APA was varied while maintaining the total concentration of the amine blends at 3.0 $kmol.m^{-3}$. Based on the zwitterion mechanism, overall reaction scheme for (APA+AMP+H_2O)-CO_2 system was established. According to the pseudo-first-order condition, the reaction rate parameters were estimated for (APA+AMP+H_2O)-CO_2 system from the kinetics measurement. A substantial enhancement of rate in comparison to the single AMP solution was observed due to the addition of a small amount of APA in the blend. A parametric sensitivity analysis has been performed to examine the effect of important physicochemical and kinetic parameters on the specific rate of absorption of CO_2 into (APA+H_2O) and (APA+AMP+H_2O) solutions. For the analyses, the involved parameters are Henry's law constant for CO_2, diffusivity of CO_2 into the amine solutions and the second order reaction rate constants for the absorption of CO_2.

Physicochemical properties such as density and viscosity of aqueous novel APA and an aqueous novel blend of APA with MDEA and AMP solutions as well as solubility and diffusivity of N_2O into these binary and ternary solutions were measured over a wide range of temperature and relative amine composition. The "N_2O-analogy" has been used to determine Henry's constant and diffusivity for CO_2 into the chosen solvents. The experimental binary and ternary density data as well as binary viscosity

data were correlated by Redlich–Kister equation whereas ternary viscosity data were correlated by Grunberg and Nissan model. On the other hand, solubility and diffusivity were correlated with different models like the semiemperical model, the modified Stokes Einstein model, arrhenius type equation and polynomial model. All the correlations based on the different model performed are capable for adequately predicting experimental physicochemical data. It is expected that the kinetics and the physicochemical properties this generated will be useful for process design.

CONTENTS

		Page No.
Dedication		*iii*
Certificate		*v*
Acknowledgements		*vii*
Vitae		*xi*
Abstract		*xv*
List of Tables		*xxiii*
List of Figures		xxxi
CHAPTER 1	**INTRODUCTION, LITERATURE REVIEW AND OBJECTIVES ON CO_2 CAPTURE**	1-25
1.1	INTRODUCTION	1-3
1.2	ACID GAS TREATING TECHNOLOGIES	3-8
1.2.1	CO_2 treating by absorption	4-8
1.2.1.1	Physical absorption	5
1.2.1.2	Chemical absorption	5-6
1.2.1 .2.1	CO_2 absorption by aqueous alkanolamine solutions	6-8
1.3	LITERATURE REVIEW ON ABSORPTION OF CO_2 BY SINGLE AND BLENDED AMINE SOLUTIONS	8-18
1.3.1	Absorption of CO_2 in single amine solvents	8-12
1.3.2	Absorption of CO_2 in blended amine solvents	12-16
1.4	IMPORTANCE AND OBJECTIVES OF PRESENT WORK	16-18
REFERENCES		18-25
CHAPTER 2	**CHEMISTRY AND THEORY OF MASS TRANSFER WITH CHEMICAL REACTION FOR ABSORPTION OF CO_2 IN ALKANOLAMINES**	27-52
2.1	INTRODUCTION	27-28

2.2 CHEMISTRY FOR CO_2 – ALKANOLAMINE SYSTEMS 28-35
2.2.1 Zwitterionic mechanism 29-32
2.2.2 Termolecular mechanism 33
2.2.3 Base-catalyzed hydration mechanism 34
2.2.4 Alcohol-group bonding of CO_2 35
2.2.5 Molecules with multiple amine functionalities 35
2.3 THEORY OF MASS TRANSFER WITH CHEMICAL REACTION 36
2.3.1 Mass transfer models 37-40
2.3.2 Effect of chemical reaction on absorption 41-42
2.4 LABORATORY GAS LIQUID CONTACTORS 42-44
NOTATIONS 44-45
REFERENCES 46-49
TABLES 50
FIGURES 51-52

CHAPTER 3 PHYSICOCHEMICAL PROPERTIES OF CO_2– AMINE SYSTEMS 53-131

3.1 INTRODUCTION 53-55
3.2 LITERATURE REVIEW 55-58
3.2.1 Density and viscosity 55-56
3.2.2 Physical solubility and diffusivity 56-58
3.3 EXPERIMENTAL 58-61
3.3.1 Materials 58-59
3.3.2 Apparatus and procedure 59-61
3.3.2.1 Density and viscosity measurement 59
3.3.2.2 Physical solubility measurement 60-61
3.3.2.3 Diffusivity measurement 61
3.4 RESULTS AND DISCUSSION 62-74
3.4.1 Density and viscosity 62-67
3.4.2 Physical solubility 67-71
3.4.2.1 Semiempirical model 68-69
3.4.2.2 Arrhenius type equation 69-70
3.4.2.3 Polynomial model 70-71
3.4.3 Diffusivity 71-74
3.4.3.1 Modified Stokes Einstein model 72

3.4.3.2 Arrhenius type equation 72-73
3.4.3.3 Polynomial model 73-74
NOTATIONS 74-76
REFERENCES 77-84
TABLES 85-125
FIGURES 126-132

CHAPTER 4 KINETICS STUDY OF ABSORPTION OF CARBONDIOXIDE ABSORPTION INTO AQUEOUS AMINE SOLUTIONS 133-199

4.1 INTRODUCTION 133-136
4.2 THEORY 137-139
4.3 EXPERIMENTAL 139-142
4.3.1 Materials 139
4.3.2 Preparation of the aqueous amine solvent and NMR measurement 139-140
4.3.3 Apparatus 140-141
4.3.4 Procedure 141-142
4.4 REACTION MECHANISM 142-152
4.4.1 Hydration of CO_2 in aqueous solutions 142
4.4.2 Reactions of CO_2 with APA 143-145
4.4.2.1 Reaction mechanism 143-145
4.4.2.2 One-dimensional and two-dimensional NMR study 145-146
4.4.2.3 Carbamate formation during absorption 146-147
4.4.3 Reactions of CO_2 with blends of (APA + MDEA) 148-150
4.4.3.1 Reaction scheme 148-149
4.4.4 Reactions of CO_2 with blends of (APA + AMP) 150-153
4.4.4.1 Reaction scheme 150-152
4.5 PHYSICOCHEMICAL PROPERTIES 153
4.6 RESULTS AND DISCUSSION 153-161
4.6.1 Validation of absorption experimental set-up 153-154
4.6.2 Determination of overall reaction rate constant and second order rate constant for aqueous APA system 154-156

4.6.3 Determination of overall reaction rate constant and second order rate constant for aqueous (APA+MDEA) 156-157
4.6.4 Determination of overall reaction rate constant and second order rate constant for aqueous (APA+AMP) solutions. 158-159
4.6.5 Enhancement of CO_2 absorption using APA activated MDEA 159-160
4.6.6 Parametric sensitivity analysis 160-161
NOTATIONS 161-162
REFERENCES 162-168
TABLES 169-180
FIGURES 181-199

CHAPTER 5 CONCLUSIONS AND FUTURE DIRECTIONS 201-205

5.1 CONCLUSIONS 201-204
5.2 RECOMMENDATIONS ON FUTURE DIRECTIONS 204-205
APPENDIX I Calculation of Uncertainty in the Experimental Measurements 206-208
APPENDIX II Tabulated Representation of Different Physicochemical Properties 209-225
APPENDIX III Sample Calculations 226-232
APPENDIX IV Typical M-files and program outputs 233-266

LIST OF TABLES

		Page No.
Table 2.1	Carbamate stability constants for conventional and hindered amines by ^{13}C NMR	**50**
Table 3.1	Comparison of the Densities (ρ) of Pure MDEA and Aqueous MDEA Solutions (Mass % w) Measured in This Work with Literature Values at Temperature (T) at a Pressure of 0.1 MPa[a]	**85**
Table 3.2	Comparison of the Viscosities (η) of Pure MDEA and Aqueous MDEA Solutions (Mass % *w*) Measured in This Work with Literature Values at Temperature (*T*) at a Pressure of 0.1 MPa[a]	**86**
Table 3.3	Density (ρ), Viscosity (η) and Henry's Constant (H_{N_2O}) of Pure APA at Different Temperature (T)[a]	**87**
Table 3.4	Parameters of Density, Viscosity and Henry's Constant for Pure APA	**88**
Table 3.5a	Density (ρ) and Viscosity (η) for APA + H_2O at Different Molar Concentration (*m*) and Temperature (*T*) at a Pressure of 0.1 MPa[a]	**88**
Table 3.5b	Density (ρ) and Viscosity (η) for APA+H_2O at Different Molar Concentration (*m*) and Temperature (*T*) at a Pressure of 0.1 MPa[a]	**89**
Table 3.5c	Density (ρ) and Viscosity (η) for APA+H_2O at Different Molar Concentration (*m*) and Temperature (*T*) at a Pressure of 0.1 MPa[a]	**90**
Table 3.6a	Density (ρ) for APA+MDEA+H_2O at Different Molar Concentration (*m*) and Temperature (*T*) at a Pressure of 0.1 MPa[a]	**91**
Table 3.6b	Density (ρ) for APA+MDEA+H_2O at Different Molar Concentration (*m*) and Temperature (*T*) at a Pressure of 0.1 MPa[a]	**92**

Table 3.6c	Density (ρ) for APA+MDEA+H_2O at Different Molar Concentration (m) and Temperature (T) at a Pressure of 0.1 MPa[a]	**93**
Table 3.7a	Viscosity (η) for APA+MDEA+H_2O at Different Molar Concentration (m) and Temperature (T) at a Pressure of 0.1 MPa[a]	**94**
Table 3.7b	Viscosity (η) for APA+MDEA+H_2O at Different Molar Concentration (m) and Temperature (T) at a Pressure of 0.1 MPa[a]	**95**
Table 3.7c	Viscosity (η) for APA+MDEA+H_2O at Different Molar Concentration (m) and Temperature (T) at a Pressure of 0.1 MPa[a]	**96**
Table 3.8a	Density (ρ) for APA+AMP+H_2O at Different Molar Concentration (m') and Temperature (T) at a Pressure of 0.1 MPa[a]	**97**
Table 3.8b	Density (ρ) for APA+AMP+H_2O at Different Molar Concentration (m') and Temperature (T) at a Pressure of 0.1 MPa[a]	**98**
Table 3.8c	Density (ρ) for APA+AMP+H_2O at Different Molar Concentration (m') and Temperature (T) at a Pressure of 0.1 MPa[a]	**99**
Table 3.9a	Viscosity (η) for APA+AMP+H_2O at Different Molar Concentration (m') and Temperature (T) at a Pressure of 0.1 MPa[a]	**100**
Table 3.9b	Viscosity (η) for APA+AMP+H_2O at Different Molar Concentration (m') and Temperature (T) at a Pressure of 0.1 MPa[a]	**101**
Table 3.9c	Viscosity (η) for APA+AMP+H_2O at Different Molar Concentration (m') and Temperature (T) at a Pressure of 0.1 MPa[a]	**102**

Table 3.10	Binary Redlich-Kister Parameters A_0, A_1, A_2 for the Excess Volume of density (ρ) and kinematic viscosity (υ) for APA+H_2O (Equations 3.4, 3.5, 3.10 and 3.11)	**103**
Table 3.11	Ternary Redlich-Kister Parameters A_0, A_1, A_2 for the Excess Volume of Density for APA+MDEA+H_2O (Equations 3.4 and 3.5)	**104**
Table 3.12	Ternary Redlich-Kister Parameters A_0, A_1, A_2 for the Excess Volume of Density for APA+AMP+H_2O (Equations 3.4 and 3.5)	**105**
Table 3.13a	Excess molar volume, (V^E), thermal expansion coefficient (α), viscosity deviation ($\Delta\eta$) of ternary blend X_1 APA (1) + X_2 AMP (2) + (1-X_1- X_2) H_2O (3) system at different temperature and molar concentration (m') (X_1, X_2 = mole fraction)[a]	**106**
Table 3.13b	Excess molar volume, (V^E), thermal expansion coefficient (α), viscosity deviation ($\Delta\eta$) of ternary blend X_1 APA (1) + X_2 AMP (2) + (1-X_1- X_2) H_2O (3) system at different temperature and molar concentration (m') (X_1, X_2 = mole fraction)[a]	**107**
Table 3.13c	Excess molar volume, (V^E), thermal expansion coefficient (α), viscosity deviation ($\Delta\eta$) of ternary blend X_1 APA (1) + X_2 AMP (2) + (1-X_1- X_2) H_2O (3) system at different temperature and molar concentration (m') (X_1, X_2 = mole fraction)[a]	**108**
Table 3.14	Parameters of Grunberg and Nissan Model G_{12}, G_{23}, G_{13} for Ternary Viscosity of APA+MDEA+H_2O and APA+AMP+H_2O (Equations 3.12 and 3.13)	**109**
Table 3.15	Values of ΔH and ΔS as a Function of Concentration from (298 to 323) K and ΔG Against APA Mole Fraction at 298 K.	**110**
Table 3.16a	Estimated Henry's Constant of CO_2 in APA+H_2O Using the N_2O Analogy as a Function of Molar Concentration (m) at a Pressure of 0.1 MPa[a]	**111**
Table 3.16b	Estimated Henry's Constant of CO_2 in APA+H_2O Using the N_2O Analogy as a Function of Molar Concentration (m) at a Pressure of 0.1 MPa[a]	**112**

Table 3.17a	Estimated Henry's Constant of CO_2 in APA+MDEA+H_2O Using the N_2O Analogy as a Function of Molar Concentration (m) at a Pressure of 0.1 MPa[a]	**113**
Table 3.17b	Estimated Henry's Constant of CO_2 in APA+MDEA+H_2O Using the N_2O Analogy as a Function of Molar Concentration (m) at a Pressure of 0.1 MPa[a]	**114**
Table 3.18a	Estimated Henry's Constant of CO_2 in APA+AMP+H_2O Using the N_2O Analogy as a Function of Molar Concentration (m) at a Pressure of 0.1 MPa[a]	**115**
Table 3.18b	Estimated Henry's Constant of CO_2 in APA+AMP+H_2O Using the N_2O Analogy as a Function of Molar Concentration (m) at a Pressure of 0.1 MPa[a]	**116**
Table 3.19	Parameters k_1, k_2, k_3, k_4, α_{123} for the Excess Henry's Constant for the Binary and Ternary Solvent Systems and AAD for N_2O Solubility of APA+MDEA+H_2O (Equations 3.19 and 3.20)	**117**
Table 3.20	Parameters for Solubility of N_2O in the Binary Solution of APA+H_2O and Ternary Solution of APA+MDEA+H_2O, APA+AMP+H_2O with AAD using Arrhenius Type Equation (Equations 3.21 and 3.22)	**118**
Table 3.21	Parameters A_1, A_2, A_3, A_4, A_5, A_6 for Solubility of N_2O in the Binary Solutions of APA+H_2O and Ternary Solutions of APA+MDEA+H_2O, APA+AMP+ H_2O with AAD using Polynomial Models (Equations 3.23, 3.24 and 3.25)	**118**
Table 3.22a	Estimated Diffusivity of CO_2 (D_{CO_2}) in APA+H_2O at Temperature (T) Using the N_2O Analogy as a Function of Molar Concentration (m) at a Pressure of 0.1 MPa[a]	**119**
Table 3.22b	Estimated Diffusivity of CO_2 (D_{CO_2}) in APA+H_2O at Temperature (T) Using the N_2O Analogy as a Function of Molar Concentration (m) at a Pressure of 0.1 MPa[a]	**120**
Table 3.23a	Estimated Diffusivity of CO_2 (D_{CO_2}) in APA+MDEA+H_2O at Temperature (T) Using the N_2O Analogy as a Function of Molar Concentration (m) at a Pressure of 0.1 MPa[a]	**121**

Table 3.23b	Estimated Diffusivity of CO_2 (D_{CO_2}) in APA+MDEA+H_2O at Temperature (T) Using the N_2O Analogy as a Function of Molar Concentration (m) at a Pressure of 0.1 MPa[a]	**122**
Table 3.24a	Estimated Diffusivity of CO_2 (D_{CO_2}) in APA+AMP+H_2O at Temperature (T) Using the N_2O Analogy as a Function of Molar Concentration (m) at a Pressure of 0.1 MPa[a]	**123**
Table 3.24b	Estimated Diffusivity of CO_2 (D_{CO_2}) in APA+AMP+H_2O at Temperature (T) Using the N_2O Analogy as a Function of Molar Concentration (m) at a Pressure of 0.1 MPa[a]	**124**
Table 3.25	Parameters for Diffusivity of N_2O in the Binary Solution of APA+H_2O and Ternary Solution of APA+MDEA+H_2O, APA+AMP+H_2O with AAD using Arrhenius Type Equation (Equations 3.28, 3.29 and 3.30)	**125**
Table 3.26	Parameters A_1, A_2, A_3, A_4, A_5, A_6 for Diffusivity of N_2O in the Binary Solutions of APA+H_2O and Ternary Solutions of APA+MDEA+H_2O, APA+AMP+H_2O with AAD using Polynomial Models (Equations 3.31, 3.32 and 3.33)	**125**
Table 4.1	NMR analysis parameters at room temperature	**169**
Table 4.2a	Kinetic data for the absorption of CO_2 into (APA+ H_2O)	**170**
Table 4.2b	Kinetic data for the absorption of CO_2 into (APA+ H_2O)	**171**
Table 4.3a	Kinetic constant for the absorption of CO_2 into (APA+ H_2O)	**172**
Table 4.3b	Kinetic constant for the absorption of CO_2 into (APA+ H_2O).	**173**
Table 4.4	Kinetic data for the absorption of CO_2 into (APA+MDEA+ H_2O).	**174**
Table 4.5	Kinetic constant for the absorption of CO_2 into (APA+MDEA+ H_2O)	**175**
Table 4.6a	Results of the interpretation of the experimental kinetic data for CO_2 -APA-AMP- H_2O system	**176**

Table 4.6b	Results of the interpretation of the experimental kinetic data for CO_2-APA-AMP-H_2O system	**177**
Table 4.7a	Kinetics constant for the absorption of CO_2 into aqueous blend solutions of AMP and APA	**178**
Table 4.7b	Kinetics constant for the absorption of CO_2 into aqueous blend solutions of AMP and APA	**179**
Table 4.7c	Kinetics constant for the absorption of CO_2 into aqueous blend solutions of AMP and APA	**180**
Table II.1	Summary of the literature survey about density of different binary aqueous amine solutions	**210**
Table II.2a	Summary of the literature survey about density of different ternary aqueous amine solutions	**211**
Table II.2b	Summary of the literature survey about density of different ternary aqueous amine solutions	**212**
Table II.2c	Summary of the literature survey about density of different ternary aqueous amine solutions	**213**
Table II.2d	Summary of the literature survey about density of different ternary aqueous amine solutions	**214**
Table II.3	Summary of the literature survey about viscosity of different binary aqueous amine solutions	**215**
Table II.4a	Summary of the literature survey about viscosity of different ternary aqueous amine solutions	**216**
Table II.4b	Summary of the literature survey about viscosity of different ternary aqueous amine solutions	**217**
Table II.4c	Summary of the literature survey about viscosity of different ternary aqueous amine solutions	**218**
Table II.4d	Summary of the literature survey about viscosity of different ternary aqueous amine solutions	**219**

Table II.5	Summary of the literature survey about solubility of N_2O into different binary aqueous amine solutions	**220**
Table II.6	Summary of the literature survey about diffusivity of N_2O into different binary aqueous amine solutions	**221**
Table II.7a	Summary of the literature survey about solubility and diffusivity of N_2O into different ternary aqueous amine solutions	**222**
Table II.7b	Summary of the literature survey about solubility and diffusivity of N_2O into different ternary aqueous amine solutions	**223**
Table II.7c	Summary of the literature survey about solubility and diffusivity of N_2O into different ternary aqueous amine solutions	**224**
Table II.7d	Summary of the literature survey about solubility and diffusivity of N_2O into different ternary aqueous amine solutions	**225**

LIST OF FIGURES

		Page No.
Figure 2.1	Structural formulae for important alkanolamines for gas treating	**51**
Figure 2.2	Formation of carbamate by termolecular mechanism	**52**
Figure 2.3	Alcohol bonding with CO_2	**52**
Figure 3.1	Schematic of experimental set-up for solubility measurement	**126**
Figure 3.2	Excess molar volume (V^E) values of APA (1) + AMP (2) + H_2O (3) systems as a function of APA mole fraction	**127**
Figure 3.3	Thermal expansion coefficient (α) values of APA (1) + AMP (2) + H_2O (3) system at various mole fraction of APA	**128**
Figure 3.4	Viscosity deviation ($\Delta\eta$) values of APA (1) + AMP (2) + H_2O (3) system against APA mole fraction	**129**
Figure 3.5	($H_{CO_2-H_20}$) as a function of temperature (T)	**130**
Figure 3.6	($H_{N_2O-H_20}$) as a function of temperature (T)	**130**
Figure 3.7	($D_{CO_2-H_20}$) as a function of temperature	**131**
Figure 3.8	($D_{N_2O-H_2O}$) as a function of temperature	**131**
Figure 4.1	^{1}H NMR spectra for (a) aqueous APA solution (b) CO_2-loaded aqueous APA solution	**181**
Figure 4.2	TOCSY NMR spectra for CO_2-loaded aqueous APA solution	**182**
Figure 4.3	Dept-135 NMR spectra for CO_2 -loaded aqueous APA solution.	**183**
Figure 4.4	^{13}C NMR spectra for (a) aqueous APA solution (b) CO_2-loaded aqueous APA solution	**184**
Figure 4.5	HMBC spectra for CO_2-loaded aqueous APA solution	**185**
Figure 4.6	HSQC spectra for CO_2-loaded aqueous APA solution.	**186**

Figure 4.7	Enlarged version of ^{1}H NMR spectra for CO_2-loaded aqueous APA solution.	**187**
Figure 4.8	Enlarged version of HMBC spectra for CO_2-loaded aqueous APA solution.	**188**
Figure 4.9	HSQC spectra for aqueous APA solution.	**189**
Figure 4.10	The structure of important reaction intermediates and product of CO_2-(MDEA-APA-H_2O) system	**190**
Figure 4.11	CO_2 absorption rate as a function of CO_2 partial pressure apparently measured for 2 kmol m^{-3} MDEA solutions in the pseudo-first-order regime at different temperature	**191**
Figure 4.12	Effect of contact time on specific rate of absorption in aqueous MDEA at different temperatures for gas compositions of 10% CO_2 and 90% N_2. V_G: 180×10^{-6} m^3 s^{-1}; 2.0 kmol m^{-3} of MDEA.	**191**
Figure 4.13	Specific absorption rates of CO_2 into aqueous solutions of APA at different temperatures for gas compositions (a) 5% CO_2 and 95% N_2 (b) 10% CO_2 and 90% N_2 (c) 15% CO_2 and 85% N_2.	**192**
Figure 4.14	Overall reaction rate constants for the reaction of CO_2 with aqueous APA solutions as a function of amine concentration.	**193**
Figure 4.15	Arrhenius plots of second order reaction rate constants for APA, PZ and PZEA aqueous solutions.	**194**
Figure 4.16	Comparison of the calculated rates to the experimental rates of absorption for CO_2 into aqueous solutions of APA.	**194**
Figure 4.17	Overall reaction rate constants for the reaction of CO_2 with aqueous (APA+MDEA) solutions as a function of amine concentration	**195**
Figure 4.18	Comparison of the calculated rates to the experimental rates of absorption for CO_2 into aqueous solutions of (APA+MDEA)	**195**
Figure 4.19	Specific absorption rates of CO_2 into aqueous solutions of (APA +AMP) at different temperatures for gas compositions 5% CO_2 and 95% N_2	**196**

Figure 4.20 Specific absorption rates of CO_2 into aqueous solutions of (APA +AMP) at different temperatures for gas compositions 10% CO_2 and 90% N_2 **196**

Figure 4.21 Specific absorption rates of CO_2 into aqueous solutions of (APA +AMP) at different temperatures for gas compositions 15% CO_2 and 85% N_2 **197**

Figure 4.22 Overall reaction rate constants for the reaction of CO_2 with aqueous (APA+AMP) solutions as a function of amine concentration **197**

Figure 4.23 Comparison of the calculated rates to the experimental rates of absorption for CO_2 into aqueous solutions of (APA+AMP) **198**

Figure 4.24 Enhancement of MDEA using APA promoter at different temperature **198**

Figure 4.25 Effect of error in Henry's law constant and diffusivity of CO_2 on the calculated rate of absorption of CO_2 in aqueous solutions of (APA +AMP) **199**

Figure 4.26 Effect of error in second order rate coefficient ($k_{2\text{-APA}}$) on the calculated rate of absorption of CO_2 in aqueous solutions of (APA +AMP) **199**

CHAPTER 1

INTRODUCTION, LITERATURE REVIEW AND OBJECTIVES ON CO_2 CAPTURE

This chapter discusses about the release of CO_2 in the earth's atmosphere and its adverse impact on environment such as global warming, climate change issues and greenhouse effect. The features of different CO_2 absorption technologies are also reported in this chapter. The background of the present study and importance and objectives of the research work are discussed in this chapter. Detailed literature review, which includes chemical absorption of CO_2 into different single and blended amine solvents, are also included in this chapter.

1.1 INTRODUCTION

Global warming and climate change issues, which are caused by greenhouse gas emission and its inherent effects, have got an extensive attention in recent years (Kerr, 2007; Sema et al., 2012). It has been reported that owing to the effect of global warming, the earth's temperature will enhance nearly 1.4 to 5.8 °C until the end of 21st century (Bajpai et al., 2013). In the earth's atmosphere, the greenhouse gases (GHG) such as nitrous oxide, methane and CO_2 have a prolonged life span. Among the greenhouse gases, CO_2 has a great role due to its abundance. Currently about 85% of the world energy requirement is largely met by carbon-based fossil fuel resources (BCNet Staff, 2016). The coal-fired power generation sectors are the world's major source of

electricity. They significantly contribute to the runaway anthropogenic greenhouse gas like CO_2 emissions (Richner et al., 2015). The energy-related global CO_2 emissions will keep on growing from 31.3 gt (gigatonnes) in 2011 to about 45 gt in 2035 as per report of the International Energy Agency (2012). Hence, persistent attempts are essential to achieving the target of stabilizing GHG concentrations at 450 ppm CO_2-e (carbon dioxide equivalent). India experiences large fossil-fuel CO_2 emissions (~5.8 % per year) during the period 1950 to 2004 due to dramatic industrial growth. Although, CO_2 emission through coal was decreased from 87 % in 1950 to 70 % in 2004, the emission from oil industries increases from 11% to 22% (Marland et al., 2007). It is anticipated that in between 2010 and 2035, global energy demand will increase by 35%, out of which 59% will be carbon based fossil fuel resources (Richner et al., 2015).

Besides these, to avoid corrosion of pipeline and equipment as well as to meet the fuel gas composition in the natural gas processing unit, CO_2 removal is essential to a level less than 1 %. The ammonia plants and polymerization units contain syngas which must be free of CO_2 to prevent catalyst poisoning. Furthermore, to avoid freezing in cryogenic equipment in natural gas liquefaction plants, CO_2 reduction is mandatory to a level of 50 ppm (Mandal et al., 2006). Hence, to control the earth's surface temperature and enhance the sustainable development of society, CO_2 emissions need to be reduced. In recent years, unwarranted growth in energy consumption and stringent environmental regulations has motivated extensive research and development in suitable technology to economically capture CO_2 from large point sources (e.g., flue gas streams from power plants) of CO_2 emissions (Das et al., 2017).

Various factors such as CO_2 concentration in the feed stream, nature of other components present in the feed stream, pressure and temperature at which the feed stream is available are taken into account for the selection of method for CO_2 capture. The separation of acid gas components (such as CO_2) from natural gas, refinery off-gases, synthesis gas and other industrial gases are carried out in many industrial gas processing. Also the removal of CO_2 is important in many cases such as industrial

organic chemicals like cracking of petroleum fractions, salicylic acid, manufacture of synthetic gasoline, atmosphere control in submarines and space-crafts. Hence, it is highly desirable to capture, utilize or sequester CO_2 from the various point sources.

1.2 ACID GAS TREATING TECHNOLOGIES

Treating of CO_2 from a mixture of gases can be accomplished through various means: cryogenic distillation, membrane separation, adsorption and most commonly physical and chemical absorption. Treating of CO_2 from flue gas through membranes have not been widely explored because it requires flue gas pressurization and comparatively high mixture flows. Apart from this, it requires two-stage system to achieve good separation and cost are double in comparison to conventional amine absorption process (Meisen and Shuai, 1997). Adsorption based process is not yet a highly acceptable process because CO_2 selectivity and capacity of available adsorbent is low (Meisen and Shuai, 1997). Although, there is a possibility when adsorption is combined with another capture technology then it becomes attractive. Low-temperature distillation is used commercially for the purpose of purification and liquefaction of CO_2 from streams containing > 90% CO_2. The CO_2 separation through the cryogenic process would produce a high pressure liquid CO_2 stream and this process is energy intensive (Meisen and Shuai, 1997). The refrigeration and the removal of water increases the overall cost of this process. This process is usually considered when stream containing highly concentrated CO_2.

Among the various separation techniques, chemical absorption and physical absorption are the most promising for capturing post-combustion CO_2. Absorption using a chemical solvent is the present frontline commercial technology to chemically and reversibly bind the CO_2 (Mondal et al., 2015). In order to develop potential post-combustion carbon capture (PCC) using alkanolamine based solvent systems,

significant advancements need to be made (Conway et al., 2015). However, stainless steel absorber/stripping columns and energy associated with the regeneration of solvent from CO_2-rich amine solvent bring high capital cost, which are the key barriers to a large-scale industrial process. These factors demand significant improvements to facilitate the up-scaling (Barzagli et al., 2009; Conway et al., 2013). To see the merits and versatility of chemical absorption process, CO_2 removal using this process is considered in the present work. These methods are discussed in details as given below.

1.2.1 CO_2 treating by absorption

The transfer of one or more substances from the gas phase to the liquid phase through the vapor-liquid phase boundary is the main principle of all separation processes using gas absorption. The substance absorbed in liquid phase is occurred by physical dissolution, which may also be followed by a chemical reaction. However, the prospect of significant improvements towards current generation solvent which can provide faster reaction kinetics, high equilibrium loading capacity, smaller size of equipment, reduction in the overall energy penalty, higher degradation resistance, less corrosivity and ultimately, lower capital cost is one of the most pivotal point of PCC technology (Liu et al., 2014). Beside this, it would provide an additional degree of freedom for achieving the desired separation of treated gas by judiciously mixing amines with different proportion. Different industries like natural and synthesis gas processing plants, coal-based power plants, and cement plants are proved the potentiality of the absorption based technique. Although, the primary focus is on the coal-based power plant towards CO_2 capture and storage technology (CCS) (Dash et al., 2011). Separation of CO_2 using absorption generally falls into two broad categories: physical absorption; and chemical absorption. This depends upon the nature of the interaction between the absorbate and absorbent.

1.2.1.1 Physical absorption

For acid gas treating processes, chilled methanol (Rectisol® process licensed by Linde AG), *N*-methyl-2-pyrolidone (Purisol® process licensed by Lurgi GmbH), dimethylether of polyethylene glycol (Selexol® process licensed by UOP LLC) and propylene carbonate (Flour® process licensed by Fluor Daniel, Inc.) are normally used as physical absorbents. The advantages of physical solvents are very good equilibrium loading capacity for the gaseous impurities and less energy requirement for regeneration. Beside this, it separates acid gases very easily from the loaded solution and it is applicable when partial pressure of acid gases to be removed is relatively higher. However, higher cost and co-absorption of hydrocarbons are the major disadvantages of these solvents (Kazemi et al., 2016).

1.2.1.2 Chemical absorption

Like in a physical absorption, the substance of gas phase is absorbed into the liquid phase in chemical absorption process. The reaction between substance and absorbent formed a semi-stable complex. In natural gas processing, reaction kinetics and economy play a vital role. So chemical solvents are usually employed though their regeneration is relatively tough. Aqueous alkanolamine and promoted hot potassium carbonate processes are mostly used. This study falls under the category of chemical absorption process.

The CO_2 removal from mixture of gases using potassium carbonate has been known for many years. The hot potassium carbonate process requires relatively high partial pressures of CO_2 and it is capable to remove several trace sulfur compound coming from sour gas streams. For the economical sweetening of natural gases, the hot potassium carbonate process is commonly used. Ammonia-based processes are very

rarely applicable compared to the alkanolamine and hot potassium carbonate-based processes due to the higher corrosive nature of the loaded solutions and complex flow scheme.

The alkanolamine technology is the most commonly applicable today to separate CO_2 from sour gas streams due to the following reasons:

- Alkanolamine can remove CO_2 to a very low level.
- Alkanolamine-based CO_2 capture streams are a proven technology that is commercially available and in use today.
- Alkanolamine-based system typically used in power plants, are operated at ordinary temperature and pressure.
- Lower cost compared to that of the physical solvents.

1.2.1.2.1 CO_2 absorption by aqueous alkanolamine solutions

Alkanolamine are commonly preferred solution to separate acid gases as the amino group delivered the required alkalinity in water solution to make the absorption of acid gases and the hydroxyl group helps to increase the solubility of the amines in water. This effect reduces the vapour pressure of amine and therefore, amines are hardly lost out of the top of the absorber and stripper. Approximately 90% of the acid gas treating processes uses alkanolamine solvents because of their versatility and their ability to remove acid gases to very low levels (Paul et al., 2007). A blended alkanolamine solvent, which involves a primary or secondary alkanolamine with a mixture of tertiary or sterically hindered alkanolamine, combine the higher CO_2 reaction rates of the primary or secondary alkanolamine with the higher CO_2 loading capacity of the tertiary or sterically hindered alkanolamine. Thus, both higher CO_2 reaction rate and higher CO_2 equilibrium capacity are provided by blended alkanolamine solvent and it may also delivered substantial lower solvent circulation

rates compared to a single alkanolamine solvent. Solvent circulation rate is the single most important factor in determining the economics of a gas treating process using chemical solvent.

Alkanolamine mainly classified in three categories; primary, secondary and tertiary. The mostly used alkanolamines are the primary amine: monoethanolamine (MEA); the secondary amine: diethanolamine (DEA); and the tertiary amines: MDEA and triethanolamine (TEA). The reactions between CO_2 and primary or secondary alkanolamines are very rapid and they formed carbamate ions. When a primary or secondary alkanolamine is added to a purely physical solvent such as water (H_2O), the CO_2 absorption capacity and rate is enhanced manifold. However, the cost of regenerating primary and secondary amines is high because there is a relatively high heat of absorption released with the formation of carbamate ions. Primary and secondary alkanolamines required two moles of amine to react with one mole of CO_2 and therefore their loadings are limited to a maximum of 0.5 which is also the disadvantage to use these amines. In case of tertiary amine, they do not form the carbamate ion because of lack of N-H bond. However, tertiary alkanolamine in aqueous medium promote CO_2 hydrolysis reaction to form bicarbonate and protonated alkanolamine. This hydrolysis reaction is much slower than the direct reaction of primary or secondary amine with CO_2, and therefore the kinetics of CO_2 reaction in tertiary amine is very poor (Das et al., 2017). The formation of bicarbonate ions associated with the heat of reaction released is much lower than that of carbamate formation. Therefore, the regeneration costs are lower for tertiary alkanolamine than that for the primary and secondary amines. Compared to primary and secondary amines, tertiary amines have a higher absorption capacity (1 mole of CO_2/mole of amine) as well as higher degradation resistance (Das et al., 2016). So in other words, while tertiary alkanolamines are thermodynamically selective toward CO_2, primary and secondary alkanolamines are kinetically selective toward CO_2.

One important class of alkanolamines (sterically hindered form of primary amine) i.e., 2-amino-2-methyl-1-propanol (AMP) is considered to be a potential absorbent for CO_2 absorption process (Gabrielsen et al., 2007). Despite the fact that AMP absorbs CO_2 more slowly than MEA from the flue gas stream, but the theoretical cyclic capacity of AMP on a molar basis is twice than MEA (Dash et al., 2011).

Given this, an economically viable and improved process for CO_2 capture is needed to mitigate the problem of global warming. Out of various solvents used in regenerative chemical absorption processes, interest has recently grown towards activated alkanolamine absorbents where a small amount of rate activator is employed into the alkanolamine solution to increase the significant reaction rate of CO_2. As for example, piperazine (PZ) activated MDEA or AMP solutions could combine the high reaction rate of CO_2 with PZ and the high CO_2 loading capacity of MDEA or AMP and a relatively small cost to regenerate the activated solvent (Appl et al., 1982; Paul et al., 2009a).

1.3 LITERATURE REVIEW ON ABSORPTION OF CO_2 BY SINGLE AND BLENDED AMINE SOLUTIONS

1.3.1 Absorption of CO_2 in single amine solvents

Numerous literature on acid gas absorption into a primary amine MEA (extensive studies on the kinetics of CO_2 absorption) were conducted by several authors (Astarita, 1961; Leder, 1971; Sada et al., 1976; Hikita et al., 1977; Danckwerts, 1979; blauwhoff et al., 1984; Barth et al., 1986; Saha, 1994). There is a very good agreement for the data reported by them and their investigation for rate of reaction between CO_2 and MEA was found to be a first-order dependence. Blauwhoff et al. (1984) examined the huge number of literature data on CO_2-MEA kinetics and concluded that the data were fitted well with the rate expression given by Hikita et al. (1977) over the temperature range

of 278-353 K. A few years later, Barth et al. (1986) conducted the experiment on CO_2-MEA kinetics and their results provided very good agreement with previous literature data.

A secondary category of amine i.e., DEA is widely popular solvent in the field of gas treating industry because it has a reasonable reactivity towards CO_2. However, it is much less corrosive than MEA and its exothermic heat of reaction is lower. Numerous literature are available for DEA because of its prevalence (Blauwhoff et al., 1984; Barth et al., 1986; Donaldson and Nguyen, 1980; Hikita et al.,1977; Ladha and Danckwerts, 1981). Caplow (1968) originally proposed two-step zwitterion mechanism which was reintroduced by Danckwarts (1979) is widely accepted reaction mechanism for the reactions between CO_2 and primary or secondary amines (Blauwhoff et al., 1984; Versteeg and Oyevaar, 1989; Versteeg and van Swaaij, 1988; Glasscock et al., 1991; Little et al., 1992a; Little et al., 1992b; Versteeg et al., 1990). This mechanism has two limiting cases. One is the reaction rate appears to be first order with respect to both amine and CO_2 concentrations when the zwitterion formation reaction is rate determining. The other one is the overall reaction rate appears in between 1 and 2 as a fractional order with respect to amine concentration when the zwitterion deprotonation reactions are rate limiting. A primary amine, mostly in MEA, the zwitterion formation has been reported to be the rate-determining step (Blauwhoff et al., 1984; Versteeg and van Swaaij, 1988; Little et al., 1992; Sada et al., 1985). Whereas, the secondary category of amines i.e., DEA and DIPA, the rate coefficients reported by several authors (Blauwhoff et al., 1984; Versteeg and van Swaaij, 1988; Glasscock et al., 1991) using zwitterion mechanism considered zwitterion deprotonation to be rate limiting cases. Usually the reaction of CO_2 with secondary amines provided only fractional orders (Versteeg and Oyevaar, 1989; Little et al., 1992a; Sada et al., 1985).

In acid gas treating technology, commercially used first ethanolamine was a tertiary category of amine i.e., TEA. It has been largely displaced by a low molecular

weight MDEA or more reactive MEA and DEA towards CO_2. The reason why MDEA considered to be superior over TEA is that in a given volume of solution the moles of amine are present more. Now a days TEA has only the scientific interest and its industrial significance is limited.

MDEA is a potential solvent as it has low heat of reaction and currently being studied more due to its industrial significance (Versteeg and van Swaaij, 1988; Little et al., 1992; Rinker et al., 1995). Rinker et al. (1995) studied the reaction between CO_2 and MDEA over the range of temperature. Their results are in good agreement with the proposed base catalysed hydrolysis of CO_2.

Now a days, commercially attractive proposed CO_2 absorbents are sterically hindered class of AMP and 2- piperidineethanol (2-PE) because of their benefit in absorption rate, CO_2 loading capacity, and regeneration energy. Sharma (1965) reported that steric effects influence the stability of the carbamates which formed between the reaction of amine and CO_2. They found out a second order rate in a laminar jet absorber for the CO_2-AMP reaction. Sharma (1965) also reported that the use of highly branched amine i.e., AMP for CO_2 absorption could show considerable advantages such as high reaction rate with CO_2 compared to tertiary amines and requiring less energy for regeneration over primary or secondary alkanolamines i.e., MEA or DEA. Sartori and Savage (1983) studied on CO_2 absorption into AMP and few other hindered amines as well.

In a CO_2 capture process typically a feed gas along with the acidic components is contacted countercurrently in a packed column with the aqueous amine solutions. The reason for the countercurrent contacting is that the reactions are equilibrium limited. The ‘sweet gas’ comes out from the top of the absorption column. The loaded solution is then fed to the stripper where it is typically heated at slightly above ambient pressure. Energy is provided to the reboiler for two reasons: (i) to produce enough water vapour so that the vapour-phase partial pressure of CO_2 is low enough to provide a driving force for desorption, and (ii) to provide enough energy to reverse the reactions which occur in the absorber. In fact, the reactions of CO_2 with aqueous alkanolamine solutions are exothermic, releasing energy in the absorber and requiring energy in the stripper.

The lean solvent is then cooled to the desired temperature and fed back at the top of the absorption tower. In this process, there is little loss of amine and hence some make arrangement are usually made at the top of the absorption tower. Hence, the amine regenerative and solvent is reused.

Xu et al. (1996) determined the kinetics for the reaction between CO_2 and AMP from the measurements of rate of absorption of CO_2 into both aqueous and non-aqueous (1-propanol) AMP solutions in a stirred-cell reactor. Their study varied the temperatures from 288 to 318 K and the concentration from 0.25 to 3.5 kmol m^{-3} of AMP. The zwitterion mechanism was found to be suitable for modeling the absorption of CO_2 into the aqueous and organic (1-propanol) solutions of AMP. The order of reaction in amine was reported to be greater than one for both cases.

Saha et al. (1999) investigated the absorption of CO_2 into aqueous solutions of sterically hindered amine (AMP) at 288.0-301.5 K over CO_2 partial pressure of (5-15 kPa) and amine concentration of 1-2 kmol m^{-3} in a mechanically agitated contactors. Their experimental and predicted CO_2 loadings were found to be good agreement when CO_2 loading is below 0.5. However, the predicted values of CO_2 loadings from the experimental values is only about 3% and this occurs only when the total liquid-phase CO_2 loadings is greater than 0.5 mol CO_2 per mol of AMP.

Paul et al. (2009b) investigated the kinetics of absorption of CO_2 with aqueous AHPD solutions at 303, 313 and 323 K within the amine concentration range of 0.179-1.789 kmol m^{-3} in a wetted wall column absorber. It was reported that the absorption into 2-PE are higher than AHPD solutions at temperature range of around 303-313 K, whereas at 323 K the CO_2 absorption coefficient of aqueous AHPD solutions was higher than aqueous 2-PE solutions. Therefore, at higher temperatures, AHPD is more preferable solvent than 2-PE for the absorption of CO_2. It was also been reported that the absorption of CO_2 into (AHPD +H_2O) is better than that for the absorption into other sterically hindered amines like 2-amino-2-ethyl-1,3- propanediol (AEPD) and 2-amino-2-methyl-1,3-propanediol (AMPD).

Bougie and Iliuta (2009) studied the kinetics of CO_2 into sterically hindered alkanolamine, 2-amino-2-hydroxymethyl-1, 3-propanediol (AHPD) and they determined kinetics of reaction at the temperatures ranges of 303.15-323.15 K in a wetted wall column contactor. In their experiment, AHPD concentration was varied in the range of 0.5-2.4 kmol m^{-3}. They determined the overall pseudo-first-order rate constants based on the pseudo-first-order principle for the absorption of CO_2. They found that the zwitterion mechanism fits the experimental data very well.

1.3.2 Absorption of CO_2 in blended amine solvents

Horng and Li (2002) investigated the kinetics of the absorption of CO_2 into (MEA + TEA +H_2O) at 303, 308 and 313 K in a wetted wall column. Ten systems of which 0.5 and 1.0 kmol m^{-3} TEA mixed with various MEA concentrations (0.1, 0.2, 0.3, 0.4, and 0.5 kmol m^{-3}) were conducted in their study. It was reported that there is significant increase of reaction rate of CO_2 with even a small amount of MEA.

Hagewiesche et al. (1995) investigated the rates of absorption of CO_2 into aqueous blends of MDEA and MEA. They reported that the small addition of MEA to aqueous solution of MDEA results in significant increase in the enhancement factor and rate of absorption.

Mandal and Bandyopadhyay (2006) investigated experimentally and theoretically the rate of absorption of CO_2 into aqueous blends of (AMP+MEA) with 30 mass% total amine concentration in a wetted wall-column at 313 K. They observed that on the addition of small amounts of MEA, there is increase in the enhancement in the rates of absorption.

Adeosun et al. (2013) reported four piperazine (PZ)-based blends such as (10 wt.% MEA + 20 wt.% PZ), (10 wt.% DEA + 20 wt.% PZ) , (10 wt.% AMP + 20 wt.% PZ), (10 wt.% MDEA + 20 wt.% PZ), (10 wt.% DEA + 20 wt.% PZ). Among these (10 wt.% AMP + 20 wt.% PZ) blend recorded the highest CO_2 absorption capacity of 0.99 mol CO_2 /molamine.

Dubois and Thomas (2011) studied the CO_2 absorption into aqueous amine based solvents at 298 K in a laboratory cables-bundle scrubber. Their study was to compare CO_2 absorption performances for different type of single and blended amine solutions contaning MEA, MDEA, AMP, PZ and 2-(1-piperazinl)-ethylamine (PZEA). They stated that the different absorption experiments clearly showed the very positive effect of an activator on the absorption performances and particularly with PZ. A gradual increase in the CO_2 absorption efficiencies can be reached by mixing different types of amine tertiary (MDEA) or sterically hindered amine (AMP) with an activator (PZ or PZEA) or a primary amine (MEA).

Muraleedharan et al. (2012) investigated the absorption of CO_2 into aqueous blends of 2-amino-2- hydroxymethyl-1, 3-propanediol (AHPD) and monoethanolamine (MEA) at 303, 313 and 323 K as well as physicochemical properties of this blended amine solvent over the temperature range from 293 to 323 K. They showed that the absorption flux for CO_2 in this amine blend is higher compared to the single amine (AHPD) as obtained in earlier work (Paul et al., 2009b). The absorption flux of CO_2 into the aqueous blends increased with the increase in temperature from 303 to 323 K. The absorption flux decreased when the concentration of AHPD increased in the blends. They started the experiment with the total amine concentration at 30 % mass, with the AHPD mass fractions ranging from 30% to 0% in the solutions and MEA mass fraction ranging from 0 % to 30 %.

Xiao et al. (2000) measured the kinetics of the absorption of CO_2 into (AMP + MEA+ H_2O) at 303, 308 and 313 K using a laboratory wetted wall column. They used ten systems of which 1.7 and 1.5 kmol m^{-3} AMP mixed with various MEA concentrations (0.1, 0.2, 0.3 and 0.4 kmol m^{-3}) for experimentation. The overall pseudo-first order reaction rate constants were determined based on the pseudo-first order for the CO_2 absorption from the kinetic measurements.

Mandal et al. (2001) worked on the absorption of CO_2 into aqueous blends of MDEA and MEA as well as on the blend of AMP and MEA. They observed that on the addition of small amount of MEA to aqueous solution of MDEA enhances the

enhancement factor and rate of absorption significantly. It was also reported that the enhancement factor for CO_2-(AMP + MEA + H_2O) is higher than the CO_2-(MDEA + MEA+ H_2O) system.

Liao and Li (2002) investigated the kinetics of the absorption of carbon dioxide into aqueous blends of MEA and MDEA in a wetted wall column absorber over the temperature range of 303–313 K. Ten systems of which 1.0 and 1.5 kmol m^{-3} MDEA mixed with MEA concentrations of 0.1, 0.2, 0.3, 0.4 and 0.5 kmol m^{-3} were studied. They reported in their work that the small addition of MEA to MDEA results in great enhancement of CO_2 absorption rates. The reaction model developed was found to be in great agreement for prediction of the CO_2 absorption rate into (MEA + MDEA + H_2O) systems.

Wang and Li (2004) determined the rates of absorption into aqueous blends of AMP and DEA in a wetted wall column absorber in the temperature range 303–313 K. Eight systems of which 1.0 and 1.5 kmol m^{-3} AMP mixed with DEA concentrations of 0.1, 0.2, 0.3, 0.4, and 0.5 kmol m^{-3} were studied. They reported in their work that the small addition of DEA to AMP results in great enhancement of CO_2 absorption rates.

Jamal et al. (2006a, 2006b) determined the kinetics of CO_2 absorption into aqueous solutions of MEA, DEA, MDEA and AMP and their mixtures (i.e., MEA+AMP, MEA+MDEA, DEA+AMP and DEA+MDEA) using a hemispherical contactor. For this absorption study, MEA, DEA, MDEA and AMP concentrations were varied in the range of 2–35 wt.%. In their study the reaction between CO_2 and carbamate-forming amines such as MEA, DEA and AMP under both absorption and desorption conditions were presented.

Ramachandran et al. (2006) determined the kinetics of CO_2 into loaded blend MDEA and MEA solutions using laminar jet apparatus over the temperature range of 298–333 K with total amine concentration of 30 wt.%, and CO_2 loading from 0.005-0.15 (mole of CO_2 per mole of total amine). To interpret the kinetic data they used both zwitterion and termolecular reaction mechanisms. Their results showed that the zwitterion mechanism in its original form could not forecast the individual kinetic rate constants. Similarly, the termolecular mechanism with water could not yield any

reasonable results to estimate the apparent reaction rate. A modified termolecular mechanism included the contribution of hydroxide ions was applied in their work to estimate the kinetics of a CO_2 loaded mixed alkanolamine solutions with MDEA not participating with MEA in the kinetics. Based on the modified termolecular mechanism, they estimated individual reaction rate constants.

Vaidya and Kenig (2007) investigated the kinetics of the reaction of CO_2 into aqueous blend of *N*-ethylethanolamine (EEA) and *N*,*N*-diethylethanolamine (DEEA) solutions in a stirred cell reactor with a plane, horizontal gas–liquid interface over the temperatures range of 298–308 K. They investigated those solvents which becomes potentially attractive chemical solvents for gas purification as they can prepared from renewable resources. Their results stated that EEA acted as an effective activator in aqueous DEEA solutions. The overall reaction of CO_2 into aqueous blends containing DEEA and EEA could be considered as a reaction between CO_2 and DEEA in parallel with the reaction of CO_2 with EEA.

Zoghi et al. (2012) experimentally investigated the kinetics of absorption of CO_2 into aqueous solutions of MDEA in the presence of different activators like PZ, DIPA, AMP, DGA and aminoethylethanolamine (AEEA). Their results suggest that AEEA at activator/MDEA ratio of 0.125 shows the best result on the enhancement effect of CO_2 absorption rate among other potential activators investigated. At low ratio of DIPA /MDEA, DIPA has moderate enhancement effect on CO_2 absorption rate, but its enhancement effect becomes reduces significantly with increasing its ratio to MDEA. Similarly at low ratio of DGA /MDEA, DGA did not show a significant activation effect but its effect becomes higher by increasing the ratio to 0.25.

Conway et al. (2013) studied in details that a fundamental chemical understanding of the relationship between the amine structure and chemical properties of the amine which are relevant for post combustion capture of CO_2 (PCC) applications. They investigated the kinetics of absorption of CO_2 (aq) with a series of linear and methyl substituted primary amines and alkanolamines using stopped-flow spectrophotometry and ^1H NMR measurements at 298 K. The specific mechanism of

absorption include CO_2 hydration and/or carbamate formation for each of the amines is discussed. According to this mechanism, the kinetic and equilibrium constants following the formation of carbamic acid/carbamates for amines are investigated. The kinetic rate constants and equilibrium constants for the formation of carbamic acid/carbamates with the protonation constant of the amine relating with Brønsted correlation is investigated. This type of relationship facilitates the effects of steric and electronic properties of the amine toward its reaction of CO_2.

1.4 IMPORTANCE AND OBJECTIVES OF PRESENT WORK

It is prominent from the comprehensive literature review that acid gas (such as CO_2) absorption using activated alkanolamine solutions are needed for its immense industrial significance. Therefore, a novel amine activator was essential having faster reaction kinetics, high equilibrium loading capacity, to provide reduce solvent circulation rate, higher degradation resistance and less corrosivity, which will ultimately provide lower capital cost. Due to carbamate formation by Lewis acid–base reaction, carbamate forming amine or fast-reacting amine is getting an advantage because of their reactivity with CO_2 involve much faster kinetics compared to water/hydroxide with CO_2 (Conway et al., 2013). Fast reaction results in significantly smaller size of the absorber column, and hence cost will be less. Similarly, as the pH of the solution increases, the rate of reaction increases and if it is greater than 8.5 then eventually it surpasses the reaction with water. So amines under the same conditions with high protonation will give higher rate of reaction. As we know Lewis acid-base interaction was observed during the reaction of CO_2 and amine, therefore Lewis basicity is an important property of the amine which governs the rate as well as the equilibrium constant for the reaction with CO_2. However, Brønsted basicity is taken into account as a simplest approximation in place of Lewis basicity because protonation constant is straightforwardly defined by Brønsted basicity (Conway et al., 2013).

A bis(3-aminopropyle)amine (APA), which contains two primary amine groups and one secondary amine group (structure is given as: 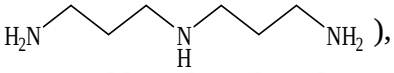), has more pK_a (10.85) value than PZ (9.73) (Das et al., 2016) and based on the relation of cyclic and noncyclic amines given by Conway et al. (2013), the reaction rate of APA expected to be higher than PZ. Three amine groups are present in a single molecule of APA and hence it is expected to provide higher equilibrium loading capacity than PZ. Also, the high molecular weight of APA leads to less evaporation loss than PZ. Furthermore, according to our knowledge no such amine activator was found in the literature which occurs naturally in some species of plants, bacteria, and algae. Since APA occurs naturally in renewable resources, it is expected to be more promising rate activator than others (Das et al., 2016). As we know that the typical solvent regeneration temperature range is 353 to 393 K. So within this range, APA with loaded CO_2 does not form any cyclic urea (Wu et al., 2010). In this study, APA was chosen as a novel activator for different amine blends towards absorption of CO_2. Also, considering the potentially of AMP and MDEA, two novel aqueous blends such as (APA+MDEA+H_2O), (APA+AMP+H_2O) were chosen in this research. Physicochemical properties and kinetics are important for any new solvent system for its commercial application. Hence, the objectives of the present research work are as follows:

- To determine the physicochemical properties as well as specific rate of CO_2 absorption into aqueous solutions of APA. This in turn will help us to develop a reaction mechanism and kinetics of the CO_2-APA-H_2O system.
- To study the performance of APA as an accelerator when blended with other amines like MDEA and AMP instead of an individual solvent for a wide range of temperature and amine concentration using a wetted wall column absorber.
- Measurement of required physicochemical properties of (APA+MDEA+H_2O) and (APA+AMP+ H_2O) system (i.e., density and viscosity of the above alkanolamine

solutions as well as diffusivity and physical solubility of CO_2 into the above alkanolamine solutions) over wide range of temperature and amine concentrations.

- Development of useful correlations for the measured properties as well as kinetics and validation with the experimental data.

REFERENCES

Adeosun, A., Hadri, N.E., Goetheer, E., Abu-Zahra, M.R., 2013. Absorption of CO_2 by amine blends solution: an experimental evaluation. International Journal of Engineering and Science, 3, 12-23.

Appl, M., Fuerst, E., Henrici, H.J., Kuessner, K., Volkamer, K., Wagner, U., 1982. Removal of CO_2 and/or H_2S and/or COS from gases containing these constituents. US Pat 4, 336, 233.

Astarita, G., 1961. Carbon dioxide absorption in aqueous monoethanolamine solutions. Chemical Engineering Science 16, 202-207.

Barth, D., Tondre, C., Delpuech, J.J., 1986. Stopped-flow investigations of the reaction kinetics of carbon dioxide with some primary and secondary alkanolamines in aqueous solutions. International Journal of Chemical Kinetics 18, 445-457.

Barzagli, F., Mani, F., Peruzzini, M., 2009. A ^{13}C NMR study of the carbon dioxide absorption and desorption equilibria by aqueous 2-aminoethanol and N-methyl-substituted 2-aminoethanol. Energy & Environmental Science 2, 322-330.

Bajpai, A., Mondal, M.K., 2013. Equilibrium solubility of CO_2 in aqueous mixtures of DEA and AEEA. Journal of Chemical & Engineering Data 58, 1490-1495.

Boston Commons High Tech Network http://bostoncommons.net/85-of-worlds-energy-still-comes-from-fossil-fuels/ Feb 26, 2016 by BCNet Staff.

Bougie F., Iliuta M.C., 2009. Kinetics of absorption of carbon dioxide into aqueous solutions of 2-amino-2-hydroxymethyl-1,3-propanediol. Chemical Engineering Science 64,153-162.

Blauwhoff, P.M.M., Versteeg, G.F., Van Swaaij, W.P.M., 1984. A study on the reaction between CO_2 and alkanolamines in aqueous solutions. Chemical Engineering Science 39, 207-225.

Caplow, M., 1968. Kinetics of carbamate formation and breakdown. Journal of the American Chemical Society 90, 6795-6803.

Conway, W., Wang, X., Fernandes, D., Burns, R., Lawrance, G., Puxty, G., Maeder, M., 2013. Toward the understanding of chemical absorption processes for post-combustion capture of carbon dioxide: electronic and steric considerations from the kinetics of reactions of CO_2 (aq) with sterically hindered amines. Environmental Science & Technology 47, 1163-1169.

Conway, W., Beyad, Y., Richner, G., Puxty, G., Feron, P., 2015. Rapid CO_2 absorption into aqueous benzylamine (BZA) solutions and its formulations with monoethanolamine (MEA), and 2-amino-2-methyl-1-propanol (AMP) as components for post combustion capture processes. Chemical Engineering Journal 264, 954-961.

Danckwerts, P.V., 1979. The reaction of CO_2 with ethanolamines. Chemical Engineering Science 34, 443-446.

Das, B., Deogam, B., Agrawal, Y and Mandal, B., 2016. Measurement and correlation of the physicochemical properties of novel aqueous bis(3-aminopropyl)amine and its blend with n-methyldiethanolamine for CO_2 capture. Journal of Chemical & Engineering Data 61, 2226-2235.

Das, B., Deogam, B., Mandal, B., 2017. Absorption of CO_2 into novel aqueous bis(3-aminopropyl)amine and enhancement of CO_2 absorption into its blends with n-methyldiethanolamine. International Journal of Greenhouse Gas Control 60, 172-185.

Dash, S.K., Samanta, A., Nath Samanta, A., Bandyopadhyay, S.S., 2011. Absorption of carbon dioxide in piperazine activated concentrated aqueous 2-amino-2-methyl-1-propanol solvent. Chemical Engineering Science 66, 3223-3233.

Donaldson, T.L., Nguyen, Y.N., 1980. Carbon dioxide reaction kinetics and transport in aqueous amine membranes. Industrial & Engineering Chemistry Fundamentals 19, 260-266.

Dubois, L., Thomas, D., 2011. Carbon dioxide absorption into aqueous amine based solvents: Modeling and absorption tests. Energy Procedia 4, 1353-1360.

Gabrielsen, J., Svendsen, H.F., Michelsen, M.L., Stenby, E.H., Kontogeorgis, G.M., 2007. Experimental validation of a rate-based model for CO_2 capture using an AMP solution. Chemical Engineering Science 62, 2397-2413.

Glasscock, D.A., Critchfield, J.E., Rochelle, G.T., 1991. CO_2 absorption/desorption in mixtures of methyldiethanolamine with monoethanolamine or diethanolamine. Chemical Engineering Science 46, 2829-2845.

Hagewiesche, D.P., Ashour, S.S., Al-Ghawas, H.A., Sandal, O.C., 1995. Absorption of carbon dioxide into aqueous blends of monoethanolamine and N-methyldiethanolamine. Chemical Engineering Science 50, 1071-1079.

Hikita, H., Asai, S., Ishikawa, H., Honda, M., 1977. The kinetics of reactions of carbon dioxide with monoethanolamine, diethanolamine and triethanolamine by a rapid mixing method. The Chemical Engineering Journal 13, 7-12.

Horng, S.-Y., Li, M.-H., 2002. Kinetics of absorption of carbon dioxide into aqueous solutions of monoethanolamine + triethanolamine. Industrial & Engineering Chemistry Research 41, 257-266.

Jamal, A., Meisen, A., Jim Lim, C., 2006a. Kinetics of carbon dioxide absorption and desorption in aqueous alkanolamine solutions using a novel hemispherical contactor—

I. Experimental apparatus and mathematical modeling. Chemical Engineering Science 61, 6571-6589.

Jamal, A., Meisen, A., Jim Lim, C., 2006b. Kinetics of carbon dioxide absorption and desorption in aqueous alkanolamine solutions using a novel hemispherical contactor—II: Experimental results and parameter estimation. Chemical Engineering Science 61, 6590-6603.

Kazemi, A., Kazemi Joujili, A., Mehrabani-Zeinabad, A., Hajian, Z., Salehi, R., 2016. Influence of CO_2 Residual of regenerated amine on the performance of natural gas sweetening processes using alkanolamine solutions. Energy & Fuels 30, 4263-4273.

Kerr, R.A., 2007. Global warming is changing the world. Science 316, 188-190.

Laddha, S.S., Danckwerts, P.V., 1981. Reaction of CO_2 with ethanolamines: kinetics from gas-absorption. Chemical Engineering Science 36, 479-482.

Leder, F., 1971. The absorption of CO_2 into chemically reactive solutions at high temperatures. Chemical Engineering Science 26, 1381-1390.

Liang, Z., Rongwong, W., Liu, H., Fu, K., Gao, H., Cao, F., Zhang, R., Sema, T., Henni, A., Sumon, K., Nath, D., Gelowitz, D., Srisang, W., Saiwan, C., Benamor, A., Al-Marri, M., Shi, H., Supap, T., Chan, C., Zhou, Q., Abu-Zahra, M., Wilson, M., Olson, W., Idem, R., Tontiwachwuthikul, P., 2015. Recent progress and new developments in post-combustion carbon-capture technology with amine based solvents. International Journal of Greenhouse Gas Control 40, 26-54.

Liao, C.-H., Li, M.-H., 2002. Kinetics of absorption of carbon dioxide into aqueous solutions of monoethanolamine+N-methyldiethanolamine. Chemical Engineering Science 57, 4569-4582.

Littel, R.J., Versteeg, G.F., Van Swaaij, W.P.M., 1992a. Kinetics of CO_2 with primary and secondary amines in aqueous solutions - II. Influence of temperature on zwitterion formation and deprotonation rates. Chemical Engineering Science 47, 2037-2045.

Littel, R.J., Versteeg, G.F., Van Swaaij, W.P.M., 1992b. Kinetics of CO_2 with primary and secondary amines in aqueous solutions—I. Zwitterion deprotonation kinetics for DEA and DIPA in aqueous blends of alkanolamines. Chemical Engineering Science 47, 2027-2035.

Liu, H., Liang, Z., Sema, T., Rongwong, W., Li, C., Na, Y., Idem, R., Tontiwachwuthikul, P., 2014. Kinetics of CO_2 absorption into a novel 1-diethylamino-2-propanol solvent using stopped-flow technique. AIChE Journal 60, 3502-3510.

Mandal, B.P., Bandyopadhyay, S.S., 2006. Absorption of carbon dioxide into aqueous blends of 2-amino-2-methyl-1-propanol and monoethanolamine. Chemical Engineering Science 61, 5440-5447.

Mandal, B.P., Guha, M., Biswas, A.K., Bandyopadhyay, S.S., 2001. Removal of carbon dioxide by absorption in mixed amines: modelling of absorption in aqueous MDEA/MEA and AMP/MEA solutions. Chemical Engineering Science 56, 6217-6224.

Marland, G., Boden, T., Andres. R., 2007. Global, regional, and national CO_2 emissions in trends: a compendium of data on global change, carbon dioxide. Information Analysis Center, Oak Ridge National Laboratory, U.S. Department of Energy, Oak Ridge, TN, USA.

Meisen, A., Shuai, X., 1997. Research and development issues in CO_2 capture. Energy Conversion and Management 38, S37-S42.

Mondal, A., Barooah, M., Mandal, B., 2015. Effect of single and blended amine carriers on CO_2 separation from CO_2/N_2 mixtures using crosslinked thin-film poly(vinyl alcohol) composite membrane. International Journal of Greenhouse Gas Control 39, 27-38.

Muraleedharan, R., Mondal, A., Mandal, B., 2012. Absorption of carbon dioxide into aqueous blends of 2-amino-2-hydroxymethyl-1,3-propanediol and monoethanolamine. Separation and Purification Technology 94, 92-96.

Paul, S., 2008. Absorption of CO_2 by single and blended amine solvents in various gas–liquid contactors. PhD Dissertation. Indian Institute of Technology Guwahati, India.

Paul, S., Ghoshal, A.K., Mandal, B., 2007. Removal of CO_2 by single and blended aqueous alkanolamine solvents in hollow-fiber membrane contactor: modeling and simulation. Industrial & Engineering Chemistry Research 46, 2576-2588.

Paul, S., Ghoshal, A.K., Mandal, B., 2009a. Kinetics of absorption of carbon dioxide into aqueous solution of 2-(1-piperazinyl)-ethylamine. Chemical Engineering Science 64, 313-321.

Paul, S., Ghoshal, A.K., Mandal, B., 2009b. Kinetics of absorption of carbon dioxide into aqueous solutions of 2-amino-2-hydroxymethyl-1,3-propanediol. Separation and Purification Technology 68, 422-427.

Pei, Z., Yao, S.H.I., Jianwen, W.E.I., Wei, Z., Qing, Y.E., 2008. Regeneration of 2-amino-2-methyl-1-propanol used for carbon dioxide absorption. Journal of Environmental Sciences 20, 39-44.

Puxty, G., Rowland, R., 2011. Modeling CO_2 mass transfer in amine mixtures: PZ-AMP and PZ-MDEA. Environmental Science & Technology 45, 2398-2405.

Ramachandran, N., Aboudheir, A., Idem, R., Tontiwachwuthikul, P., 2006. Kinetics of the absorption of CO_2 into mixed aqueous loaded solutions of monoethanolamine and methyldiethanolamine. Industrial & Engineering Chemistry Research 45, 2608-2616.

Richner, G., Puxty, G., Carnal, A., Conway, W., Maeder, M., Pearson, P., 2015. Thermokinetic properties and performance evaluation of benzylamine-based solvents for CO_2 capture. Chemical Engineering Journal 264, 230-240.

Rinker, E.B., Ashour, S.S., Sandal, O.C., 1996. Kinetics and modeling of carbon dioxide absorption into aqueous solutions of diethanolamine. Industrial & Engineering Chemistry Research 35, 1107-1114.

Sada, E., Kumazawa, H., Butt, M.A., 1976. Gas absorption with consecutive chemical reaction: Absorption of carbon dioxide into aqueous amine solutions. The Canadian Journal of Chemical Engineering 54, 421-424.

Sada, E., Kumazawa, H., Han, Z.Q., Matsuyama, H., 1985. Chemical kinetics of the reaction of carbon dioxide with ethanolamines in nonaqueous solvents. AIChE Journal 31, 1297-1303.

Saha, A.K., 1994. Absorption of carbon dioxide into aqueous solutions of 2-amino-2-methyl-1-propanol, PhD Dissertation. Indian Institute of Technology Kharagpur, India.

Saha, A.K., Biswas, A.K., Bandyopadhyay, S.S., 1999. Absorption of CO_2 in a sterically hindered amine: modeling absorption in a mechanically agitated contactor. Separation and Purification Technology 15, 101-112.

Sartori, G., Savage, D.W., 1983. Sterically hindered amines for carbon dioxide removal from gases. Industrial & Engineering Chemistry Fundamentals 22, 239-249.

Sema, T., Edali, M., Naami, A., Idem, R., Tontiwachwuthikul, P., 2012. Solubility and diffusivity of N_2O in aqueous 4-(diethylamino)-2-butanol solutions for use in postcombustion CO_2 capture. Industrial & Engineering Chemistry Research 51, 925-930.

Sharma, M.M., 1965. Kinetics of reactions of carbonyl sulphide and carbon dioxide with amines and catalysis by Bronsted bases of the hydrolysis of COS. Transactions of the Faraday Society 61, 681-688.

Vaidya, P.D., Kenig, E.Y., 2007. Absorption of CO_2 into aqueous blends of alkanolamines prepared from renewable resources. Chemical Engineering Science 62, 7344-7350.

Versteeg, G.F., van Swaaij, W.P.M., 1988. Solubility and diffusivity of acid gases (carbon dioxide, nitrous oxide) in aqueous alkanolamine solutions. Journal of Chemical & Engineering Data 33, 29-34.

Versteeg, G.F., Oyevaar, M.H., 1989. The reaction between CO_2 and diethanolamine at 298 K. Chemical Engineering Science 44, 1264-1268.

Versteeg, G.F., Kuipers, J.A.M., Beckum, F.P.H.V., van Swaaij, W.P.M., 1990. Mass transfer with complex reversible chemical reactions. II: Parallel reversible chemical reactions. Chemical Engineering Science 45, 183-197.

Wang, H.M., Li, M.H., 2004. Kinetics of absorption of carbon dioxide into aqueous solutions of 2-amino-2-methyl-1-propanol + diethanolamine. Journal of Chemical Engineering of Japan 37, 267-278.

Wu, C., Cheng, H., Liu, R., Wang, Q., Hao, Y., Yu, Y., Zhao, F., 2010. Synthesis of urea derivatives from amines and CO_2 in the absence of catalyst and solvent. Green Chemistry 12, 1811-1816.

Xiao, J., Li, C.-W., Li, M.-H., 2000. Kinetics of absorption of carbon dioxide into aqueous solutions of 2-amino-2-methyl-1-propanol+monoethanolamine. Chemical Engineering Science 55, 161-175.

Xu, S., Wang, Y.-W., Otto, F.D., Mather, A.E., 1996. Kinetics of the reaction of carbon dioxide with 2-amino-2-methyl-1-propanol solutions. Chemical Engineering Science 51, 841-850.

Zoghi, A.T., Feyzi, F., Zarrinpashneh, S., 2012. Experimental investigation on the effect of addition of amine activators to aqueous solutions of N-methyldiethanolamine on the rate of carbon dioxide absorption. International Journal of Greenhouse Gas Control 7, 12-19.

CHAPTER 2

CHEMISTRY AND THEORY OF MASS TRANSFER WITH CHEMICAL REACTION FOR ABSORPTION OF CO_2 IN ALKANOLAMINES

This chapter presents a discussion of the chemistry involved in the absorption of CO_2 into aqueous alkanolamine solutions. The chemical reactions, rate expressions and an overview of possible reaction mechanisms are presented in this chapter. This chapter also elaborates the basic theory of mass transfer with chemical reaction which applied to heterogeneous reaction system relevant to this study.

2.1 INTRODUCTION

Removal of CO_2 to a very low level is very often done by regenerative absorption using chemical solvents which involve chemical reactions between CO_2 and amines. With very slow reactions, the overall mass transfer rate is not appreciably increased because the dissolved molecules apparently migrate well into the body of the liquid before reaction occurs. Whereas with the very rapid reactions, dissolved molecules migrate only a very short distance before reaction occurs. And in between i.e., moderately fast and fast

reactions provides different absorption kinetics. Hence to determine the overall absorption kinetics, the types of chemical reactions involved and the reaction regimes are very important. The reaction between CO_2 and alkanolamine are not fully understood yet. However, significant advancement has been made to understand the proper reaction mechanism of CO_2-amine system.

To determine the rate of absorption with chemical reaction in a contactor, the hydrodynamic conditions (such as flow-rate, geometry of packing or plate of absorption column), physical properties of liquid, physicochemical properties of the gas-liquid system (such as solubility's of CO_2 in the absorbent, diffusivities of dissolved gases and reactants in solutions), kinetics of reactions occurring in solution, etc. are taken into accounts. In this perspective, to predict the rate of absorption with chemical reaction numerous theories or hydrodynamic models as for example the film model and various surface renewal models can be effectively used.

2.2 CHEMISTRY FOR CO_2–ALKANOLAMINE SYSTEMS

The amine is classified as a primary, secondary or tertiary amine when one, two or three carbon containing groups are attached to the nitrogen atom, respectively. Now for many applications it is known that the traditional aqueous alkanolamine systems has to be competitive with so called hindered amines. Sterically hindered form of amine (e.g., 2-amino 2-methyl-1-propanol) is referred to as 'a primary amine' where the amino group is attached to a tertiary carbon atom, or 'a secondary amine' where the amino-group is attached to at least one secondary or tertiary carbon atom (Sartori and Savage, 1983). The structure of some important amine and sterically hindered amines for acid-gas treating are represented in Figure 2.1. It is obvious that the development of a reaction mechanism is the prerequisite for the modeling of CO_2 absorption in amine systems.

The reaction between CO_2 and primary, secondary as well as sterically hindered amines are described by two-step zwitterionic mechanism, whereas the reaction between CO_2 and tertiary amines is described by the base-catalyzed hydration of CO_2. The CO_2 reacts in aqueous amine systems to form either bicarbonate or carbamate.

2.2.1 Zwitterion mechanism

The zwitterionic mechanism was first proposed by Caplow (1968) and later reintroduced by Danckwerts (1979). In this mechanism, CO_2 forms a bond to the amine functional group in the first step. An amine-proton is transferred to a second molecule is the second step. The second molecule can be any base-molecule but in Caplow's article the second molecule was water. Here the reaction intermediate species is a zwitterion. Caplow (1968) assumed that before the amine reacts with the CO_2 molecule a hydrogen bond is formed in between the amine and a water molecule. However, Danckwerts (1979), Versteeg et al. (1996) and Kumar et al. (2003) omitted this feature in the later published literature. So, the reaction of CO_2 with amine (here denoted as Amn) proceeds through the formation of a zwitterion as an intermediate:

$$CO_2 + Amn \underset{k_{-1}}{\overset{k_2}{\rightleftharpoons}} Amn^+COO^- \tag{2.1}$$

This zwitterion undergoes deprotonation by a base (or bases) b, thereby carbamate formation occurs:

$$Amn^+COO^- + b \xrightarrow{k_b} AmnCOO^- + bH^+ \tag{2.2}$$

Here, an amine, OH^- or H_2O can be the base (b). However, the contribution of OH^- can be neglected because its concentration is very low compared with those of amine and H_2O (Xu et al., 1996).

The rate of reaction of CO_2 in aqueous solutions using the steady-state principle to an intermediate zwitterion can be given as follows:

$$r = \frac{k_2[CO_2][Amn]}{1 + \frac{1}{\left(k_b / k_{-1}\right)[b]}} \tag{2.3}$$

For the above equation two asymptotic situations exist.

i. The term $(k_{-1} \ll k_b[b])$. When zwitterion deprotonation reaction is fast in comparison with the reversion rate of CO_2 and rate determining step is zwitterion formation, the kinetics rate expression becomes second order kinetics as given below:

$$r = k_2[CO_2][Amn] \tag{2.4}$$

ii. The term $(k_{-1} \gg k_b[b])$. When zwitterion deprotonation is rate-determining, the more complex expressions for the kinetics is as follows:

$$r = \frac{k_2[CO_2][Amn]\left(k_b[b]\right)}{k_{-1}} \tag{2.5}$$

This expression suggest that the overall reaction order is three if the contribution of water towards the deprotonation of the zwitterion is negligible. Here, the reaction order changes in the transition region (between the two asymptotic cases) from two to three. The overall

reaction is of the second order with respect to amine when the contribution of amine to zwitterion deprotonation is much more significant than that of other bases i.e., H_2O and OH^-. The kinetics of the reaction between CO_2 and monoethanolamine (MEA) has been extensively studied and adequately explained by zwitterionic mechanism (Versteeg et al., 1996; Mahajani et al., 1988; Mimura et al., 1998). The reaction is of the first order with respect to both CO_2 and MEA in aqueous systems which indicates zwitterion deprotonation is instantaneous. Versteeg et al. (1996) outlined previous studies on the absorption of CO_2 by an aqueous diglycolamine (DGA) solution and suggest that the overall reaction order has a value of two. One of the most popular secondary category of alkanolamine used for CO_2 removal is diethanolamine (DEA), was reviewed earlier (Rinker et al., 1996), which exhibits complex kinetic behavior. The reaction order with respect to DEA lies between one and two, depending on the rate-limiting step (zwitterion formation or deprotonation) and the amine concentration. Camacho et al. (2005) studied another secondary category of alkanolamine used for CO_2 removal is diisopropanolamine (DIPA). The reaction was determined to be of the second order with respect to DIPA, and hence, overall of the third order.

If the base (b), in the reaction described by Eq. (2.2) is the amine itself, the carbamate formation can be expressed as:

$$Amn^+COO^- + Amn \rightarrow AmnCOO^- + AmnH^+ \tag{2.6}$$

Following the case, the overall reaction, which includes for carbamate formation in a solution, is expressed by the sum of reactions represented by Eqs. (2.1) and (2.6):

$$CO_2 + 2Amn \rightleftharpoons Amn\,COO^- + AmnH^+ \tag{2.7}$$

In case of sterically hindered amine, the zwitterion reacts more easily with water than with Amn and bicarbonate formation occurred:

$$Amn^{+}COO^{-} + H_2O \rightarrow HCO_3^{-} + AmnH^{+} \quad (2.8)$$

The overall bicarbonate formation reaction is expressed by the sum of reactions represented by Eqs. (2.1) and (2.8):

$$CO_2 + Amn + H_2O \rightleftharpoons HCO_3^{-} + AmnH^{+} \quad (2.9)$$

The carbamates of sterically hindered amines may also readily undergo hydrolysis, forming bicarbonates and releasing free amine molecules due to its low stability. Thus it can be given by:

$$AmnCOO^{-} + H_2O \rightarrow HCO_3^{-} + Amn \quad (2.10)$$

Again these free amine molecules will react with CO_2. Therefore, bicarbonate ions will be present in larger amounts than carbamate ions. However, at high pressures a certain amount of carbamate hydrolysis (reaction (2.10)) take place with all amines. The carbamate stability constants (Sartori et al., 1987) for aqueous MEA, DEA and AMP have been determined by ^{13}C NMR at 313 K. These are represented in Table 2.1. From the values of K_c presented in Table 2.1, the substantial differences in carbamate stability of hindered amine with conventional amines are observed.

2.2.2 Termolecular mechanism

Crooks and Donnellan (1989) originally proposed termolecular mechanism and recently revisited by da Silva and Svendsen (2004) is widely accepted reaction mechanism for CO_2 and tertiary amines reaction. This mechanism involved the simultaneous bonding of amine with CO_2 and proton transfer to a base, b (Figure 2.2). A single step reaction takes place in this mechanism by forming a loosely-bound encounter complex as the intermediate. This can be given as follows:

$$CO_2 + Amn \cdots b \rightleftharpoons AmnCOO^- \cdots bH^+ \tag{2.11}$$

The reactant molecules i.e., CO_2 and amine again appear via breaking down of intermediate complex, while ionic product was formed by small fraction of intermediate reacts with a second molecule of the amine or a water molecule. The forward reaction rate for this mechanism is represented as:

$$r = k_{ov}[CO_2] \tag{2.12}$$

where k_{ov} is represented as

$$k_{ov} = \left[k^*_{OH^-}[OH^-] + k_{Amn}[Amn]\right][Amn] \tag{2.13}$$

The Eq. (2.12) can describe fractional and higher-order kinetics (da Silva and Svendsen, 2004) similar to that of the limiting case of the zwitterion mechanism, which is represented by Eq. (2.5).

2.2.3 Base-catalyzed hydration mechanism

The tertiary alkanolamines (here R_3N) as suggested by Donaldson and Nguyen (1980) can not react directly with CO_2. A base-catalytic effect was observed in these type of amines on the hydration of CO_2. This can be presented as follows:

$$CO_2 + R_3N + H_2O \xrightarrow{k_{2,R_3N}} R_3NH^+ + HCO_3^- \tag{2.14}$$

In aqueous solutions, an amine dissociation reaction may also take place:

$$R_3N + H_2O \rightleftharpoons R_3NH^+ + OH^- \tag{2.15}$$

Jørgensen and Faurholt (1954) reported that a direct reaction between CO_2 and tertiary amines may stand up at high pH, therefore resulting in monoalkylcarbonate formation. Although, the rate of this reaction can be neglected at pH values lower than 12 (Benitez-Garciaet al., 1991). The sum of the reaction rates of bicarbonate formation and the rate given by Eq. (2.14) is accounted for the total rate of all CO_2 reactions in an aqueous solution. Thus the equation is presented as follows:

$$r_{ov} = \left[k^*_{OH^-}\left[OH^-\right] + k_{2,R_3N}[R_3N]\right]\left[CO_2\right] = k_{ov}\left[CO_2\right] \tag{2.16}$$

Where, k_{ov} is given by:

$$k_{ov} = \left[k^*_{OH^-}\left[OH^-\right] + k_{2,R_3N}[R_3N]\right] \tag{2.17}$$

and k_{app} by:

$$k_{app} = k_{2,R_3N}[R_3N] \tag{2.18}$$

The base-catalysis reaction which is earlier proposed by Yu et al. (1985) could also be described through a zwitterion-type mechanism.

$$CO_2 + R_3N \rightleftharpoons R_3N^+COO^- \tag{2.19}$$

$$R_3N^+COO^- + H_2O \rightarrow R_3NH^+ + HCO_3^- \tag{2.20}$$

Here, a reaction of the amine with CO_2 to form an unstable complex is presented by Eq. (2.19). The homogeneous hydrolysis reaction where water reacts with the zwitterion-type complex to form bicarbonate is explained through Eq. (2.20).

2.2.4 Alcohol-group bonding with CO_2

Alcohol-group bonding of CO_2 is occurred at very high pH values where CO_2 can make bond with alcohol groups (Jørgensen and Faurholt, 1954). The carbamate formation (Figure 2.3) is the analogous form of this mechanism. This type of reaction is not recognised to play a significant role in industrial CO_2 absorption processes because pH of the solution is low (Versteeg et al., 1996).

2.2.5 Molecules with multiple amine functionalities

Solvents being considered for CO_2 absorption having more than one amine functionality is common now a days. Molecules such as piperazine (PZ), 2-(1-piperazinl)-ethylamine (PZEA), aminoethylethanolamine (AEEA) have multiple amine functionalities. Similar nature of such molecules as in simpler amines was observed for the multiple functional groups containing amines. Therefore, the form of interactions between

CO_2 and amine is also likely to be the same. However, the huge number of species can be formed in the case of multiple amine functionalities.

In the present study, the primary and secondary amines reaction with CO_2 has been explained by zwitterionic mechanism as it is widely accepted reaction mechanism due to its versatility. In many primary and secondary amines reaction with CO_2 fall shifting reaction orders in which the overall reaction order changes between 2 and 3, can be covered by zwitterion mechanism (Ramachandran et al., 2006). Whereas the fractional reaction orders with respect to alkanolamine can't cover by termolecular mechanism (Rinker et al., 1996). In this study, the base-catalyzed hydration of CO_2 has been described for the reaction between CO_2 and tertiary alkanolamine.

2.3 THEORY OF MASS TRANSFER WITH CHEMICAL REACTION

Gas absorption through simultaneous mass transfer with chemical reaction has two different effects on the overall behaviour of the system. The first one is given as: Component A is absorbed into the liquid phase emphasized that it is consumed by the chemical reactions and, thus, its concentration in the bulk of the liquid ($[A_o]$) is kept low. Thus, the driving force for additional absorption remains higher than it would be if there is no chemical reaction. The rate of enhancement may vary largely due to significant increase in mass transfer coefficient which is up to two orders of magnitude or even more.

The rate enhancement concept was stated above and it would be formalized as follows. When there is no chemical reactions, the rate of absorption in the liquid phase is presented by

$$R_A a = k_L a([A^*] - [A_o]) \tag{2.21}$$

The actual rate in which chemical reactions are occurred may be larger than the value given by Eq. (2.21) and a "chemical" mass transfer coefficient, k_{LR}, can be presented as bellow:

$$R_A a = k_{LR} a([A^*] - [A_o]) \tag{2.22}$$

The rate enhancement factor, E_A, is defined as the ratio of the actual rate and the rate which would be observed in the absence of chemical reactions under the same driving force. Therefore,

$$E_A = \frac{k_{LR} a([A^*] - [A_o])}{k_L a([A^*] - [A_o])} = \frac{k_{LR}}{k_L} \tag{2.23}$$

As we know, the exact nature of the hydrodynamics at a free gas-liquid interface cannot be determined, we must make the assumption for the proposed behaviour of the absorption and reaction processes. The form of the well-known film, penetration and surface renewal theories are accounts for these simplified assumptions.

2.3.1 Mass transfer models

The film theory (Lewis and Whitman, 1924) which is the oldest mass transfer theory, stated that a stagnant film of liquid rests at the gas-liquid interface, and mass transfer by molecular diffusion through this stagnant film of thickness δ occurs from gas to the liquid phase only. The composition is uniform below this film due to turbulence. By nature, film theory is a steady-state theory and at a gas-liquid interface to determine concentration profiles in the boundary layer, the solution of ordinary differential equations is essential. A steady state concentration profile (falls from [A*] at its surface to $[A_o]$ at its inner edge), beyond which the composition of the liquid is assumed to be homogeneous, prevails across

the film. Depending on the boundary condition of a fixed driving force ([A*] - [A_o]) and steady state condition, integration of the diffusion equation form the following expression for the flux rate, R_A:

$$R_A = \frac{D_A([A^*]-[A_o])}{\delta} = k_L([\mathrm{A}^*]-[\mathrm{A_o}]) \tag{2.24}$$

Thus, film theory suggests that

$$k_L = \frac{D_A}{\delta} \tag{2.25}$$

The parameter δ is accounted for the hydrodynamic properties of the system, which depends on the geometry, physical properties, liquid agitation, etc.

The Penetration theory proposed by Higbie (1935) considers as more realistic alternative to film theory. According to Higbie (1935) the liquid surface to be composed of tiny liquid elements. These elements rise from the surface to the bulk of the liquid and vice-versa by the motion of liquid phase. The period of time these element remain at the interface is called as the contact time. Danckwerts (1951) studied that the time of contact is not the same for all elements and hence improved the assumption that time of contact provided by a distribution of times. So surface renewal theory is introduced by him and the fraction of surface renewed per unit time is the characterized by this theory. In general, more tractable analytical solutions for the absorption rate are provided by surface renewal theory whereas penetration theory is faster to solve numerically. Both the theories are known as unsteady-state theories and hence the solution of partial differential equations are required to explain these theories.

The Penetration theory assumes that all the liquid elements have equal period of exposure time, say t, to the gas. While the liquid element is at the interface and is exposed

to the gas, it absorbs equal amount Q of gas per unit area as though it were quiescent and infinitely deep. Therefore, Q/t, is the average rate of absorption and this is also the rate of absorption (R_A) per unit area averaged over the interface in a representative region of a steady-state absorption system in which the bulk composition is statistically uniform. The hydrodynamic properties of the system are used to determine the exposure-time t and it is the only parameter essential to account for their effect on the transfer coefficient k_L.

The relation between t and k_L for physical absorption is derived as given bellow.

$$R_A = \frac{Q}{t} = \frac{1}{t}\int_0^{\infty} -D_{\mathrm{A}} \left.\frac{\partial[\mathrm{A}]}{\partial x}\right|_{x=0} \mathrm{dt} = 2\sqrt{\frac{D_{\mathrm{A}}}{\pi t}}([\mathrm{A}]-[\mathrm{A_o}]) \tag{2.26}$$

Which implies

$$k_L = 2\sqrt{\frac{D_A}{\pi t}} \tag{2.27}$$

The Danckwerts surface renewal model (Danckwerts, 1951) instead supposes that the chance of liquid element of interface being replaced with fresh liquid element is independent of period of time in which it has been exposed. This phenomena indicates to a stationary distribution of surface 'ages' in which the fraction of the surface at any given instant has been exposed to the surface for times between t and (t + dt) is se^{-st}dt. The fraction of the area of surface, which is replaced with fresh liquid in unit time is denoted by s. Therefore, the instantaneous rate of physical absorption per unit area of surface (R_A) that has been exposed for time t is given by

$$R_A = ([\mathrm{A}^*]-[\mathrm{A_o}])\sqrt{\frac{D_A}{\pi t}} \tag{2.28}$$

then the value of R_A averaged over all elements of the surface having ages between 0 and ∞ is

$$R_A = s\int_0^{\infty} R_A e^{-st}\,\mathrm{dt} \tag{2.29}$$

$$= ([\mathrm{A}^*]-[\mathrm{A_o}])\, s\sqrt{\frac{D_A}{\pi}}\int_0^{\infty}\frac{e^{-st}}{\sqrt{t}}\mathrm{dt} \tag{2.30}$$

$$= ([\mathrm{A}^*]-[\mathrm{A_o}])\sqrt{(D_A s)} \tag{2.31}$$

or

$$k_L = \sqrt{(D_A s)} \tag{2.32}$$

Like the penetration theory, the surface renewal theory also a square root dependence of mass transfer coefficient on the diffusivity of the solute and in a few situations this has been verified somewhat satisfactorily. Also, the surface renewal theory is a better representation of an absorption process. Apart from above discussed theories, various other theories such as the film penetration theory of Toor and Marchello (1958) and the boundary layer theory of Vieth et al. (1963) have also been proposed for the mass transfer processes.

In this study the film theory is used to analyse the experimental results. When time taken to establish concentration gradient is very small compared with the time of transfer (Coulson and Richardson, 1999), then this theory can be applied. The reactions between CO_2 and amines are fast reaction and therefore the concentration gradient in the liquid phase develops very fast and it confines within a very thin film. In such scenario, the film model and the various versions of the surface-renewal models provides almost the same quantitative predictions (Danckwerts and Kennedy, 1954; Danckwerts et al., 1963).

2.3.2 Effect of chemical reaction on absorption

When gas phase is comes in contact with liquid phase to achieve the separation of components in a gas mixture then liquid phase can selectively absorb either the desired component or the diluent. In general both the rate of mass transfer and the capacity of the liquid for the gas are increased when the liquid contains a constituent which can reacts with the dissolving gas.

Hatta (1928) for the first time modified the film concept of mass transfer to include simple simultaneous chemical reaction. Each reaction is characterized by its kinetic order, degree of reversibility and the relative rates of the diffusional and chemical reaction. Therefore, the absorption of CO_2 into caustic solution by Hatta's (1928) early investigation pertained to a reaction kinetics of second order, irreversible and infinitely rapid compared to the diffusional rates involved. A number of cases for reversible first order and second order chemical reactions in the stagnant film is considered by Olander (1960) whereas Danckwerts (1970) considered a number of reactants in solution to consequently generalize the solution of his model. In the case of chemical absorption of a gas in an agitated liquid, Lightfoot (1958) and Bird et al. (1960) provided the expression for the rate of mass transfer. They assumed the film theory to be valid in this case. Assuming the validity of the penetration and surface renewal theories, effect of liquid phase chemical reaction on the rate of absorption of gas has been studied. The solution for the rate of absorption accompanied by first order chemical reaction is obtained by Danckwerts (1951). The case of instantaneous chemical reaction of the absorbed gas with a dissolved solute is also considered by Danckwerts (1970). The film and penetration theory solutions for gas absorption escorted by a two-step second order chemical reaction including a transient

intermediate species is studied by Brian and Beaverstock (1965). The two theories were found to agree within 6% for the case of equal diffusivities of the reactants.

In many cases, different hydrodynamic models applied towards the theoretical predictions for the effect of chemical reaction on the rate of absorption of a gas are in close agreement. When the diffusion coefficients of all the reacting species are equal, then this agreement is remarkable. Even when the physical systems depart considerably from the idealized models, the insensitivity of the theoretical predictions to the fluid-mechanical models adopted recommends that these will be good approximations of the actual rates of absorption.

2.4 LABORATORY GAS-LIQUID CONTACTORS

In chemical process industries, gas-liquid contactors are frequently encountered. A gas phase come in contact with liquid phase into these contactors and mass transfer between the liquid and the gas phase occurred. Sometime, the mass transfer is accompanied by the simultaneous occurrence of a chemical reaction. To design a gas-liquid contactors, a good knowledge of the behaviour of gas-liquid contactors is necessary.

A number of configurations exist in gas-liquid contactors. Mass transfer can occur from the gas phase to the liquid phase or vies versa. Chemical reactions may take place in the gas and/or in the liquid phase, respectively. The various mixing patterns of gas and liquid phases includes plug flow, well stirred, plug flow with axial dispersion, etc.

It has been reported that measuring the rates of absorption and discerning the controlling mechanism, previous workers are used various model contactors. They may be collected under two categories. In one category the hydrodynamics is well established and these include the wetted wall column, the laminar jet apparatus, the wetted sphere column, and the like. In the other category the hydrodynamics is not well established and these

involve the stirred cell, the stirred contactor and the mechanically agitated contactor. Apart from the mechanically agitated contactor, both the categories have known interfacial area for mass transfer. Danckwerts (1970) and Doraiswamy and Sharma (1984) explained the details of these type of contactors.

A jet of liquid in case of the laminar jet absorber and a film of liquid in the case of a wetted wall column moves continuously through the gas, to which it is exposed for a known length of time. The contact time for these absorption range from a few seconds to 10^{-3} s or lower. A jet of liquid in case of laminar jet apparatus enters the gas space through a circular hole, and leaves through a slightly larger hole. We can conveniently vary the concentration of A as well as of B. In case of the jet apparatus, the contact time is uniquely determined by the jet length and diameter and the liquid flow rate, and is independent of the viscosity and the density of the liquid. This is an important advantage of this apparatus. The contact time of this apparatus can be varied over a range of (0.001 – 0.1) s.

The liquid flows in the form of a film under the influence of gravity down a surface which is usually a vertical tube or rod in the wetted wall column. The concentration of both A and B can be varied easily. Due care should be taken either to eliminate the gas phase resistance to mass transfer or evaluate it by adopting an appropriate method when an inert gas is used to vary partial pressure of A. By changing the absorption length or the liquid-flow rate or both, the contact time in a wetted wall column can be varied in the range of (0.1 – 2) s.

A cross shaped stirrer with vertical flat blades just skims the surface of the liquid are the main features of a stirred cell. This type of arrangement provides higher values of k_L than are obtainable when the blades are completely immersed. The area of the flat liquid surface minus the area occupied by the stirrer blades is the known gas-liquid interfacial area of the stirred cell. Here by changing the total pressure of the system the concentration of A in the stirred cell can be varied. However in some scenario, it may be possible by

using an inert gas to change the partial pressure of A and hence the concentration of A. The concentration range of B should be such that the viscosity of the liquid does not change significantly. As we know normal stirrer speed of 20 to 150 rpm resist the vortex formation and hence the agitation speed should be varied accordingly under such conditions. Here the volume of the liquid per unit transfer area can also be conveniently varied without significantly affecting the value of k_L at least by a factor of 2. Although using an inert diluent for the solute gas, the gas side resistance (in many cases) cannot be eliminated conveniently in a stirred cell.

In the present experimental work, a model laboratory contactor i.e., wetted wall column is used for the specific rate of absorption of CO_2 into a novel alkanolamine solvents.

NOTATIONS

A gas phase species

Amn amine

a gas-liquid mass interfacial area per unit volume of contactor or dispersion, $m^2\ m^{-3}$

A^* concentration of A in the gas-liquid interface, kmol m^{-3}

A_0 concentration of A in the bulk liquid phase, kmol m^{-3}

b base

D diffusivity, $m^2\ s^{-1}$

E_A enhancement factor

Ha Hatta number

k_{-1} backward rate constant in Eq. (2.1), s^{-1}

k_2 second order forward reaction rate constant, $m^3\ mol^{-1}\ s^{-1}$

k_{Amn} reaction rate constant in Eq. (2.13), $m^6\ kmol^{-2}\ s^{-1}$

k_{ov} observed overall reaction rate constant, s^{-1}

k_b reaction rate constant for base b in Eq. (2.5), $m^3\ kmol^{-1}\ s^{-1}$

k_L liquid side mass transfer coefficient in absence of reaction, $m\ s^{-1}$

k_{LR} liquid side mass transfer coefficient in presence of reaction, m s-1

$k^*_{OH^-}$ reaction rate constant for CO_2 hydration, $m^3\ kmol^{-1}\ s^{-1}$

k_{app} apparent reaction rate constant, s^{-1}

Q amount of gas per unit area, $kmol\ m^{-2}$

r reaction rate, $kmol\ m^{-3}\ s^{-1}$

S fractional rate of surface-renewal, s^{-1}

R_3N tertiary alkanolamine

R_A specific rate of absorption of species A, $kmol\ m^{-2}\ s^{-1}$

[ ] concentration, $kmol\ m^{-3}$

Greek letters

α loading of CO_2 in amine, kmol of CO_2 per kmol of amine

δ thickness of diffusion film (liquid) in the film theory of mass transfer, m

t contact time, s

Subscripts

b base for zwitterions deprotonation

i gas-liquid interface

L liquid

ov overall reaction rate

REFERENCES

Benitez-Garcia, J., Ruiz-Ibanez, G., Al-Ghawas, H.A., Sandal, O.C., 1991. On the effect of basicity on the kinetics of CO_2 absorption in tertiary amines. Chemical Engineering Science 46, 2927-2931.

Bird, R.B., 1960. Stewart, WE, and Lightfoot, EN. Transport Phenomena, 655.

Brian, P., Beaverstock, M., 1965. Gas absorption accompanied by a two-step chemical reaction. Chemical Engineering Science 20, 47-56.

Camacho, F., Sánchez, S., Pacheco, R., Sánchez, A., La Rubia, M.D., 2005. Absorption of carbon dioxide at high partial pressures in aqueous solutions of di-isopropanolamine. Industrial & Engineering Chemistry Research 44, 7451-7457.

Caplow, M., 1968. Kinetics of carbamate formation and breakdown. Journal of the American Chemical Society 90, 6795-6803.

Coulson, J., Richardson, J., 1999. Chemical engineering, Vol. 1, RK Butterworth. Heinemann, Oxford.

Crooks, J.E., Donnellan, J.P., 1989. Kinetics and mechanism of the reaction between carbon dioxide and amines in aqueous solution. Journal of the Chemical Society, Perkin Transactions 2, 331-333.

da Silva, E.F., Svendsen, H.F., 2004. Ab initio study of the reaction of carbamate formation from CO_2 and alkanolamines. Industrial & Engineering Chemistry Research 43, 3413-3418.

Danckwerts, P., 1951. Significance of liquid-film coefficients in gas absorption. Industrial & Engineering Chemistry 43, 1460-1467.

Danckwerts, P., 1970. Gas-Liquid Reactions. McGraw-Hill Chemical Engineering Series.

Danckwerts, P., 1979. The reaction of CO_2 with ethanolamines. Chemical Engineering Science 34, 443-446.

Danckwerts, P., Kennedy, A., 1997. Kinetics of liquid-film process in gas absorption. Part I: Models of the absorption process. Chemical Engineering Research and Design 75, S101-S104.

Danckwerts, P., Kennedy, A., 1954. Kinetics of liquid-film process in gas absorption. part 1: models of the absorption process. Transactions of the Institution of Chemical Engineers 32, S49 – S53.

Donaldson, T.L., Nguyen, Y.N., 1980. Carbon dioxide reaction kinetics and transport in aqueous amine membranes. Industrial & Engineering Chemistry Fundamentals 19, 260-266.

Doraiswamy, L.K., Sharma, M.M., 1984. Heterogeneous reactions: analysis, examples and reactor design. vol. 2, Fluid-fluid-solid Reactions. Wiley.

Hatta, S., 1928. Absorption velocity of gases by liquids. I. absorption of carbon dioxide by potassium hydroxide solution. Technology Reports of the Tohoku Imperial University, 8, 1 – 25.

Higbie, R., 1935. The rate of absorption of a pure gas into a still liquid during short periods of exposure. Trans. AIChE 31, 365-389.

Jorgensen, E., Faurholt, C., 1954. Reactions between carbon dioxide and amino alcohols. 2. triethanolamine. Acta Chemica Scandinavica 8, 1141-1144.

Kumar, P., Hogendoorn, J., Versteeg, G., Feron, P., 2003. Kinetics of the reaction of CO_2 with aqueous potassium salt of taurine and glycine. AIChE Journal 49, 203-213.

Lewis, W., Whitman, W., 1924. Principles of gas absorption. Industrial & Engineering Chemistry 16, 1215-1220.

Lightfoot, E., 1958. Steady state absorption of a sparingly soluble gas in an agitated tank with simultaneous irreversible first-order reaction. AIChE Journal 4, 499-500.

Mahajani, V., Joshi, J., 1988. Kinetics of reactions between carbon dioxide and alkanolamines. Gas Separation & Purification 2, 50-64.

Mimura, T., Suda, T., Iwaki, I., Honda, A., Kumazawa, H., 1998. Kinetics of reaction between carbon dioxide and sterically hindered amines for carbon dioxide recovery from power plant flue gases. Chemical Engineering Communications 170, 245-260.

Olander, D.R., 1960. Simultaneous mass transfer and equilibrium chemical reaction. AIChE Journal 6, 233-239.

Ramachandran, N., Aboudheir, A., Idem, R., Tontiwachwuthikul, P., 2006. Kinetics of the absorption of CO_2 into mixed aqueous loaded solutions of monoethanolamine and methyldiethanolamine. Industrial & Engineering Chemistry Research 45, 2608-2616.

Rinker, E.B., Ashour, S.S., Sandall, O.C., 1996. Kinetics and modeling of carbon dioxide absorption into aqueous solutions of diethanolamine. Industrial & Engineering Chemistry Research 35, 1107-1114.

Sartori, G., Savage, D.W., 1983. Sterically hindered amines for CO_2 removal from gases. Industrial & Engineering Chemistry Fundamentals 22, 239 – 249.

Sartori, G., Ho, W., Savage, D., Chludzinski, G., Wlechert, S., 1987. Sterically-hindered amines for acid-gas absorption. Separation and Purification Methods 16, 171-200.

Toor, H., Marchello, J., 1958. Film-penetration model for mass and heat transfer. AIChE Journal 4, 97-101.

Versteeg, G., Van Dijck, L., van Swaaij, W.P.M., 1996. On the kinetics between CO_2 and alkanolamines both in aqueous and non-aqueous solutions. An overview. Chemical Engineering Communications 144, 113-158.

Vieth, W., Porter, J., Sherwood, T., 1963. Mass transfer and chemical reaction in a turbulent boundary layer. Industrial & Engineering Chemistry Fundamentals 2, 1-3.

Xu, S., Wang, Y.-W., Otto, F.D., Mather, A.E., 1996. Kinetics of the reaction of carbon dioxide with 2-amino-2-methyl-1-propanol solutions. Chemical Engineering Science 51, 841-850.

Yu, W.-C., Astarita, G., Savage, D., 1985. Kinetics of carbon dioxide absorption in solutions of methyldiethanolamine. Chemical Engineering Science 40, 1585-1590.

Table 2.1

Carbamate stability constants for conventional and hindered amines by ^{13}C NMR (da Silva et al., 2004)

$k_C = \frac{[\text{AmnCOO}^-]}{[\text{HCO}_3^-][\text{AmnH}]}$	
Amine	K_C at 313 K (m^3 $kmol^{-1}$)
MEA	12.5
DEA	2
AMP	<0.1

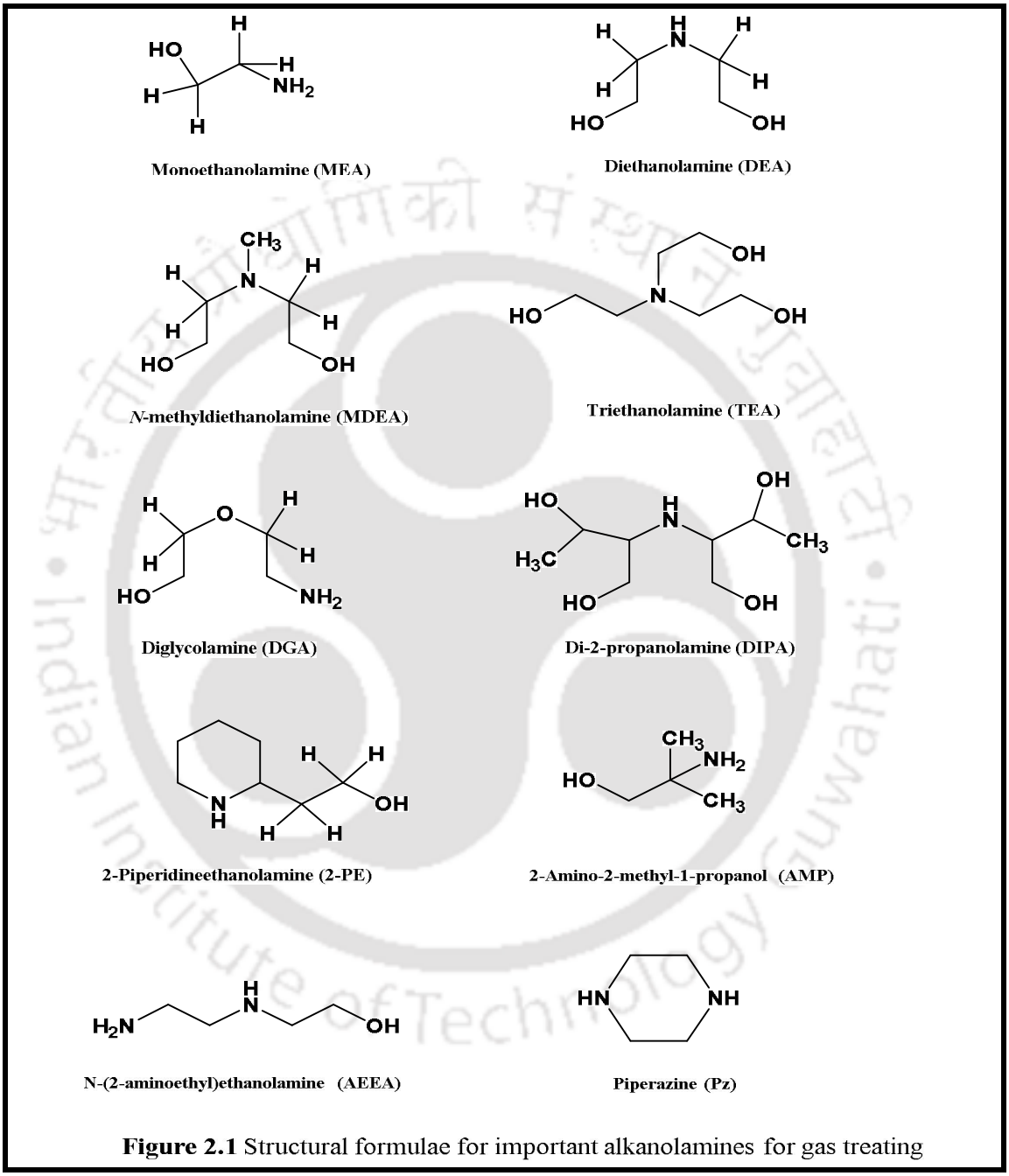

Figure 2.1 Structural formulae for important alkanolamines for gas treating

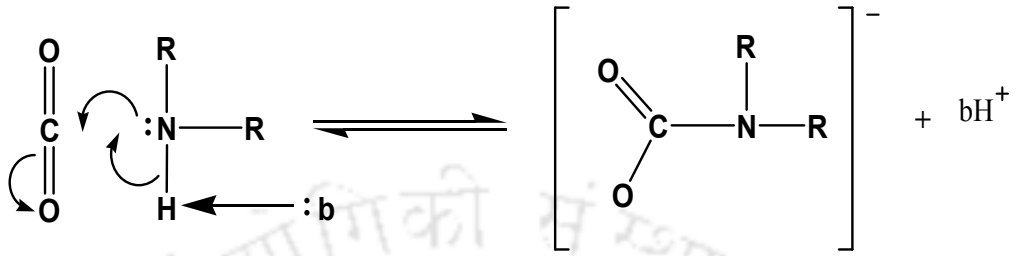

Figure 2.2 Formation of carbamate by termolecular mechanism

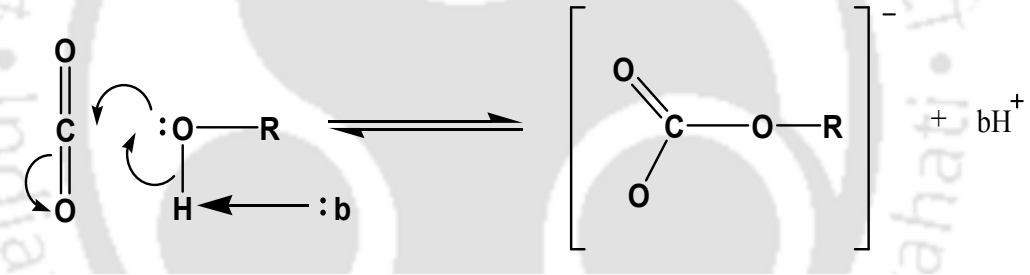

Figure 2.3 Alcohol bonding with CO_2

CHAPTER 3

PHYSICOCHEMICAL PROPERTIES OF CO_2–AMINE SYSTEMS

This chapter presents a discussion about the experimental and theoretical study of physicochemical properties of CO_2 and the novel aqueous alkanolamine solvents. Literature review specific to the physicochemical properties that include density and viscosity of the novel solvents and the diffusivity and physical solubility of CO_2 into the novel solvents are also elaborated in this chapter. These properties are unique for each novel solvent and they are dependent on solution composition and/or temperature. The effect of thermodynamic properties on liquid-liquid interaction of aqueous blend solvents are discussed and assessed. The diffusion coefficients and physical solubilities of N_2O in the novel solvents have been experimentally measured and the diffusivities and physical solubilities of CO_2 in these solvents have been estimated by "N_2O-analogy".

3.1 INTRODUCTION

Several physicochemical properties are necessary for the rational design of gas treatment units and operation of absorption and desorption columns as well as these data are basic requirements to finding the mass transfer coefficient by using mass transfer rate modeling (Paul et al., 2010). For the operation of equipment involved in

the processes, such as pumps and heat exchangers in a gas-treatment unit, information of the physicochemical properties of process solutions are essential. These important physicochemical properties include density, viscosity, Henry's law constant and diffusivity of CO_2 in the aqueous amine solutions. The 10% discrepancy in the measurement of CO_2 solubility may lead to 20% inconsistency in reaction kinetics constant because the kinetic rate constant varies with square of Henry's law constant. Besides mass transfer rate modeling, solubility data of CO_2 is also used in thermodynamic modeling to calculate real activity coefficient (Aronu et al., 2012). For the mass-transfer-rate modeling of absorbers and regenerators, solution density and viscosity are also important parameters because these parameters influence the values of liquid side mass transfer coefficient, k_L. The physicochemical properties are essential to analyse the kinetics data for absorption of CO_2 into aqueous alkanolamine which is presented in Chapter 4. In addition, different models were exploited to correlate the experimental data in the entire range of temperature and concentration.

Physical solubility and diffusivity of CO_2 are not possible to be measured directly due to the chemical reactions between CO_2 and amine solution (Paul et al., 2010; Das et al., 2017[a]). To overcome the above problem "N_2O analogy", proposed by Clarke (1964) was used to estimate the solubility and diffusivity of CO_2 using N_2O because of similar properties like electronic structure, configuration, molecular weight, molar volume, and it is a nonreactive gas in amine solvents (Aronu et al., 2012). Thus, solubility and diffusivity of N_2O in amine solutions were measured experimentally and the solubility and diffusivity of CO_2 was determined in aqueous amine solutions by using N_2O analogy as shown below

$$H_{CO_2\text{-Amn}} = \left(\frac{H_{CO_2\text{-}H_2O}}{H_{N_2O\text{-}H_2O}} \right) H_{N_2O\text{-Amn}} \tag{3.1}$$

[a] Das, B., Deogam, B., Agrawal, Y and Mandal, B., 2016. Measurement and correlation of the physicochemical properties of novel aqueous bis(3-aminopropyl)amine and its blend with n-methyldiethanolamine for CO_2 capture. Journal of Chemical & Engineering Data 61, 2226-2235.

where, $H_{CO_2-water}$ and H_{CO_2-Amn} are measured and estimated Henry's law constants of CO_2 in H_2O and amine solutions, respectively. $H_{N_2O-water}$ and H_{N_2O-Amn} are measured Henry's law constants of N_2O in H_2O and amine solutions, respectively.

$$D_{CO_2\text{-}Amn} = \left(\frac{D_{CO_2\text{-}H_2O}}{D_{N_2O\text{-}H_2O}} \right) D_{N_2O\text{-}Amn} \tag{3.2}$$

where, $D_{CO_2-water}$ and D_{CO_2-Amn} are the measured and the estimated diffusivities of CO_2 in water and amine solutions, respectively. $D_{N_2O-water}$ and D_{N_2O-Amn} are the measured diffusivities of N_2O in water and amine solutions, respectively.

3.2 LITERATURE REVIEW

3.2.1 Density and viscosity

The density and viscosity data for aqueous single amine solvents such as (PZ + H_2O) (Derks et al., 2005; Sun et al., 2005; Samanta and Bandyopadhyay, 2006), (AEPD + H_2O) (Yoon et al., 2002b), (AMPD + H_2O) (Yoon et al., 2003; Baek et al., 2000), (MEA + H_2O) (Li and Shen, 1992; Li and Lie, 1994; Song et al., 1996), (DEA + H_2O) (Rinker et al., 1994; Hsu and Li, 1997a, 1997b), (MDEA + H_2O) (Al-Ghawas et al., 1989; Hagewiesche et al., 1995; Li and Shen, 1992; Li and Lie, 1994; Rinker et al., 1994; Maham et al., 1995) (AMP + H_2O) (Hagewiesche et al., 1995; Li and Lie, 1994) [34, 46], (2-PE + H_2O) (Xu et al., 1992; Shen et al., 1991) have been reported in the literature. The density and viscosity data for some aqueous blended amine solvents such as (PZ + AMP + H_2O) (Derks et al., 2005; Sun et al., 2005; Samanta and Bandyopadhyay, 2006), (PZ + MDEA + H_2O) (Derks et al., 2008), (MEA + MDEA + H_2O) (Hagewiesche et al., 1995; Li and Shen, 1992; Li and Lie, 1994; Mandal et al.,

2003), (MEA + AMP + H_2O) (Li and Lie, 1994; Mandal et al., 2003), (DEA + MDEA + H_2O) (Rinker et al., 1994; Hsu and Li, 1997a,1997b; Mandal et al., 2003; Teng et al., 1994), (DEA + AMP + H_2O) (Hsu and Li, 1997a, 1997b; Mandal et al., 2003), (MEA + TEA + H_2O) (Horng et al., 2002) and (MEA + 2-PE + H_2O) (Hsu and Li, 1997a,1997b) have been reported in the literature. The studied temperature ranges for the measurement of density and viscosity by different researchers and the details concentration ranges for different single and blended alkanolamine solutions are given in Tables II.1- II.4 of Appendix II.

In the present work, the density and viscosity of aqueous solutions of (0.10 to 1.10) kmol·m^3 APA, aqueous blend of (0 to 1.1) kmol·m^3 APA and (1.9 to 2.9) kmol·m^3 MDEA, and aqueous blend of (0 to 1.1) kmol·m^3 APA and (1.9 to 2.9) kmol·m^3 AMP solutions were measured at atmospheric pressure and over the temperature range of 298–323 K. At the same time different models were exploited to correlate the experimental data in the entire range of temperature and concentration. The importance of thermodynamic properties of new amine based solvent such as (AMP+APA) on both technical (thermodynamic model) and economical considerations (Wong et al., 2016) are assessed and the role of these on ternary liquid mixture are discussed. Several models were introduced in our work to implement the measured density and viscosity data. Uncertainty analysis was carried out with a 95% level of confidence to interpret all the measured density and viscosity data.

3.2.2 Physical solubility and diffusivity

To estimate the solubility and diffusivity of CO_2 in various amine solutions, the concept of "N_2O analogy" has been used by almost all the researchers in this area such as Versteeg and van Swaaij (1988), Sada et al. (1977, 1978), Al-Ghawas et al. (1989), Haimour (1990), Xu et al. (1991, 1992), Tsai et al. (2000), Ko et al. (2001), Saha et al. (1993), and Mandal et al. (2004, 2005). The solubility of N_2O and CO_2 in aqueous

solutions of organic alcohols that are non-reacting with respect to both solutes have been investigated by Laddha et al. (1981). Their study demonstrate that the solubilities of CO_2 and N_2O in the different solutions have a constant ratio of 1.37. According to them if the temperature change from 288 K to 303 K, the ratio of solubilities in water has been changed by within 2% of 1.37.

In general, the value of $\left(\frac{H_{N_2O\text{-}H_2O}}{H_{CO_2\text{-}H_2O}}\right)$ in Eqs. (3.1) is 1.37. However, it is desirable to find the value of this for better accuracy of the estimated solubility of CO_2 at the particular temperature at which the CO_2 solubility is required to be estimated. In this study, this value has been obtained to be 1.32 at 303 K.

The "N_2O analogy" considered by Al-Ghawas et al. (1989), Sada et al. (1977, 1978) and Haimour and Al (1984) are suggested to estimate the diffusivity of CO_2 using this analogy. From the measurements in aqueous alcohol solutions, Diaz et al. (1988) have proved this analogy. Xu et al. (1991) and Saha et al. (1993) have deliberated that it is preferred to use the N_2O analogy to estimate the diffusivity of CO_2 in aqueous AMP rather than to estimate it using the Stokes-Einstein relation. Also, the analogue was not a general relation suggested by Versteeg and van Swaaij (1988) and to calculate the diffusivity of CO_2 in amine solutions they reported a modified Stokes-Einstein relation.

The solubility and diffusivity data of N_2O in aqueous amine solutions (for the binary and ternary systems) were reported extensively in the literature, such as (PZ + H_2O) (Derks et al., 2005; Sun et al., 2005; Samanta et al., 2007); (AEPD + H_2O) (Yoon et al., 2002b); (AMPD + H_2O) (Yoon et al., 2003); (MEA + H_2O) (Clarke et al., 1964; Little et al., 1992; Li and Lai, 1995); (DEA + H_2O) (Versteeg et al., 1988; Sada et al., 1977; Haimour, 1990; Versteeg et al., 1989; Li and Lee, 1996); (AMP + H_2O) (Xu et al., 1991; Saha et al., 1993; Little et al., 1992; Bosch et al., 1990); (MDEA + H_2O) (Versteeg et al., 1988; Al-Ghawas et al., 1989; Haimour et al., 1984; Ko and Li, 2000); (2-PE + H_2O) (Xu et al., 1992; Xu et al., 1993); (MEA + AMP + H_2O) (Mandal et al., 2005; Li and Lai, 1995; Xiao et al., 2000); (MEA + MDEA + H_2O) (Mandal et al.,

2005; Li and Lai, 1995; Hagewiesche et al., 1995; Liao and Li, 2002); (DEA + AMP + H_2O) (Mandal et al., 2004; Li and Lee, 1996; Wang et al., 2004); (DEA + MDEA + H_2O) (Mandal et al., 2004; Li and Lee, 1996; Rinker et al., 1995); (MEA + TEA + H_2O) (Horng et al., 2002); (PZ + MDEA + H_2O) (Samanta et al., 2007) and (PZ + AMP + H_2O) (Sun et al., 2005). The studied temperature ranges for the measurement of solubility and diffusivity of N_2O by different researchers and the details concentration ranges for different single and blended alkanolamine solutions are given in Tables II.4-II.7 of Appendix II.

In this study, the solubility and diffusivity of N_2O into aqueous solutions of (0.10 to 1.10) kmol·m^3 APA, aqueous blend of (0 to 1.1) kmol·m^3 APA and (1.9 to 2.9) kmol·m^3 MDEA, and aqueous blend of (0 to 1.1) kmol·m^3 APA and (1.9 to 2.9) kmol·m^3 AMP solutions were measured at atmospheric pressure and over the temperature range of 298–323 K. Based on these results the estimated solubilities and diffusivities of CO_2 in the aqueous amine solutions were calculated using the N_2O analogy.

3.3 EXPERIMENTAL

3.3.1 Materials

Reagent-grade APA (98% purity) and MDEA (98% purity) were procured from Sigma-Aldrich (USA). AMP (97% purity) was purchased from E. Merck (Germany). Assam Air Products (India) provided zero grade N_2O gas for measurement of diffusivity and solubility. These chemicals used without any further purification. In the present study, water purification has been done by a Millipore water purification system whose conductivity and surface tension were 1 $\times 10^{-7}$ Ω^{-1}cm^{-1} and 72 mN·m^{-1} (at 298 K), respectively. Water de–gassing was carried out through the prolonged boiling followed by cooling to an ambient temperature under the vacuum, and then used for preparing amine solutions. To clarify the strength of amine solutions, titration against

standard HCl using an autotitrator (DL-50, Mettler Toledo, Switzerland) was conducted. The uncertainty of the concentration measurement of amine solutions was within 0.01 %.

3.3.2 Apparatus and procedure

3.3.2.1 Density and viscosity measurement

A $34.73 \cdot 10^{-6}$ m^3 Pyrex pycnometer (Sigma Aldrich) was used for the density measurement of the aqueous amine solutions in the temperature T = (298 to 323) K. The pycnometer along with the amine solution was immersed in a constant temperature bath where a circulating temperature controller (RW 2025G, Jeio Tech) was used to control the desired temperature. The approximate uncertainty of bath temperature was 0.25 K. After reaching the desired temperature of a constant temperature bath, the pycnometer along with the amine solution was weighed with an analytical balance (BSA 224S-CW). A minimum of three experiments were done before reporting every density data. The combined expanded uncertainty in the experimental measured density was estimated to be 4.17 $kg \cdot m^{-3}$, 4.41 $kg \cdot m^{-3}$ and 3.97 $kg.m^{-3}$ for APA, (APA + MDEA) and (APA+AMP) solutions, respectively.

For the viscosity measurement of the amine solutions, an Ostwald viscometer (Model: 11619/01, Stanhope-seta, UK) was used. The viscometer along with the amine solution was immersed in a thermostatic bath where a circulating temperature controller, similar to density measurement, was used to control the desired temperature. Each reported value was the average of three measurements. For the viscosity measurement, the combined expanded uncertainty was estimated to be 0.0153 mPa·s, 0.068 mPa·s and 0.058 mPa·s for aqueous APA, (APA + MDEA) and (APA + AMP) solutions, respectively.

3.3.2.2 Physical solubility measurement

The physical solubility experiment was performed in a corning glass equilibrium cell which was similar to one used by Paul et al. (2010) with the volume of $6.5 \cdot 10^{-4}$ m^3. Amount of N_2O absorbed at equilibrium inside a closed vessel of the known volume of liquid with gas at constant temperature and atmospheric pressure was used to determine solubility (Henry's law constants) of N_2O. For quickly attaining equilibrium, a magnetic stirrer was used for enhancing the liquid phase mass transfer and two four-bladed impellers mounted on a shaft were used for enhancing the gas phase mass transfer driven by DC motor. The temperature and pressure of the equilibrium cell were controlled with a circulating temperature controller operated on external control mode (RW 2025G, Jeio Tech) and precise U-tube manometric device with an adjustable limb, respectively. The schematic of the experimental set-up is shown in Figure 3.1. Here the uncertainty of the temperature measurement was 0.25 K.

For every solubility measurement, the attainment of thermal equilibrium inside the equilibrium cell was allowed to reach the desired temperature. Then purging was done with desired gas. To ensure uniform gas phase concentration throughout the cell, gas phase stirrer was run at 70 rpm during purging. The temperature of the gas stream was maintained by passing the gas through water vapor saturator. Then the cell was sealed after filling 10 ml of a freshly prepared aqueous amine solution of known concentration and the stirrer was turned on to commence absorption. The attainment of equilibrium was considered once there was no change in volume of absorption for at least 1 hour. Equilibrium was established within 5 to 6 hours. To maintain atmospheric pressure in the equilibrium cell throughout the experiment, a precise manomatric device was employed. The difference between the initial and final level of the cell side limb (precise U-tube manometric device) was the absorbed amount of N_2O. The value of vapor pressure of the solution was taken to correct the partial pressure of N_2O in the cell.

The calculation for Henry's law constant was done as described by our group elsewhere (Paul et al., 2009b). The combined expanded uncertainties in the determining Henry's law constant for N_2O were estimated to be 66.2 $kPa \cdot m^3 \cdot kmol^{-1}$, 66.0 $kPa \cdot m^3 \cdot kmol^{-1}$ and 66.5 $kPa.m^3.kmol^{-1}$ for aqueous APA, (APA+MDEA) and (APA+AMP) solutions, respectively. The reproducibility between the different experiments at the same condition was within ± 1.0 %.

3.3.2.3 Diffusivity measurement

The diffusivity of N_2O in aqueous amine solutions was performed using a stainless steel wetted wall column absorber whose outer diameter $2.81 \cdot 10^{-2}$ m. The apparatus and procedure were the same for measuring the diffusivity as described by Paul et al. (2010). The height of the absorption column during the experiment was kept at $7 \cdot 10^{-2}$ m. The volume uptake method was adopted to measure the rate of absorption of gas with the help of a soap film meter. A calibrated rotameter was used to measure the flow rate of liquid. During every experiment absorption chamber reached the thermal equilibrium at the desired temperature by using a circulator temperature controller (RW 2025G, Jeio Tech) with uncertainty 0.25 K. The pressure inside the absorption chamber was nearly 100 kPa. The combined expanded uncertainties in the experimental diffusivity measurement were estimated to be $35.1 \cdot 10^{-12}$ $m^2 \cdot s^{-1}$, $18.2 \cdot 10^{-12}$ $m^2 \cdot s^{-1}$ and 19.3×10^{-12} $m^2.s^{-1}$ for aqueous APA, (APA+MDEA) and (APA+AMP) solutions, respectively. Among the various diffusivity experiments at the same condition, the repeatability was within ± 1.0 %.

3.4 RESULTS AND DISCUSSION

3.4.1 Density and viscosity

Experimentally measured values of density as well as viscosity of pure MDEA and its aqueous solutions at various temperatures were exploited for validation of pycnometer, the viscometer and the experimental procedure of the measurements. These values were compared with data reported by Al-Ghawas et al. (1989) as shown in Tables 3.1 and 3.2. There was an excellent agreement with the average absolute deviations (AAD) for density and viscosity were 0.06% and 0.79%, respectively. The average absolute deviation was calculated by the following equation (Shaikh et al., 2013).

$$\%\text{AAD} = \frac{1}{n}\sum_{i=1}^{n}\left|\frac{X_{\text{exptl,i}} - X_{\text{calcd,i}}}{X_{\text{exptl,i}}}\right|.100 \tag{3.3}$$

The density and viscosity of pure APA were experimentally measured, correlated, and these are presented in Tables 3.3 and 3.4. The obtained densities and viscosities of aqueous APA and (APA+MDEA) solutions are given in Tables 3.5 – 3.6, respectively. For binary (APA+H_2O) and ternary (APA+MDEA+H_2O) solutions, both densities and viscosities decreased with increasing temperature whereas with increasing molar concentration of APA in both the solutions densities decreased and viscosities increased. Also, for ternary (APA + AMP + H_2O) solutions, both densities and viscosities decreased with increasing temperature while both densities and viscosities increased with increasing APA concentration in the blend (Tables 3.8 and 3.9). The experimental data of densities were correlated using Redlich–Kister equation (Paul and Mandal., 2006; Idris et al., 2015) for binary and ternary solutions as shown in Eq. (3.4).

$$V_{jk}^{E}/\mathrm{m}^3\cdot\mathrm{kmol}^{-1} = x_j x_k \sum_{i=0}^{n} A_i \left(x_j - x_k\right)^i \tag{3.4}$$

$$A_i = a + b\left(T/\mathrm{K}\right) + c\left(T/\mathrm{K}\right)^2 \tag{3.5}$$

where A_i is pair parameters and these are function of temperature as shown in Eq. (3.5). The excess volume (V^E) of binary system is V_{12}^E and for the ternary system, it is the sum of V_{12}^E, V_{23}^E and V_{13}^E were calculated by Eq. (3.6). The molar volumes (V_m) of the solutions were calculated by Eq. (3.7).

$$V^E = V_m - \sum x_i V_i^0 \tag{3.6}$$

$$V_m = \frac{\sum x_i M_i}{\rho_m} \tag{3.7}$$

where V_i^0 and M_i are the molar volume and molar mass of pure components at the system temperature. ρ_m is the measured liquid density and x_i is the mole fraction of the pure fluid i. In this density measurement, the computed values using Redlich–Kister equation deviates (AAD) from experimental values of (APA+H_2O), (APA+MDEA+H_2O) and (APA+AMP+H_2O) solutions by 0.08 %, 0.16 % and 0.12%, respectively. The parameters of Eq. (3.4) are presented in Tables 3.10 – 3.12.

Total excess volume, V^E, in case of (APA+AMP+H_2O) solutions varies with the change of mole fraction of APA (x_1) as shown in Figure 3.2. In the studied composition and the entire temperature range, the values of V^E are negative. These V^E describes the physical, structural and chemical contribution of the components between the molecules upon mixing. The dispersion of forces or weak dipole-dipole interaction accounts for physical contribution, which leads to positive contribution of V^E. The structural contribution of different size molecule present in mixture provides geometrical effect to fit each other's structure, which leads to negative contribution of

V^E. Lastly, the chemical contribution while V^E are negative involves formation of hydrogen bonding, the specific interaction, formation of charge transfer complex, other complex forming interactions and strong dipole-dipole interaction among the components (Kumar et al., 2012; Kassim et al., 2016). This study indicates that the packing effect and the intermolecular interaction (hydrogen bond) are exists in the mixture. While V^E are negative a contraction of volume occurred by strong intermolecular interaction in the system upon mixing. The AAD of this system is 0.12 % for 42 data points. The values of V^E are given in Table 3.13. Here, a correlation developed by Hsu and Li (1997) was used to calculate the density of pure AMP.

The thermal expansion coefficient (α), of the blend was estimated from the experimentally measured density values according to the Eq. (3.8) (Geppert-Rybczynska et al., 2014)

$$\alpha = -\frac{1}{\rho_m}\left(\frac{\delta\rho_m}{\delta T}\right)_p \tag{3.8}$$

where, ρ_m , T and p are the measured liquid density, temperature, and pressure, respectively. The values of thermal expansion coefficient (α) are incorporated in Table 3.13. Figure 3.3 demonstrate the values of α against APA concentration at various temperatures. It was observed that the values of α were all positive. The values of α for (APA+AMP+H_2O) increases with increasing APA concentration indicating the further expansion in the volume with the addition of more APA in the blend. The values of α of the blend increases with increase in the temperature demonstrating higher expansivities for the mixtures.

The experimental data of viscosities were also correlated using Redlich–Kister equation (Paul and Mandal, 2006) for the binary solutions taking kinematic viscosity as a variable. The modified viscosity deviation expression (Paul and Mandal, 2006) is given in Eqs. (3.9) and (3.10).

$$\delta\nu / 10^{-3}\mathrm{m}^2 \cdot \mathrm{s}^{-1} = \ln \nu_m - \sum_{i=1}^{n} x_i \ln \nu_i \tag{3.9}$$

$$\delta\nu_{12} / 10^{-3}\mathrm{m}^2 \cdot \mathrm{s}^{-1} = x_1 x_2 \sum_{i=0}^{n} A_i \left(x_1 - x_2\right)^i \tag{3.10}$$

$$A_i = a + \frac{b}{\left(T / \mathrm{K}\right) + c} \tag{3.11}$$

where υ (η/ρ) is the kinematic viscosity, η is the viscosity, ρ is the density, A_i are pair parameters and are a function of temperature as shown in Eq. (3.11). In this binary viscosity measurement, the correlated values using Eq. (3.10) are in excellent agreement with the experimental data where AAD value was 1.42%. The regressed parameters from Eq. (3.10) are given in Table 3.10. Grunberg and Nissan model (Paul and Mandal, 2006) was used to correlate viscosity data of ternary solutions as shown below.

$$\ln(\eta / \mathrm{mPa.s}) = \sum x_i \ln \eta_i + \sum \sum x_i x_j G_{ij} \tag{3.12}$$

$$G_{ij} = a + b(T / \mathrm{K}) + c(T / \mathrm{K})^2 \tag{3.13}$$

where, G_{ij} in Eq. (3.12) are function of temperature as shown in Eq (3.13). The viscosity data of pure AMP are taken from Mandal et al. (2003). The deviation of correlated values from experimental data of (APA+MDEA+H_2O) and (APA+AMP+H_2O) were reasonable with AAD of 2.28% and 2.23% and the parameters are presented in Table 3.14.

In this studied (APA+AMP+H_2O) system, the viscosity deviation ($\Delta\eta$) of the blend was calculated from the experimental value of viscosity and viscosity of pure components values using the Eq. (3.14) (Qian et al., 2012)

$$\Delta\eta = \eta_m - (x_1\eta_1 + x_2\eta_2 + x_3\eta_3) \quad (3.14)$$

where x_1, x_2 and x_3 are the mole fraction of components 1, 2 and 3, respectively while η_m, η_1, η_2 and η_3 are the viscosity values of the mixture and components 1, 2 and 3, respectively.

The calculated values of viscosity deviation ($\Delta\eta$) are given in Table 3.13. Figure 3.4 demonstrate the values of $\Delta\eta$ against APA mole fraction at different temperatures. It was observed that the values of $\Delta\eta$ increased with increasing temperature at constant concentration prompting to the positive value of $\Delta\eta$. Vogel and Weiss (1982) expressed that different components present in a blend system with strong interaction show positive viscosity deviation. The dipole interaction amongst AMP and H_2O is less at low temperature. The interaction between the molecules of the system increases when APA was introduced in the system and temperature was increased. The values of $\Delta\eta$ increases with the increment in both the temperature and mole fraction of APA, expressing that dipole interaction between the molecules in the system is more prominent at higher temperature and increases with the mole fraction of APA in the mixture. The negative $\Delta\eta$ values indicates that interaction amongst AMP and H_2O is weak which becomes stronger with the addition of APA in the mixture. The values of $\Delta\eta$ tends to increase on an account of the increase of viscosity in the blend with the introduction of APA in the blend. Thus, overall it is described that at low APA concentration and low temperature the dipole association is less prevailing which increases with the temperature and APA concentration.

Eyring equation Eq. (3.15) (Aguila-Hernandez et al., 2008) has been used to calculate the activation molar enthalpy (ΔH), molar entropy (ΔS) and the Gibbs free energy (ΔG) of the ternary blends using experimental viscosity data,

$$\eta = \left(\frac{h'N_A}{V_m}\right)\exp\left(\frac{-\Delta S}{R}\right)\exp\left(\frac{\Delta H}{RT}\right) \tag{3.15}$$

where, h', N_A, V_m, ΔS, ΔH, R, and T are Planck constant, Avogadro's constant, the molar volume, molar entropy, molar enthalpy, the gas constant and the temperature, respectively. A rearrangement of Eq. (3.15) can be done according to Eq. (3.16) as a linear equation of $R\ln\left(\eta V_m / h'N_A\right)$ against $1/T$ in which the slope and the intercept were estimated for ΔH and ΔS values, respectively.

$$R\ln\left(\frac{\eta V_m}{h'N_A}\right) = \frac{\Delta H}{T} - \Delta S \tag{3.16}$$

From the obtained values of ΔH and ΔS, molar Gibbs free energy (ΔG) can be calculated at a particular temperature according to Eq. (3.17),

$$\Delta G = \Delta H - T\Delta S \tag{3.17}$$

Based on the experimental viscosity as a function of concentration, the estimated values of ΔH and ΔS from Eq. (3.17) for entire temperature range and ΔG at T = 298 K are incorporated in Table 3.15. It was observed from the Table 3.15 that the values of ΔH were positive in the blend which indicate strong interaction in the molecule (Kumar et al., 2012) while the values of ΔH were greater than $T\Delta S$. These observation suggests that the contribution of enthalpy to the change of molar Gibbs free energy was more predominant than entropy.

3.4.2 Physical solubility

The experimental values of solubility of N_2O (in terms of Henry's constant) in aqueous APA, (APA+MDEA) and (APA+AMP) solutions at T = (298 to 323) K and

various concentrations of APA are tabulated in Tables 3.16 – 3.18. The measured values of solubility of pure APA and correlation parameters are presented in Tables 3.3 and 3.4. To validate the experimental method and data for solubility measurement, we considered the solubility measurements of CO_2 and N_2O in water at T =(298 to 323) K and compared the values with the literature data reported by different authors (Al-Ghawas et al., 1989; Paul et al., 2009a; Mandal et al., 2005; Li and Lai., 1995) as shown in Figures 3.5 and 3.6. It demonstrates that the experimental data were in good agreement with the literature data.

It was elucidated from the experimental results that Henry's constant (H_{N_2O}) of both in aqueous APA and (APA+MDEA) solutions increased with increasing temperature as well as increasing APA concentration in amine solutions. As observed from the Table 3.18, Henry's constant (H_{N_2O}) of aqueous (APA+AMP) solutions increased with increase in temperature. This is may be due to the exothermic nature of the gas absorption. However, Henry's constant decreased with increasing APA concentration in ternary solutions may be due to larger affinity of APA towards N_2O. To correlate experimental solubility data at various temperature and composition, several models were applied in literature such as the semiemperical model (Sema et al., 2012; Wang et al., 1992), Arrhenius type equation (Paul et al., 2010) and polynomial model (Wang et al., 1992). In this study, the experimental data of the solubility of N_2O in amine solutions were also correlated by different models as presented in the following sections.

3.4.2.1 Semiempirical model

A semi-empirical model was used to correlate excess Henry's constant (R') shown in Eq. (3.18), that is a function of the volume fraction and the temperature as shown in Eqs. (3.19) and (3.20).

$$R' = \ln(H_{\mathrm{N_2O\text{-}Solution}}) - \sum_{i=1}^{n} \varphi_i \ln(H_i) \tag{3.18}$$

$$R' = \frac{1}{2}\sum_{i=1}^{n}\sum_{i\neq j=1}^{n} \alpha_{ij}\varphi_i\varphi_j + \varphi_1\varphi_2\varphi_3\alpha_{123} \tag{3.19}$$

$$\alpha_{ij} = k_1 + k_2 T + k_3 T^2 + k_4 \varphi_j \tag{3.20}$$

where φ_i is the volume fraction of amines and water, α_{123} is a constant of three body interaction parameter, and k_1, k_2, k_3 and k_4 are constants for two body interaction parameter. An attempt was made to validate the constants of Eq. (3.20) for MDEA and water solutions by the solubility data obtained from Mandal et al. (2004) and determined value of AAD was 0.82% whereas the authors reported value was 0.81%. The values of Henry's constant of pure AMP and an aqueous solution of AMP were obtained from Wang et al. (1992) and Mandal et al. (2005), respectively, to calculate the excess property. The values of AAD for the aqueous APA, (APA+MDEA) and (APA+AMP) solutions were 7.03%, 0.65% and 0.95%, respectively. So predicted results from this model do not correlate well with the experimental results for the binary system but gave good estimation for ternary solutions. The values of parameters are given in Table 3.19, for aqueous APA, (APA+MDEA) and (APA+AMP) solutions.

3.4.2.2. Arrhenius type equation

The Arrhenius type equation is suggested to correlate solubility data at various concentrations (molarity) of APA (m_1) and MDEA (m_2), and temperature (T) as follows:

$$H_{\mathrm{N_2O}} \Big/ \mathrm{kPa \cdot m^3 \cdot kmol^{-1}} = \left(a + bm_1 + cm_1^2 + dm_2 + em_2^2 + fm_1m_2\right)\exp\left(-h\Big/\left(T/\mathrm{K}\right)\right) \tag{3.21}$$

In the above equation when the concentration of MDEA is zero then this equation is applicable to binary system of APA and water. The values of constant used are given

in Table 3.20 for binary and ternary solutions, respectively. The values of AAD for APA and (APA+MDEA) solutions were 0.57 % and 0.77 %, respectively.

For aqueous blends of (APA+AMP) solution, the measured solubility of N_2O are also estimated by the Arrhenius type equation as shown below in terms of different APA (m'_1) and AMP (m'_2) concentrations (kmol.m^{-3}) and temperature (T).

$$H_{N_2O} \Big/ \mathrm{kPa \cdot m^3 \cdot kmol^{-1}} = \left(a + bm'_1 + cm'^2_1 + dm'_2 + em'^2_2 + fm'_1 m'_2\right) \exp\left(-h/(T/\mathrm{K})\right) \qquad (3.22)$$

The values of parameters are presented in Tables 3.20 and the values of AAD was 0.38 %.

3.4.2.3. Polynomial model

Polynomial models are proposed to predict solubility of binary solutions as a function of mole fraction of APA (x_1) and ternary solution as a function of the mole fraction of APA (x_1) and MDEA (x_2), and the temperature (T). These are given in Eqs. (3.23) and (3.24), respectively.

$$H_{N_2O} \Big/ \mathrm{kPa \cdot m^3 \cdot kmol^{-1}} = A_1 + A_2 x_1 + A_3 x_1^2 + A_4 (T/\mathrm{K}) + A_5 x_1 (T/\mathrm{K}) + A_6 x_1^2 (T/\mathrm{K}) \qquad (3.23)$$

$$H_{N_2O} \Big/ \mathrm{kPa \cdot m^3 \cdot kmol^{-1}} = A_1 + A_2 x_1 + A_3 x_2^2 + A_4 (T/\mathrm{K}) + A_5 x_1 (T/\mathrm{K}) + A_6 x_2^2 (T/\mathrm{K}) \qquad (3.24)$$

where, A_i is the parameters for binary and ternary solutions. The values of the constant are tabulated in Table 3.21 for binary and ternary solutions. It was observed that the computed values using this model gave good agreement with the experimental results and had AAD of 0.35% and 0.58%, respectively.

The solubility of N_2O into blend aqueous solution of (APA+AMP) as a function of the mole fraction of APA (x'_1), AMP (x'_2), and the temperature (T) can be obtained from the following equation:

$$H_{N_2O}/\text{kPa}\cdot\text{m}^3\cdot\text{kmol}^{-1} = A_1 + A_2 x_1' + A_3 x_2'^2 + A_4 (T/\text{K}) + A_5 x_1' (T/\text{K}) + A_6 x_2'^2 (T/\text{K}) \quad (3.25)$$

The values of parameters are presented in Tables 3.21 and the values of AAD of (APA+AMP) was 0.28 %.

By comparing the experimental values with three predicting models (the semiempirical model, Arrhenius type equation, and polynomial model) for N_2O solubility in aqueous APA, (APA + MDEA) and (APA + AMP) solutions, it was found that the polynomial model led to best fit among the three models.

3.4.3 Diffusivity

The experimental values of diffusivity of N_2O in aqueous APA, (APA+MDEA) and (APA+AMP) solutions at T = (298 to 323) K and various concentrations of APA, MDEA and AMP are presented in Tables 3.22 – 3.24. The diffusivity measurement of CO_2 and N_2O in water were considered, similar to solubility measurement, at T = (298 to 323) K and compared values with the literature data reported by different authors (Al–Ghawas et al., 1989; Paul et al., 2009; Mandal et al., 2005; Li and Lai, 1995; Versteeg et al., 1988) as shown in Figures 3.7 and 3.8. As depicted from these figures, the experimental data were in good agreement with the literature data.

From the investigation of the present experimental data, we observed that D_{N_2O} in aqueous APA, (APA+MDEA) and (APA+AMP) solutions increased with increasing temperature as well as decreased with increasing APA concentration in amine solutions. To correlate experimental diffusivity data at various temperature and composition several models was reported in literature such as the modified Stokes Einstein model (Sema et al., 2012), Arrhenius type equation (Sema et al., 2012) and polynomial model. The experimental data of the diffusivity of N_2O in amine solutions were correlated by different models as follows.

3.4.3.1. Modified Stokes Einstein model

The experimental values of diffusivity of N_2O in aqueous APA and (APA+MDEA) solutions are proposed to correlate by the modified Stokes Einstein model. This model relates the viscosity of solution (η), which is a function of temperature and concentration, to diffusivity of solution (D_{N_2O}) as follows.

$$\frac{(D_{N_2O}/\mathrm{m^2\cdot s^{-1}})\cdot(\eta/\mathrm{mPa\cdot s})^{p}}{(T/\mathrm{K})} = C \tag{3.26}$$

where, p and C are constant parameters. For the binary system, the values of p and C were 1.1255 and $5.3552\cdot10^{-12}$, and for the ternary system, the values of p and C were 0.8087 and $7.6392\cdot10^{-12}$. The AAD values for binary and ternary solutions were 8.48 % and 3.73 %, respectively.

For aqueous solutions of (APA+AMP), modified Stokes Einstein model based on viscosity of the solutions (η) with different temperature and measured diffusivity of N_2O is suggested to estimate the diffusivity of N_2O (D_{N_2O}) as follows:

$$\frac{(D_{N_2O}/\mathrm{m^2\cdot s^{-1}})\cdot(\eta/\mathrm{mPa\cdot s})^{p'}}{(T/\mathrm{K})} = C' \tag{3.27}$$

where p' and C' are constant parameters. For the ternary system, the values of p' and C' were 0.907 and $6.74\cdot10^{-12}$. The AAD value for this model predicted diffusivity of N_2O was 3.05 %.

3.4.3.2. Arrhenius type equation

The Arrhenius type equation for N_2O diffusivity of aqueous APA solutions were used to correlate experimental data at various molar concentration of APA (m_1) and temperature (T) as given in Eq. (3.28). Diffusivity of (APA+MDEA) solutions were correlated as the function of concentration of APA (m_1) and MDEA (m_2), and

temperature as shown in Eq. (3.29). Diffusivity of N_2O (D_{N_2O}) into aqueous (APA+AMP) solutions were also correlated as the function of the molar concentration of APA (m'_1) and AMP (m'_2), and temperature as shown in Eq. (3.30).

$$D_{N_2O}/\mathrm{m^2\cdot s^{-1}} = \left(a + bm_1 + cm_1^2\right)\exp\left((d + hm_1)/(T/\mathrm{K})\right) \tag{3.28}$$

$$D_{N_2O}/\mathrm{m^2\cdot s^{-1}} = \left(a + bm_1 + cm_1^{\,2} + dm_2 + em_2^{\,2} + fm_1m_2\right)\exp\left(-h/(T/\mathrm{K})\right) \tag{3.29}$$

$$D_{N_2O}/\mathrm{m^2\cdot s^{-1}} = \left(a + bm'_1 + cm'^2_1 + dm'_2 + em'^2_2 + fm'_1m'_2\right)\exp\left(-h/(T/\mathrm{K})\right) \tag{3.30}$$

The values of parameter in above Eqs. (3.28), (3.29) and (3.30) are also given in Table 3.25. The values of AAD for aqueous APA, (APA+MDEA) and (APA+AMP) solutions were 4.6 %, 2.98 %, 2.57 %, respectively.

3.4.3.3. Polynomial model

Polynomial models are considered to correlate diffusivity data, for binary solutions as a function of the mole fraction of APA (x_1) and temperature (T), and for ternary solutions as a function of mole fraction of APA (x_1), MDEA (x_2) and temperature (T) are given below

$$\ln\left(D_{N_2O}/\mathrm{m^2\cdot s^{-1}}\right) = A_1 + A_2x_1 + A_3(T/\mathrm{K}) + A_4x_1(T/\mathrm{K}) + A_5x_1(T/\mathrm{K})^2 + A_6x_1^2(T/\mathrm{K})^2 \tag{3.31}$$

$$\ln(D_{N_2O}/\mathrm{m^2\cdot s^{-1}}) = A_1 + A_2x_1 + A_3x_2^2 + A_4(T/\mathrm{K}) + A_5x_1(T/\mathrm{K}) + A_6x_2^2(T/\mathrm{K}) \tag{3.32}$$

Parameters of Eqs. (3.31) and (3.32) are also included in Table 3.26 for both binary and ternary solutions. The values of AAD for aqueous APA and (APA+MDEA) solutions were 1.75% and 2.17%, respectively.

The diffusivity of N_2O for ternary solutions as the function of the mole fraction of APA (x_1'), AMP (x_2'), and temperature (T) is correlated as given below.

$$\ln(D_{N_2O} / \mathrm{m}^2 \cdot \mathrm{s}^{-1}) = A_1 + A_2 x_1' + A_3 x_2'^2 + A_4 (T / \mathrm{K}) + A_5 x_1' (T / \mathrm{K}) + A_6 x_2'^2 (T / \mathrm{K}) \quad (3.33)$$

Parameters of Eq. (3.33) are given in Table 3.26 along with the AAD of 2.44%.

All the model parameters for solubility and diffusivity were obtained using regression performed by Matlab® software (2013). The experimental values with three predicting models (the modified Stokes Einstein model, Arrhenius type equation and polynomial model) for N_2O diffusivity in aqueous APA, (APA+MDEA) and (APA+AMP) solutions were compared. It was observed that polynomial model gave the best fit among the three models.

NOTATIONS

A_i	constant in Eqs. (3.4), (3.10), (3.23), (3.24), (3.25), (3.31), (3.32) and (3.33)
A	constant in Eqs. (3.5), (3.11), (3.13), (3.21), (3.22), (3.28), (3.29) and (3.30)
b	constant in Eqs. (3.5), (3.11), (3.13), (3.21), (3.22), (3.28), (3.29) and (3.30)
c	constant in Eqs. (3.5), (3.11), (3.13), (3.21), (3.22), (3.28), (3.29) and (3.30)
d	constant in Eqs. (3.21), (3.22), (3.28), (3.29) and (3.30)
e	constant in Eqs. (3.21), (3.22), (3.29) and (3.30)
f	constant in Eqs. (3.21), (3.22), (3.29) and (3.30)
h	constant in Eq. (3.21), (3.22), (3.28), (3.29) and (3.30)
x	mole fraction
[ ]	concentration, kmol m^{-3}
AEPD	2-Amino-2-ethyl-1,3-propanediol
AMPD	2-Amino-2-methyl-1,3-propanediol
APA	Bis(3-aminopropyl)amine

MDEA	N-Methyldiethanolamine
T	temperature, K
Pka	the acid dissociation constant
MEA	monoethanolamine
DIPA	di-isopropanolamine
DEA	diethanolamine
DGA	diglycolamine
TEA	triethanolamine
AMP	N-2-amino-2-methyl-l-propanol
PZ	piperazine
2-PE	2-piperidineethanol
AAD	average absolute deviations
V^E	excess volume, $m^3 \cdot kmol^{-1}$
V_m	molar volumes of solution, $m^3 \cdot kmol^{-1}$
V_i^0	molar volume of pure components, $m^3 \cdot kmol^{-1}$
M_i	molar mass of pure components, $kg \cdot kmol^{-1}$
x_i	mole fraction of the pure fluid *i*
H_{N_2O}	Henry constant for solubility, kPa m^3 $kmol^{-1}$
H_i	Henry constant of pure component, kPa m^3 $kmol^{-1}$
R	excess Henry's constant
φ_i	volume fraction of amines and water
α_{ij}	two body interaction parameter

α_{123} three body interaction parameter

D_{N_2O} diffusivity of N_2O, $m^2 \cdot s^{-1}$

H_{CO_2} Henry constant of CO_2, kPa m^3 $kmol^{-1}$

D_{CO_2} Diffusivity of CO_2, $m^2 \cdot s^{-1}$

Greek letters

η viscosity, mPa s

υ kinematic viscosity, $m^2 \cdot s^{-1}$

ρ density, kg m^{-3} or g cm^{-3}

Subscripts

Amn amine

I componet

j componet

k componet

m mixture

REFERENCES

Al-Ghawas, H.A., Hagewiesche, D.P., Ruiz-Ibanez, G., Sandal, O.C., 1989. Physicochemical properties important for carbon dioxide absorption in aqueous methyldiethanolamine. Journal of Chemical & Engineering Data 34, 385-391.

Águila-Hernández, J., Trejo, A., García-Flores, B.E., Molnar, R., 2008. Viscometric and volumetric behaviour of binary mixtures of sulfolane and N-methylpyrrolidone with monoethanolamine and diethanolamine in the range 303–373K. Fluid Phase Equilibria 267, 172-180.

Aronu, U.E., Hartono, A., Svendsen, H.F., 2012. Density, viscosity, and N_2O solubility of aqueous amino acid salt and amine amino acid salt solutions. The Journal of Chemical Thermodynamics 45, 90-99.

Baek, J.I., Yoon, J.H., Eum, H.M., 2000. Physical and thermodynamic properties of aqueous 2-amino-2-methyl-1,3-propanediol solutions. International Journal of Thermophysics 21, 1175-1184.

Bosch, H., Versteeg, G., Van Swaaij, W.P.M., 1990. Kinetics of the reaction of CO_2 with the sterically hindered amine 2-amino-2-methylpropanol at 298 K. Chemical Engineering Science 45, 1167-1173.

Clarke, J., 1964. Kinetics of absorption of cardon dioxide in monoethanolamine solutions at short contact times. Industrial & Engineering Chemistry Fundamentals 3, 239-245.

Derks, P.W., Hamborg, E.S., Hogendoorn, J., Niederer, J.P., Versteeg, G.F., 2008. Densities, viscosities, and liquid diffusivities in aqueous piperazine and aqueous (piperazine + N-methyldiethanolamine) solutions. Journal of Chemical & Engineering Data 53, 1179-1185.

Derks, P.W., Hogendoorn, K.J., Versteeg, G.F., 2005. Solubility of N_2O in and density, viscosity, and surface tension of aqueous piperazine solutions. Journal of Chemical & Engineering Data 50, 1947-1950.

Diaz, J. M., Vega, A., Coca, J., 1988. Diffusivities of carbon dioxide and nitrous oxide in aqueous alcohol solutions. Journal of Chemical & Engineering Data 33, 10 – 12.

Geppert-Rybczyńska, M., Lehmann, J.K., Heintz, A., 2014. Physicochemical properties of two 1-alkyl-1-methylpyrrolidinium bis [(trifluoromethyl) sulfonyl] imide ionic liquids and of binary mixtures of 1-butyl-1-methylpyrrolidinium bis [(trifluoromethyl) sulfonyl] imide with methanol or acetonitrile. The Journal of Chemical Thermodynamics 71, 171-181.

Haimour, N., Sandal, O.C., 1984. Absorption of carbon dioxide into aqueous methyldiethanolamine. Chemical Engineering Science 39, 1791-1796.

Haimour, N.M., 1990. Solubility of nitrous oxide in aqueous solutions of diethanolamine at different temperatures. Journal of Chemical and Engineering Data 35, 177-178.

Hagewiesche, D.P., Ashour, S.S., Sandal, O.C., 1995. Solubility and diffusivity of nitrous oxide in ternary mixtures of water, monoethanolamine and N-Methyldiethanolamine and solution densities and viscosities. Journal of Chemical and Engineering Data 40, 627-629.

Horng, S.-Y., Li, M.-H., 2002. Kinetics of absorption of carbon dioxide into aqueous solutions of monoethanolamine + triethanolamine. Industrial & Engineering Chemistry Research 41, 257-266.

Hsu, C.-H., Li, M.-H., 1997a. Densities of aqueous blended amines. Journal of Chemical & Engineering Data 42, 502-507.

Hsu, C.-H., Li, M.-H., 1997b. Viscosities of aqueous blended amines. Journal of Chemical & Engineering Data 42, 714-720.

Idris, Z., Ang, L., Eimer, D.A., Ying, J., 2015. Density measurements of unloaded and CO_2-loaded 1-dimethylamino-2-propanol at temperatures (298.15 to 353.15) K. Journal of Chemical & Engineering Data 60, 1419-1425.

Kassim, M.A., Sairi, N.A., Yusoff, R., Ramalingam, A., Alias, Y., Aroua, M.K., 2016. Experimental densities and viscosities of binary mixture of 1-butyl-3-methylimidazolium bis (trifluoromethylsulfonyl) imide or glycerol with sulfolane and their molecular interaction by COSMO-RS. Thermochimica Acta 639, 130-147.

Ko, J.-J., Li, M.-H., 2000. Kinetics of absorption of carbon dioxide into solutions of N-methyldiethanolamine + water. Chemical Engineering Science 55, 4139-4147.

Ko, J.-J., Tsai, T.-C., Lin, C.-Y., Wang, H.-M., Li, M.-H., 2001. Diffusivity of nitrous oxide in aqueous alkanolamine solutions. Journal of Chemical & Engineering Data 46, 160-165.

Kumar, D.B.K., Reddy, K.R., Rao, G.S., Rao, G.R., Rambabu, C., 2012. Thermodynamic and spectroscopic study of molecular interactions in the binary liquid mixtures of N-methyl-2-pyrrolidone and some substituted benzenes at different temperatures. Journal of Molecular Liquids 174, 100-111.

Laddha, S., Diaz, J., Danckwerts, P., 1981. The N_2O analogy: the solubilities of CO_2 and N_2O in aqueous solutions of organic compounds. Chemical Engineering Science 36, 228-229.

Li, M.H., Shen, K.P., 1992. Densities and solubilities of solutions of carbon dioxide in water + monoethanolamine + N-methyldiethanolamine. Journal of Chemical and Engineering Data 37, 288-290.

Li, M.-H., Lie, Y.-C., 1994. Densities and viscosities of solutions of monoethanolamine + N-methyldiethanolamine + water and monoethanolamine + 2-amino-2-methyl-1-propanol + water. Journal of Chemical and Engineering Data 39, 444-447.

Li, M.-H., Lai, M.-D., 1995. Solubility and Diffusivity of N_2O and CO_2 in (Monoethanolamine + N-Methyldiethanolamine + Water) and in (Monoethanolamine + 2-Amino-2-methyl-1-propanol + Water). Journal of Chemical and Engineering Data 40, 486-492.

Li, M.-H., Lee, W.-C., 1996. Solubility and diffusivity of N_2O and CO_2 in (Diethanolamine + N-Methyldiethanolamine + Water) and in (Diethanolamine + 2-Amino-2-methyl-1-propanol+ Water). Journal of Chemical & Engineering Data 41, 551-556.

Liao, C.-H., Li, M.-H., 2002. Kinetics of absorption of carbon dioxide into aqueous solutions of monoethanolamine + N-methyldiethanolamine. Chemical Engineering Science 57, 4569-4582.

Littel, R.J., Versteeg, G.F., Van Swaaij, W.P., 1992. Solubility and diffusivity data for the absorption of carbonyl sulfide, carbon dioxide, and nitrous oxide in amine solutions. Journal of Chemical and Engineering Data 37, 49-55.

Mandal, B.P., Kundu, M., Bandyopadhyay, S.S., 2003. Density and viscosity of aqueous solutions of (N-methyldiethanolamine + monoethanolamine), (N-methyldiethanolamine + diethanolamine), (2-amino-2-methyl-1-propanol + monoethanolamine), and (2-amino-2-methyl-1-propanol + diethanolamine). Journal of Chemical & Engineering Data 48, 703-707.

Mandal, B.P., Kundu, M., Padhiyar, N.U., Bandyopadhyay, S.S., 2004. Physical solubility and diffusivity of N_2O and CO_2 into aqueous solutions of (2-amino-2-methyl-1-propanol + diethanolamine) and (N-methyldiethanolamine+ diethanolamine). Journal of Chemical & Engineering Data 49, 264-270.

Mandal, B.P., Kundu, M., Bandyopadhyay, S.S., 2005. Physical solubility and diffusivity of N_2O and CO_2 into aqueous solutions of (2-amino-2-methyl-1-propanol + monoethanolamine) and (N-methyldiethanolamine + monoethanolamine). Journal of Chemical & Engineering Data 50, 352-358.

Maham, Y., Teng, T.T., Mather, A.E., Hepler, L.G., 1995. Volumetric properties of (water+ diethanolamine) systems. Canadian Journal of Chemistry 73, 1514-1519.

Paul, S., Ghoshal, A.K., Mandal, B., 2009a. Kinetics of absorption of carbon dioxide into aqueous solution of 2-(1-piperazinyl)-ethylamine. Chemical Engineering Science 64, 313-321.

Paul, S., Ghoshal, A.K., Mandal, B., 2009b. Physicochemical Properties of Aqueous Solutions of 2-Amino-2-hydroxymethyl-1,3-propanediol. Journal of Chemical & Engineering Data 54, 444-447.

Paul, S., Ghoshal, A.K., Mandal, B., 2010. Physicochemical Properties of Aqueous Solutions of 2-(1-Piperazinyl)-ethylamine. Journal of Chemical & Engineering Data 55, 1359-1363.

Paul, S., Mandal, B., 2006. Density and Viscosity of Aqueous Solutions of 2-Piperidineethanol, (2-Piperidineethanol + Monoethanolamine), and (2-Piperidineethanol + Diethanolamine) from (288 to 333) K. Journal of Chemical & Engineering Data 51, 1406-1410.

Qian, W., Xu, Y., Zhu, H., Yu, C., 2012. Properties of pure 1-methylimidazolium acetate ionic liquid and its binary mixtures with alcohols. The Journal of Chemical Thermodynamics 49, 87-94.

Rinker, E.B., Oelschlager, D.W., Colussi, A.T., Henry, K.R., Sandal, O.C., 1994. Viscosity, density, and surface tension of binary mixtures of water and N-Methyldiethanolamine and water and diethanolamine and tertiary mixtures of these amines with water over the temperature range 20-100. degree. C. Journal of Chemical and Engineering Data 39, 392-395.

Rinker, E., Russell, J., Tamimi, A., Sandal, O., 1995. Diffusivity of nitrous oxide in N-methyldiethanolamine + diethanolamine + water. Journal of Chemical and Engineering Data 40, 630-631.

Sada, E., Kumazawa, H., Butt, M., 1977. Solubilities of gases in aqueous solutions of amine. Journal of Chemical and Engineering Data 22, 277-278.

Sada, E., Kumazawa, H., Butt, M. A., 1978. Solubilities and diffusivities of gases in aqueous solutions of amines. Journal of Chemical and Engineering Data 23, 161 – 163.

Saha, A.K., Bandyopadhyay, S.S., Biswas, A.K., 1993. Solubility and diffusivity of nitrous oxide and carbon dioxide in aqueous solutions of 2-amino-2-methyl-1-propanol. Journal of Chemical and Engineering Data 38, 78-82.

Samanta, A., Bandyopadhyay, S.S., 2006. Density and viscosity of aqueous solutions of piperazine and (2-Amino-2-methyl-1-propanol + Piperazine) from 298 to 333 K. Journal of Chemical & Engineering Data 51, 467-470.

Samanta, A., Roy, S., Bandyopadhyay, S.S., 2007. Physical solubility and diffusivity of N_2O and CO_2 in aqueous solutions of piperazine and (N-methyldiethanolamine+ piperazine). Journal of Chemical & Engineering Data 52, 1381-1385.

Sema, T., Edali, M., Naami, A., Idem, R., Tontiwachwuthikul, P., 2012. Solubility and diffusivity of N_2O in Aqueous 4-(Diethylamino)-2-butanol solutions for use in postcombustion CO_2 capture. Industrial & Engineering Chemistry Research 51, 925 −930.

Shaikh, M.S., Shariff, A.M., Bustam, M.A., Murshid, G., 2013. Physical properties of aqueous blends of sodium glycinate (SG) and piperazine (pz) as a solvent for CO_2 capture. Journal of Chemical & Engineering Data 58, 634-638.

Shen, K.P., Li, M.H., Yih, S.M., 1991. Kinetics of carbon dioxide reaction with sterically hindered 2-piperidineethanol aqueous solutions. Industrial & Engineering Chemistry Research 30, 1811-1813.

Song, J.-H., Park, S.-B., Yoon, J.-H., Lee, H., Lee, K.-H., 1996. Densities and viscosities of monoethanolamine+ ethylene glycol + water. Journal of Chemical & Engineering Data 41, 1152-1154.

Sun, W.-C., Yong, C.-B., Li, M.-H., 2005. Kinetics of the absorption of carbon dioxide into mixed aqueous solutions of 2-amino-2-methyl-l-propanol and piperazine. Chemical Engineering Science 60, 503-516.

Teng, T.T., Maham, Y., Hepler, L.G., Mather, A.E., 1994. Viscosity of aqueous solutions of N-methyldiethanolamine and of diethanolamine. Journal of Chemical and Engineering Data 39, 290-293.

Tsai, T.-C., Ko, J.-J., Wang, H.-M., Lin, C.-Y., Li, M.-H., 2000. Solubility of nitrous oxide in alkanolamine aqueous solutions. Journal of Chemical & Engineering Data 45, 341-347.

Versteeg, G., Oyevaar, M., 1989. The reaction between CO_2 and diethanolamine at 298 K. Chemical Engineering Science 44, 1264-1268.

Versteeg, G.F., Van Swaalj, W., 1988. Solubility and diffusivity of acid gases (carbon dioxide, nitrous oxide) in aqueous alkanolamine solutions. Journal of Chemical and Engineering Data 33, 29-34.

Vogel, H., Weiss, A., 1982. Transport properties of liquids, III. Viscosity of athermal liquid mixtures. Berichte der Bunsengesellschaft für physikalische Chemie 86, 193-198.

Wang, Y.W., Xu, S., Otto, F.D., Mather, A.E., 1992. Solubility of N_2O in alkanolamines and in mixed solvents. Chemical Engineering Journal, 48, 31 −40.

Wang, H.-M., Li, M.-H., 2004. Kinetics of absorption of carbon dioxide into aqueous solutions of 2-amino-2-methyl-l-propanol + diethanolamine. Journal of chemical engineering of Japan 37, 267-278.

Wong, M., Shariff, A., Bustam, M., 2016. Raman spectroscopic study on the equilibrium of carbon dioxide in aqueous monoethanolamine. RSC Advances 6, 10816-10823.

Xiao, J., Li, C.-W., Li, M.-H., 2000. Kinetics of absorption of carbon dioxide into aqueous solutions of 2-amino-2-methyl-1-propanol + monoethanolamine. Chemical Engineering Science 55, 161-175.

Xu, S., Otto, F.D., Mather, A.E., 1991. Physical properties of aqueous AMP solutions. Journal of Chemical and Engineering Data 36, 71-75.

Xu, S., Wang, Y., Otto, F.D., Mather, A.E., 1992. Physicochemical properties of 2-piperidineethanol and its aqueous solutions. Journal of Chemical and Engineering Data 37, 407-411.

Xu, S., Wang, Y.W., Otto, F.D., Mather, A.E., 1993. Kinetics of the reaction of carbon dioxide with aqueous 2-piperidineethanol solutions. AIChE Journal 39, 1721-1725.

Yoon, J.-H., Baek, J.-I., Yamamoto, Y., Komai, T., Kawamura, T., 2003. Kinetics of removal of carbon dioxide by aqueous 2-amino-2-methyl-1,3-propanediol. Chemical Engineering Science 58, 5229-5237.

Yoon, S.J., Lee, H., Yoon, J.-H., Shim, J.-G., Lee, J.K., Min, B.-Y., Eum, H.-M., 2002a. Kinetics of absorption of carbon dioxide into aqueous 2-amino-2-ethyl-1,3-propanediol solutions. Industrial & Engineering Chemistry Research 41, 3651-3656.

Yoon, S.J., Lee, H.-S., Lee, H., Baek, J.-I., Yoon, J.-H., Eum, H.-M., 2002b. Densities, viscosities, and surface tensions of aqueous 2-Amino-2-ethyl-1,3-propanediol solutions. Journal of Chemical & Engineering Data 47, 30-32.

Table 3.1

Comparison of the Densities (ρ) of Pure MDEA and Aqueous MDEA Solutions (Mass % w) Measured in This Work with Literature Values at Temperature (T) at a Pressure of 0.1 MPa[a]

Mass% MDEA	Temperature T(K)	ρ (kg·m^{-3})	
		Al-Ghawas et al.	this work
Pure	298	1037.4	1036.7
	308	1030.2	1029.4
	323	1019.4	1018.5
10	298	1005.4	1005.7
	308	1002.5	1001.9
	323	996.0	995.9
20	298	1015.2	1015.0
	308	1011.3	1010.9
	323	1004.7	1003.4
30	298	1025.0	1024.6
	308	1020.5	1020.2
	323	1013.0	1012.0

[a]Standard uncertainties u are $u(T)$ = 0.25 K, $u(w)$ = 0.01%, and u(p) = 0.2 kPa. The combined expanded uncertainty for density measurement $U_c(\rho)$ = 4.11 kg·m^{-3} (95% level of confidence, k = 2).

Table 3.2

Comparison of the Viscosities (η) of Pure MDEA and Aqueous MDEA Solutions (Mass % w) Measured in This Work with Literature Values at Temperature (T) at a Pressure of 0.1 MPa[a]

Mass% MDEA	Temperature T(K)	η mPa·s	
		Al-Ghawas et al.	this work
Pure	298	76.900	77.600
	308	44.140	44.330
	323	21.980	22.300
10	298	1.290	1.295
	308	1.011	1.007
	323	0.748	0.748
20	298	1.941	1.925
	308	1.474	1.468
	323	1.051	1.033
30	298	3.092	3.031
	308	2.250	2.251
	323	1.505	1.491

[a]Standard uncertainties u are $u(T)$ = 0.25 K, $u(w)$ = 0.01%, and u(p) = 0.2 kPa. The combined expanded uncertainty for viscosity measurement $U_c(\eta)$ =0.725 mPa·s (95% level of confidence, k = 2).

Table 3.3

Density (ρ), Viscosity (η) and Henry's Constant (H_{N_2O}) of Pure APA at Different Temperature (T)[a]

T (K)	ρ kg·m^{-3}	η mPa·s	H_{N_2O} kPa·m^3·kmol^{-1}
298	927.36	8.51	2215
303	923.34	7.04	2355
308	919.32	5.92	2495
313	915.28	5.05	2645
318	911.18	4.62	2805
323	906.97	3.99	2971

[a]Standard uncertainties (u) for density, viscosity and Henry's Constant $u(T)$ = 0.25 K. The combined expanded uncertainty for density measurement $U_c(\rho)$ = 3.69 kg·m^{-3}, for viscosity measurement $U_c(\eta)$ = 0.093 mPa·s and for solubility measurement $U_c(H_{N_2O})$ = 18.30 kPa·m^3·kmol^{-1} (95% level of confidence, k = 2).

Table 3.4

Parameters of Density, Viscosity and Henry's Constant for Pure APA

parameters	density	Viscosity	Henry's Constant
a	1032.1	539.31	$9.743 \cdot 10^{4}$
b	$79.61 \cdot 10^{-2}$	-3.262	$-1.1281 \cdot 10^{3}$
c	$14.47 \cdot 10^{-4}$	$4.971 \cdot 10^{-3}$	
AAD%	$1.56 \cdot 10^{-2}$	1.38	0.15

Table 3.5a

Density (ρ) and Viscosity (η) for APA + H_2O at Different Molar Concentration (m) and Temperature (T) at a Pressure of 0.1 MPa[a]

T (K)	[APA](m_1) kmol·m^3	ρ kg·m^{-3}	η mPa·s
298	0.1	997.56	0.95
303	0.1	996.21	0.84
308	0.1	994.48	0.76
313	0.1	992.55	0.69
318	0.1	990.18	0.61
323	0.1	987.58	0.55

Table 3.5b

Density (ρ) and Viscosity (η) for APA+H_2O at Different Molar Concentration (m) and Temperature (T) at a Pressure of 0.1 MPa[a]

T (K)	[APA](m_1) kmol·m^3	ρ kg·m^{-3}	η mPa·s
298	0.3	997.47	1.07
303	0.3	996.12	0.95
308	0.3	994.37	0.85
313	0.3	992.43	0.77
318	0.3	989.94	0.69
323	0.3	987.36	0.63
298	0.5	997.32	1.23
303	0.5	995.98	1.09
308	0.5	994.17	0.98
313	0.5	992.27	0.88
318	0.5	989.71	0.8
323	0.5	987.13	0.73
298	0.7	997.12	1.41
303	0.7	995.83	1.24
308	0.7	994	1.1
313	0.7	992.1	0.99
318	0.7	989.48	0.9
323	0.7	986.93	0.81

Table 3.5c

Density (ρ) and Viscosity (η) for APA+H_2O at Different Molar Concentration (m) and Temperature (T) at a Pressure of 0.1 MPa[a]

T (K)	[APA](m_1) kmol·m^3	ρ kg·m^{-3}	η mPa·s
298	0.9	996.9	1.57
303	0.9	995.67	1.39
308	0.9	993.82	1.24
313	0.9	991.92	1.11
318	0.9	989.3	1
323	0.9	986.74	0.9
298	1.1	996.71	1.74
303	1.1	995.53	1.55
308	1.1	993.64	1.38
313	1.1	991.73	1.23
318	1.1	989.09	1.11
323	1.1	986.55	0.98

[a]Standard uncertainties u are $u(T) = 0.25$ K, $u(m) = 0.001$ kmol·m^3, and u(p) = 0.2 kPa. The combined expanded uncertainty for density measurement $U_c(\rho) = 3.98$ kg·m^{-3} and for viscosity measurement $U_c(\eta) = 0.012$ mPa·s (95% level of confidence, k = 2).

Table 3.6a

Density (ρ) for APA+MDEA+H_2O at Different Molar Concentration (m) and Temperature (T) at a Pressure of 0.1 MPa[a]

T (K)	[APA](m_1) kmol·m^3	[MDEA](m_2) kmol·m^3	ρ kg·m^{-3}
298	0	3.0	1036.91
303	0	3.0	1034.27
308	0	3.0	1030.94
313	0	3.0	1027.61
318	0	3.0	1024.05
323	0	3.0	1020.68
298	0.1	2.9	1034.21
303	0.1	2.9	1031.54
308	0.1	2.9	1028.71
313	0.1	2.9	1025.06
318	0.1	2.9	1021.52
323	0.1	2.9	1018.53
298	0.3	2.7	1031.94
303	0.3	2.7	1029.05
308	0.3	2.7	1025.64
313	0.3	2.7	1022.81
318	0.3	2.7	1019.54
323	0.3	2.7	1016.34

Table 3.6b

Density (ρ) for APA+MDEA+H_2O at Different Molar Concentration (m) and Temperature (T) at a Pressure of 0.1 MPa[a]

T (K)	[APA](m_1) kmol·m^3	[MDEA](m_2) kmol·m^3	ρ kg·m^{-3}
298	0.5	2.5	1029.81
303	0.5	2.5	1026.64
308	0.5	2.5	1023.62
313	0.5	2.5	1020.71
318	0.5	2.5	1017.34
323	0.5	2.5	1013.8
298	0.7	2.3	1027.4
303	0.7	2.3	1024.71
308	0.7	2.3	1021.6
313	0.7	2.3	1018.61
318	0.7	2.3	1015.14
323	0.7	2.3	1011.26
298	0.9	2.1	1024.98
303	0.9	2.1	1022.78
308	0.9	2.1	1019.58
313	0.9	2.1	1016.51
318	0.9	2.1	1012.94
323	0.9	2.1	1008.72

Table 3.6c

Density (ρ) for APA+MDEA+H_2O at Different Molar Concentration (m) and Temperature (T) at a Pressure of 0.1 MPa[a]

T (K)	[APA](m_1) kmol·m^3	[MDEA](m_2) kmol·m^3	ρ kg·m^{-3}
298	1.1	1.9	1022.67
303	1.1	1.9	1020.45
308	1.1	1.9	1017.56
313	1.1	1.9	1014.26
318	1.1	1.9	1010.74
323	1.1	1.9	1006.18

[a]Standard uncertainties u are $u(T) = 0.25$ K, $u(m) = 0.001$ kmol·m^3, and u(p) = 0.2 kPa. The combined expanded uncertainty for density measurement $U_c(\rho) = 4.10$ kg·m^{-3} (95% level of confidence, k = 2).

Table 3.7a

Viscosity (η) for APA+MDEA+H_2O at Different Molar Concentration (m) and Temperature (T) at a Pressure of 0.1 MPa[a]

T (K)	[APA](m_1) kmol·m^3	[MDEA](m_2) kmol·m^3	η mPa·s
298	0	3.0	3.851
303	0	3.0	3.22
308	0	3.0	2.7
313	0	3.0	2.215
318	0	3.0	1.89
323	0	3.0	1.62
298	0.1	2.9	4.21
303	0.1	2.9	3.468
308	0.1	2.9	2.903
313	0.1	2.9	2.368
318	0.1	2.9	2.04
323	0.1	2.9	1.773
298	0.3	2.7	4.54
303	0.3	2.7	3.763
308	0.3	2.7	3.14
313	0.3	2.7	2.61
318	0.3	2.7	2.2
323	0.3	2.7	1.94

Table 3.7b

Viscosity (η) for APA+MDEA+H_2O at Different Molar Concentration (m) and Temperature (T) at a Pressure of 0.1 MPa[a]

T (K)	[APA](m_1) kmol·m^3	[MDEA](m_2) kmol·m^3	η mPa·s
298	0.5	2.5	4.86
303	0.5	2.5	3.98
308	0.5	2.5	3.35
313	0.5	2.5	2.77
318	0.5	2.5	2.39
323	0.5	2.5	2.06
298	0.7	2.3	5.18
303	0.7	2.3	4.207
308	0.7	2.3	3.561
313	0.7	2.3	2.949
318	0.7	2.3	2.57
323	0.7	2.3	2.2
298	0.9	2.1	5.5
303	0.9	2.1	4.434
308	0.9	2.1	3.771
313	0.9	2.1	3.128
318	0.9	2.1	2.731
323	0.9	2.1	2.354

Table 3.7c

Viscosity (η) for APA+MDEA+H_2O at Different Molar Concentration (m) and Temperature (T) at a Pressure of 0.1 MPa[a]

T (K)	[APA](m_1) kmol·m^3	[MDEA](m_2) kmol·m^3	η mPa·s
298	1.1	1.9	5.82
303	1.1	1.9	4.661
308	1.1	1.9	3.982
313	1.1	1.9	3.307
318	1.1	1.9	2.892
323	1.1	1.9	2.508

[a]Standard uncertainties u are $u(T)$ = 0.25 K, $u(m)$ = 0.001 kmol·m^3, and u(p) = 0.2 kPa. The combined expanded uncertainty for viscosity measurement $U_c(\eta)$ = 0.068 mPa·s (95% level of confidence, k = 2).

Table 3.8a

Density (ρ) for APA+AMP+H_2O at Different Molar Concentration (m') and Temperature (T) at a Pressure of 0.1 MPa[a]

T (K)	[APA](m'_1) kmol·m^3	[AMP](m'_2) kmol·m^3	ρ kg·m^{-3}
298	0	3.0	994.97
303	0	3.0	992.54
308	0	3.0	989.4
313	0	3.0	986.5
318	0	3.0	983.2
323	0	3.0	979.7
298	0.1	2.9	995.9
303	0.1	2.9	993.58
308	0.1	2.9	990.69
313	0.1	2.9	987.81
318	0.1	2.9	984
323	0.1	2.9	981
298	0.3	2.7	997.3
303	0.3	2.7	994.87
308	0.3	2.7	991.71
313	0.3	2.7	988.91
318	0.3	2.7	985.2
323	0.3	2.7	982.2

Table 3.8b

Density (ρ) for APA+AMP+H_2O at Different Molar Concentration (m') and Temperature (T) at a Pressure of 0.1 MPa[a]

T (K)	[APA](m'_1) kmol·m^3	[AMP](m'_2) kmol·m^3	ρ kg·m^{-3}
298	0.5	2.5	998.86
303	0.5	2.5	995.88
308	0.5	2.5	992.9
313	0.5	2.5	989.63
318	0.5	2.5	986.4
323	0.5	2.5	982.9
298	0.7	2.3	1000.3
303	0.7	2.3	996.9
308	0.7	2.3	994.2
313	0.7	2.3	991.3
318	0.7	2.3	987.7
323	0.7	2.3	983.8
298	0.9	2.1	1001.7
303	0.9	2.1	998.5
308	0.9	2.1	995.5
313	0.9	2.1	992.3
318	0.9	2.1	989
323	0.9	2.1	984.9

Table 3.8c

Density (ρ) for APA+AMP+H_2O at Different Molar Concentration (*m′*) and Temperature (*T*) at a Pressure of 0.1 MPa[a]

T (K)	[APA](m'$_1$) kmol·m^3	[AMP](m'$_2$) kmol·m^3	ρ kg·m^{-3}
298	1.1	1.9	1003.2
303	1.1	1.9	1000.1
308	1.1	1.9	996.9
313	1.1	1.9	993.6
318	1.1	1.9	990.3
323	1.1	1.9	986.3

[a]Standard uncertainties *u* are $u(T) = 0.25$ K, $u(m') = 0.001$ kmol·m^3 and $u(p) = 0.2$ kPa. The combined expanded uncertainty for density measurement $U_c(\rho) = 3.97$ kg·m^{-3} (95% level of confidence, k = 2).

Table 3.9a

Viscosity (η) for APA+AMP+H_2O at Different Molar Concentration (*m′*) and Temperature (*T*) at a Pressure of 0.1 MPa[a]

T (K)	[APA](m'_1) kmol·m^3	[AMP](m'_2) kmol·m^3	*η* mPa·s
298	0	3.0	3.55
303	0	3.0	2.8
308	0	3.0	2.32
313	0	3.0	1.95
318	0	3.0	1.62
323	0	3.0	1.4
298	0.1	2.9	3.71
303	0.1	2.9	2.95
308	0.1	2.9	2.42
313	0.1	2.9	2.04
318	0.1	2.9	1.75
323	0.1	2.9	1.5
298	0.3	2.7	3.85
303	0.3	2.7	3.05
308	0.3	2.7	2.56
313	0.3	2.7	2.16
318	0.3	2.7	1.85
323	0.3	2.7	1.6

Table 3.9b

Viscosity (η) for APA+AMP+H_2O at Different Molar Concentration (*m′*) and Temperature (*T*) at a Pressure of 0.1 MPa[a]

T (K)	[APA](m'_1) kmol·m^3	[AMP](m'_2) kmol·m^3	*η* mPa·s
298	0	3.0	4.05
303	0	3.0	3.29
308	0	3.0	2.72
313	0	3.0	2.29
318	0	3.0	1.98
323	0	3.0	1.72
298	0.1	2.9	4.31
303	0.1	2.9	3.54
308	0.1	2.9	2.94
313	0.1	2.9	2.48
318	0.1	2.9	2.13
323	0.1	2.9	1.85
298	0.3	2.7	4.57
303	0.3	2.7	3.79
308	0.3	2.7	3.16
313	0.3	2.7	2.68
318	0.3	2.7	2.28
323	0.3	2.7	1.98

Table 3.9c

Viscosity (η) for APA+AMP+H_2O at Different Molar Concentration (m') and Temperature (T) at a Pressure of 0.1 MPa[a]

T (K)	[APA](m'_1) kmol·m^3	[AMP](m'_2) kmol·m^3	η mPa·s
298	1.1	1.9	4.84
303	1.1	1.9	4.05
308	1.1	1.9	3.38
313	1.1	1.9	2.89
318	1.1	1.9	2.43
323	1.1	1.9	2.13

[a]Standard uncertainties u are $u(T) = 0.25$ K, $u(m') = 0.001$ kmol·m^3 and $u(p) = 0.2$ kPa. The combined expanded uncertainty for viscosity measurement $U_c(\eta)$ =0.049 mPa·s (95% level of confidence, k = 2).

Table 3.10

Binary Redlich-Kister Parameters A_0, A_1, A_2 for the Excess Volume of density (ρ) and kinematic viscosity (υ) for APA+H_2O (Equations 3.4, 3.5, 3.10 and 3.11)

Parameters		APA + H_2O	
		Binary pair (ρ)	Binary pair (υ)
A_0	*a*	517.68	-42.575
	b	-3.4618	214.25
	c	$5.7639 \cdot 10^{-3}$	245.36
A_1	*a*	1080.1	-55.098
	b	-7.2228	-1670.6
	c	$12.026 \cdot 10^{-3}$	-211.49
A_2	*a*	563.72	
	b	-3.7697	
	c	$6.2764 \cdot 10^{-3}$	
AAD		0.08%	1.42%

Table 3.11

Ternary Redlich-Kister Parameters A_0, A_1, A_2 for the Excess Volume of Density for APA+MDEA+H_2O (Equations 3.4 and 3.5)

Parameters		Binary pair		
		APA + MDEA	MDEA + H_2O	APA + H_2O
A_0	*a*	2.4338	1.4403	-1.6031
	b	-0.1069	0.518	-1.1156
	c	0.0562	0.3536	0.2168
A_1	*a*	-3.402	-0.1320	-6.1226
	b	-0.8171	1.2175	-2.4746
	c	-0.0856	0.8287	0.4410
A_2	*a*	-1.5899	-2.1	-4.7438
	b	1.5981	0.7151	-1.368
	c	-0.3623	0.4856	0.2178
AAD		0.16%		

Table 3.12

Ternary Redlich-Kister Parameters A_0, A_1, A_2 for the Excess Volume of Density for APA+AMP+H_2O (Equations 3.4 and 3.5)

Parameters		Binary pair		
		APA + AMP	AMP + H_2O	APA + H_2O
A_0	*a*	3.0289	1.3901	4.8559
	b	-0.30397	0.55637	-1.2786
	c	0.072131	0.38635	0.44933
A_1	*a*	-2.1136	-0.029089	-1.6548
	b	-0.82476	1.2527	-2.6081
	c	0.25637	0.89446	0.9783
A_2	*a*	-3.091	-1.8248	-8.0982
	b	2.1344	0.70382	-1.2998
	c	0.04018	0.5177	0.52785
AAD		0.12%		

Table 3.13a

Excess molar volume, (V^E), thermal expansion coefficient (α), viscosity deviation ($\Delta\eta$) of ternary blend X_1 APA (1) + X_2 AMP (2) + (1-X_1- X_2) H_2O (3) system at different temperature and molar concentration (m') (X_1, X_2 = mole fraction)[a]

APA(1) + AMP(2) + H_2O(3)					
m_1/m_2 kmol·m^3	X_1	X_2	V^E (cm^3 mol^{-1})	$\alpha \times 10^3$ (K^{-1})	$\Delta\eta$ (mPa s)
T=298 K					
0/3	0	0.0691	-0.3904	0.6161	-6.4297
0.1/2.9	0.0023	0.0671	-0.4219	0.6089	-6.0244
0.3/2.7	0.007	0.063	-0.4751	0.6149	-5.3815
0.5/2.5	0.0118	0.0589	-0.5336	0.6379	-4.6793
0.7/2.3	0.0166	0.0547	-0.5893	0.6455	-3.9039
0.9/2.1	0.0216	0.0504	-0.6461	0.66	-3.1169
1.1/1.9	0.0266	0.046	-0.7053	0.6676	-2.3068
T=303 K					
0/3	0	0.0691	-0.3876	0.6176	-4.8607
0.1/2.9	0.0023	0.0671	-0.422	0.6103	-4.5277
0.3/2.7	0.007	0.063	-0.4733	0.6164	-4.0524
0.5/2.5	0.0118	0.0589	-0.5196	0.6398	-3.4378
0.7/2.3	0.0166	0.0547	-0.5658	0.6477	-2.8032
0.9/2.1	0.0216	0.0504	-0.628	0.6621	-2.16
1.1/1.9	0.0266	0.046	-0.6901	0.6696	-1.497

Table 3.13b

Excess molar volume, (V^E), thermal expansion coefficient (α), viscosity deviation ($\Delta\eta$) of ternary blend X_1 APA (1) + X_2 AMP (2) + (1-X_1- X_2) H_2O (3) system at different temperature and molar concentration (m') (X_1, X_2 = mole fraction)[a]

APA(1) + AMP(2) + H_2O(3)					
m_1/m_2 kmol·m^3	X_1	X_2	V^E (cm^3 mol^{-1})	$\alpha \times 10^3$ (K^{-1})	$\Delta\eta$ (mPa s)
T=308 K					
0/3	0	0.0691	-0.3717	0.6196	-3.2603
0.1/2.9	0.0023	0.0671	-0.4123	0.6121	-3.0338
0.3/2.7	0.007	0.063	-0.4578	0.6183	-2.6342
0.5/2.5	0.0118	0.0589	-0.5088	0.6418	-2.2152
0.7/2.3	0.0166	0.0547	-0.5624	0.6495	-1.7291
0.9/2.1	0.0216	0.0504	-0.6179	0.6641	-1.2373
1.1/1.9	0.0266	0.046	-0.6758	0.6718	-0.7385
T=313 K					
0/3	0	0.0691	-0.3647	0.6214	-1.914
0.1/2.9	0.0023	0.0671	-0.4062	0.6139	-1.7416
0.3/2.7	0.007	0.063	-0.4541	0.6201	-1.4526
0.5/2.5	0.0118	0.0589	-0.4945	0.6439	-1.154
0.7/2.3	0.0166	0.0547	-0.5575	0.6514	-0.7907
0.9/2.1	0.0216	0.0504	-0.6064	0.6662	-0.4138
1.1/1.9	0.0266	0.046	-0.6625	0.674	-0.0222

Table 3.13c

Excess molar volume, (V^E), thermal expansion coefficient (α), viscosity deviation ($\Delta\eta$) of ternary blend X_1 APA (1) + X_2 AMP (2) + (1-X_1- X_2) H_2O (3) system at different temperature and molar concentration (m') (X_1, X_2 = mole fraction)[a]

APA(1) + AMP(2) + H_2O(3)					
m_1/m_2 kmol·m^3	X_1	X_2	V^E (cm^3 mol^{-1})	$\alpha \times 10^3$ (K^{-1})	$\Delta\eta$ (mPa s)
T=318 K					
0/3	0	0.0691	-0.3524	0.6235	-1.208
0.1/2.9	0.0023	0.0671	-0.3821	0.6163	-1.0241
0.3/2.7	0.007	0.063	-0.4328	0.6224	-0.8136
0.5/2.5	0.0118	0.0589	-0.4852	0.646	-0.5734
0.7/2.3	0.0166	0.0547	-0.5399	0.6537	-0.31
0.9/2.1	0.0216	0.0504	-0.5966	0.6685	-0.0444
1.1/1.9	0.0266	0.046	-0.6532	0.6763	0.2245
T=323 K					
0/3	0	0.0691	-0.3379	0.6257	-0.7933
0.1/2.9	0.0023	0.0671	-0.3799	0.6181	-0.6539
0.3/2.7	0.007	0.063	-0.4314	0.6243	-0.473
0.5/2.5	0.0118	0.0589	-0.4723	0.6483	-0.2726
0.7/2.3	0.0166	0.0547	-0.5178	0.6563	-0.0597
0.9/2.1	0.0216	0.0504	-0.5701	0.6712	0.1549
1.1/1.9	0.0266	0.046	-0.6298	0.679	0.3918

Table 3.14

Parameters of Grunberg and Nissan Model G_{12}, G_{23}, G_{13} for Ternary Viscosity of APA+MDEA+H_2O and APA+AMP+H_2O (Equations 3.12 and 3.13)

Parameters		Ternary pairs	
		APA+MDEA+H_2O	APA+AMP+ H_2O
G_{12}	*a*	3149.3	43971
	b	-18.5	-289.8
	c	$29.3 \cdot 10^{-3}$	477.04
G_{23}	*a*	620.61	951.42
	b	-3.7123	-5.8358
	c	$5.658 \cdot 10^{-3}$	9.048
G_{13}	*a*	936.62	-2146.1
	b	-5.8117	14.421
	c	$9.1678 \cdot 10^{-3}$	$-23.888 \cdot 10^{-3}$
AAD		2.28%	2.23%

Table 3.15

Values of Δ*H* and Δ*S* as a Function of Concentration from (298 to 323) K and Δ*G* Against APA Mole Fraction at 298 K.

X_1	APA (1) + AMP (2) + H_2O (3)		
	ΔH, (kJ mol^{-1})	$T\Delta S$, (kJ mol^{-1})	ΔG, (kJ mol^{-1})
0.0000	26.623	13.424	13.199
0.0023	27.718	14.402	13.316
0.0070	26.767	13.340	13.427
0.0118	26.350	12.778	13.572
0.0166	26.079	12.335	13.744
0.0216	25.810	11.901	13.909
0.0266	25.434	11.364	14.070

Table 3.16a

Estimated Henry's Constant of CO_2 in APA+H_2O Using the N_2O Analogy as a Function of Molar Concentration (*m*) at a Pressure of 0.1 MPa[a]

T (K)	In water		In aqueous amine solutions		
	$H_{N_2O-water}$ kPa·m^3·kmol^{-1}	$H_{CO_2-water}$ kPa·m^3·kmol^{-1}	[APA] kmol·m^3	H_{N_2O-Am} kPa·m^3·kmol^{-1}	H_{CO_2-Am} kPa·m^3·kmol^{-1}
298	4075	3089	0.10	4065	3081
			0.30	4235	3210
			0.50	4395	3331
			0.70	4535	3437
			0.90	4670	3540
			1.10	4765	3612
303	4438	3358	0.10	4505	3409
			0.30	4663	3529
			0.50	4803	3634
			0.70	4925	3726
			0.90	5035	3810
			1.10	5158	3903
308	5023	3809	0.10	4830	3663
			0.30	5019	3806
			0.50	5180	3928
			0.70	5295	4015
			0.90	5428	4116
			1.10	5575	4228

Table 3.16b

Estimated Henry's Constant of CO_2 in APA+H_2O Using the N_2O Analogy as a Function of Molar Concentration (m) at a Pressure of 0.1 MPa[a]

T (K)	In water		In aqueous amine solutions		
	$H_{N_2O-water}$ kPa·m^3·kmol^{-1}	$H_{CO_2-water}$ kPa·m^3·kmol^{-1}	[APA] kmol·m^3	H_{N_2O-Am} kPa·m^3·kmol^{-1}	H_{CO_2-Am} kPa·m^3·kmol^{-1}
313	4075	3089	0.10	5309	3828
			0.30	5479	3951
			0.50	5655	4077
			0.70	5778	4166
			0.90	5908	4260
			1.10	6098	4397
318	6480	4652	0.10	5810	4171
			0.30	5985	4297
			0.50	6135	4405
			0.70	6284	4512
			0.90	6435	4620
			1.10	6595	4735
323	7215	5123	0.10	6335	4498
			0.30	6495	4611
			0.50	6665	4732
			0.70	6825	4846
			0.90	6945	4931
			1.10	7125	5059

[a]Standard uncertainties u are $u(T)$ = 0.25 K, $u(m)$ = 0.001 kmol·m^3 and $u(p)$ = 0.2 kPa. The combined expanded uncertainty for solubility measurement $U_c(H_{N_2O})$ = 50.83 kPa·m^3·kmol^{-1} (95% level of confidence, k = 2).

Table 3.17a

Estimated Henry's Constant of CO_2 in APA+MDEA+H_2O Using the N_2O Analogy as a Function of Molar Concentration (*m*) at a Pressure of 0.1 MPa[a]

T (K)	In water		In aqueous amine solutions			
	$H_{N_2O-water}$ kPa·m^3·kmol^{-1}	$H_{CO_2-water}$ kPa·m^3·kmol^{-1}	[APA] kmol·m^3	[MDEA] kmol·m^3	H_{N_2O-Am} kPa·m^3·kmol^{-1}	H_{CO_2-Am} kPa·m^3·kmol^{-1}
298	4075	3089	0.00	3.00	5035	3816
			0.10	2.90	5056	3832
			0.30	2.70	5101	3866
			0.50	2.50	5145	3900
			0.70	2.30	5171	3919
			0.90	2.10	5193	3936
			1.10	1.90	5219	3956
303	4438	3358	0.00	3.00	5325	4029
			0.10	2.90	5364	4059
			0.30	2.70	5398	4084
			0.50	2.50	5435	4112
			0.70	2.30	5458	4130
			0.90	2.10	5484	4149
			1.10	1.90	5508	4168
308	5023	3809	0.00	3.00	5665	4296
			0.10	2.90	5715	4334
			0.30	2.70	5778	4382
			0.50	2.50	5808	4404
			0.70	2.30	5835	4425
			0.90	2.10	5863	4446
			1.10	1.90	5890	4465

Table 3.17b

Estimated Henry's Constant of CO_2 in APA+MDEA+H_2O Using the N_2O Analogy as a Function of Molar Concentration (m) at a Pressure of 0.1 MPa[a]

T (K)	In water			In aqueous amine solutions		
	$H_{N_2O-water}$ kPa·m^3·kmol^{-1}	$H_{CO_2-water}$ kPa·m^3·kmol^{-1}	[APA] kmol·m^3	[MDEA] kmol·m^3	H_{N_2O-Am} kPa·m^3·kmol^{-1}	H_{CO_2-Am} kPa·m^3·kmol^{-1}
313	5745	4142	0.00	3.00	6125	4416
			0.10	2.90	6170	4448
			0.30	2.70	6205	4474
			0.50	2.50	6245	4502
			0.70	2.30	6269	4520
			0.90	2.10	6295	4539
			1.10	1.90	6315	4553
318	6480	4652	0.00	3.00	6595	4735
			0.10	2.90	6641	4768
			0.30	2.70	6698	4809
			0.50	2.50	6735	4835
			0.70	2.30	6772	4862
			0.90	2.10	6798	4881
			1.10	1.90	6821	4897
323	7215	5123	0.00	3.00	7135	5066
			0.10	2.90	7184	5101
			0.30	2.70	7205	5116
			0.50	2.50	7248	5146
			0.70	2.30	7276	5166
			0.90	2.10	7296	5180
			1.10	1.90	7316	5194

[a]Standard uncertainties u are $u(T)$ = 0.25 K, $u(m)$ = 0.001 kmol·m^3 and $u(p)$ = 0.2 kPa. The combined expanded uncertainty for solubility measurement $U_c(H_{N_2O})$ = 48.68 kPa·m^3·kmol^{-1} (95% level of confidence, k = 2).

Table 3.18a

Estimated Henry's Constant of CO_2 in APA+AMP+H_2O Using the N_2O Analogy as a Function of Molar Concentration (*m*) at a Pressure of 0.1 MPa[a]

T (K)	In water			In aqueous amine solutions		
	$H_{N_2O-water}$ kPa·m³·kmol⁻¹	$H_{CO_2-water}$ kPa·m³·kmol⁻¹	[APA] kmol·m³	[AMP] kmol·m³	H_{N_2O-Am} kPa·m³·kmol⁻¹	H_{CO_2-Am} kPa·m³·kmol⁻¹
298	4075	3089	0.00	3.00	5025	3809
			0.10	2.90	4955	3756
			0.30	2.70	4895	3710
			0.50	2.50	4851	3677
			0.70	2.30	4795	3634
			0.90	2.10	4730	3585
			1.10	1.90	4688	3553
303	4438	3358	0.00	3.00	5471	4140
			0.10	2.90	5405	4090
			0.30	2.70	5341	4041
			0.50	2.50	5285	3999
			0.70	2.30	5225	3953
			0.90	2.10	5165	3908
			1.10	1.90	5135	3885
308	5023	3809	0.00	3.00	6015	4561
			0.10	2.90	5968	4526
			0.30	2.70	5910	4482
			0.50	2.50	5860	4444
			0.70	2.30	5785	4387
			0.90	2.10	5728	4344
			1.10	1.90	5690	4315

Table 3.18b

Estimated Henry's Constant of CO_2 in APA+AMP+H_2O Using the N_2O Analogy as a Function of Molar Concentration (m) at a Pressure of 0.1 MPa[a]

T (K)	In water		In aqueous amine solutions			
	$H_{N_2O-water}$ kPa·m^3·kmol^{-1}	$H_{CO_2-water}$ kPa·m^3·kmol^{-1}	[APA] kmol·m^3	[AMP] kmol·m^3	H_{N_2O-Am} kPa·m^3·kmol^{-1}	H_{CO_2-Am} kPa·m^3·kmol^{-1}
313	5745	4142	0.00	3.00	6590	4751
			0.10	2.90	6550	4722
			0.30	2.70	6487	4677
			0.50	2.50	6405	4618
			0.70	2.30	6345	4575
			0.90	2.10	6310	4549
			1.10	1.90	6272	4522
318	6480	4652	0.00	3.00	7285	5230
			0.10	2.90	7203	5171
			0.30	2.70	7097	5095
			0.50	2.50	7025	5044
			0.70	2.30	6935	4979
			0.90	2.10	6880	4940
			1.10	1.90	6845	4914
323	7215	5123	0.00	3.00	7924	5626
			0.10	2.90	7875	5591
			0.30	2.70	7807	5543
			0.50	2.50	7721	5482
			0.70	2.30	7605	5400
			0.90	2.10	7555	5364
			1.10	1.90	7521	5340

[a]Standard uncertainties u are $u(T)$ = 0.25 K, $u(m)$ = 0.001 kmol·m^3, and u(p) = 0.2 kPa. The combined expanded uncertainty for solubility measurement $U_c(H_{N_2O})$ = 62.46 kPa·m^3·kmol^{-1} (95% level of confidence, k = 2).

Table 3.19

Parameters k_1, k_2, k_3, k_4, α_{123} for the Excess Henry's Constant for the Binary and Ternary Solvent Systems and AAD for N_2O Solubility of APA+MDEA+H_2O (Equations 3.19 and 3.20)

System	k_1	k_2	$10^4 \cdot k_3$	k_4	α_{123}	AAD%
APA+H_2O	249.973	-1.284	18.4	-31.347		7.03
MDEA+H_2O	61.911	-0.339	4.921	-3.632		0.82
APA+MDEA	-410.21	1.809	-23.514	73.948		
APA+MDEA+H_2O					61.145	0.65
APA+AMP	-447.95	2.505	-32.31	180.23		
APA+AMP+H_2O					-111.8	0.95

Table 3.20 Parameters for Solubility of N_2O in the Binary Solution of APA+H_2O and Ternary Solution of APA+MDEA+H_2O, APA+AMP+H_2O with AAD using Arrhenius Type Equation (Equations 3.21 and 3.22)

Parameters	Systems		
	APA+H_2O	APA+MDEA+H_2O	APA+AMP+H_2O
a	$8.8966 \cdot 10^5$	$-2.8325 \cdot 10^9$	$7.6867 \cdot 10^7$
b	$1.4585 \cdot 10^5$	$2.0224 \cdot 10^9$	$1.5537 \cdot 10^5$
c	-15780	$-3.5934 \cdot 10^8$	$-8.3652 \cdot 10^6$
d		$2.1179 \cdot 10^9$	$3.4288 \cdot 10^8$
e		$-3.9119 \cdot 10^8$	$-1.22 \cdot 10^8$
f		$-7.5053 \cdot 10^8$	$-1.31 \cdot 10^8$
h	1606.4	1357.4	1809.2
AAD%	0.57	0.77	0.38

Table 3.21 Parameters A_1, A_2, A_3, A_4, A_5, A_6 for Solubility of N_2O in the Binary Solutions of APA+H_2O and Ternary Solutions of APA+MDEA+H_2O, APA+AMP+H_2O with AAD using Polynomial Models (Equations 3.23, 3.24 and 3.25)

Parameters	Systems		
	APA+H_2O	APA+MDEA+H_2O	APA+AMP+H_2O
A_1	6.3966	4.8068	3.7394
A_2	53.252	-4.7536	-22.37
$10^2 \cdot A_3$	-50272	-9199.1	-159.45
$10^3 \cdot A_4$	6.318	13.084	15.456
$10^3 \cdot A_5$	-98.986	7.191	79.144
$10^3 \cdot A_6$	1275.3	189.84	0.655
AAD%	0.35	0.58	0.28

Table 3.22a

Estimated Diffusivity of CO_2 (D_{CO_2}) in APA+H_2O at Temperature (T) Using the N_2O Analogy as a Function of Molar Concentration (m) at a Pressure of 0.1 MPa[a]

T (K)	In water		In aqueous amine solutions		
	$D_{N_2O-water}$ $10^9 \cdot m^2 \cdot s^{-1}$	$D_{CO_2-water}$ $10^9 \cdot m^2 \cdot s^{-1}$	[APA] $kmol \cdot m^3$	D_{N_2O-Am} $10^9 \cdot m^2 \cdot s^{-1}$	D_{CO_2-Am} $10^9 \cdot m^2 \cdot s^{-1}$
298	1.77	1.91	0.10	1.48	1.6
			0.30	1.31	1.41
			0.50	1.14	1.23
			0.70	0.99	1.07
			0.90	0.84	0.91
			1.10	0.68	0.73
303	1.96	2.15	0.10	1.74	1.91
			0.30	1.57	1.72
			0.50	1.41	1.55
			0.70	1.26	1.38
			0.90	1.12	1.23
			1.10	0.96	1.05
308	2.27	2.45	0.1	2.2	2.37
			0.3	1.91	2.06
			0.5	1.72	1.86
			0.7	1.54	1.66
			0.9	1.4	1.51
			1.1	1.25	1.35

Table 3.22b

Estimated Diffusivity of CO_2 (D_{CO_2}) in APA+H_2O at Temperature (T) Using the N_2O Analogy as a Function of Molar Concentration (m) at a Pressure of 0.1 MPa[a]

T (K)	In water		In aqueous amine solutions		
	$D_{N_2O-water}$ $10^9 \cdot m^2 \cdot s^{-1}$	$D_{CO_2-water}$ $10^9 \cdot m^2 \cdot s^{-1}$	[APA] $kmol \cdot m^3$	D_{N_2O-Am} $10^9 \cdot m^2 \cdot s^{-1}$	D_{CO_2-Am} $10^9 \cdot m^2 \cdot s^{-1}$
313	2.55	2.83	0.10	2.44	2.71
			0.30	2.26	2.51
			0.50	2.05	2.28
			0.70	1.86	2.06
			0.90	1.7	1.89
			1.10	1.54	1.71
318	2.86	3.2	0.10	2.76	3.03
			0.30	2.51	2.81
			0.50	2.32	2.6
			0.70	2.14	2.39
			0.90	2	2.24
			1.10	1.84	2.06
323	3.26	3.68	0.1	2.95	3.33
			0.3	2.72	3.07
			0.5	2.48	2.87
			0.7	2.35	2.65
			0.9	2.2	2.48
			1.1	2.05	2.31

[a]Standard uncertainties u are $u(T)$ = 0.25 K, $u(m)$ = 0.001 $kmol \cdot m^3$ and $u(p)$ = 0.2 kPa. The combined expanded uncertainty for diffusivity measurement $U_c(D_{N_2O}) = 28.9 \cdot 10^{-12}\ m^2 \cdot s^{-1}$ (95% level of confidence, k = 2).

Table 3.23a

Estimated Diffusivity of CO_2 (D_{CO_2}) in APA+MDEA+H_2O at Temperature (T) Using the N_2O Analogy as a Function of Molar Concentration (m) at a Pressure of 0.1 MPa[a]

T (K)	In water		In aqueous amine solutions			
	$D_{N_2O-water}$ $10^9 \cdot m^2 \cdot s^{-1}$	$D_{CO_2-water}$ $10^9 \cdot m^2 \cdot s^{-1}$	[APA] $kmol \cdot m^3$	[MDEA] $kmol \cdot m^3$	D_{N_2O-Am} $10^9 \cdot m^2 \cdot s^{-1}$	D_{CO_2-Am} $10^9 \cdot m^2 \cdot s^{-1}$
298	1.77	1.91	0.00	3.00	0.82	0.88
			0.10	2.90	0.77	0.83
			0.30	2.70	0.71	0.77
			0.50	2.50	0.65	0.7
			0.70	2.30	0.59	0.64
			0.90	2.10	0.53	0.57
			1.10	1.90	0.47	0.51
303	1.96	2.15	0	3	0.95	1.04
			0.1	2.9	0.9	0.99
			0.3	2.7	0.85	0.93
			0.5	2.5	0.78	0.86
			0.7	2.3	0.72	0.79
			0.9	2.1	0.66	0.72
			1.1	1.9	0.6	0.66
308	2.27	2.45	0	3	1.09	1.18
			0.1	2.9	1.05	1.13
			0.3	2.7	0.99	1.07
			0.5	2.5	0.93	1
			0.7	2.3	0.87	0.94
			0.9	2.1	0.81	0.87
			1.1	1.9	0.74	0.8

Table 3.23b Estimated Diffusivity of CO_2 (D_{CO_2}) in APA+MDEA+H_2O at Temperature (T) Using the N_2O Analogy as a Function of Molar Concentration (m) at a Pressure of 0.1 MPa[a]

T	In water		In aqueous amine solutions			
(K)	$D_{N_2O-water}$ $10^9 \cdot m^2 \cdot s^{-1}$	$D_{CO_2-water}$ $10^9 \cdot m^2 \cdot s^{-1}$	[APA] $kmol \cdot m^3$	[MDEA] $kmol \cdot m^3$	D_{N_2O-Am} $10^9 \cdot m^2 \cdot s^{-1}$	D_{CO_2-Am} $10^9 \cdot m^2 \cdot s^{-1}$
313	2.55	2.83	0.00	3.00	1.24	1.38
			0.10	2.90	1.19	1.32
			0.30	2.70	1.13	1.25
			0.50	2.50	1.07	1.19
			0.70	2.30	1.01	1.12
			0.90	2.10	0.94	1.04
			1.10	1.90	0.88	0.98
318	2.86	3.2	0	3	1.37	1.53
			0.1	2.9	1.33	1.49
			0.3	2.7	1.28	1.43
			0.5	2.5	1.22	1.37
			0.7	2.3	1.15	1.29
			0.9	2.1	1.08	1.21
			1.1	1.9	1.01	1.13
323	3.26	3.68	0	3	1.54	1.74
			0.1	2.9	1.48	1.67
			0.3	2.7	1.43	1.61
			0.5	2.5	1.37	1.55
			0.7	2.3	1.3	1.47
			0.9	2.1	1.23	1.39
			1.1	1.9	1.16	1.31

[a]Standard uncertainties u are $u(T)$ = 0.25 K, $u(m)$ = 0.001 $mol \cdot kg^{-1}$, $u(p)$ = 0.2 kPa. The combined expanded uncertainty for diffusivity measurement $U_c(D_{N_2O})$ = 14.83·10^{-12} $m^2 \cdot s^{-1}$ (95% level of confidence, k = 2).

Table 3.24a

Estimated Diffusivity of CO_2 (D_{CO_2}) in APA+AMP+H_2O at Temperature (*T*) Using the N_2O Analogy as a Function of Molar Concentration (*m*) at a Pressure of 0.1 MPa[a]

T (K)	In water		In aqueous amine solutions			
	$D_{N_2O-water}$ $10^9 \cdot m^2 \cdot s^{-1}$	$D_{CO_2-water}$ $10^9 \cdot m^2 \cdot s^{-1}$	[APA] kmol·m^3	[AMP] kmol·m^3	D_{N_2O-Am} $10^9 \cdot m^2 \cdot s^{-1}$	D_{CO_2-Am} $10^9 \cdot m^2 \cdot s^{-1}$
298	1.77	1.91	0.00	3.00	0.68	0.73
			0.10	2.90	0.64	0.69
			0.30	2.70	0.6	0.65
			0.50	2.50	0.56	0.6
			0.70	2.30	0.52	0.56
			0.90	2.10	0.47	0.51
			1.10	1.90	0.43	0.46
303	1.96	2.15	0	3	0.82	0.9
			0.1	2.9	0.76	0.83
			0.3	2.7	0.72	0.79
			0.5	2.5	0.68	0.75
			0.7	2.3	0.64	0.7
			0.9	2.1	0.61	0.67
			1.1	1.9	0.57	0.63
308	2.27	2.45	0	3	0.97	1.05
			0.1	2.9	0.91	0.98
			0.3	2.7	0.87	0.94
			0.5	2.5	0.83	0.9
			0.7	2.3	0.79	0.85
			0.9	2.1	0.75	0.81
			1.1	1.9	0.7	0.76

Table 3.24b Estimated Diffusivity of CO_2 (D_{CO_2}) in APA+AMP+H_2O at Temperature (T) Using the N_2O Analogy as a Function of Molar Concentration (m) at a Pressure of 0.1 MPa[a]

T	In water		In aqueous amine solutions			
(K)	$D_{N_2O-water}$ $10^9 \cdot m^2 \cdot s^{-1}$	$D_{CO_2-water}$ $10^9 \cdot m^2 \cdot s^{-1}$	[APA] kmol·m^3	[AMP] kmol·m^3	D_{N_2O-Am} $10^9 \cdot m^2 \cdot s^{-1}$	D_{CO_2-Am} $10^9 \cdot m^2 \cdot s^{-1}$
313	2.55	2.83	0.00	3.00	1.16	1.29
			0.10	2.90	1.1	1.22
			0.30	2.70	1.05	1.17
			0.50	2.50	1	1.11
			0.70	2.30	0.96	1.07
			0.90	2.10	0.92	1.02
			1.10	1.90	0.86	0.95
318	2.86	3.2	0	3	1.31	1.47
			0.1	2.9	1.25	1.4
			0.3	2.7	1.2	1.34
			0.5	2.5	1.15	1.29
			0.7	2.3	1.1	1.23
			0.9	2.1	1.05	1.17
			1.1	1.9	1	1.12
323	3.26	3.68	0	3	1.49	1.69
			0.1	2.9	1.42	1.61
			0.3	2.7	1.38	1.57
			0.5	2.5	1.34	1.52
			0.7	2.3	1.29	1.47
			0.9	2.1	1.24	1.41
			1.1	1.9	1.18	1.34

[a]Standard uncertainties u are $u(T)$ = 0.25 K, $u(m)$ = 0.001 kmol·m^{3}and $u(p)$ = 0.2 kPa. The combined expanded uncertainty for diffusivity measurement $U_c(D_{N_2O})$ = 16.1·10^{-12} m^2·s^{-1} (95% level of confidence, k = 2).

Table 3.25 Parameters for Diffusivity of N_2O in the Binary Solution of APA+H_2O and Ternary Solution of APA+MDEA+H_2O, APA+AMP+H_2O with AAD using Arrhenius Type Equation (Equations 3.28, 3.29 and 3.30)

Parameters	Systems		
	APA+H_2O	APA+MDEA+H_2O	APA+AMP+H_2O
a	$1.3931 \cdot 10^{-5}$	$3.5 \cdot 10^{-6}$	$1.5219 \cdot 10^{-6}$
b	$1.1236 \cdot 10^{-5}$	$1 \cdot 10^{-6}$	$1.5621 \cdot 10^{-6}$
c	$2.2984 \cdot 10^{-5}$	$5.6 \cdot 10^{-7}$	$1.57 \cdot 10^{-6}$
d	-2690.3	$3 \cdot 10^{-6}$	$3.0287 \cdot 10^{-6}$
e		$2.77 \cdot 10^{-6}$	$2.7701 \cdot 10^{-6}$
f		$2.4 \cdot 10^{-6}$	$2.994 \cdot 10^{-6}$
h	-546.9	3228	3248.3
AAD%	4.61	3.89	2.57

Table 3.26 Parameters A_1, A_2, A_3, A_4, A_5, A_6 for Diffusivity of N_2O in the Binary Solutions of APA+H_2O and Ternary Solutions of APA+MDEA+H_2O, APA+AMP+H_2O with AAD using Polynomial Models (Equations 3.31, 3.32 and 3.33)

Parameters	Systems		
	APA+H_2O	APA+MDEA+H_2O	APA+AMP+H_2O
A_1	-27.88	-25.745	-29.028
A_2	-5385.46	-183.493	-136.92
$10^2 \cdot A_3$	2.573	-48968.7	-310.4
$10^3 \cdot A_4$	33812	18.317	26.212
$10^3 \cdot A_5$	-53.2	512.004	416.54
$10^3 \cdot A_6$	0.7168	1256.51	1.1248
AAD%	1.75	2.17	2.44

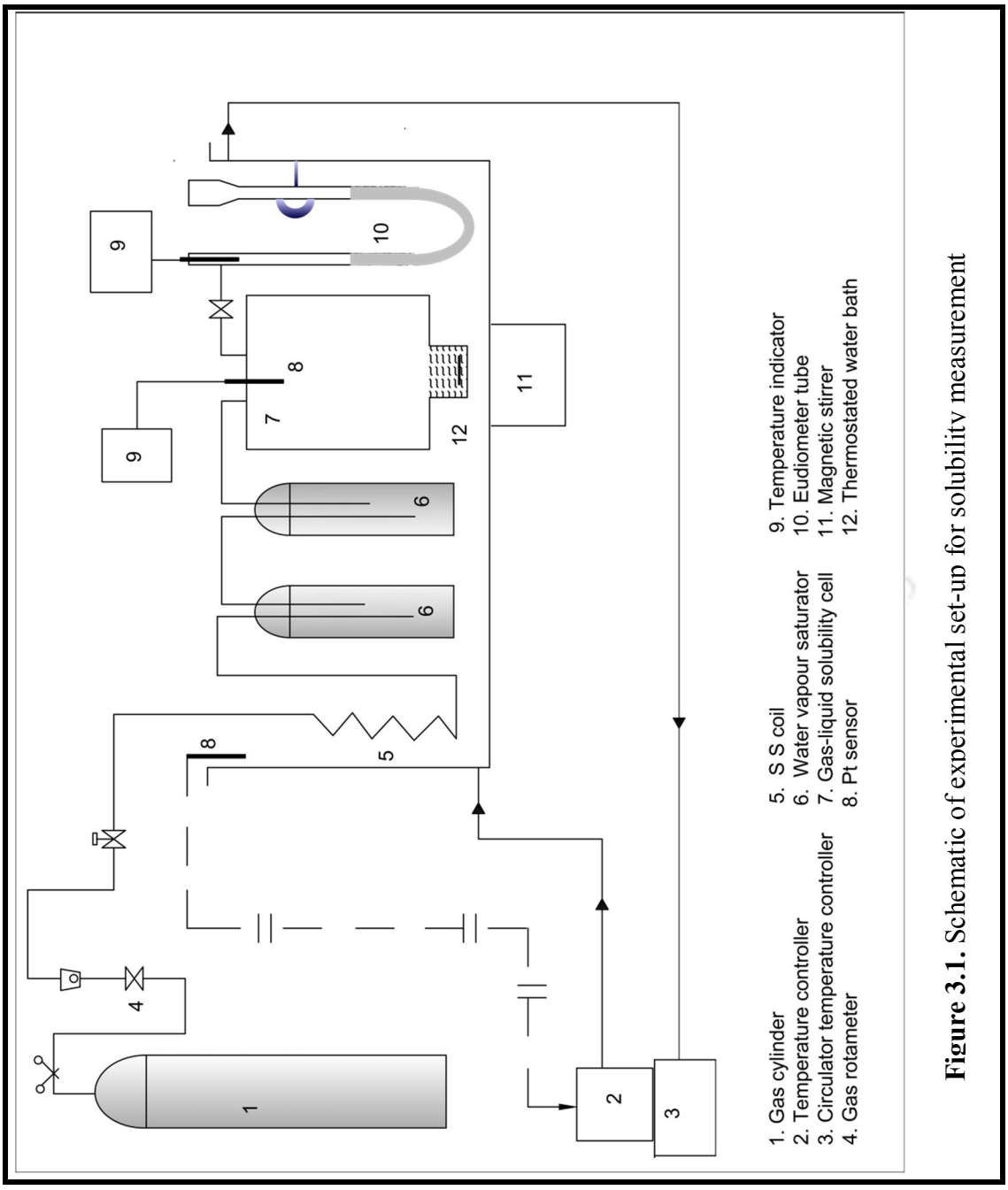

Figure 3.1. Schematic of experimental set-up for solubility measurement

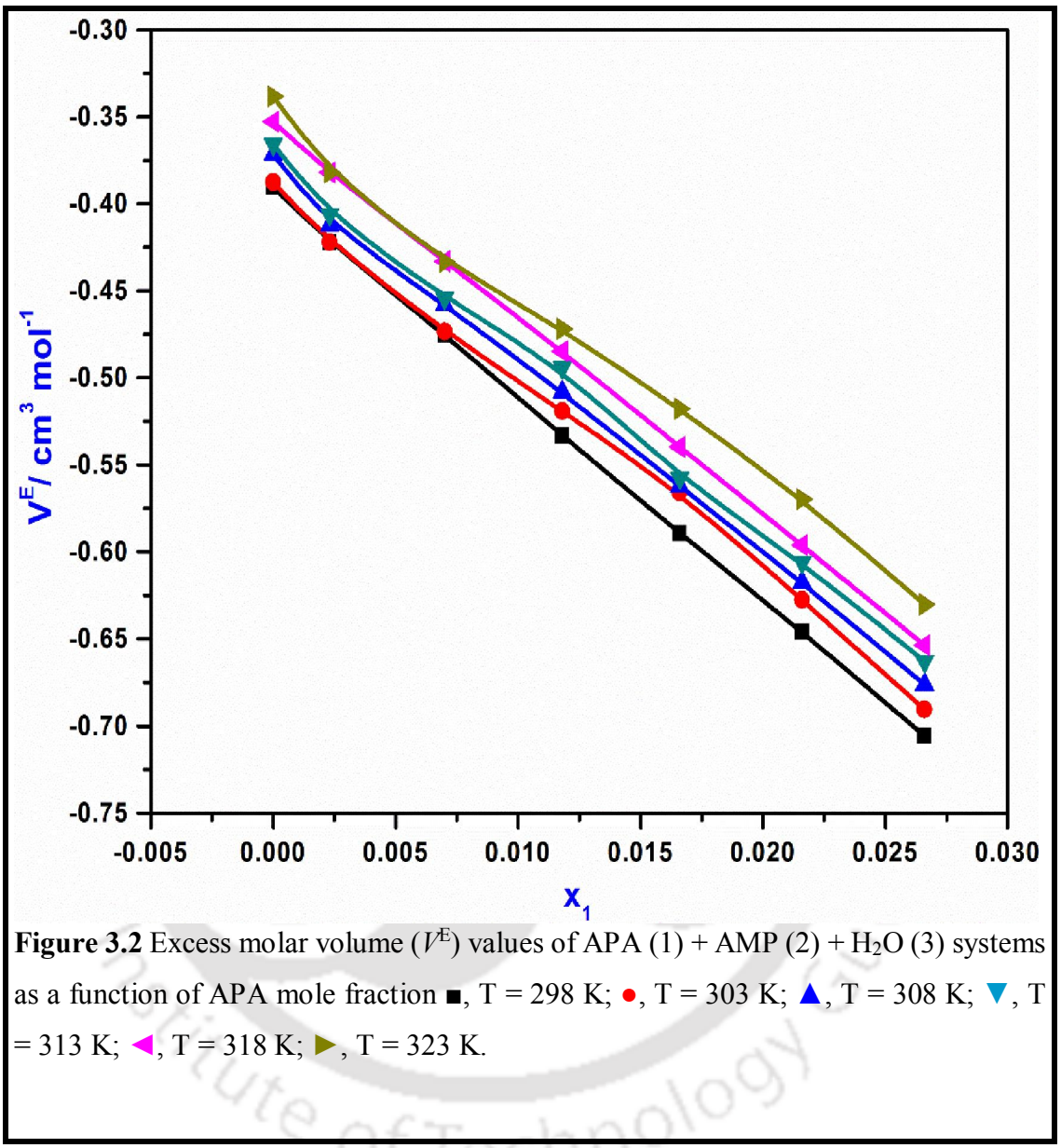

Figure 3.2 Excess molar volume (V^E) values of APA (1) + AMP (2) + H_2O (3) systems as a function of APA mole fraction ■, T = 298 K; ●, T = 303 K; ▲, T = 308 K; ▼, T = 313 K; ◄, T = 318 K; ►, T = 323 K.

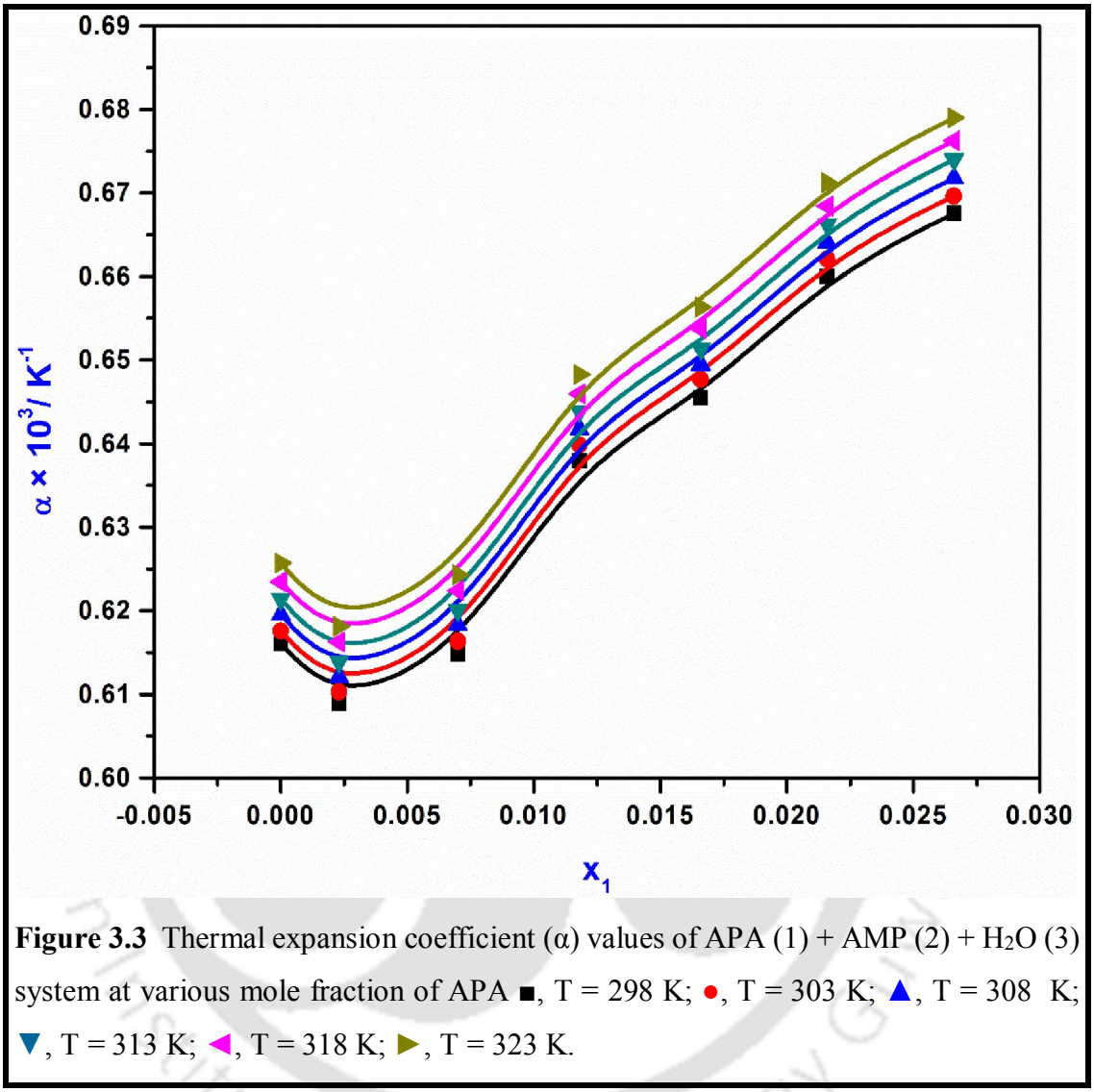

Figure 3.3 Thermal expansion coefficient (α) values of APA (1) + AMP (2) + H_2O (3) system at various mole fraction of APA ■, T = 298 K; ●, T = 303 K; ▲, T = 308 K; ▼, T = 313 K; ◄, T = 318 K; ►, T = 323 K.

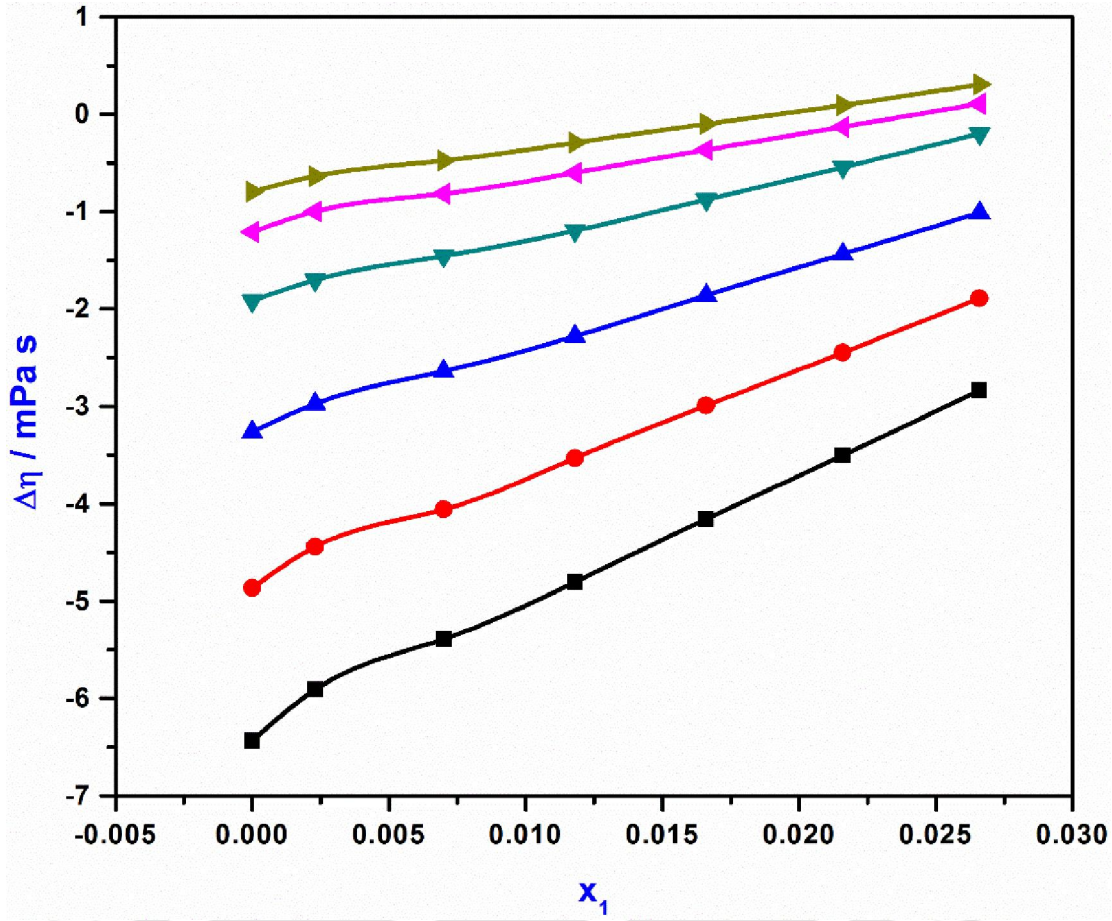

Figure 3.4 Viscosity deviation ($\Delta\eta$) values of APA (1) + AMP (2) + H_2O (3) system against APA mole fraction ■, T = 298 K; ●, T = 303 K; ▲, T = 308 K; ▼, T =313 K; ◀, T = 318 K; ▶, T = 323 K.

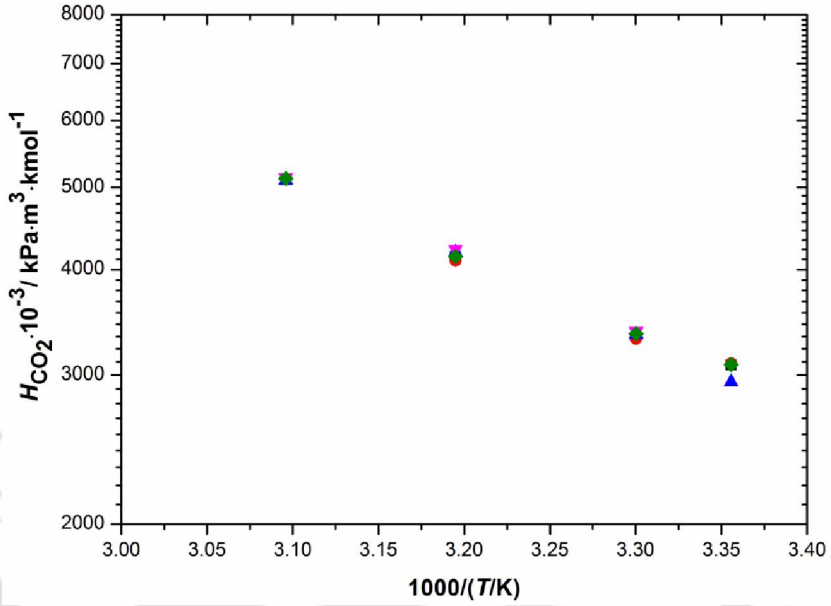

Figure 3.5 ($H_{CO_2-H_2O}$) as a function of temperature (T): ■, Paul et al.(2009a); ●, Mandal et al.(2005); ▲, Al-Ghawas et al.(1989); ▼, Li and Lai (1995); ♦, this study.

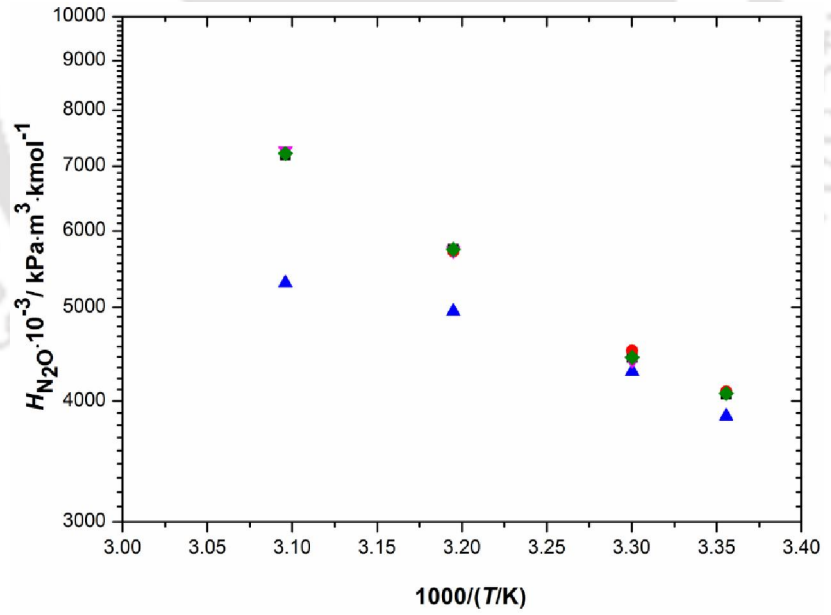

Figure 3.6 ($H_{N_2O-H_2O}$) as a function of temperature (T): ■, Paul et al.(2009a); ●, Mandal et al.(2005); ▲, Al-Ghawas et al.(1989); ▼, Li and Lai (1995); ♦, this study.

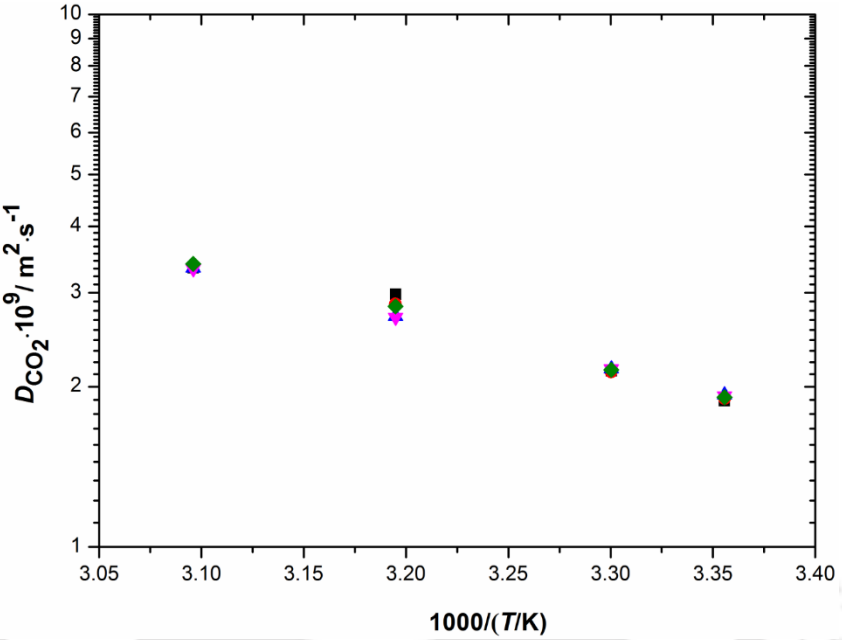

Figure 3.7 ($D_{CO_2-H_2O}$) as a function of temperature: ■, Paul et al.(2009a); ●, Mandal et al.(2005); ▲, Al-Ghawas et al.(1989); ▼, Li and Lai (1995); ♦, this study.

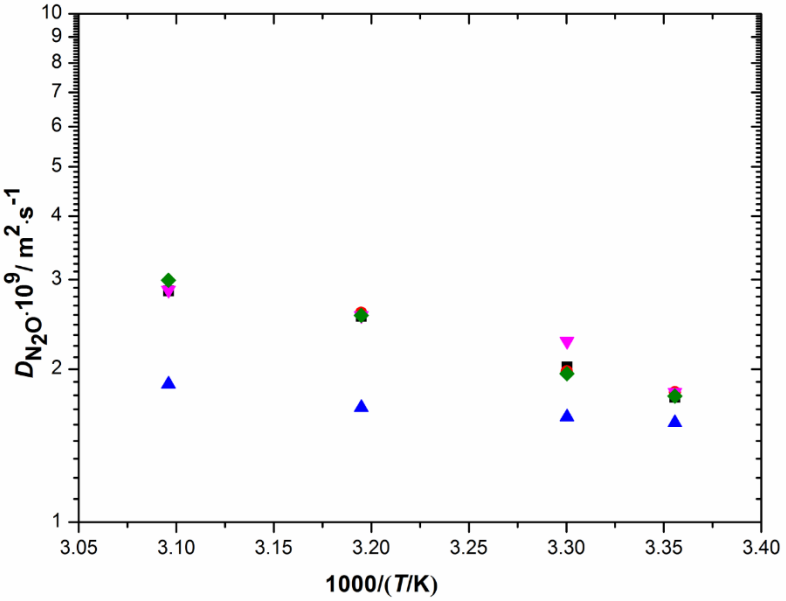

Figure 3.8 ($D_{N_2O-H_2O}$) as a function of temperature: ■, Paul et al.(2009a); ●, Mandal et al.(2005); ▲, Al-Ghawas et al.(1989); ▼, Versteeg and van Swaaij. (1988); ♦, this study.

CHAPTER 4

KINETICS STUDY OF ABSORPTION OF CARBON DIOXIDE INTO AQUEOUS AMINE SOLUTIONS

This chapter describes the CO_2 absorption into novel aqueous amine solutions of APA as well as aqueous blends of APA with MDEA and AMP. A fabricated short wetted wall contactor was used for this kinetics measurements. A qualitative nuclear magnetic resonance [NMR (1D and 2D)] spectroscopy method has been applied to confirm the final reaction products and to describe the reaction mechanism of novel APA-CO_2 reactions. Based on the pseudo-first-order condition for the CO_2 absorption, kinetic data for novel amine solvent measurement are reported. A substantial enhancement of rate in comparison to the single AMP or MDEA solution were observed due to the addition of a small amount of APA in the blend. A parametric sensitivity analysis has been investigated to examine the effect of important physicochemical and kinetic parameters on the specific rate of absorption of CO_2 into novel amines solutions.

4.1 INTRODUCTION

Globally, the capture of anthropogenic CO_2 from power plants and other industrial sources has become a critical environmental concern because CO_2 is a root cause for global warming (Khan et al., 2015; Paul and Thomsen, 2012; Wong et al., 2016; Nugent et al., 2013; Das et al., 2017[a]). Different industries like natural and

[a] Das, B., Deogam, B., Mandal, B., 2017. Absorption of CO_2 into novel aqueous bis(3-aminopropyl)amine and enhancement of CO_2 absorption into its blends with N-methyldiethanolamine. International Journal of Greenhouse Gas Control 60, 172–185.

synthesis gas processing plants, coal-based power plants, and cement plants are proved the potentiality of the absorption based technique (Dash et al., 2011).

Out of various solvents, researchers primarily draw attention towards the use of amines and alkanolamines as a solvent due to its basicity, since CO_2 is acidic in nature. A broad variety of conventional alkanolamines like monoethanolamine (MEA), diethanolamine (DEA), di-2-propanolamine (DIPA), N-methyldiethanolamine (MDEA), triethanolamine (TEA), 2-amino-2-methyl-l-propanol (AMP) have been investigated for industrial gas treatment (Kohl and Nielsen, 1997). The solvent systems studied so far, has many drawbacks which include the inability to fulfil the desired physicochemical properties as well as the flexibility required for CO_2 removal. In order to develop potential post-combustion carbon capture (PCC) using alkanolamine based solvent systems, significant advancements need to be made (Conway et al., 2015). For effective design of a CO_2 treating plant and process simulation, reaction kinetics play a vital role. Although there are many characteristics which determine the physical size and footprint of the absorber, reaction kinetics is the most important one. In an amine-based post-combustion carbon capture (PCC) system at 90% CO_2 recovery, more than half of the overall energy requirement accounts for solvent regeneration. Besides this, the stoichiometric CO_2 loading capacity of MEA is 0.5 mole CO_2 per mole amine. More volatility and the high rate of degradation, i.e., degradation product, can be an environmental issue and dealing with them can increase overall cost. The large size of the stainless steel absorber and stripping columns, and solvent regeneration contributes 70% to the overall capital cost of MEA-based PCC process (Artanto et al., 2014; Conway et al., 2013). Thus, the higher cost of CO_2 capture from power plant flue gas reduces the motivation of up-scaling in the MEA-based PCC process. Generally, tertiary amine has the capacity to absorb the proton released from carbonic acid, which is formed by the reaction between CO_2 and water but tertiary amines do not from carbamates in the reaction with CO_2. In addition, MDEA offers great savings in regeneration energy demand i.e., less heat for regeneration as well as less corrosivity than primary and secondary amines (Details of MDEA are discussed in Chapter 1,

Section 1.2.1.2.1). The sterically hindered form of primary amine (Gabrielsen et al., 2007) i.e., AMP absorbs CO_2 more slowly than MEA. But thermal degradation is much more resistant than MEA, and oxidative degradation is two order of magnitude slower than MEA (Dash et al., 2011; Dash et al., 2014). No degradation product was observed for both MDEA and AMP after heating for 14 days at 403 K in the study conducted by Barzagli et al. (2010) (Details of AMP are discussed in Chapter 1, Section 1.2.1.2.1).

While MDEA and AMP acts only as a base in solution and consequently being slower in reaction kinetics, the addition of a small amount of fast reacting amine like single molecule containing two or more amine groups is necessary for enhancing the overall absorption rate into the formulated amine solutions (Conway et al., 2015). Mixtures of primary and tertiary or secondary and tertiary alkanolamine are also formulated which offer to outperform conventional single alkanolamine solution (Mandal et al., 2006). However, the prospect of significant improvements towards current generation solvent which can provide faster reaction kinetics, high equilibrium loading capacity, smaller size of equipment, reduction in the overall energy penalty, higher degradation resistance, less corrosivity and ultimately, lower capital cost is one of the most pivotal point of PCC technology (Liu et al., 2014).

In recent years, extensive research focused towards the finding of rate activators which are far superior to conventional rate accelerators. Sun et al. (2005) described the reaction kinetics of CO_2-Piperazine (PZ)-H_2O system employing a wetted wall column absorber (303-313 K) and showed a pseudo first-order reaction rate constant at (303 K) to be 29185 $m^3\ kmol^{-1}\ s^{-1}$. However, Bindwal et al. (2011) reported the values of rate constant for the CO_2-PZ-H_2O system an identical condition at (303 K) to be 25800 $m^3\ kmol^{-1}\ s^{-1}$. Paul et al. (2009a) studied absorption of CO_2 in aqueous 2-(1-piperazinl)-ethylamine (PZEA) solutions and rate constant was 31867.6 $m^3\ kmol^{-1}\ s^{-1}$ at 303 K. While, Dubois et al. (2010) experimentally estimated and clearly visualized the positive effect of blending of PZEA to MDEA and MEA solutions. PZ as well as PZEA are considered to be efficient activators than conventional rate accelerators and the rate constant of PZ is one order of magnitude higher than MEA (Samanta et al., 2011). CO_2

capture technique using activated solvents such as blends of PZ or PZEA with MDEA/AMP has been reported to have a more CO_2 absorption capacity due to the high reaction rate and high CO_2 loading. Moreover, the cost of regeneration of such activated solvents is relatively low (Paul et al., 2009b; Appl et al., 1982; Das et al., 2017[b]). Furthermore, it may able to fulfil towards the requirements of lower capital cost (Liu et al., 2014).

Keeping this in view, a novel amine bis(3-aminopropyl)amine (APA) is proposed as an activator in this study. The kinetics of CO_2 absorption into APA is essential for a better understanding of the mechanism and working principle towards CO_2 absorption. Moreover, the reaction kinetics is necessary to provide the input parameter for diffusion reaction-based model. However, the major objective of this study is to find out how APA performs as an accelerator when blended with other amines like MDEA, AMP instead of an individual solvent and to develop a reaction mechanism of the CO_2-(MDEA-APA-H_2O) and CO_2-(AMP-APA-H_2O) system. Hence, in this study, the rates of absorption in the CO_2-(APA-H_2O) system are determined within the concentration range of 0.1-0.5 kmol m^{-3} and temperatures of 303, 308, 313 and 323 K. The kinetic rate parameters have been calculated on the basis of CO_2 absorption rate under the above mentioned experimental conditions. At the same time one-dimensional (1D) and two-dimensional (2D) (^1H and ^{13}C) NMR spectroscopic methods have been applied to confirm the reaction scheme of CO_2-(APA-H_2O) system. Furthermore, due to the immense commercial significance of novel blended amine solvent (APA+MDEA+H_2O) and (APA+AMP+H_2O), the kinetics of CO_2 absorption into (APA+MDEA+H_2O) and (APA+AMP+H_2O) which were not published in open literature so far, have been investigated. To observe the enhancement of overall CO_2 absorption rate, APA concentration as an activator was varied from 0 to 0.5 kmol m^{-3} into aqueous MDEA and AMP whereas total concentration of amine was kept at 3 kmol m^{-3}.

[b] Das, B., Deogam, B., Mandal, B., 2017. Experimental and theoretical studies on efficient carbon dioxide capture using novel bis(3-minopropyl)amine (APA)-activated aqueous 2-amino-2-methyl-1-propanol (AMP) solutions. RSC Advance 7, 21518–21530.

4.2 THEORY

The absorption flux is enhanced by the chemical reaction in the liquid phase in a gas-liquid contactor and is presented by Eq. (4.1)

$$N_{CO_2} = E_A k_L [CO_2]_i \tag{4.1}$$

The above equation is valid when the liquid bulk does not contain any CO_2 and the gas-side mass transfer coefficient is completely negligible. The enhancement factor, E_A, describes the mass transfer rate which is influenced by a chemical reaction. The enhancement factor is defined as the ratio of the flux of CO_2 in the presence of chemical reactions to the flux of CO_2 in the absence of chemical reactions used an identical CO_2 concentration difference between the interface and the liquid bulk of the absorbing gas. It is necessary because this single term incorporates the possible effects of all chemical reactions on the absorption rate. For certain reaction regimes, to predict the enhancement factor based on the different mass transfer models, several approximate solutions are available in the literature (Kierzkowska-Pawlak et al., 2015). Doraiswamy et al. (1984) presented the specific rate of mass transfer of CO_2 as:

$$N_{CO_2} = -D_{CO_2}\left(\frac{d[CO_2]}{dw}\right)_{w=0} = [CO_2]_i \frac{\sqrt{D_{CO_2} k_{ov}}}{\tanh\left(\sqrt{D_{CO_2} k_{ov}}/k_L\right)} \tag{4.2}$$

In Eq. (4.2), the interfacial (gas-liquid interface) concentrations of CO_2 were denoted by $[CO_2]_i$

To ensure that absorption has been carried out in the pseudo-first-order reaction regime, the absorption conditions of the CO_2-(APA-H_2O), CO_2-(APA-MDEA-H_2O) and CO_2-(APA-AMP-H_2O) systems were selected accordingly. The linear relationship of the flux versus CO_2 partial pressure is expected in this regime. When the *Hatta*

number is greater than 3, then tanh Ha in above equation is close to one and it is assumed that enhancement factor is equal to dimensionless Hatta number ($E_A = Ha$) with

$$Ha = \sqrt{k_{ov} D_{CO_2}} / k_L \tag{4.3}$$

Also, the defining condition in the fast-pseudo-first order regime is $3 < Ha << E_\infty$. The infinite enhancement factor (E_∞) can defined as follows:

$$E_\infty = \sqrt{\frac{D_{CO_2}}{D_{Amn}}} + \frac{[Amn]}{Z[CO_2]_i}\sqrt{\frac{D_{Amn}}{D_{CO_2}}} \tag{4.4}$$

The determination of the exact value of infinite enhancements factor is very difficult. However, independency of contact time on flux and linear relationship of flux versus CO_2 partial pressure satisfies the fast-pseudo-first order regime (Singh et al., 2011). Using Eqs. (4.1) and (4.3), the specific rate of mass transfer of CO_2 becomes

$$N_{CO_2} = [CO_2]_i \sqrt{D_{CO_2} k_{ov}} \tag{4.5}$$

From the above equation, it can be concluded that rate of absorption does not depend on liquid side mass transfer coefficient, k_L, and therefore, independent of the hydrodynamic conditions. The interfacial concentrations of CO_2 were denoted by $[CO_2]_i$ and obtained from Henry's law:

$$[CO_2]_i = \frac{p_{CO_2}}{H_{CO_2}} \tag{4.6}$$

After incorporation of Eq. (4.6), Eq. (4.7) is transformed to:

$$N_{CO_2} = \frac{p_{CO_2}}{H_{CO_2}} \sqrt{D_{CO_2} k_{ov}} \tag{4.7}$$

Hence, the absorption kinetics measurements were interpreted on the basis of Eq. (4.7). On the other hand, to find $k_{ov,}$ (in the fast-pseudo-first-order regime) determination of H_{CO_2}, D_{CO_2} and the absorption rate for CO_2 into the amine is essential.

4.3 EXPERIMENTAL

4.3.1 Materials

The solvents APA, MDEA and AMP used for this kinetics study were similar as described in details of the previous Chapter in Section 3.3.1. CO_2 gas had a purity of 99.995%. Similarly, Vadilal Gases, India provided calibrated CO_2 and N_2 gas mixtures for the experiment where absorption was carried out. Deuterium oxide (D_2O) was used for NMR measurement while concentrated HCl was utilized for desorption cell. Neutral EXTRAN (N) cleaning solution was procured from E. Merck (India).

4.3.2 Preparation of the aqueous amine solvent and NMR measurement

The solutions required for all the experiments were prepared using Millipore water of surface tension and conductivity of the magnitude 72 mN/m and 1×10^{-7} Ω^{-1} cm^{-1} at 298 K, respectively (Rahaman et al., 2010). For the preparation of each amine solutions, a Sartorious balance (BSA 224S-CW) with an accuracy of 0.001% was used. Prior to preparation of amine solutions, the water degassing was conducted using prolonged boiling followed by cooling under vacuum. To determine the actual concentration of amine solutions, a quality control step, acid-base titration against standard HCL was carried out using an auto-titrator (DL–50, Mettler Toledo,

Switzerland). Thus the uncertainty in the determination of amine concentrations was found out to be within 0.01 %. For the experimental findings, three different APA concentration (0.1-0.5 kmol m^{-3}) and eight amine blends of MDEA/AMP, APA i.e., (3 kmol m^{-3} MDEA/AMP), (2.9 kmol m^{-3} MDEA/AMP+ 0.1 kmol m^{-3} APA), (2.7 kmol m^{-3} MDEA/AMP+ 0.3 kmol m^{-3} APA), (2.5 kmol m^{-3} MDEA/AMP + 0.5 kmol m^{-3} APA) were used with total concentration of 3 kmol m^{-3} for absorption of CO_2. The aqueous solution of 2 kmol m^{-3} MDEA as reference absorbent was used to validate the experimental set-up.

A batch solution was prepared using APA into Millipore water (unloaded solution) for the present NMR measurement. CO_2/N_2 gas mixture (15% CO_2) was bubbled into the amine solution and it was continued in the measurements to ensure complete equilibration of the reaction (Barzagli et al., 2010; Conway et al., 2013; Lim et al., 2012). In equilibrium condition, the inlet and outlet CO_2 concentration are same which was checked by GC analysis. This equilibrium solution and unloaded solutions were collected and studied using 600 MHz NMR spectrometer (Ascend^{TM} aeon 600 NMR spectrometer, Bruker). D_2O was used to get a signal lock for NMR measurement. ^{1}H and ^{13}C NMR measurements of 1D and 2D study were performed in details. NMR analysis parameters at room temperature are given in Table 4.1.

4.3.3 Apparatus

A wetted-wall column contactor (Paul et al., 2009a; Conway et al., 2015; Choi et al., 2014) which consist of three concentric stainless steel tubes was used to determine the reaction kinetics of the CO_2-APA-H_2O, CO_2-APA-MDEA-H_2O, CO_2-APA-AMP-H_2O system. The outside diameter of wetted-wall contactor was 2.81×10^{-2} m. The outer surface of the tube provides an interfacial area for capturing the solute gas. The length of the column was adjusted manually at length of 7×10^{-2} m throughout this work. In this absorption study, a jacketed glass shroud formed the gas phase enclosure which

consists a gas inlet at the top and three equally shroud gas outlets at the bottom. A water circulating temperature controller was used to maintain the temperature of the gas phase enclosure at the desired level. An overhead vessel was employed to store the aqueous amine solution. A constant liquid flow through an outside part of the tube and gas were monitored using calibrated rotameters. Thermostated water was circulated through the middle of a concentric tube, which forms a two-pass heat exchanger, to maintain the liquid film temperature. At the end of the absorption length, three samples of CO_2 loaded aqueous solutions were collected in the liquid receiver at a fixed interval to obtain steady state absorption flux. Each data was the average value of three liquid solutions. A thermostated gas cell with a manometric device was used to measure the total CO_2 content of a loaded liquid (Mandal and Bandyopadhyay, 2006).

4.3.4 Procedure

Neutral EXTRAN (N) cleaning solution was used to clean thoroughly the absorption surface of the column and to ensure cleanness of outer surface of the column distilled water was used before each run for getting continuous ripple free film. To establish the thermal equilibrium for gas absorption in liquid, thermostated water was circulated through wetted wall column, the jacket of the glass shroud and through the bath, whereas the gas inlet coil was immersed in that bath.

Through the saturators immersed in the controlled temperature bath and the coil immersed in the same bath, the gas mixtures of CO_2 and N_2 or Pure CO_2 were passed for absorption of CO_2. From the top of absorption space of the wetted wall column, the gas which saturated with water vapour at the desired temperature of absorption was fed. The amine solution, thermostated at the desired temperature for the absorption of CO_2, was taken in the overhead storage. Then the liquid was provided to the contactor at the desired flow rate. The temperature of absorption was controlled by the circulator

temperature controller within about ± 0.25 K. All experiments were conducted with initial CO_2-free solution under atmospheric pressure.

Total CO_2 content of the loaded liquid sample was found out through acidulating a known liquid sample, placed in a thermostated bath and measurement of evolved gas with the help of gas burette. At first temperature of the room controlled such a way that cell as well as burette was maintained within ± 0.5 K of 298 K. Then (10×10^{-6} m^3) of liquid solution was introduced in the cell and 4 N HCl solution was fed to it in excess and well stirred by magnetic stirrer. The whole system was allowed to attain thermal equilibrium and the evolved gas was measured by the gas burette. The measurement of volume in gas was corrected for the vapour pressure of liquid at the test temperature. Hence, the liquid phase analysis by acidulation was considered to estimate the specific rate of CO_2 in this study which are used several authors in before (Hikita et al., 1979; Glasscock, 1990; Glasscock et al., 1991; Saha et al., 1995).

4.4 REACTION MECHANISM

4.4.1 Hydration of CO_2 in aqueous solutions

The following reactions are involved in hydration of CO_2 and formation of bicarbonate:

$$CO_2 + H_2O \rightleftharpoons HCO_3^- + H^+ \quad (4.8)$$

$$CO_2 + OH^- \rightleftharpoons HCO_3^- \quad (4.9)$$

The reaction (4.8) contributes very less to the overall reaction rate since it has a negligible rate constant (k = 0.026 s^{-1} at 298 K) (Pinsent et al., 1956) and hence can be avoided for the experimental condition in the present study. The reaction (4.9) doesn't show a significant contribution to the overall reaction. Therefore, the reaction between the CO_2 and OH^- ion is neglected as well.

4.4.2 Reactions of CO_2 with APA

4.4.2.1 Reaction mechanism

Caplow (1968) and Danckwerts (1979) proposed the two-step zwitterion mechanism which is the widely accepted reaction mechanism for the reaction between CO_2 and amines (primary and secondary). Presuming this zwitterion mechanism for APA, although it is not an alkanolamine, the formation of an intermediate zwitterion in the reaction of CO_2 and APA should occur as follows:

$$CO_2 + APA \underset{}{\overset{k_{2,APA}, k_{-1}}{\rightleftharpoons}} APAH^+COO^- \tag{4.10}$$

In Eq. (4.10) the intermediate zwitterion formed in the reaction undergoes deprotonation by either a base or a number of bases, such as H_2O, OH^- or amine, APA to form carbamate:

$$APAH^+COO^- + B \xrightarrow{\hat{k}_B} APACOO^- + BH^+ \tag{4.11}$$

The reaction mechanism of APA with CO_2 is illustrated below:

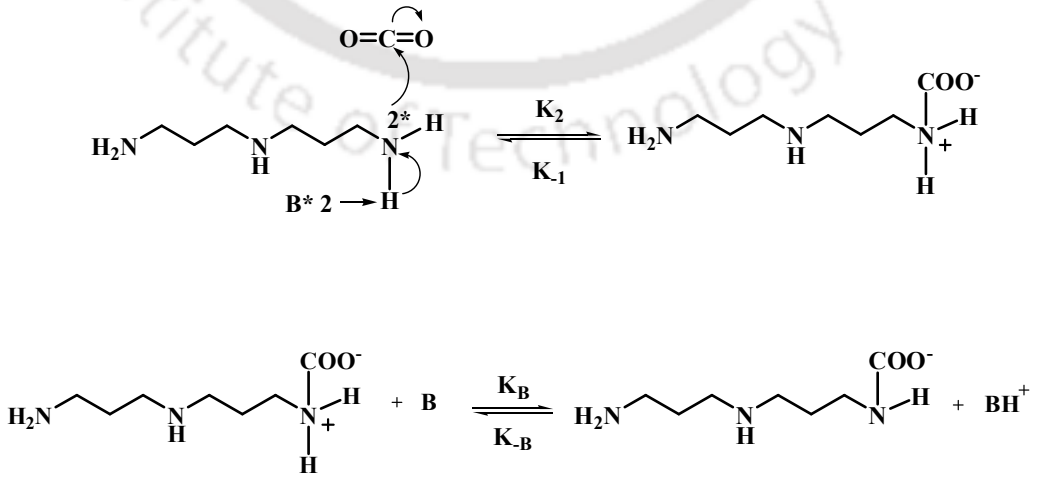

Two lone electrons present at nitrogen and at base atom in above mechanism are denotes as '*2'.

The overall rate of the reaction of CO_2 in aqueous amine solutions using the steady-state principle via intermediate zwitterion as given in Eq. (4.10) can be written as follows:

$$r_{CO_2\text{-APA}} = \frac{[APA][CO_2]}{\frac{1}{k_{2,APA}} + \frac{k_{-1}}{\overset{\Lambda}{k}_B(B)k_{2,APA}}} = \frac{[APA][CO_2]}{\frac{1}{k_{2,APA}} + \frac{1}{k_B(B)}} \quad (4.12)$$

A combination of bases which is represented by the kinetic constant $\overset{\Lambda}{k}_B(B)$, where $k_B = k_{2,APA}\overset{\Lambda}{k}_B / k_{-1}$.

The two asymptotic situations are exist for the above rate equation.

Case I. When deprotonation reaction is very high in comparison to reverse reaction and rate determining step is zwitterion formation, the kinetics rate expression becomes simple second order kinetics as given bellow:

$$r_{CO_2\text{-APA}} = k_{2,APA}[CO_2][APA] \qquad \text{when } (k_{-1} \ll \overset{\Lambda}{k}_B(B)) \quad (4.13)$$

Case II. The opposite condition i.e., when $(k_{-1} \gg \overset{\Lambda}{k}_B(B))$ and zwitterion deprotonation is rate-determining, then the rate equation becomes

$$r_{CO_2\text{-APA}} = \frac{k_{2,APA}\overset{\Lambda}{k}_B(B)}{k_{-1}}[CO_2][APA] \quad (4.14)$$

This expression is suggested for shift in reaction order between one and two with respect to amine concentration, since the contribution of individual bases to deprotonate the zwitterions are considered to estimate the reaction order.

The reaction rate depends on the concentration of each base and its strength. However, the contribution of the hydroxide ion is very less and hence it doesn't affect the accuracy much because [OH^-] has a low concentration in amines' reaction with CO_2 (Paul et al., 2009a). Laddha et al. (1981) also considered only the amines as the base for aqueous alkanolamine solutions in their studies.

4.4.2.2 One-dimensional and two-dimensional NMR study

Figure 4.1 show the ^1H spectra of aqueous APA solution before and after the reaction with CO_2. In ^1H NMR spectra (Figure 4.1) of the reaction mixture, several overlapping regions were observed that indicate the presence of CH_2 groups, which correspond to different CH_2 groups of mono- and di-carbamates. As we know Total Correlation Spectroscopy (TCOSY) represents a separate spin system of a compound depending on the mixing time. In our TOCSY (^1H–^1H) spectra as shown in Figure 4.2, many separate regions were visualized which represent a different spin system of different compounds. So from that spectrum, we can say mono-carbamate and di-carbamate corresponding to primary and secondary amine groups were present. But no clear evidence of the presence of tri-carbamate was found. The presence of different CH_2 groups in the reaction mixture was confirmed by Distortionless Enhancement by Polarization Transfer (DEPT–135) experiment (shown in Figure 4.3). From the ^{13}C NMR spectra (as shown in Figure 4.4) of CO_2 loaded APA solution, four peaks were observed at different positions in the low field range (163–165 ppm) corresponding to carbonyl carbon, which represent the different carbamate groups. In the higher field range (26–45 ppm), different CH_2 carbons were present, which corresponds to different CH_2 carbon from a different set of products. These were also confirmed by

Heteronuclear Multiple Bond Coherence (HMBC) and Heteronuclear Single Quantum Coherence (HSQC) experiments (Figures 4.5 and 4.6). The enlarged version of ^{1}H spectra as well as the HMBC (^{1}H–^{13}C) of CO_2-loaded APA and HSQC (^{1}H–^{13}C) spectra of starting APA solutions are given in Figures 4.7 to 4.9, respectively. Hence, the formulation of mono and di-carbamates corresponding to primary and secondary amine groups were visualized based on the desired peaks in the NMR spectra.

4.4.2.3 Carbamate formation during absorption

The chemistry of the CO_2-APA-H_2O reaction system is very complex since APA contains multiple amine functional groups. This leads to a large number of possible chemical reactions and formation of liquid phase species (e.g., carbamate and dicarbamate corresponding to primary and secondary amine groups). Hence it is tough to find out the most important reaction(s), and the effects of these reactions on an overall absorption rate are not easily predictable. However, by utilizing Brønsted dependency of the reactivity (pK_a value), an initial prediction on these reactions can be made. This is because of the existence of a linear relationship between amine's pK_a value with the logarithm of a forward rate constant (Conway et al., 2013; Singh et al., 2011; Paul et al., 2009a). If Brønsted relation to APA is assumed, then the formation of carbamates (primary and secondary) due to the reaction of CO_2 with amine groups (primary and secondary) should be taken into account. Now, through the concentration of the major reactants APA and carbamates (primary and secondary), the possible formulation of di-carbamate can be assessed. To ensure the absorption regime, the absorption conditions (amine concentrations and partial pressures of CO_2) were selected accordingly. Owing to the reaction with CO_2, the interfacial concentration of APA in this regime is not noticeably decreasing. Therefore, reaction products of the mono-carbamates concentrations are small, even near to the gas-liquid interface. In comparison with the remaining APA concentrations, mono-carbamates concentrations are small and this

gave a small contribution to the formulation of di-carbamates. Hence, the concentrations of di-carbamates were negligible.

Since bis(3-aminopropyle)amine contains two primary amine groups and one secondary amine group it is expected to be faster than other rate promoters like *N*-(2-Aminoethyl) ethanolamine, PZ and PZEA. It was established in the literature that at a small loading of CO_2, the primary amine group reacts faster than the secondary amine group (Barzagli et al., 2009; Kierzkowska-Pawlak et al., 2015). Therefore, using similar pathways the reaction of CO_2 with both amine groups of APA can be described since carbamate are formed by both amine groups. The reactions are given as follows.

$$CO_2 + APA + B \rightleftharpoons APACOO^-_p + BH^+ \tag{4.15}$$

$$CO_2 + APA + B \rightleftharpoons APACOO^-_s + BH^+ \tag{4.16}$$

where, $APACOO^-_p$ and $APACOO^-_s$ denotes primary and secondary carbamates, respectively. But finding the actual concentration of APA which contributes to a particular reaction is troublesome. Therefore, to estimate the comparative donation of each reaction towards the overall reaction rate is also difficult (Paul et al., 2009a). Hence, the reaction was assumed to be of first order with respect to both CO_2 and APA. In later discussions, the justifiability of this assumption is substantiated experimentally. Therefore, the reaction rate of CO_2 with APA can be expressed based on Eq. (4.13) as:

$$r_{CO_2\text{-}APA} = k_{2,APA}[CO_2][APA] = k_{ov\text{-}APA}[CO_2] \tag{4.17}$$

Here $k_{ov\text{-}APA}$ and $k_{2,APA}$ denotes the overall rate constant and the second order reaction rate constant, respectively.

4.4.3 Reactions of CO_2 with blends of (APA + MDEA)

4.4.3.1 Reaction scheme

Absorption of CO_2 into aqueous blends of tertiary amine, MDEA and rate activator, APA proceed via several reversible reactions. These reactions are discussed below.

Base-catalysed hydration reaction

$$CO_2 + MDEA + H_2O \xleftrightarrow{K_a, k_{2a}} MDEAH^+ + HCO_3^- \quad (4.18)$$

Monocarbamate formation by APA-H_2O:

$$CO_2 + APA + H_2O \xleftrightarrow{K_b, k_{2b}} APACOO^- + H_3O^+ \quad (4.19)$$

Monocarbamate formation by MDEA-APA:

$$CO_2 + APA + MDEA \xleftrightarrow{K_c, k_{2c}} APACOO^- + MDEAH^+ \quad (4.20)$$

Dicarbamate formation by APA-H_2O:

$$CO_2 + APACOO^- + H_2O \xleftrightarrow{K_d, k_{2d}} APA\left(COO^-\right)_2 + H_3O^+ \quad (4.21)$$

Dicarbamate formation by MDEA-$APACOO^-$:

$$CO_2 + APACOO^- + MDEA \xleftrightarrow{K_e, k_{2e}} APA\left(COO^-\right)_2 + MDEAH^+ \quad (4.22)$$

Bicarbonate formation by direct reaction of CO_2 with H_2O:

$$CO_2 + 2H_2O \xleftrightarrow{K_f, k_{2f}} HCO_3^- + H_3O^+ \quad (4.23)$$

Formation of carbonate:

$$HCO_3^- + H_2O \xleftrightarrow{K_g} CO_3^- + H_3O^+ \quad (4.24)$$

Protonation of APA:

$$APA + H_3O^+ \xleftrightarrow{K_h} APAH^+ + H_2O \quad (4.25)$$

Protonation of mono-carbamate formed:

$$APACOO^- + H_3O^+ \xleftrightarrow{K_i} H^+APACOO^- + H_2O \quad (4.26)$$

Protonation of MDEA:

$$MDEA + H_3O^+ \xleftrightarrow{K_j} MDEAH^+ + H_2O \quad (4.27)$$

Dissociation of water molecule:

$$2H_2O \xleftrightarrow{K_m} H_3O^+ + OH^- \quad (4.28)$$

where, $K_{x(x = a,....m)}$, $k_{2y(y = a,...f)}$ denotes as equilibrium constant for reaction (x) and second-order forward rate coefficient for reaction (y), respectively. The structure of important reaction intermediates and product are shown in Figure 4.10.

The tertiary alkanolamine cannot react directly with CO_2 to form carbamates because of lack of hydrogen atom attached to its nitrogen atom. In an aqueous environment, tertiary amines act as a base to promote CO_2 hydrolysis reaction and forms bicarbonate ions and protonated amine.

It was reported in most of the literature that the reaction between CO_2 and tertiary

alkanolamine (such as MDEA and DEEA) is a second-order reaction (Liu et al., 2014; Paul et al., 2009b; Kierzkowska-Pawlak et al., 2015). Therefore, absorption rate of CO_2 with MDEA can be expressed as

$$r_{CO_2\text{-MDEA}} = k_{2,MDEA}[CO_2][MDEA] = k_{ov\text{-}MDEA}[CO_2] \quad (4.29)$$

So the overall absorption rate of CO_2 for the absorption into (APA+MDEA+H_2O) is presented as follows

$$\begin{aligned} r_{CO_2} &= r_{CO_2\text{-APA}} + r_{CO_2\text{-MDEA}} \\ &= k_{2,APA}[CO_2][APA] + k_{2,MDEA}[CO_2][MDEA] \\ &= k_{ov}[CO_2] \end{aligned} \quad (4.30)$$

where K_{ov} is in terms of overall rate constant and expressed as

$$k_{ov} = k_{2,APA}[APA] + k_{2,MDEA}[MDEA]$$

4.4.4 Reactions of CO_2 with blends of (APA+ AMP)

4.4.4.1 Reaction scheme

The following reversible reactions describe the reaction rate of CO_2 into an aqueous amine blend solution of sterically hindered amine, AMP and rate activator, APA:

Base-catalysed hydration reaction:

$$CO_2 + AMP + H_2O \xleftrightarrow{K_{a1}, k_{2a1}} AMPH^+ + HCO_3^- \quad (4.31)$$

Monocarbamate formation by APA/H_2O:

$$CO_2 + APA + H_2O \xleftrightarrow{K_{b1}, k_{2b1}} APACOO^- + H_3O^+ \quad (4.32)$$

Monocarbamate formation by AMP/APA:

$$CO_2 + APA + AMP \xleftrightarrow{K_{c1}, k_{2c1}} APACOO^- + AMPH^+ \quad (4.33)$$

Dicarbamate formation by APA/H_2O:

$$CO_2 + APACOO^- + H_2O \xleftrightarrow{K_{d1}, k_{2d1}} APA\left(COO^-\right)_2 + H_3O^+ \quad (4.34)$$

Dicarbamate formation by AMP/$APACOO^-$:

$$CO_2 + APACOO^- + AMP \xleftrightarrow{K_{e1}, k_{2e1}} APA\left(COO^-\right)_2 + AMPH^+ \quad (4.35)$$

Bicarbonate formation by direct reaction of CO_2 with H_2O:

$$CO_2 + 2H_2O \xleftrightarrow{K_{f1}, k_{2f1}} HCO_3^- + H_3O^+ \quad (4.36)$$

Formation of carbonate:

$$HCO_3^- + H_2O \xleftrightarrow{K_{g1}} CO_3^- + H_3O^+ \quad (4.37)$$

Protonation of APA:

$$APA + H_3O^+ \xleftrightarrow{K_{h1}} APAH^+ + H_2O \quad (4.38)$$

Protonation of monocarbamate formed:

$$APACOO^- + H_3O^+ \xleftrightarrow{K_{i1}} H^+ APACOO^- + H_2O \quad (4.39)$$

Protonation of AMP:

$$AMP + H_3O^+ \xleftrightarrow{K_{j1}} AMPH^+ + H_2O \quad (4.40)$$

Dissociation of the water molecule:

$$2H_2O \xleftrightarrow{K_{m1}} H_3O^+ + OH^- \tag{4.41}$$

where, the equilibrium constants and second-order forward rate coefficients for reactions x, y are represented as $K_{x(x=a1,\ldots m1)}$ and $k_{2y(y=a1,\ldots f1),}$ respectively.

In the case of sterically hindered amine such as AMP, the only significant reaction of CO_2 with AMP is suggested to be a hydration of CO_2 catalyzed by AMP which formed bicarbonate ion (Yih and Shen, 1988; Seo and Hong, 2000). However, because of very small carbamate stability constant of AMP, the formation of carbamate is much lower in comparison to the bicarbonate ion (Dash et al., 2011; Sartori and Savage, 1983). Hence it can be neglected as well. The reaction between CO_2 and sterically hindered alkanolamine, AMP, is a second-order reaction as reported in several works of literature (Pei et al., 2008; Saha and Bandyopadhyay, 1995). Therefore, the absorption rate of CO_2 with AMP can be represented as

$$r_{CO_2\text{-AMP}} = k_{2,AMP}[CO_2][AMP] = k_{ov\text{-}AMP}[CO_2] \tag{4.42}$$

As described by the zwitterion mechanism, the rate-determining step of APA should be zwitterion formation. Then the governing equation for the reaction rate of CO_2 into APA can be written as

$$r_{CO_2\text{-APA}} = k_{2,APA}[CO_2][APA] \tag{4.43}$$

Thus, the overall reaction rate of CO_2 into (AMP+APA+H_2O) is as follows:

$$\begin{aligned} r_{CO_2} &= r_{CO_2\text{-APA}} + r_{CO_2\text{-AMP}} \\ &= k_{2,APA}[CO_2][APA] + k_{2,AMP}[CO_2][AMP] \\ &= k_{ov}[CO_2] \end{aligned} \tag{4.44}$$

Where, k_{ov} denotes an overall rate constant, and it represented as

$$k_{ov} = k_{2,APA}[APA] + k_{2,AMP}[AMP]$$

4.5 PHYSICOCHEMICAL PROPERTIES

To interpret the absorption rate data as well as the determination of the overall reaction kinetic rate constant, knowledge of several physicochemical and transport properties of the gas-liquid system such as density, viscosity of the aqueous amine solutions and physical solubility, diffusivity of CO_2 into the aqueous solutions were essential. Furthermore, to find out the liquid film thickness (w) and contact time (t) in the wetted wall column contactor, value of density and viscosity of the aqueous amine solutions were necessary. Similarly, determination of the liquid side mass transfer coefficient, $k_{L,}$ that is attainable in the experimental apparatus, require the corresponding values of t along with the values of diffusivity of CO_2 into the aqueous amine solutions. For this purpose, density and viscosity of aqueous APA and an aqueous blend of MDEA or AMP with APA solutions as well as solubility and diffusivity of CO_2 into these binary and ternary solutions were measured and discussed in the previous Chapter (see Chapter 3).

4.6 RESULTS AND DISCUSSION

4.6.1 Validation of absorption experimental set-up

The experimental setup validation for kinetics study was carried out using 2 and 3 kmol m^{-3} MDEA solutions. Numerous studies of kinetics data is available in the literature for absorption of CO_2 into (MDEA+ H_2O) solution. So in the present study aqueous MDEA are used for the purpose of validation.

The experimental flux of CO_2 absorption for 3 kmol m^{-3} MDEA solutions was found to be 2.6×10^{-7} m^3 $kmol^{-1}$ s^{-1} at 313 K with a CO_2 partial pressure of 4.7 kPa. There is a good agreement between experimental and published data (Kierzkowska-Pawlak and Chacuk, 2010; Paul et al., 2009b). A graphical representation of flux versus CO_2 partial pressure for 2 kmol m^{-3} MDEA solution at 303-323 K gave a straight line as shown in Figure 4.11, which confirms the fast-pseudo-first-order regime. This regime was also verified by changing the contact time at a particular partial pressure. As depicted in Figure 4.12, the flux of CO_2 does not change with variation of contact times, which confirms the desired regime of the reaction. Hence, all other kinetics experiments are conducted following this protocol.

4.6.2 Determination of overall reaction rate constant and second order rate constant for aqueous APA system

The absorption experiments of the CO_2-APA-H_2O system were undertaken at four different temperatures (303, 308, 313 and 323 K) over the amine concentration range of 0.1-0.5 kmol m^{-3}. All experiments were conducted at an initial CO_2-free amine solution under atmospheric pressure. Throughout the experimental run, a constant aqueous amine flow rate was maintained at 2×10^{-6} m^3 s^{-1}. As we know the turbulence appears above 400 (Reynolds's number) and hence, throughout the experiment the liquid phase Reynolds's number (N_{Re}) was maintained at about 20 which lie within the laminar region. All absorption experimental measurements were conducted at a gas flow rate of 180×10^{-6} m^3 s^{-1} which is above 140×10^{-6} m^3 s^{-1} so that the contribution of gas phase resistance becomes insignificant (Mandal et al., 2004). It has also been verified earlier that the change in contact time (t) does not affect the rate of absorption of CO_2. So in our work, the contact time is maintained nearly constant throughout the experiment. The specific rate of absorption of the CO_2-APA-H_2O system is shown in Figure 4.13 and also given in Table 4.2. This figure clearly demonstrates that specific

rate of absorption of CO_2 at a particular partial pressure of CO_2 increases when the reaction temperature and concentration of APA is increased.

The calculated values of k_{ov} using Eq. (4.7) at various APA concentrations and at four different temperatures of 303, 308, 313 and 323 K are given in Table 4.3. Applying the least squares method, experimentally obtained kinetics data were fitted to an empirical power law equation. Therefore, the reaction orders were found to be in the range of (0.95-0.99*)* for four different temperatures mentioned above. Hence, the reaction order falls close to first order with respect to APA.

Utilizing k_{ov} values, the values of $k_{2,APA}$ were estimated by Eq. (4.17) as discussed subsequently. The enhancement factor values (E_A) have been calculated at different flux values of CO_2. Since the values of the calculated *Ha* numbers were greater than 3 in every case, the values of enhancement factor are equal to those of *Ha* numbers, respectively, as given in Table 4.2. However, in fast-pseudo-first-order regime determination of exact E_∞ value for reversible reaction at low amine concentration and high partial pressure of CO_2 is very difficult as mentioned earlier. For this aqueous APA solution, some E_∞ value at a different flux of CO_2 is less than *Ha* number as given in Table 4.3. However, the independency of contact time on flux and linear relationship between experimental flux and CO_2 partial pressure indicates that Eq. (4.3) is fulfilled (Singh et al., 2011).

A comparison of k_{ov} values of APA, PZ (Sun et al., 2005) and PZEA (Paul et al., 2009a) has been made at different temperatures for the absorption of CO_2 and is presented in Figure 4.14. As given by the Arrhenius plot (the discussion was made later), the values of rate constants for the CO_2-APA-H_2O system were larger than the rate constants of the CO_2-PZ-H_2O and CO_2-PZEA-H_2O system which is clearly shown in Figure 4.15.

The kinetic parameter, $k_{2,APA}$ is evaluated from the values of $k_{ov\text{-}APA}$ (as given in Table 4.3) using MATLAB® software (2013) by a nonlinear regression method and are also included in Table 4.3. This nonlinear regression gave an average deviation of ±

9.76 % for 36 data points. Over the experimental temperature range, a correlation of $k_{2,APA}$ with varying temperature is developed, and it is represented by the following equation:

$$k_{2,APA} = 5.77 \times 10^{11} \exp\left(-\frac{41833}{RT}\right) \quad (4.45)$$

From the above correlation, the average deviation is found to be about ± 0.45%. For $k_{2,APA}$, the activation energy is estimated to be 41.8 kJ mol^{-1}. The measured and estimated rate constants using Eq. (4.45) are compared in a parity plot (Figure 4.16). As observed from this plot, these values are in good agreement with each other.

In this study, the experimental and calculated values of $k_{2,APA}$ for APA as well as other literature are compared over four different temperatures as shown in an Arrhenius plot (Figure 4.15). Also, the solid line for absorption of CO_2 in APA is obtained by evaluating $k_{2,APA}$ using Eq. (4.45). As per this study, the observed $k_{2,APA}$ for the CO_2-APA-H_2O system is found to be more than that of the CO_2-PZ-H_2O (Sun et al., 2005) and CO_2-PZEA-H_2O (Paul et al., 2009a) systems.

4.6.3 Determination of overall reaction rate constant and second order rate constant for aqueous (APA+MDEA)

A novel blended amine system such as (APA+MDEA+H_2O) has been considered in this work for CO_2 absorption. It was pointed out in the introduction section that MDEA can be promoted by amines with stronger reactivity. So, formulated solvent i.e., aqueous blend of MDEA and novel activators like APA can be considered as a promising absorbent for bulk CO_2 removal. In this work, a series of experiments consisting of (MDEA+APA+H_2O) blend were conducted at three different temperatures. 3 kmol m^{-3} of MDEA is used as initial concentration and then 0.1, 0.3 and 0.5 kmol m^{-3} of promoter concentration were applied into the formulated solutions.

Several experiments with different temperature and concentration were performed and absorption rate of CO_2 in the formulated amine solution at a particular partial pressure was measured in a manner similar to a single amine solution. The enhancement factor can be estimated based on the measured rate under fast-pseudo-first-order regime using Eq. (4.3). Since the calculated enhancement factors at different fluxes of CO_2 were greater than 3 in every case as shown in Table 4.4, the values of *Ha* numbers are equal to those of enhancement factors, respectively. Here in all the cases, E_∞ value for this reversible reaction is greater than Ha number. Hence the Eq. (4.3) is fulfilled. For the aqueous blend of (APA+MDEA), the variation of k_{ov} with concentrations is shown in Figure 4.17 at three different temperatures of 303, 313 and 323 K. To evaluate the values of overall reaction rate constants (k_2), Eq. (4.30) was used and the values are shown in Table 4.5.

A nonlinear regression method using MATLAB® software (2013) was introduced to evaluate the second order reaction rate constants ($k_{2,APA}$ and $k_{2,MDEA}$) from the values of k_{ov} (as given in Table 4.5) and are also added in Table 4.5. This nonlinear regression gave an average deviation of ± 8.1 % for 12 data points. Over the experimental temperature range, the estimated $k_{2,APA}$ and $k_{2,MDEA}$ values for CO_2-(APA+MDEA+H_2O) system have been correlated according to the following Arrhenius equations.

$$k_{2,APA} = 1.246 \times 10^{12} \exp\left(-\frac{41188}{RT}\right) \tag{4.46}$$

$$k_{2,MDEA} = 3.01 \times 10^{11} \exp\left(-\frac{61669}{RT}\right) \tag{4.47}$$

Both the correlated equations depicted above gave the average deviation of about ± 0.40 % and ± 6.31 % and also the activation energy is evaluated from these equations to be 41.2 and 61.7 kJ mol^{-1}, respectively. The experimental results and calculated model values are compared by a parity plot and these are in good agreement with each other as shown in Figure 4.18.

4.6.4 Determination of overall reaction rate constant and second order rate constant for aqueous (APA+AMP) solutions.

The absorption rate of CO_2 in the aqueous blend of (APA+AMP) solutions is given in Table 4.6. Here, APA act as an activator in aqueous AMP solution. As observed from the Table 4.6, the specific rate of absorption of CO_2 into the aqueous blend of (APA+AMP) solutions increased with increasing temperature as well as increasing APA concentration. Due to presence of bulky methyl groups AMP is sterically hindered, which leads to lower reaction rate with CO_2. Whereas in APA, due to presence of six electron donating alkyl group, two amine groups at either end cannot affect each other and are equally reactive with higher pK_a value (10.85). Since the basicity of APA is higher than AMP, APA can deprotonate the zwitterion faster indicating its higher reaction rate (Mondal et al., 2017). The specific absorption rate of CO_2 at different amine concentrations are shown in Figures 4.19, 4.20 and 4.21 for 5, 10 and 15 kPa partial pressures, respectively. The Hatta numbers given in Table 4.6 are higher than 3 in all cases and E_∞ (see Table 4.7) are much higher than Ha, so ($3 < Ha << E_\infty$) condition is fulfilled. The enhancement factor which is equal to the Hatta number (Ha) are also included in Table 4.6.

The overall rate of reaction, k_{ov}, are calculated based on Eq. 4.7 and are presented in Table 4.7. Figure 4.22 shows a change of k_{ov} with the variation of APA concentration in (APA+AMP+H_2O). This figure also shows the variation of PZ concentration in (AMP+PZ+H_2O) systems, which are available in open literature (Samanta and Bandyopadhyay, 2009). The k_{ov} values for the absorption of CO_2 into the aqueous blend of (APA+AMP) solutions at 303 K are comparable with reported values of (AMP+PZ+H_2O) system by Samanta and Bandyopadhyay (2009). Whereas at some higher temperature (313 K), the values of k_{ov} for (APA+AMP+H_2O) system are little

greater than the reported values of (AMP+PZ+H_2O) systems. Thus at comparatively higher temperature range, (APA+AMP+H_2O) system is preferable to the absorption of CO_2 than (AMP+PZ+H_2O) system. On the other hand, at the temperature range of (303-313) K, the values of k_{ov} for (APA+AMP+H_2O) system are higher than the values described by Sun et al. (2005). The kinetic parameters, $k_{2,APA}$ and $k_{2,AMP}$, calculated from the values of k_{ov} by a regression method using Matlab software (2013) are included in Table 4.7. The average absolute deviation from this regression analysis is estimated to be 2.71 % for 36 data points. In order to study the effect of kinetics parameter on the calculated specific rate of absorption, parametric sensitivity analysis was performed and discussed in the next section. The second order rate constants, $k_{2,APA}$ and $k_{2,AMP}$, are correlated as a function of temperature with the following results (over the experimental range).

$$k_{2,APA} = 2.18\times10^{12}\exp\left(-\frac{41256}{RT}\right) \tag{4.48}$$

$$k_{2,AMP} = 6.33\times10^{7}\exp\left(\frac{-27717}{RT}\right) \tag{4.49}$$

The absolute average deviation for these rate constants calculated are found to be 0.87 % and 4.38 %, respectively. The activation energy for these $k_{2,APA}$ and $k_{2,AMP}$ are estimated to be approximately 41.3 and 27.7 kJ mol^{-1}, respectively. The experimental and model calculated specific rate of absorption using Eqs. 4.48 and 4.49 are depicted in parity plot (Figure 4.23). There is a good agreement between experimental and model fitted data.

4.6.5 Enhancement of CO_2 absorption using APA activated MDEA

The measured absorption rates of CO_2 and enhancement factors into

(MDEA+APA+H_2O) are presented in Table 4.4. The addition of small amount of APA into the MDEA solutions results in significant increase in absorption rate as shown in Figure 4.24. For instance, at 4.7 kPa partial pressure of CO_2 and T=313 K, the enhancement factor for aqueous solutions of (3 M MDEA), (2.9 M MDEA + 0.1 M APA), (2.7 M MDEA + 0.3 M APA) and (2.5 M MDEA + 0.5 M APA) are about 4.2, 97.2, 144.2 and 174.8, respectively. Therefore, replacing 0.1 M MDEA with an equal amount of 0.1 M APA, the enhancement factor was increased by about 2214 %. Replacing an additional 0.2 M amount of MDEA with APA, an additional 48 % enhancement was observed. A further replacement of 0.2 M amount of MDEA with APA, the additional enhancement was 21 %. So the substantial increase in the enhancement factor by replacing a small amount of MDEA with an equal amount of APA may be due to the increase in the basicity of blended amine solutions, which intern enhances the base catalysis reaction between MDEA and CO_2 in aqueous solutions. The initial enhancement factor is very high. Then it is very low and above (2.5 M MDEA + 0.5 M APA) concentration the change in enhancement factor does not follow the same trend. The reduced diffusivity of CO_2 in the solvent with the higher concentration of APA may be one of the reasons. Furthermore, a negligible increase in the equilibrium CO_2 capacity of the solvent with the higher concentration of APA also puts a limit on the absorption rate of CO_2. Similar trend in the absorption rate and enhancement factor has been observed by Samanta and Bandyopadhyay (2011) with the addition of small amount of PZ in aqueous MDEA for the absorption of CO_2 into (MDEA+PZ+H_2O) solutions.

4.6.6 Parametric sensitivity analysis

A parametric sensitivity analysis has been performed to examine the effect of important physicochemical and kinetic parameters on the specific rate of absorption of CO_2 into (APA+AMP+H_2O) solutions. The pertinent parameters, i.e., Henry's law

constant and diffusion coefficient of CO_2 into (APA+AMP+H_2O) and the kinetics constant of CO_2-(APA+AMP) reactions in aqueous solutions of (APA+AMP) are considered for this analysis. The deviations of +50% to -50% are incorporated over the pertinent parameter's value and the results are generated. The resulted deviation to Henry's law constant and diffusivity of CO_2 on the specific rate of absorption are depicted in Figure 4.25. The corresponding deviation of Henry's law constants is in the range of -33% to 100% and diffusivity is in the range of +23% to -29% on the specific rate of absorption of CO_2. Therefore, Henry's law constants are very sensitive to the specific rate of absorption of CO_2 in comparison to the diffusion constants of CO_2. It was prominent from the Figure 4.26, that significant deviation on the calculated rate of absorption of CO_2 occurred due to the error introduce in rate constant values. Here, the numerical output to this deviation is in the range of +23% to -29% with the corresponding deviation incorporated on rate constant values. Therefore, accuracy to determine rate coefficient of the CO_2-(APA+AMP+H_2O) system is very important to predict the values of CO_2 absorption rate and enhancement factor.

NOTATIONS

B	base
Amn	amine
D	diffusivity, $m^2\ s^{-1}$
E_A	enhancement factor
E_∞	enhancement factor in instantaneous reaction regime
GC	gas chromatography
h	absorption length, m
H	Henry's constant, kPa $m^3\ kmol^{-1}$
Ha	Hatta number
HCl	Hydrochloric acid

k_2	second order reaction rate constant, m^3 $kmol^{-1}$ s^{-1}
k_{-1}	the reverse reaction rate constant, m^3 $kmol^{-1}$ s^{-1}.
k_L	liquid side mass transfer coefficient, m s^{-1}
k_{ov}	observed overall reaction rate constant, s^{-1}
K_B	Zwitterion mechanism deprotonation rate constant.
PCC	post-combustion carbon capture
P	partial pressure, kPa
pk_a	the acid dissociation constant
R	gas constant, 8.314 J mol^{-1} K^{-1}
NMR	nuclear magnetic resonance
r	reaction rate, kmol m^{-3} s^{-1}
T	temperature, K
W	film thickness, m
Z	stoichiometric coefficient
[ ]	concentration, kmol m^{-3}

Subscripts

B	base for zwitterions deprotonation
I	gas-liquid interface
ov	overall reaction rate

REFERENCES

Appl, M., Wagner, U., Henrici, H.J., Kuessner, K., Volkamer, K., Fuerst, E., 1982. Removal of CO_2 and/or H_2S and/or COS from gases containing these constituents. US Pat 4, 336, 233.

Artanto, Y., Jansen, J., Pearson, P., Puxty, G., Cottrell, A., Meuleman, E., Feron, P., 2014. Pilot-scale evaluation of AMP/PZ to capture CO_2 from flue gas of an Australian brown coal–fired power station. International Journal of Greenhouse Gas Control 20, 189-195.

Barzagli, F., Mani, F., Peruzzini, M., 2009. A ^{13}C NMR study of the carbon dioxide absorption and desorption equilibria by aqueous 2-aminoethanol and N-methyl-substituted 2-aminoethanol. Energy & Environmental Science 2, 322-330.

Barzagli, F., Mani, F., Peruzzini, M., 2010. Continuous cycles of CO_2 absorption and amine regeneration with aqueous alkanolamines: a comparison of the efficiency between pure and blended DEA, MDEA and AMP solutions by ^{13}C NMR spectroscopy. Energy & Environmental Science 3, 772-779.

Bindwal, A.B., Vaidya, P.D., Kenig, E.Y., 2011. Kinetics of carbon dioxide removal by aqueous diamines. Chemical Engineering Journal 169, 144-150.

Caplow, M., 1968. Kinetics of carbamate formation and breakdown. Journal of the American Chemical Society 90, 6795-6803.

Choi, S.Y., Nam, S.C., Yoon, Y.I., Park, K.T., Park, S.-J., 2014. Carbon dioxide absorption into aqueous blends of methyldiethanolamine (MDEA) and alkyl amines containing multiple amino groups. Industrial & Engineering Chemistry Research 53, 14451-14461.

Conway, W., Beyad, Y., Richner, G., Puxty, G., Feron, P., 2015. Rapid CO_2 absorption into aqueous benzylamine (BZA) solutions and its formulations with monoethanolamine (MEA), and 2-amino-2-methyl-1-propanol (AMP) as components for post combustion capture processes. Chemical Engineering Journal 264, 954-961.

Conway, W., Wang, X., Fernandes, D., Burns, R., Lawrance, G., Puxty, G., Maeder, M., 2012. Toward the understanding of chemical absorption processes for post-combustion capture of carbon dioxide: electronic and steric considerations from the

kinetics of reactions of CO_2 (aq) with sterically hindered amines. Environmental Science & Technology 47, 1163-1169.

Danckwerts, P., 1979. The reaction of CO_2 with ethanolamines. Chemical Engineering Science 34, 443-446.

Das, B., Deogam, B., Agrawal, Y., Mandal, B., 2016. Measurement and correlation of the physicochemical properties of novel aqueous bis (3-aminopropyl) amine and its blend with n-methyldiethanolamine for co_2 capture. Journal of Chemical & Engineering Data 61, 2226-2235.

Dash, S.K., Samanta, A., Samanta, A.N., Bandyopadhyay, S.S., 2011. Absorption of carbon dioxide in piperazine activated concentrated aqueous 2-amino-2-methyl-1-propanol solvent. Chemical Engineering Science 66, 3223-3233.

Dash, S.K., Samanta, A.N., Bandyopadhyay, S.S., 2014. Simulation and parametric study of post combustion CO_2 capture process using (AMP + PZ) blended solvent. International Journal of Greenhouse Gas Control 21, 130-139.

Doraiswamy, L.K., Sharma, M.M., 1984. Heterogeneous Reactions: Analysis, Examples and Reactor Design. Vol. 2, Fluid-fluid-solid Reactions. Wiley.

Dubois, L., Kahasha Mbasha, P., Thomas, D., 2010. CO_2 absorption into aqueous solutions of a polyamine (PZEA), a sterically hindered amine (AMP), and their blends. Chemical Engineering & Technology 33, 461-467.

Gabrielsen, J., Svendsen, H.F., Michelsen, M.L., Stenby, E.H., Kontogeorgis, G.M., 2007. Experimental validation of a rate-based model for CO 2 capture using an AMP solution. Chemical Engineering Science 62, 2397-2413.

Glasscock, D. A., 1990. Modelling and experimental study of carbon dioxide absorption into aqueous alkanolamines. Ph.D dissertation, The University of Texas at Austin.

Glasscock, D.A., Critchfield, J.E., Rochelle, G.T., 1991. CO_2 absorption/desorption in mixtures of methyldiethanolamine with monoethanolamine or diethanolamine. Chemical Engineering Science 46, 2829-2845.

Hikita, H., Asai, S., Katsu, Y., Ikuno, S., 1979. Absorption of carbon dioxide into aqueous monoethanolamine solutions. AIChE Journal 25, 793-800.

Khan, A.A., Halder, G., Saha, A., 2015. Carbon dioxide capture characteristics from flue gas using aqueous 2-amino-2-methyl-1-propanol (AMP) and monoethanolamine (MEA) solutions in packed bed absorption and regeneration columns. International Journal of Greenhouse Gas Control 32, 15-23.

Kierzkowska-Pawlak, H., 2015. Kinetics of CO_2 absorption in aqueous N, N-diethylethanolamine and its blend with N-(2-aminoethyl) ethanolamine using a stirred cell reactor. International Journal of Greenhouse Gas Control 37, 76-84.

Kierzkowska-Pawlak, H., Chacuk, A., 2010. Kinetics of carbon dioxide absorption into aqueous MDEA solutions. Ecological Chemistry and Engineering S 17, 463-475.

Kohl, A.L., Nielsen, R., 1997. Gas purification. Gulf Professional Publishing.

Laddha, S., Danckwerts, P., 1981. Reaction of CO_2 with ethanolamines: kinetics from gas-absorption. Chemical Engineering Science 36, 479-482.

Lim, J.-a., Kim, D.H., Yoon, Y., Jeong, S.K., Park, K.T., Nam, S.C., 2012. Absorption of CO2 into Aqueous Potassium Salt Solutions of L-Alanine and L-Proline. Energy & Fuels 26, 3910-3918.

Liu, H., Liang, Z., Sema, T., Rongwong, W., Li, C., Na, Y., Idem, R., Tontiwachwuthikul, P., 2014. Kinetics of CO_2 absorption into a novel 1-diethylamino-2-propanol solvent using stopped-flow technique. AIChE Journal 60, 3502-3510.

Mandal, B., Bandyopadhyay, S.S., 2006. Simultaneous absorption of CO_2 and H_2S into aqueous blends of N-methyldiethanolamine and diethanolamine. Environmental Science & Technology 40, 6076-6084.

Mandal, B.P., Biswas, A., Bandyopadhyay, S., 2004. Selective absorption of H_2S from gas streams containing H_2S and CO_2 into aqueous solutions of N-methyldiethanolamine and 2-amino-2-methyl-1-propanol. Separation and Purification Technology 35, 191-202.

Mondal, B.K., Bandyopadhyay, S.S., Samanta, A.N., 2017. Kinetics of CO_2 absorption in aqueous hexamethylenediamine. International Journal of Greenhouse Gas Control 56, 116-125.

Nugent, P., Belmabkhout, Y., Burd, S.D., Cairns, A.J., Luebke, R., Forrest, K., Pham, T., Ma, S., Space, B., Wojtas, L., 2013. Porous materials with optimal adsorption thermodynamics and kinetics for CO_2 separation. Nature 495, 80.

Paul, S., Ghoshal, A.K., Mandal, B., 2009a. Kinetics of absorption of carbon dioxide into aqueous solution of 2-(1-piperazinyl)-ethylamine. Chemical Engineering Science 64, 313-321.

Paul, S., Ghoshal, A.K., Mandal, B., 2009b. Kinetics of absorption of carbon dioxide into aqueous blends of 2-(1-piperazinyl)-ethylamine and N-methyldiethanolamine. Chemical Engineering Science 64, 1618-1622.

Paul, S., Thomsen, K., 2012. Kinetics of absorption of carbon dioxide into aqueous potassium salt of proline. International Journal of Greenhouse Gas Control 8, 169-179.

Pei, Z., Yao, S.H.I., Jianwen, W.E.I., Wei, Z., Qing, Y.E., 2008. Regeneration of 2-amino-2-methyl-1-propanol used for carbon dioxide absorption. Journal of Environmental Sciences 20, 39-44.

Pinsent, B.R.W., Pearson, L., Roughton, F.J.W., 1956. The kinetics of combination of carbon dioxide with hydroxide ions. Transactions of the Faraday Society 52, 1512-1520.

Rahaman, M., Mandal, B., Ghosh, P., 2010. Nitration of nitrobenzene at high-concentrations of sulfuric acid: Mass transfer and kinetic aspects. AIChE Journal 56, 737-748.

Saha, A.K., Bandyopadhyay, S.S., Biswas, A.K., 1995. Kinetics of absorption of CO_2 into aqueous solutions of 2-amino-2-methyl-1-propanol. Chemical Engineering Science 50, 3587-3598.

Samanta, A., Bandyopadhyay, S., 2009. Absorption of carbon dioxide into aqueous solutions of piperazine activated 2-amino-2-methyl-1-propanol. Chemical Engineering Science 64, 1185-1194.

Samanta, A., Bandyopadhyay, S.S., 2011. Absorption of carbon dioxide into piperazine activated aqueous N-methyldiethanolamine. Chemical Engineering Journal 171, 734-741.

Sartori, G., Savage, D.W., 1983. Sterically hindered amines for carbon dioxide removal from gases. Industrial & Engineering Chemistry Fundamentals 22, 239-249.

Seo, D.J., Hong, W.H., 2000. Effect of piperazine on the kinetics of carbon dioxide with aqueous solutions of 2-amino-2-methyl-1-propanol. Industrial & Engineering Chemistry Research 39, 2062-2067.

Singh, P., van Swaaij, W.P.M., Brilman, D.W.F., 2011. Kinetics study of carbon dioxide absorption in aqueous solutions of 1,6-hexamethyldiamine (HMDA) and 1,6-hexamethyldiamine, N,N′ di-methyl (HMDA, N,N′). Chemical Engineering Science 66, 4521-4532.

Sun, W.-C., Yong, C.-B., Li, M.-H., 2005. Kinetics of the absorption of carbon dioxide into mixed aqueous solutions of 2-amino-2-methyl-l-propanol and piperazine. Chemical Engineering Science 60, 503-516.

Wong, M., Shariff, A., Bustam, M., 2016. Raman spectroscopic study on the equilibrium of carbon dioxide in aqueous monoethanolamine. RSC Advances 6, 10816-10823.

Yih, S.M., Shen, K.P., 1988. Kinetics of carbon dioxide reaction with sterically hindered 2-amino-2-methyl-1-propanol aqueous solutions. Industrial & Engineering Chemistry Research 27, 2237-2241.

Table 4.1

NMR analysis parameters at room temperature

NMR Analysis method	Number of points	Number of scans	Acquisition time (S)	Relaxation delay	Dwell time (μsec)
^{1}H	---	16	1.363	1	41.6
^{13}C	---	53-113	0.454	2	13.867
Dept-135	32768;	49	0.682	2	20.8
HMBC	2048(f2), 128(f1);	2	0.085	1.5	41.6
HSQC	1024(f2), 256(f1);	2	0.042	1.5	41.6
TOCSY	2048(f2), 189(f1);	8	0.085	2	41.6

Table 4.2a

Kinetic data for the absorption of CO_2 into (APA+H_2O).

T (K)	[APA] (kmol m^{-3})	P_{CO_2} (kPa)	t (s^{-1})	k_l (10^5 m s^{-1})	N_{CO_2} (10^6 kmol m^{-2} s^{-1})	Ha	E
303	0.1	4.85	0.350	8.33	4.05	34.2	34.2
	0.3		0.368	7.71	5.80	54.7	54.7
	0.5		0.383	7.18	7.10	74.1	74.1
	0.1	9.71	0.352	8.31	8.15	34.4	34.4
	0.3		0.368	7.72	11.42	53.8	53.8
	0.5		0.396	7.06	14.15	75.0	75.0
	0.1	14.60	0.354	8.29	12.12	34.2	34.2
	0.3		0.365	7.75	17.10	53.5	53.5
	0.5		0.389	7.13	21.15	74.1	74.1
308	0.1	4.78	0.347	9.32	4.82	39.7	39.7
	0.3		0.346	8.71	6.70	61.3	61.3
	0.5		0.377	7.92	8.10	84.1	84.1
	0.1	9.55	0.341	9.41	9.60	39.1	39.1
	0.3		0.347	8.70	13.00	59.6	59.6
	0.5		0.368	8.02	15.91	81.6	81.6
	0.1	14.30	0.348	9.32	14.40	39.5	39.5
	0.3		0.356	8.58	19.54	60.5	60.5
	0.5		0.359	8.12	23.95	80.8	80.8

Table 4.2b

Kinetic data for the absorption of CO_2 into (APA+H_2O).

T (K)	[APA] (kmol m^{-3})	P_{CO_2} (kPa)	t (s^{-1})	k_l (10^5 m s^{-1})	N_{CO_2} (10^6 kmol m^{-2} s^{-1})	Ha	E
313	0.1	4.70	0.321	10.40	5.65	44.4	44.4
	0.3		0.340	9.70	7.78	67.4	67.4
	0.5		0.364	8.93	9.55	92.8	92.8
	0.1	9.39	0.331	10.20	11.30	45.1	45.1
	0.3		0.337	9.74	15.59	67.3	67.3
	0.5		0.357	9.01	19.05	91.8	91.8
	0.1	14.10	0.328	10.30	16.95	44.9	44.9
	0.3		0.332	9.81	23.32	66.6	66.6
	0.5		0.354	9.06	28.65	91.5	91.5
323	0.1	4.45	0.298	11.90	6.95	58.9	58.9
	0.3		0.318	11.10	9.50	88.8	88.8
	0.5		0.343	10.30	11.00	113.3	113.3
	0.1	8.90	0.307	11.70	13.78	59.3	59.3
	0.3		0.323	11.00	18.87	88.9	88.9
	0.5		0.330	10.50	22.05	111.4	111.4
	0.1	13.65	0.305	11.80	20.75	58.0	58.0
	0.3		0.321	11.00	28.88	88.4	88.4
	0.5		0.333	10.50	33.82	111.9	111.9

Table 4.3a

Kinetic constant for the absorption of CO_2 into (APA+H_2O).

T (K)	[APA] (kmol m^{-3})	P_{co_2} (kPa)	E_∞	$k_{ov\text{-}APA}$ (s^{-1})	$k_{2,APA}$ (m^3 $kmol^{-1}$ s^{-1})
303	0.1	4.85	40.3	4242.7	
	0.3		121.4	10354.9	
	0.5		207.0	18258.7	
	0.1	9.71	21.1	4286.4	
	0.3		61.5	10015.4	35775
	0.5		104.3	18093.0	
	0.1	14.60	14.7	4221.8	
	0.3		41.7	10000.9	
	0.5		70.2	18002.0	
308	0.1	4.78	43.8	5768.6	
	0.3		132.8	13844.3	
	0.5		227.1	23870.0	
	0.1	9.55	22.8	5720.8	
	0.3		67.3	13028.1	46414
	0.5		114.5	23014.7	
	0.1	14.30	15.8	5716.8	
	0.3		45.5	13079.9	
	0.5		76.9	23171.2	

Table 4.3b

Kinetic constant for the absorption of CO_2 into (APA+H_2O).

T (K)	[APA] (kmol m^{-3})	P_{co_2} (kPa)	E_∞	$k_{ov\text{-}APA}$ (s^{-1})	$k_{2,APA}$ (m^3 $kmol^{-1}$ s^{-1})
313	0.1	4.70	46.4	7814.0	
	0.3		140.0	17041.3	
	0.5		239.4	30099.3	
	0.1	9.39	24.2	7830.6	
	0.3		71.0	17143.5	59816
	0.5		120.7	30005.8	
	0.1	14.10	16.7	7814.0	
	0.3		47.9	17012.1	
	0.5		81.0	30099.3	
323	0.1	4.45	57.2	14819.9	
	0.3		172.1	31563.0	
	0.5		293.0	47673.0	
	0.1	8.90	29.5	14565.0	
	0.3		87.0	31132.6	99220
	0.5		147.0	47889.9	
	0.1	13.65	19.9	14039.9	
	0.3		57.0	31001.3	
	0.5		96.8	47894.9	

Table 4.4

Kinetic data for the absorption of CO_2 into (APA+MDEA+H_2O).

T (K)	[APA/MDEA] (kmol m^{-3})	P_{CO_2} (kPa)	t (s^{-1})	k_l (10^5 m s^{-1})	N_{CO_2} (10^6 kmol m^{-2} s^{-1})	Ha	E
303	0/3	9.71	0.573	4.81	0.38	3.3	3.3
	0.1/2.9	4.85	0.588	4.63	4.21	76.1	76.1
	0.3/2.7	4.85	0.604	4.43	6.06	115.2	115.2
	0.5/2.5	4.85	0.617	4.21	7.40	148.9	148.9
313	0/3	9.39	0.507	5.89	0.52	4.2	4.2
	0.1/2.9	4.70	0.519	5.69	5.85	97.3	97.3
	0.3/2.7	4.70	0.537	5.45	8.25	144.2	144.2
	0.5/2.5	4.70	0.548	5.26	9.60	174.8	174.8
323	0/3	8.90	0.458	6.96	0.72	5.9	5.9
	0.1/2.9	4.45	0.472	6.71	7.30	124.6	124.64
	0.3/2.7	4.45	0.487	6.49	9.70	171.8	171.84
	0.5/2.5	4.45	0.497	6.30	11.75	215.6	215.57

Table 4.5

Kinetic constant for the absorption of CO_2 into (APA+MDEA+H_2O).

T (K)	[APA/MDEA] (kmol m^{-3})	P_{co_2} (kPa)	E_∞	k_{ov} (s^{-1})	$k_{2,APA}$ (m^3 $kmol^{-1}$ s^{-1})	$k_{2,MDEA}$ (m^3 $kmol^{-1}$ s^{-1})
303	0/3	9.71	683.6	23.9		
	0.1/2.9	4.85	1377.0	12539.6		
	0.3/2.7	4.85	1385.5	27999.5	99370	7.98
	0.5/2.5	4.85	1395.0	45770.7		
313	0/3	9.39	774.5	43.3		
	0.1/2.9	4.70	1556.9	23220.5		
	0.3/2.7	4.70	1566.0	49339.4	165736	14.45
	0.5/2.5	4.70	1575.8	71057.6		
323	0/3	8.90	937.1	96.5		
	0.1/2.9	4.45	1885.4	41929.5		
	0.3/2.7	4.45	1890.9	77242.9	272290	32.20
	0.5/2.5	4.45	1902.0	119114.2		

Table 4.6a

Results of the interpretation of the experimental kinetic data for CO_2-APA-AMP-H_2O system.

T (K)	[APA/AMP] (kmol m^{-3})	P_{CO_2} (kPa)	t (s^{-1})	k_L (10^5 m s^{-1})	N_{CO_2} (10^6 kmol m^{-2} s^{-1})	Ha	E
303	0/3	4.85	0.555	4.5	2.00	37.6	37.6
	0.1/2.9		0.564	4.33	5.60	109.1	109.1
	0.3/2.7		0.571	4.20	7.80	154.7	154.7
	0.5/2.5		0.585	4.04	9.10	185.7	185.7
	0/3	9.71	0.555	4.55	3.98	37.3	37.3
	0.1/2.9		0.564	4.33	11.25	109.5	109.5
	0.3/2.7		0.571	4.20	15.40	153.4	153.4
	0.5/2.5		0.585	4.04	18.13	184.7	184.7
	0/3	14.6	0.555	4.55	6.10	38.2	38.2
	0.1/2.9		0.564	4.33	17.00	110.4	110.4
	0.3/2.7		0.571	4.20	23.20	153.4	153.4
	0.5/2.5		0.585	4.04	27.25	185.3	185.3
313	0/3	4.70	0.493	5.77	2.31	40.4	40.4
	0.1/2.9		0.500	5.57	7.33	132.1	132.1
	0.3/2.7		0.510	5.41	10.09	186.0	186.0
	0.5/2.5		0.519	5.22	12.35	232.6	232.6
	0/3	9.39	0.493	5.77	4.55	39.9	39.9
	0.1/2.9		0.500	5.47	14.80	127.0	127.0
	0.3/2.7		0.510	5.41	20.00	184.6	184.6
	0.5/2.5		0.519	5.22	24.60	232.6	232.6

Table 4.6b

Results of the interpretation of the experimental kinetic data for CO_2-APA-AMP-H_2O system.

T (K)	[APA/AMP] (kmol m^{-3})	P_{CO_2} (kPa)	t (s^{-1})	k_L (10^5 m s^{-1})	N_{CO_2} (10^6 kmol m^{-2} s^{-1})	Ha	E
313	0/3	14.1	0.493	5.77	6.85	40.0	40.0
	0.1/2.9		0.500	5.57	22.10	132.8	132.8
	0.3/2.7		0.510	5.41	30.37	186.3	186.3
	0.5/2.5		0.519	5.22	36.70	230.4	230.4
323	0/3	4.45	0.442	6.98	2.58	46.8	46.8
	0.1/2.9		0.452	6.73	9.01	168.1	168.1
	0.3/2.7		0.462	6.58	12.18	230.6	230.6
	0.5/2.5		0.473	6.40	14.40	277.3	277.3
	0/3	8.9	0.442	6.98	5.10	46.2	46.2
	0.1/2.9		0.452	6.73	18.05	168.4	168.4
	0.3/2.7		0.462	6.58	23.97	226.9	226.9
	0.5/2.5		0.473	6.40	28.50	274.4	274.4
	0/3	13.65	0.442	6.98	7.86	46.4	46.4
	0.1/2.9		0.452	6.73	27.80	169.1	169.1
	0.3/2.7		0.462	6.58	36.60	225.9	225.9
	0.5/2.5		0.473	6.40	43.52	273.2	273.2

Table 4.7a

Kinetics constant for the absorption of CO_2 into aqueous blend solutions of AMP and APA.

T (K)	[APA/AMP] (kmol m^{-3})	P_{CO_2} (kPa)	E_∞	k_{ov} (s^{-1})	k_2 (m^3 $kmol^{-1}$ s^{-1})	$k_{2,APA}$ (m^3 $kmol^{-1}$ s^{-1})	$k_{2,AMP}$ (m^3 $kmol^{-1}$ s^{-1})
303	0/3	4.85	1404.4	3238.4	1079.5		
	0.1/2.9		1387.5	26869.6	8956.5		
	0.3/2.7		1370.9	53463.4	17821.1		
	0.5/2.5		1356.7	75065.6	25021.9		
	0/3	9.71	702.4	3199.5	1066.5		
	0.1/2.9		694.0	27054.2	9018		
	0.3/2.7		685.7	52535.6	17511.9	166062.5	1114.6
	0.5/2.5		678.6	74335.9	24778.6		
	0/3	14.6	469.4	3347.3	1115.8		
	0.1/2.9		463.7	27513.2	9171		
	0.3/2.7		458.2	52553.4	17517.8		
	0.5/2.5		453.4	74790.9	24930.3		

Table 4.7b

Kinetics constant for the absorption of CO_2 into aqueous blend solutions of AMP and APA.

T (K)	[APA/AMP] (kmol m^{-3})	P_{CO_2} (kPa)	E_∞	k_{ov} (s^{-1})	k_2 (m^3 $kmol^{-1}$ s^{-1})	$k_{2,APA}$ (m^3 $kmol^{-1}$ s^{-1})	$k_{2,AMP}$ (m^3 $kmol^{-1}$ s^{-1})
313	0/3	4.70	1662.8	4226.8	1408.9		
	0.1/2.9		1652.7	44453.3	14817.8		
	0.3/2.7		1637.0	86165.9	28722.0		
	0.5/2.5		1616.3	132654.8	44218.3		
	0/3	9.39	833.2	4108.4	1369.5		
	0.1/2.9		828.1	45403	15134.3	287057.5	1411.1
	0.3/2.7		820.3	85155.6	28385.2		
	0.5/2.5		809.9	131863.3	43954.4		
	0/3	14.1	555.5	4129.7	1376.6		
	0.1/2.9		552.1	44899	14966.4		
	0.3/2.7		546.9	86736.2	28912.1		
	0.5/2.5		540.0	130160.4	43386.8		

Table 4.7c

Kinetics constant for the absorption of CO_2 into aqueous blend solutions of AMP and APA.

T (K)	[APA/AMP] (kmol m^{-3})	P_{CO_2} (kPa)	E_∞	k_{ov} (s^{-1})	k_2 (m^3 $kmol^{-1}$ s^{-1})	$k_{2,APA}$ (m^3 $kmol^{-1}$ s^{-1})	$k_{2,AMP}$ (m^3 $kmol^{-1}$ s^{-1})
323	0/3	4.45	2079.2	6295.5	2098.5		
	0.1/2.9		2066.3	79594.4	26531.5		
	0.3/2.7		2048.5	146610.4	48870.1		
	0.5/2.5		2026.1	207032.9	69011		
	0/3	8.9	1040.5	6150.0	2050.0		
	0.1/2.9		1034.1	79859.7	26619.9	463447.6	2116.3
	0.3/2.7		1025.2	141953.5	47317.8		
	0.5/2.5		1013.9	202742.2	67580.7		
	0/3	13.65	679.1	6210.0	2070.0		
	0.1/2.9		674.9	80533.7	26844.6		
	0.3/2.7		669.1	140698	46899.2		
	0.5/2.5		661.7	200977.3	66992.4		

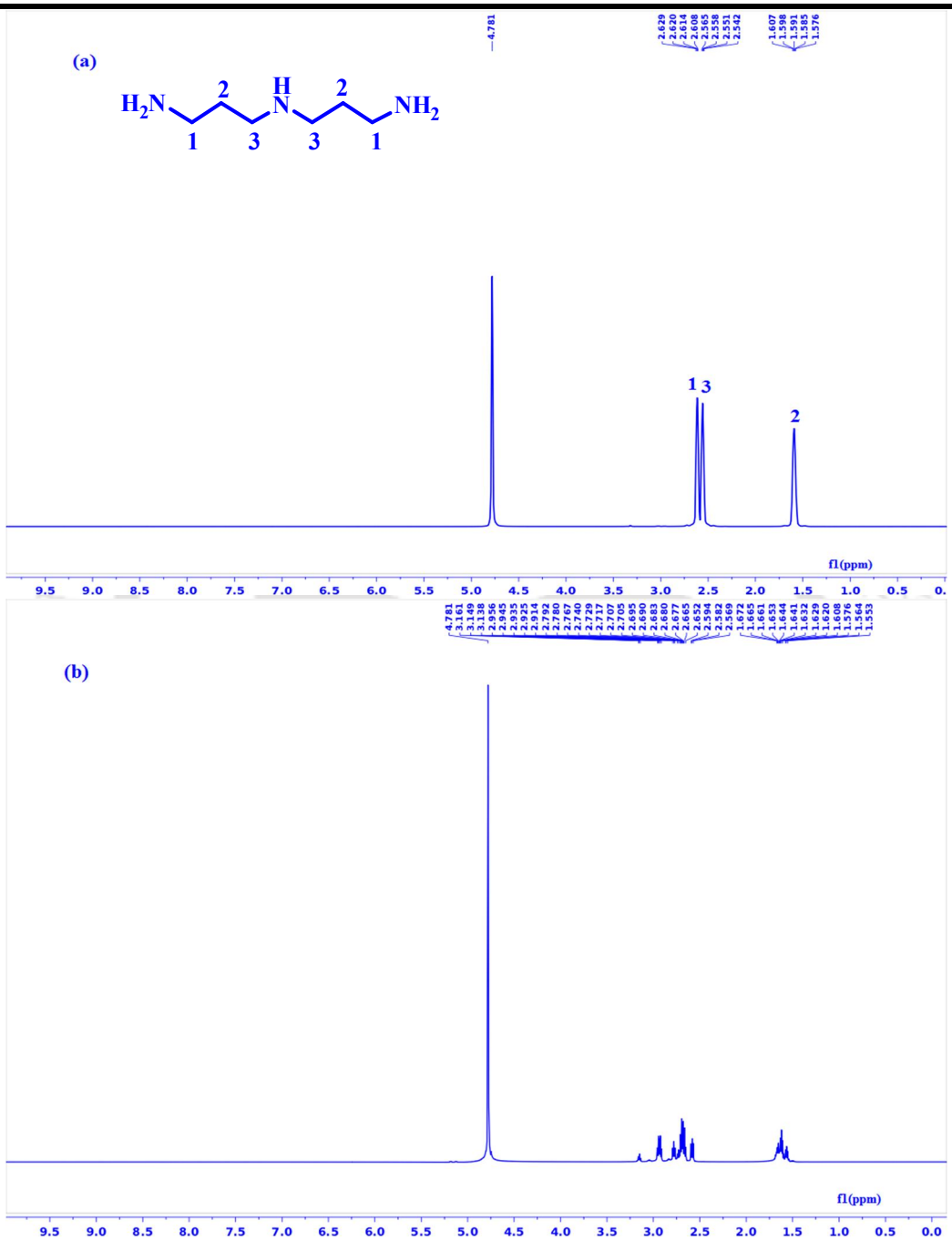

Figure 4.1 ^{1}H NMR spectra for (a) aqueous APA solution (b) CO_2-loaded aqueous APA solution.

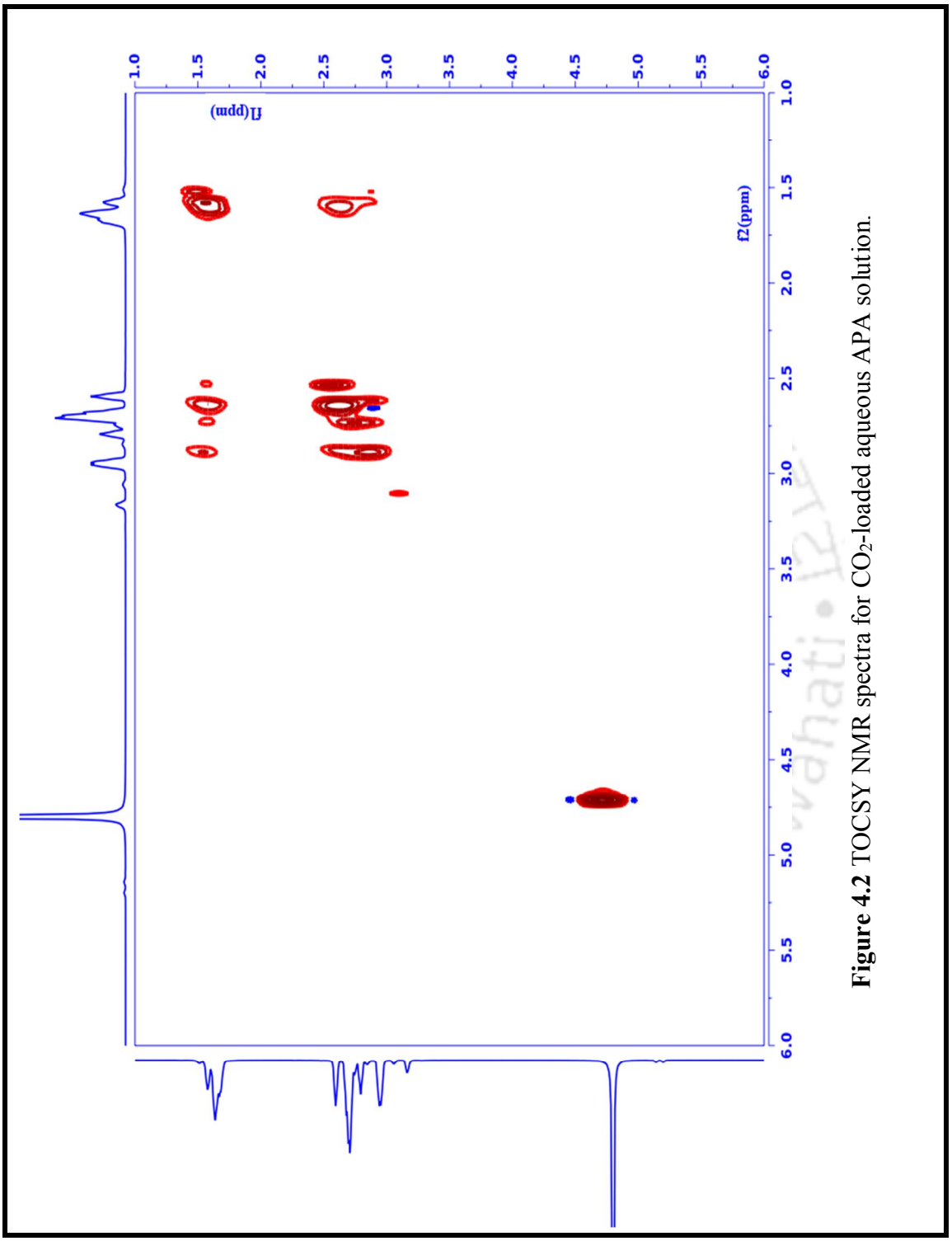

Figure 4.2 TOCSY NMR spectra for CO_2-loaded aqueous APA solution.

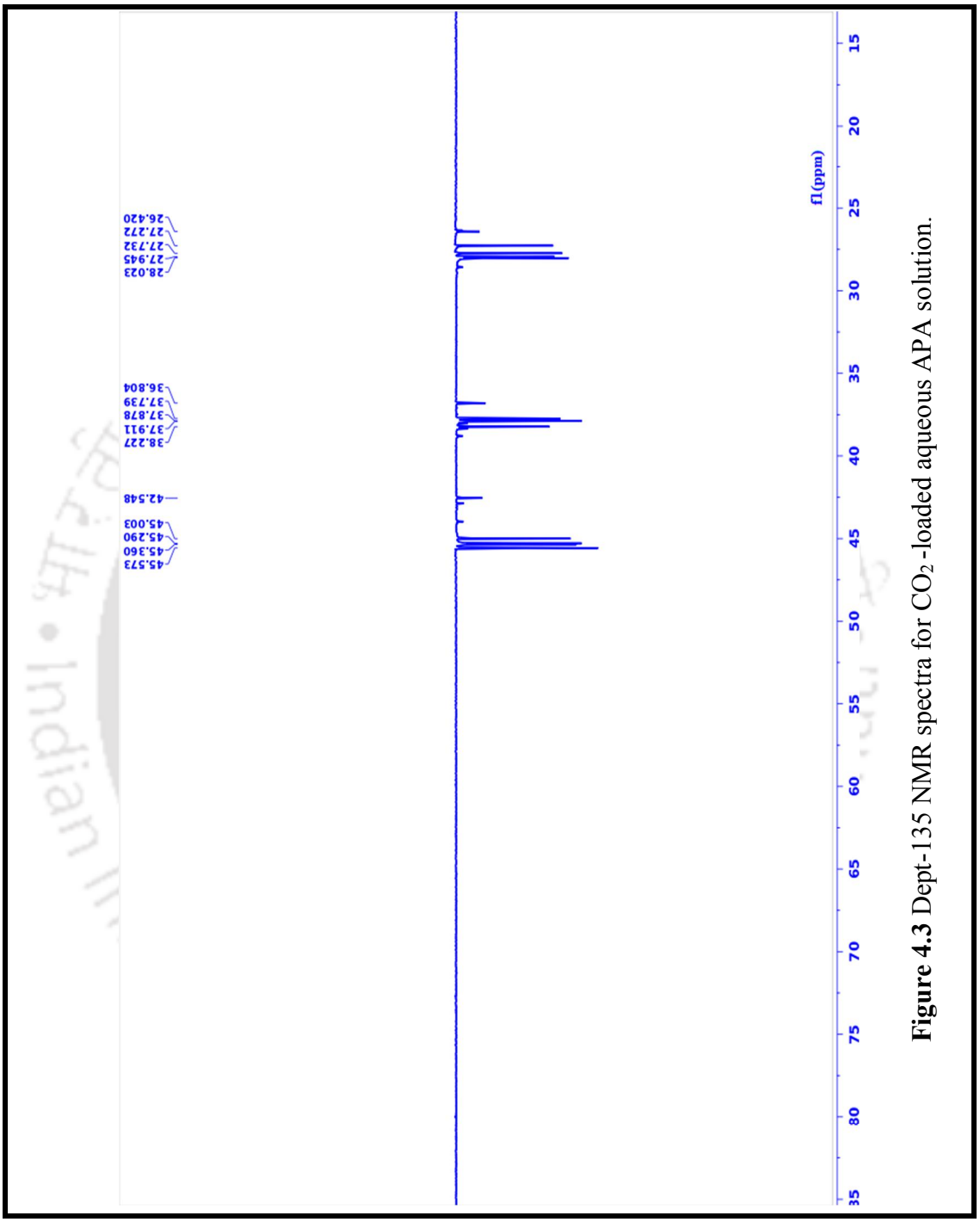

Figure 4.3 Dept-135 NMR spectra for CO_2-loaded aqueous APA solution.

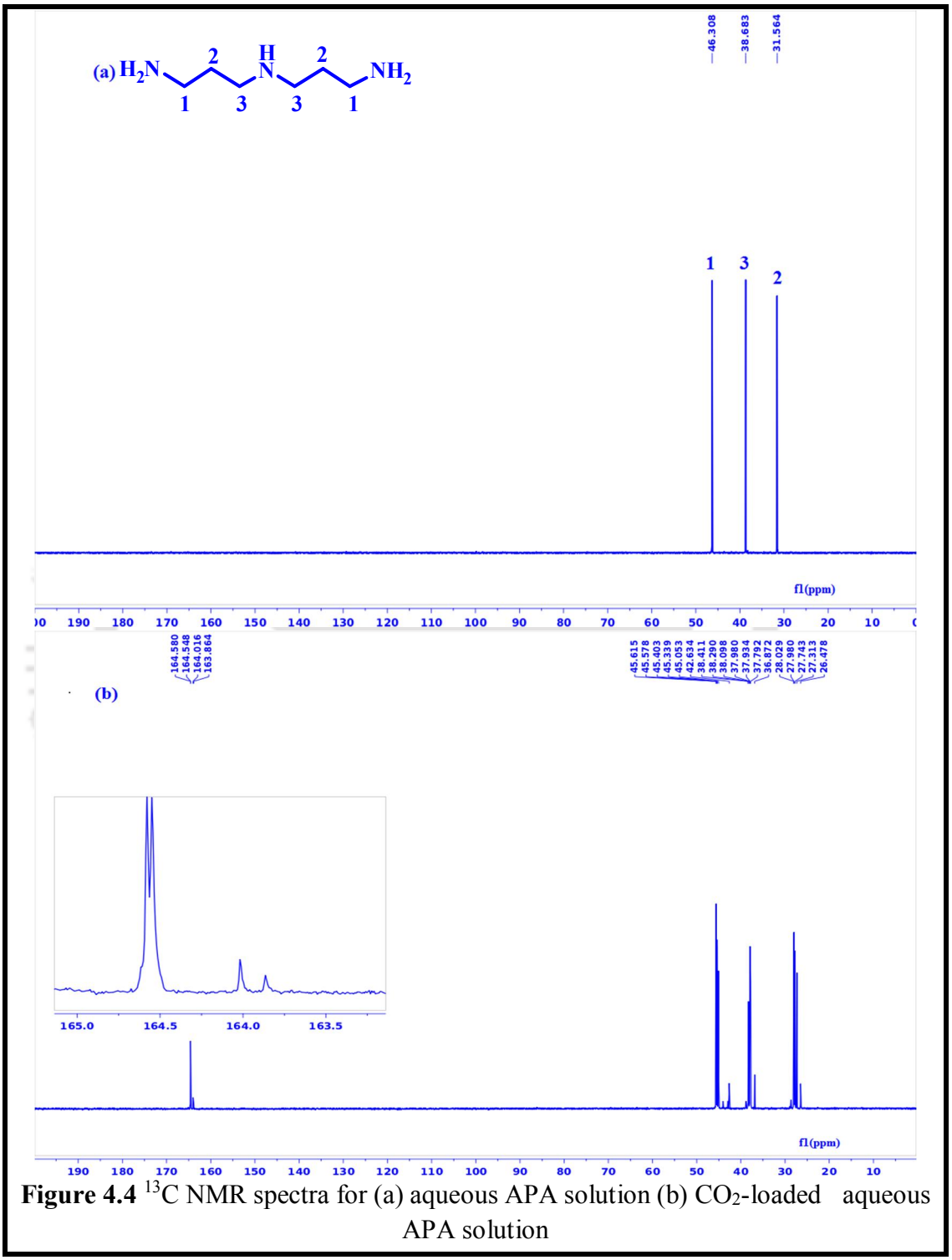

Figure 4.4 ^{13}C NMR spectra for (a) aqueous APA solution (b) CO_2-loaded aqueous APA solution

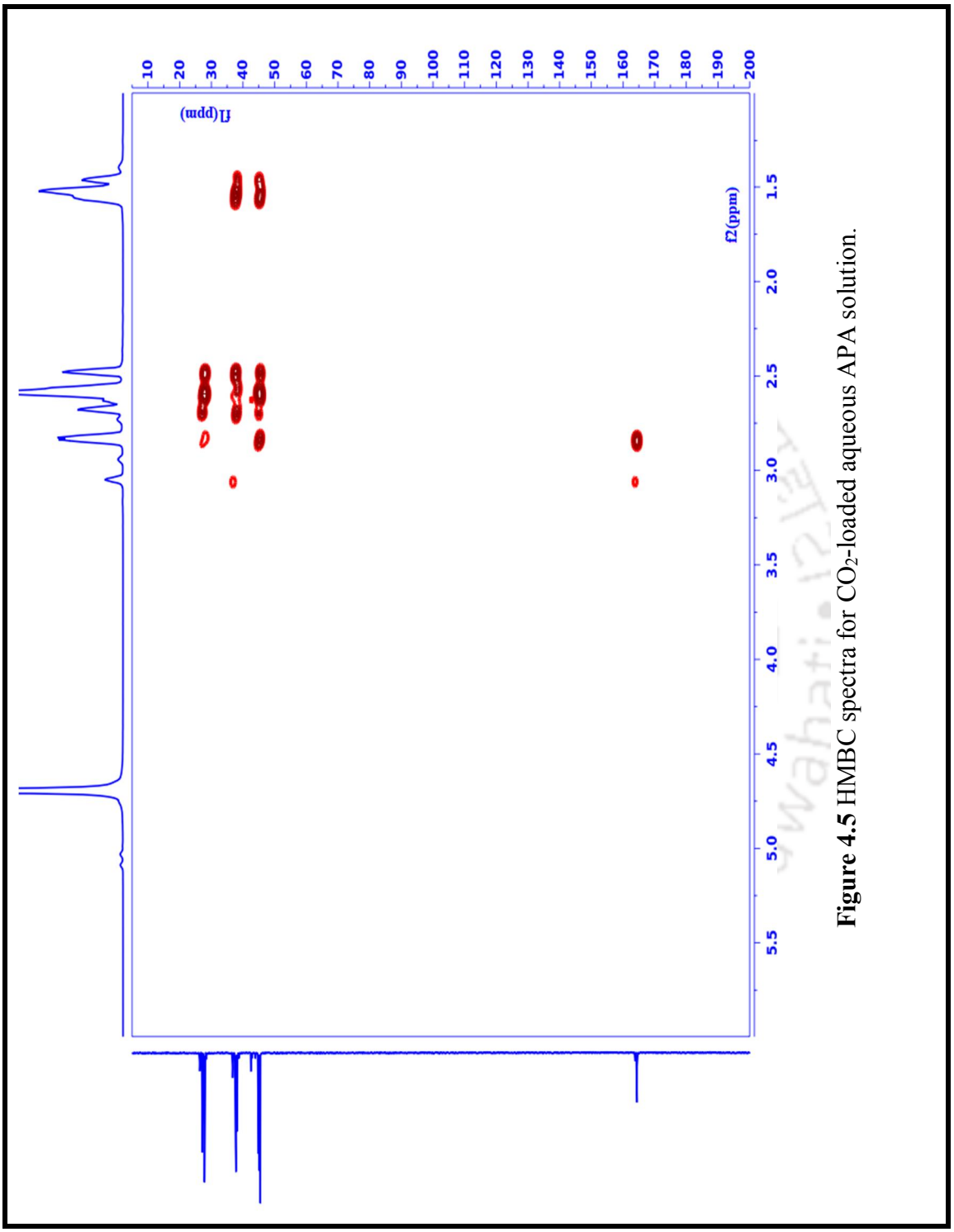

Figure 4.5 HMBC spectra for CO_2-loaded aqueous APA solution.

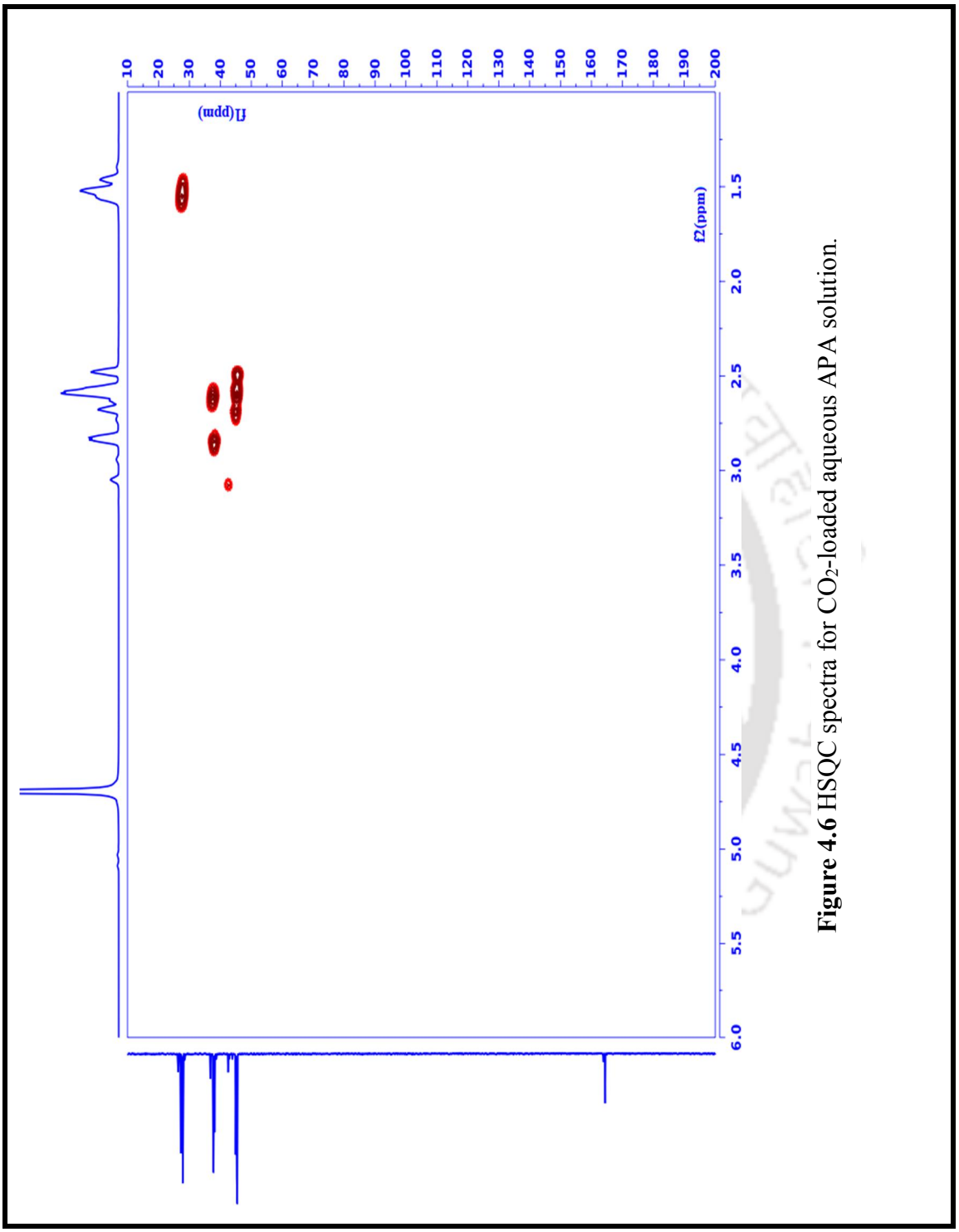

Figure 4.6 HSQC spectra for CO_2-loaded aqueous APA solution.

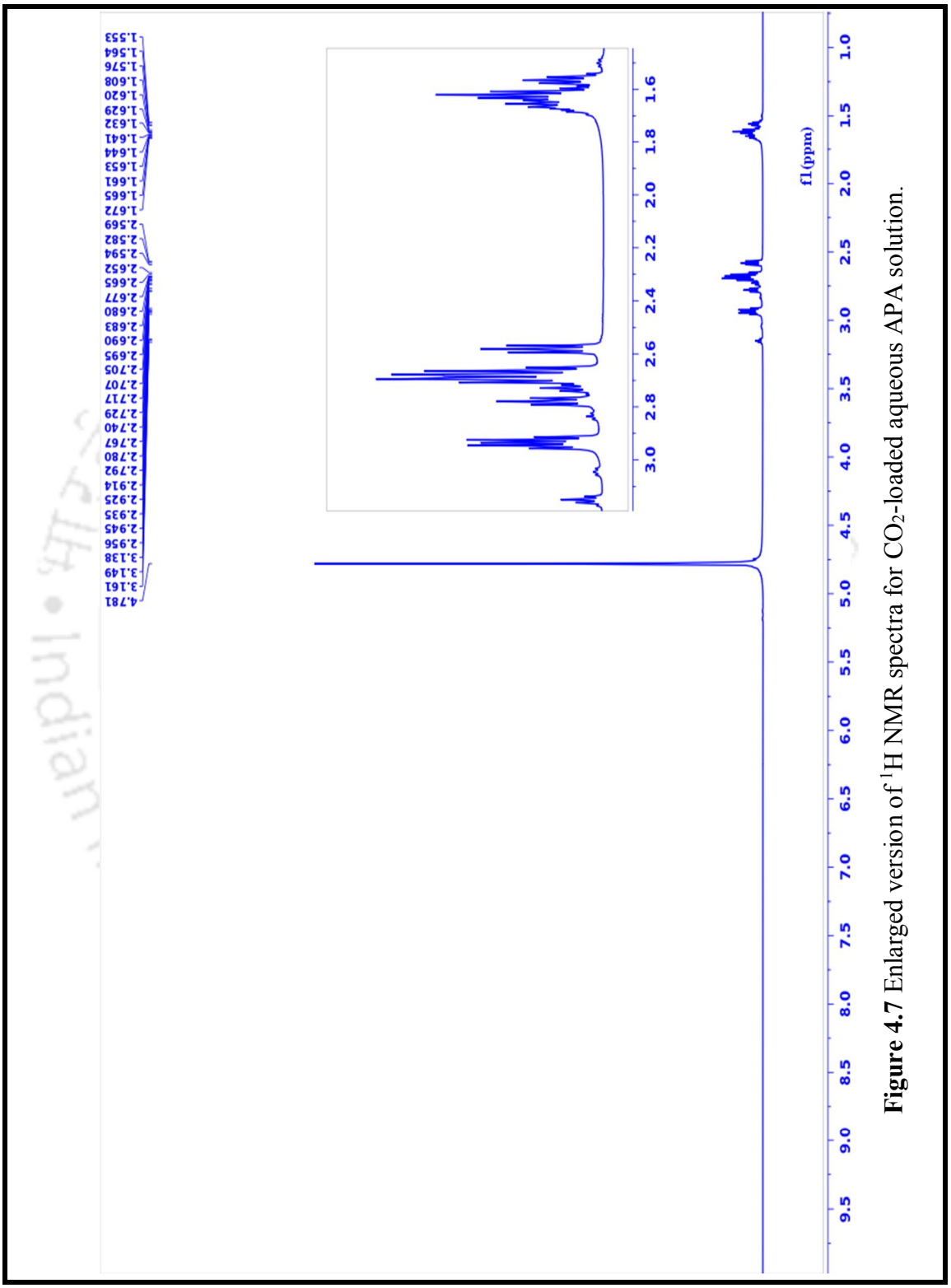

Figure 4.7 Enlarged version of ^{1}H NMR spectra for CO_2-loaded aqueous APA solution.

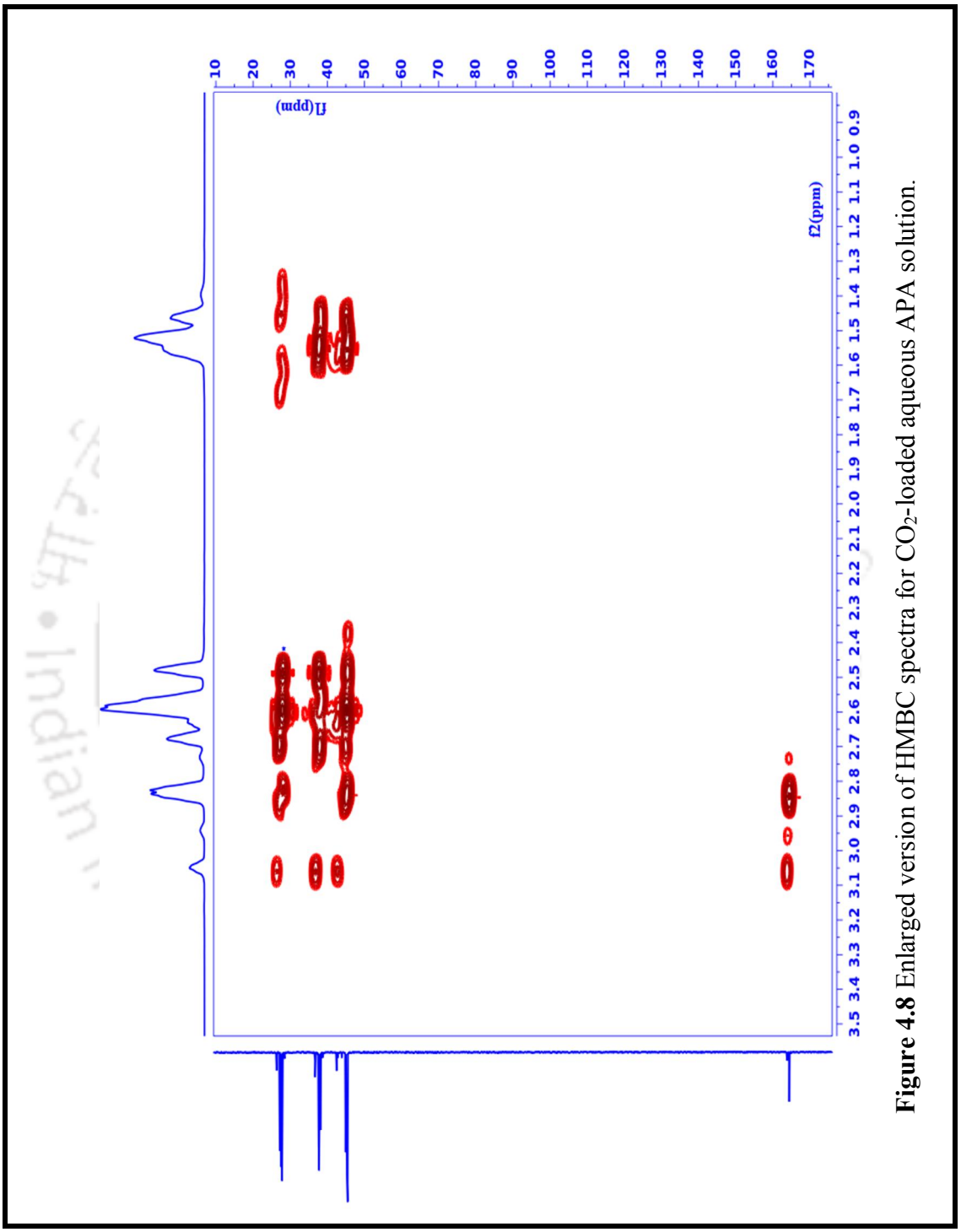

Figure 4.8 Enlarged version of HMBC spectra for CO_2-loaded aqueous APA solution.

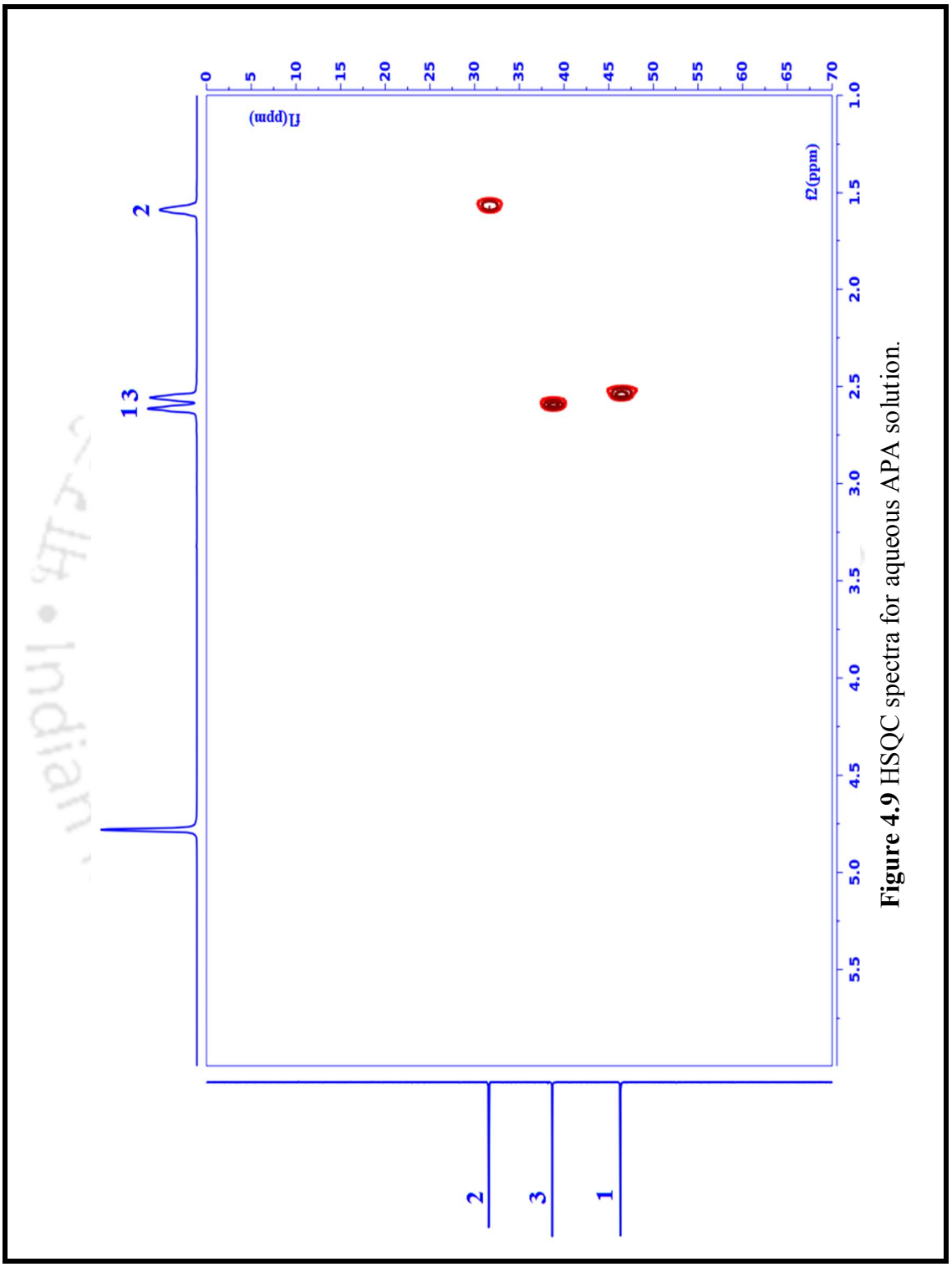

Figure 4.9 HSQC spectra for aqueous APA solution.

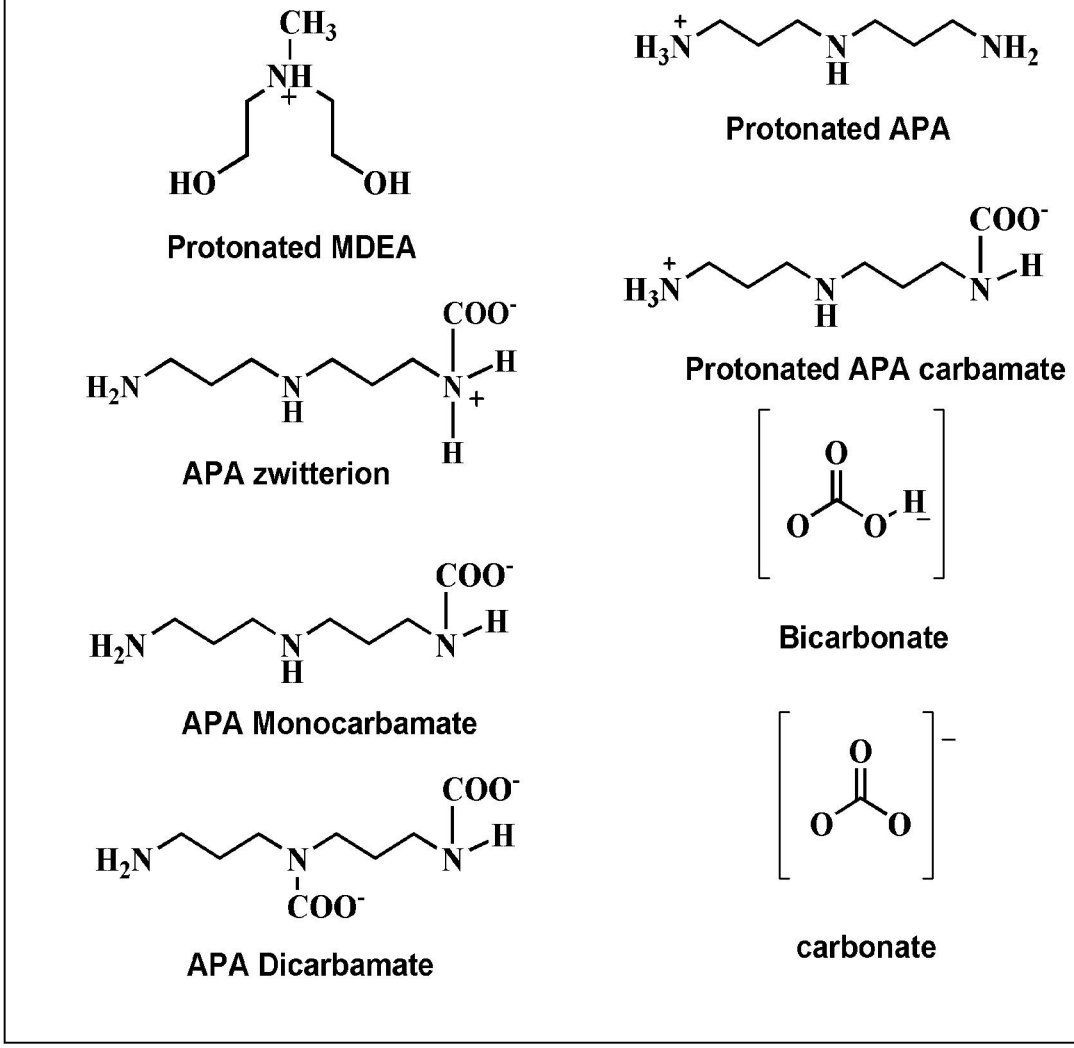

Figure 4.10 The structure of important reaction intermediates and product of CO_2-(MDEA-APA-H_2O) system

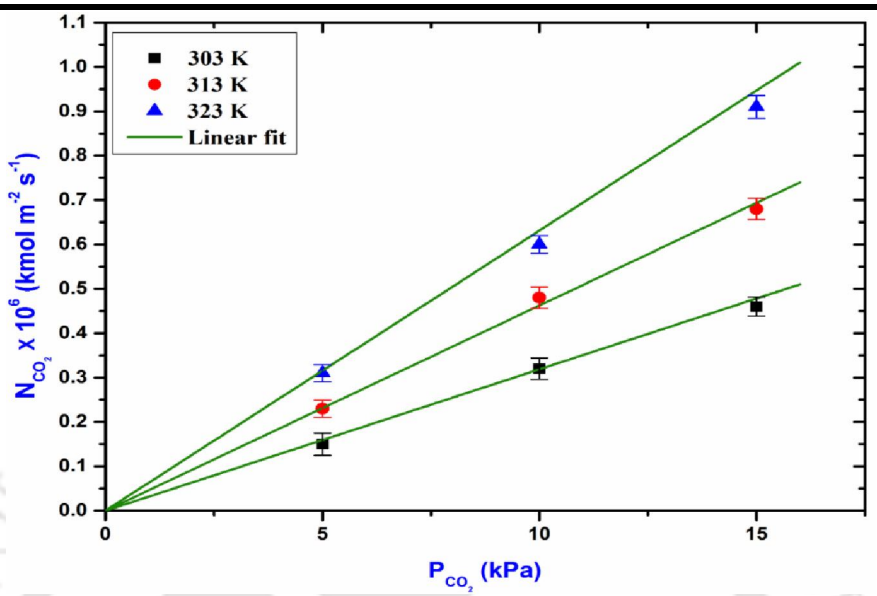

Figure 4.11 CO_2 absorption rate as a function of CO_2 partial pressure apparently measured for 2 kmol m^{-3} MDEA solutions in the pseudo-first-order regime at different temperature.

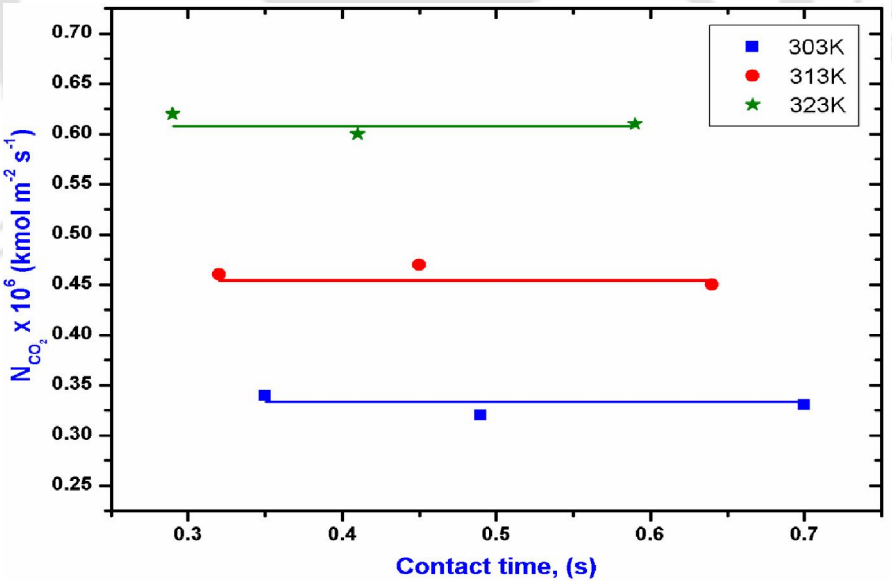

Figure 4.12 Effect of contact time on specific rate of absorption in aqueous MDEA at different temperatures for gas compositions of 10% CO_2 and 90% N_2. V_G: 180×10^{-6} m^3 s^{-1}; 2.0 kmol m^{-3} of MDEA.

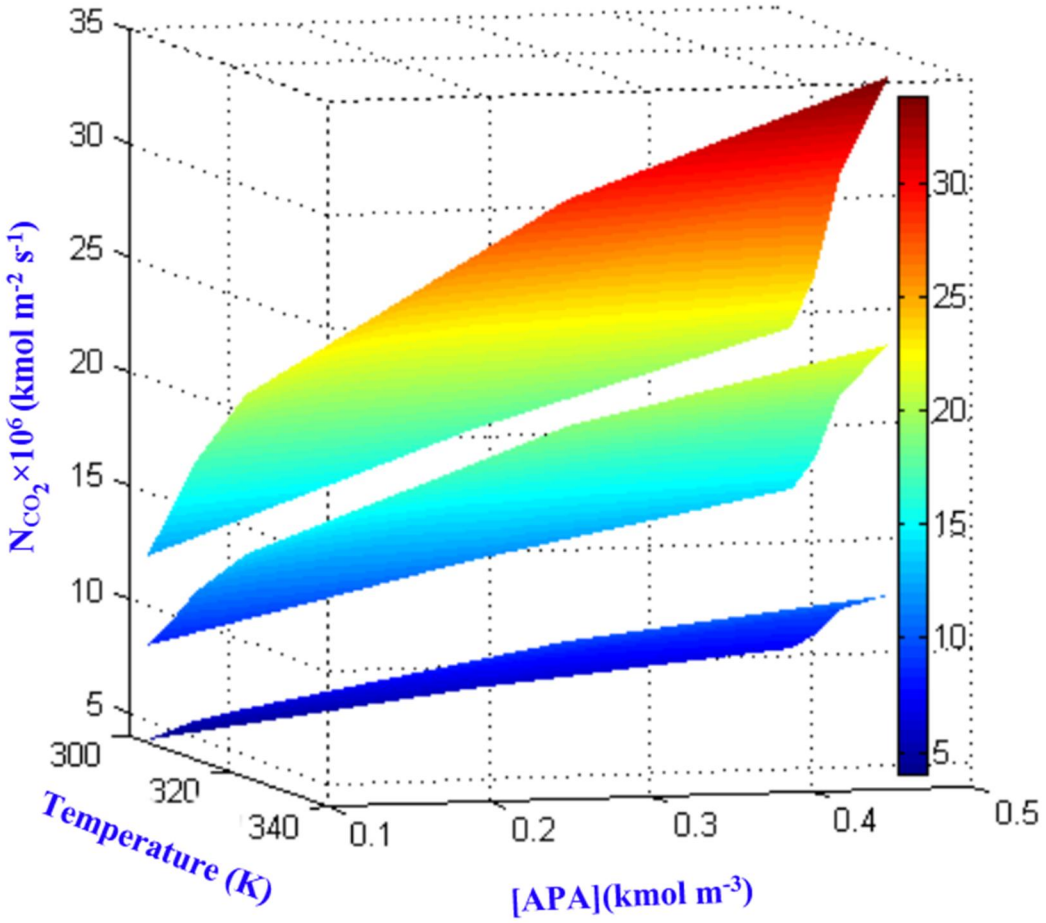

Figure 4.13 Specific absorption rates of CO_2 into aqueous solutions of APA at different temperatures for gas compositions (a) 5% CO_2 and 95% N_2 (b) 10% CO_2 and 90% N_2 (c) 15% CO_2 and 85% N_2.

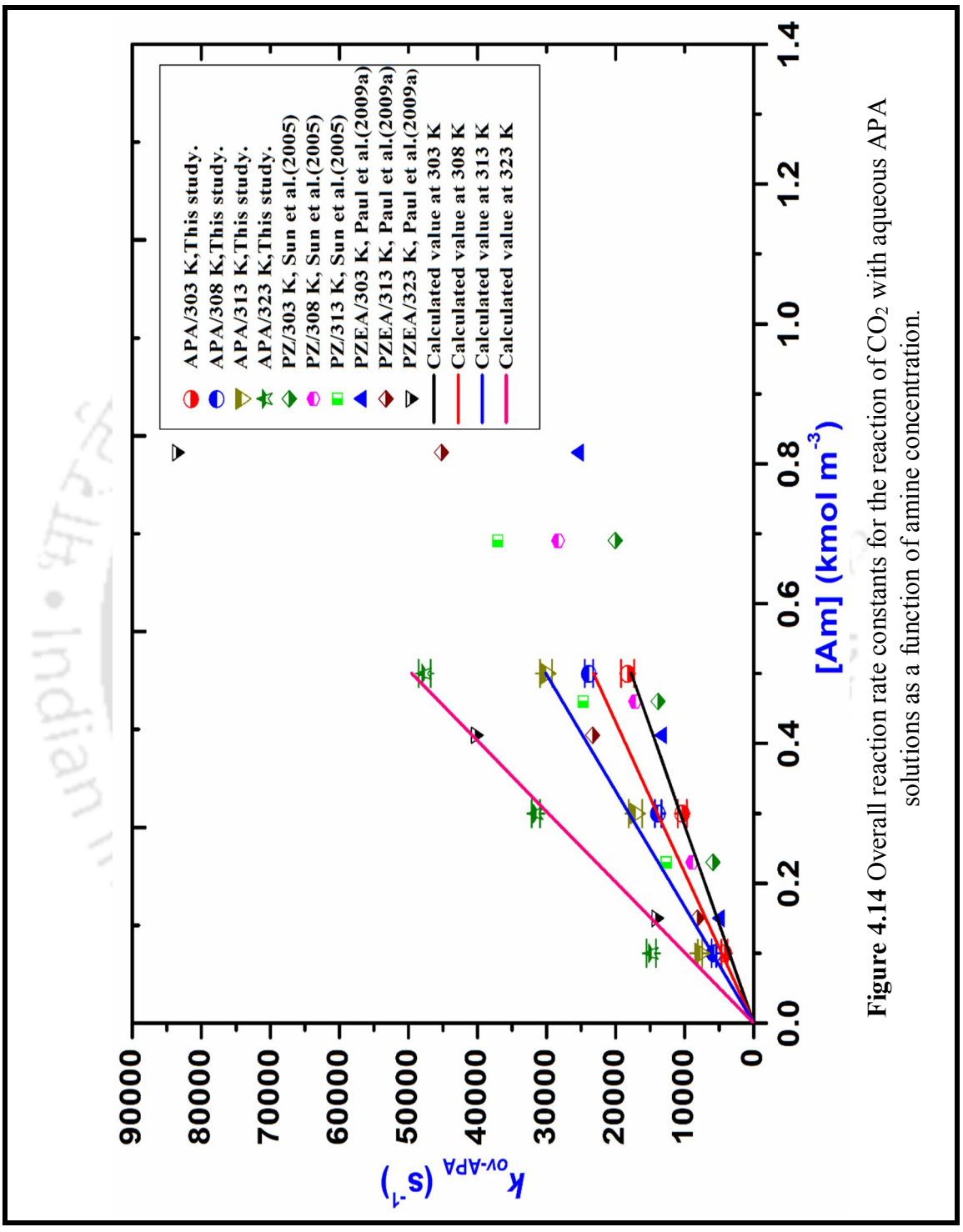

Figure 4.14 Overall reaction rate constants for the reaction of CO_2 with aqueous APA solutions as a function of amine concentration.

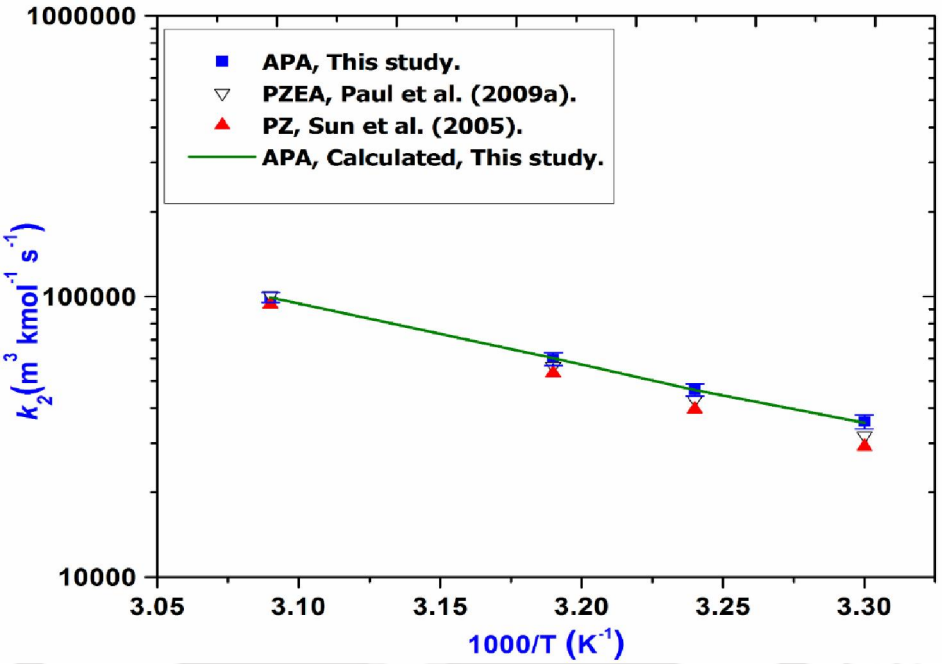

Figure 4.15 Arrhenius plots of second order reaction rate constants for APA, PZ and PZEA aqueous solutions.

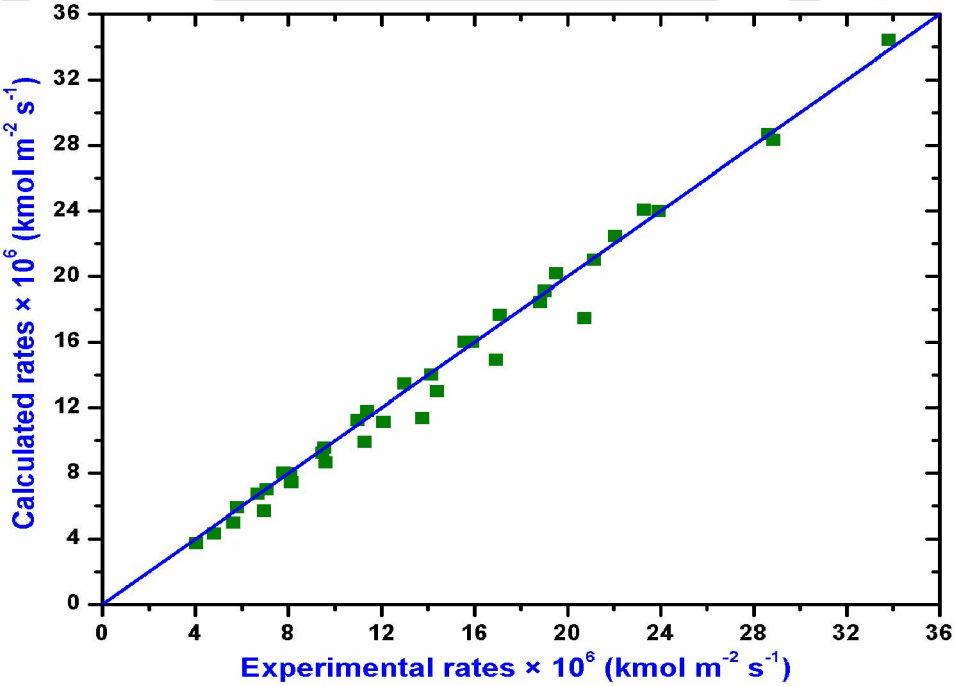

Figure 4.16 Comparison of the calculated rates to the experimental rates of absorption for CO_2 into aqueous solutions of APA.

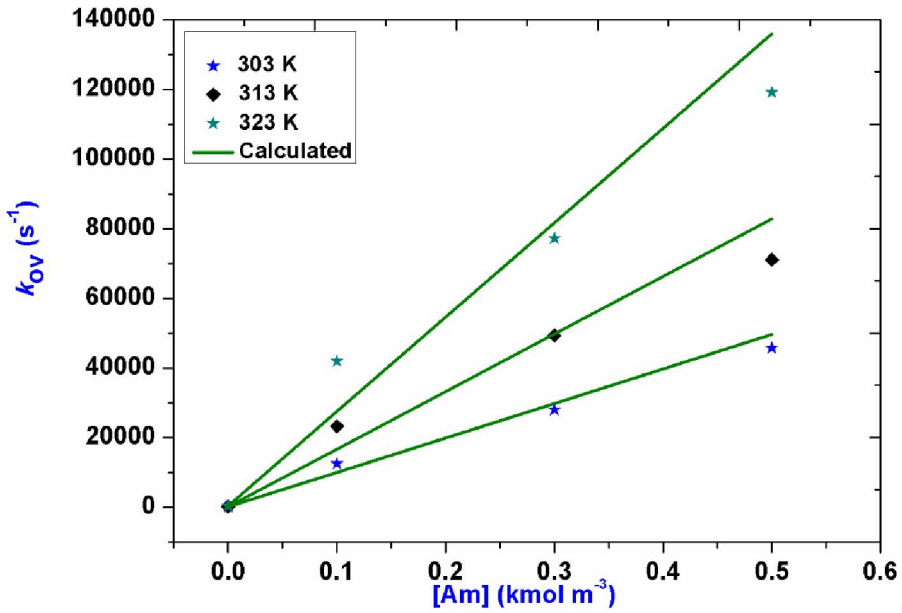

Figure 4.17 Overall reaction rate constants for the reaction of CO_2 with aqueous (APA+MDEA) solutions as a function of amine concentration.

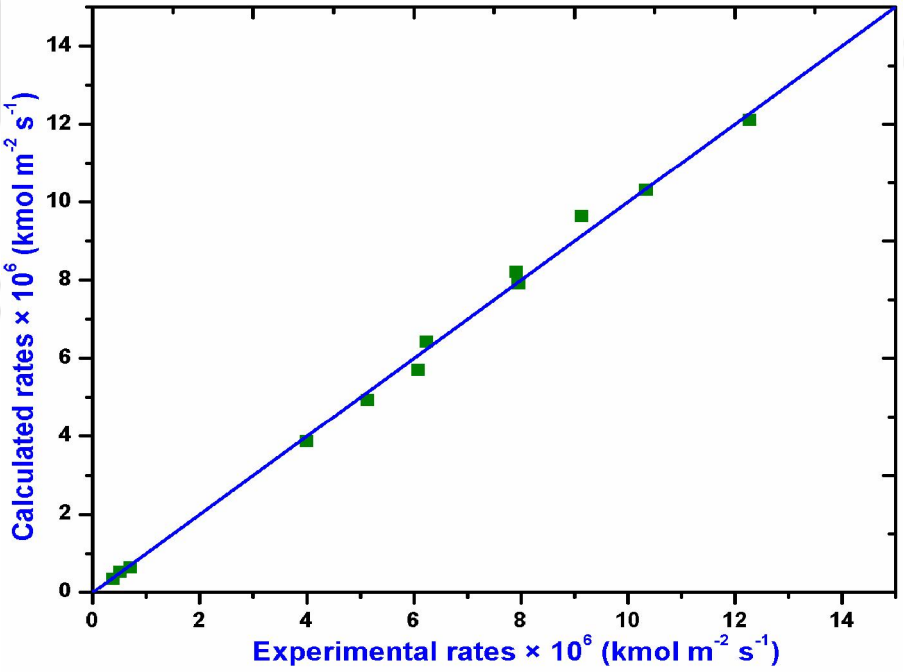

Figure 4.18 Comparison of the calculated rates to the experimental rates of absorption for CO_2 into aqueous solutions of (APA+MDEA).

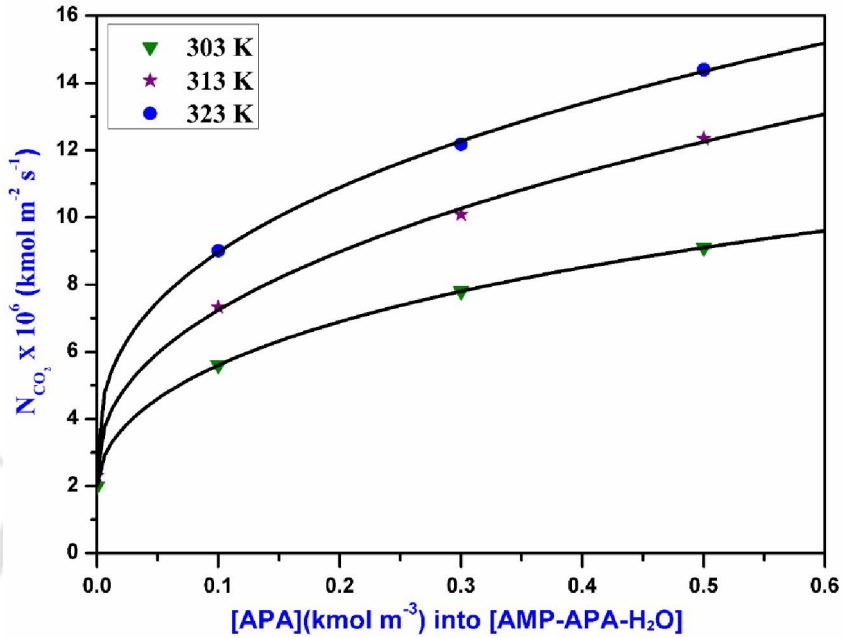

Figure 4.19 Specific absorption rates of CO_2 into aqueous solutions of (APA+AMP) at different temperatures for gas compositions 5% CO_2 and 95% N_2.

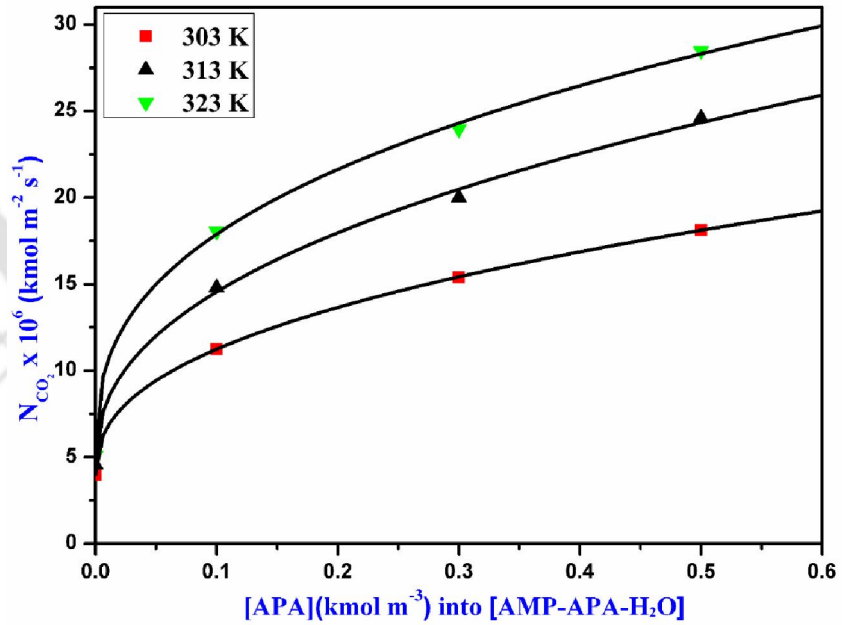

Figure 4.20 Specific absorption rates of CO_2 into aqueous solutions of (APA+AMP) at different temperatures for gas compositions 10% CO_2 and 90% N_2.

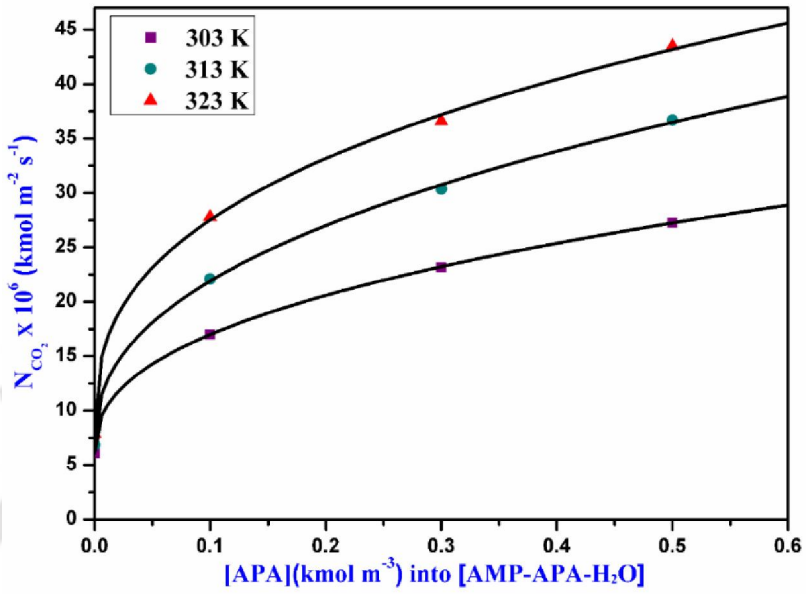

Figure 4.21 Specific absorption rates of CO_2 into aqueous solutions of (APA+AMP) at different temperatures for gas compositions 15% CO_2 and 85% N_2.

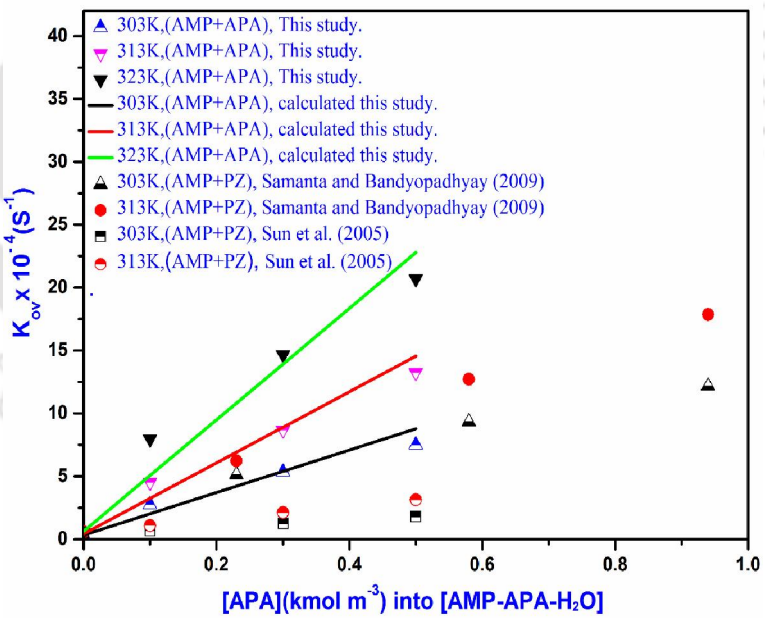

Figure 4.22 Overall reaction rate constants for the reaction of CO_2 with aqueous (APA+AMP) solutions as a function of amine concentration.

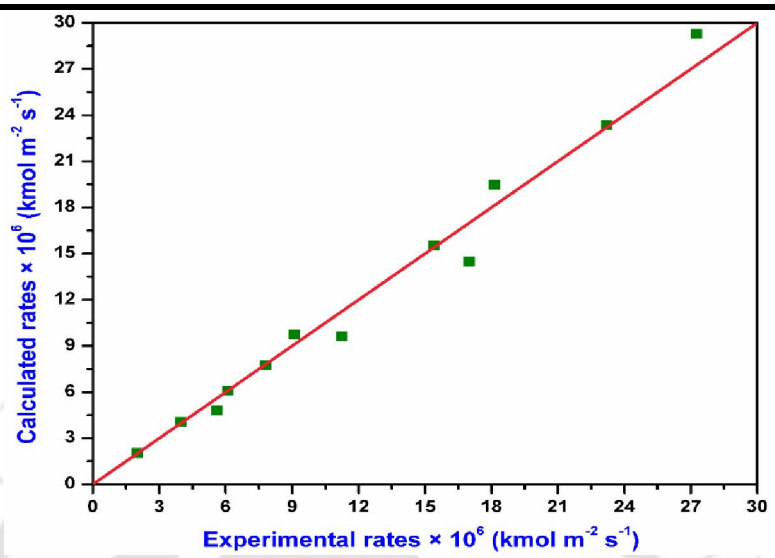

Figure 4.23 Comparison of the calculated rates to the experimental rates of absorption for CO_2 into aqueous solutions of (APA+AMP).

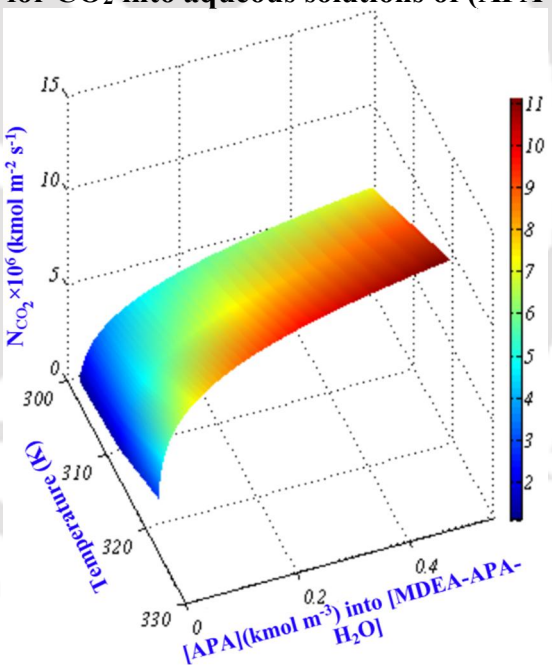

Figure 4.24 Enhancement of MDEA using APA promoter at different temperature

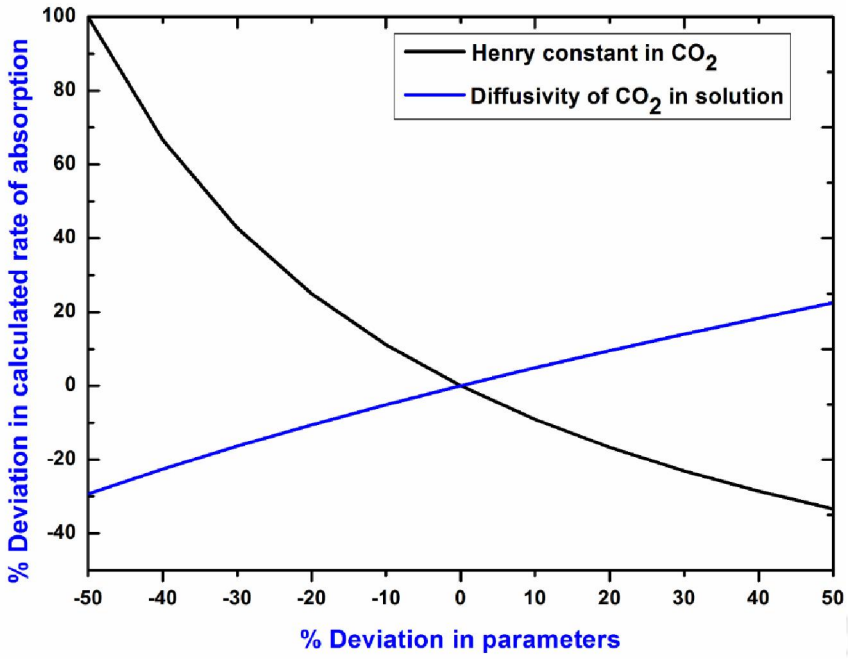

Figure 4.25 Effect of error in Henry's law constant and diffusivity of CO_2 on the calculated rate of absorption of CO_2 in aqueous solutions of (APA+AMP).

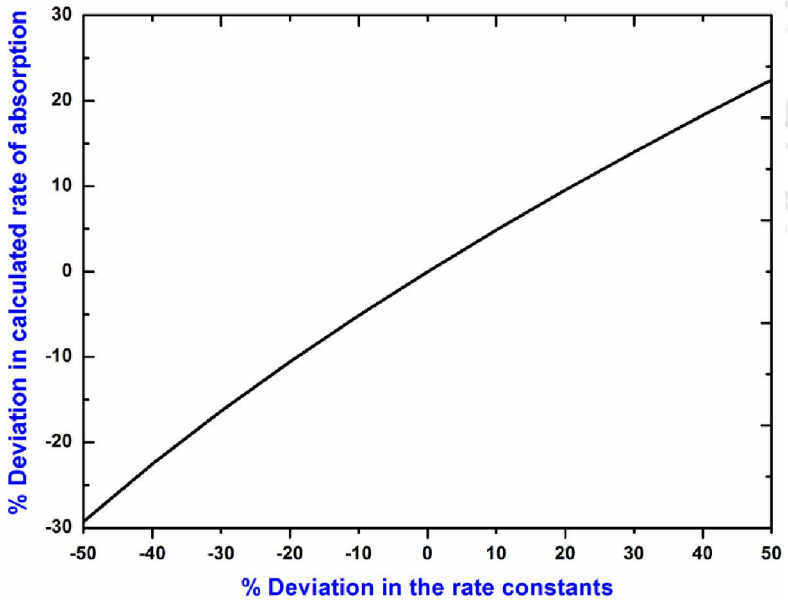

Figure 4.26 Effect of error in second order rate coefficient ($k_{2\text{-APA}}$) on the calculated rate of absorption of CO_2 in aqueous solutions of (APA+AMP).

CHAPTER 5

CONCLUSIONS AND FUTURE DIRECTIONS

This chapter summarizes the major inferences drawn from the research work presented in this dissertation and recommendation toward the future scope of research.

5.1 CONCLUSIONS

The main objective of this work was to investigate the absorption characteristics of CO_2 into selected novel amine activator and its blends with sterically hindered as well as tertiary alkanoalmines. Amine activator was judiciously chosen to represent faster reaction kinetics, high equilibrium loading capacity and higher degradation resistance. Accordingly, bis(3-aminopropyl)amine (APA) was chosen as a novel activator for the blend with N-methyldiethanolamine (MDEA) and 2-amino-2-methyl-1-propanol (AMP). The kinetics of CO_2 absorption as well as physicochemical properties of CO_2-amine systems were performed to understand the reaction mechanism towards CO_2 absorption. The salient accomplishments and major conclusions from this work are summarized below:

- The kinetics experiment of CO_2 absorption into aqueous APA and its blend with MDEA or AMP are determined using a wetted-wall model contactor at temperatures of 303-323 K. To estimate the overall pseudo-first-order reaction rate constants from the present experiments, the kinetic measurements are carried out in the fast pseudo-first-order reaction regime.

- A qualitative NMR analysis of CO_2-(APA-H_2O) reactions aided us about the formation of mono and di-carbamates which correspond to primary and secondary amine groups. However, in the fast-pseudo-first-order reaction regime, we neglected the possibility of the formations of di-carbamates. Since the relative contribution of APA to the formations of carbamates (primary and secondary) by the reactions of CO_2 with APA was very difficult to determine, hence an overall second order rate mechanism was assumed. This assumption's validity was justified by the reaction order with respect to APA (0.95-0.99).
- The values of $k_{2,APA}$ were obtained as 35775, 46414, 59816 and 99220 m^3 $kmol^{-1}$ s^{-1} at 303, 308, 313 and 323 K, respectively, whereas activation energy value is calculated to be 41.8 kJ mol^{-1}. It was found that the observed $k_{2,APA}$ for APA was more than those of PZ.
- The addition of a small amount of fast reacting APA (triamine) to a much larger amount of MDEA or AMP significantly enhances the absorption rate over conventional single amine solvents. The enhancement factors of (MDEA+APA+H_2O)-CO_2 system (at 4.7 kPa of CO_2 and T=313 K) increases from 4.2 to 174.8 when APA concentration varied in the solution from 0 to 0.5 kmol m^{-3}. It can be concluded from the kinetic rate constants of APA that it has a great potential as an activator in combination with alkanolamines like AMP and MDEA for CO_2 absorption.
- In the case of blend, the experiments were performed in the fast-pseudo-first-order reaction regime from which k_{ov} are derived. The reaction of CO_2 with APA in parallel with a reaction between CO_2 and MDEA or AMP were considered as the overall reaction for these measurements. For instance, at T=313 K, the ratio of overall reaction rate constants (k_{ov}) of APA (0.5 kmol m^{-3}) + MDEA (2.5 kmol m^{-3}) + H_2O to MDEA (3.0 kmol m^{-3}) + H_2O is about 1641.
- The rate coefficients for reaction with CO_2 of these (MDEA+APA+H_2O) system were interpreted from the experimentally measured data at different temperatures.

The values of second order rate constant, $k_{2,APA}$, and $k_{2,MDEA}$, for these amines have been correlated according to the following Arrhenius equations.

$$k_{2,APA} = 1.246\times10^{12}\exp\left(-\frac{41188}{RT}\right) \quad (5.1)$$

$$k_{2,MDEA} = 3.01\times10^{11}\exp\left(-\frac{61669}{RT}\right) \quad (5.2)$$

- Out of different compositions studied for (APA+AMP+H_2O)-CO_2 system, 2.5 kmol.m^{-3} AMP + 0.5 kmol.m^{-3} APA showed the highest peak with respect to APA concentration vis-a-vis the specific rate and enhancement factor. For instance (at 9.71 kPa of CO_2 and T=313 K), the enhancement factors increases from 37.3 to 184.7 of (APA+AMP+H_2O)-CO_2 system when APA concentration varied in the solution from 0 to 0.5 kmol m^{-3}.
- The k_{ov} value of (APA+AMP) blend solutions were found to be little higher compared to (AMP+PZ) blend solutions at comparatively higher temperature. The fast pseudo-first-order reaction regime was considered for kinetics measurement to estimate the overall pseudo-first-order reaction rate constant. The second order rate constants, $k_{2,APA}$ and $k_{2,AMP,}$ are correlated as a function of temperature with the following results

$$k_{2,APA} = 2.18\times10^{12}\exp\left(-\frac{41256}{RT}\right) \quad (5.3)$$

$$k_{2,AMP} = 6.33\times10^{7}\exp\left(\frac{-27717}{RT}\right) \quad (5.4)$$

This study demonstrated that APA activated aqueous AMP solutions i.e. formulated (APA+AMP) solutions could be a potential alternative for enhancing absorption of CO_2 compared to a single aqueous AMP solutions.

- Density and viscosity of aqueous novel APA and an aqueous novel blend of APA with MDEA and AMP solutions as well as solubility and diffusivity of N_2O into

these binary and ternary solutions were measured at (298-323) K in order to evaluate the potential of binary and ternary solutions for CO_2 removal from gas mixtures. The thermodynamic properties study indicate that specific and strong interaction like strong dipole-dipole interactions, hydrogen bonding, charge transfer interaction are present in the (APA+AMP+H_2O)-CO_2 system investigated. The physical solubility and diffusivity of CO_2 into these solutions were estimated through "N_2O-analogy". Experimentally determined density and viscosity data were correlated by the well-known model in order to compute the predicted data. In case of both the solubility and diffusivity measurements, several models are applied to correlates experimental data. The predicted data determined by the entire model in this study showed significantly in an acceptable range of less than 10 % (AAD). Hence, reported experimental data on novel amine solutions for CO_2 removal as well as developed correlation would be employed satisfactorily in engineering estimation.

- In order to evaluate the effects of different physicochemical and kinetic parameter on the specific rate of absorption of CO_2, a parametric sensitivity analysis has been performed over (APA+H_2O) and (APA+AMP+H_2O) solvents. The parameters i.e., Henry's law constant for CO_2, diffusivity of CO_2 into the amine solutions and the second order reaction rate constants for the absorption of CO_2 are considered for these analyses. These results were generated by introducing ±50% deviations for the all values of above mention parameters. The Henry's law constant of CO_2 was the most resulted sensitive one in comparison to others.

5.2 RECOMMENDATIONS ON FUTURE DIRECTIONS

- In this work, the reactions between CO_2 and different amines are described through an overall reaction. Furthermore to see the behavior of each and every species in

the liquid phase, development of rigorous mass-transfer reaction based model is essential.

- The film theory is used to describe the diffusion-reaction process to analyse the mass transfer kinetics. The other model such as Higbie's penetration theory may also be applied to compare the results.
- The aqueous blends of (APA+MDEA) and (APA+AMP) are used for kinetics study in the present work where APA acts as an activator. Further studies on APA with other sterically hindered amines such as 2-amino-2-hydroxymethyl-1,3–propanediol (AHPD) is recommended.
- Separation of acid gases such as H_2S, COS, CO_2, CS_2, and mercaptans with diferent novel amine based solvents can be performed in future studies. The present study can be extended for mixture of acid gases.
- The CO_2 absorption kinetics of the chosen activator and its blends with MDEA as well as AMP have been studied. The desorption kinetics of these solvents need to be studied.
- The kinetics and physicochemical properties obtained in this research may be used to design and develop a pilot plant to see the potential use of these solvents for CO_2 capture.

APPENDIX I

Calculation of Uncertainty in the Experimental Measurements

Any physical quantity (Y) such as density, viscosity, solubility and diffusivity depend on many factors such as temperature(X_1), concentration(X_2), pressure(X_3), etc. So we can write as shown below:

$$Y = f(X_1, X_2, X_3, ..., X_N)$$

If an experimental measurement is repeated in independent and unbiased ways, the measurement's result will be slightly different every time. So it is difficult to get "best" value. Therefore uncertainty term in the experimental measurement is considered in this work.

So how to calculate uncertainty

Step 1: It has taken the mean value of all independent variables (X_1, X_2, X_3,….., X_N) and dependent variable (Y).

Ex: Let's assume 'p' times experiment is repeated

$$\text{Mean of } X_1 \left(\overline{X_1}\right) = \frac{(X_{11} + X_{12} + X_{13} + ... + X_{1P})}{P}$$

Step 2: Now calculate standard deviation from mean of all the independent and dependent variables.

$$\text{Ex: Standard deviation of } X_1 \, (u_{X_i}) = \left\{ \frac{\sum_{i=0}^{P} \left(\overline{X_1} - X_{1i}\right)^2}{P(P-1)} \right\}^{0.5}$$

Step 3: After that calculate combined standard uncertainty (u_c^2).

Ex: $u_c^2 = \sum_{i=1}^{N} \left(\frac{\partial f}{\partial X_i} \right)^2 u_{X_i}^2$

Step 4: Finally calculate expended uncertainty (U) taking level of confidence 95% by multiplying combined uncertainty with 2. We can calculate expanded relative uncertainty (U_r)

Ex: $U_c = 2 * u_c$

$$U_r = \frac{U_c}{Y}$$

Exam: 3 Different (APA+H_2O) density (ρ) data from chapter 3 (Table 3.5a) at a given temperature and concentration is given below:

Con \ T	298	303	308	313	318	323
0.1	997.56	996.21	994.48	992.55	990.18	987.58
0.3	997.47	996.12	994.37	992.43	989.94	987.36
0.5	997.32	995.98	994.17	992.27	989.71	987.13
0.7	997.12	995.83	994	992.1	989.48	986.93
0.9	996.9	995.67	993.82	991.92	989.3	986.74
1.1	996.71	995.53	993.64	991.73	989.09	986.55

During the experiment temperature is fluctuated 0.4 K. Let's assume experiment performed at 303 K. So temperature is 303.4 K, 303 K and 302.6 K.

So mean temperature = 303 K

Standard deviation (u_T) = 0.25 K

Uncertainty in Concentration (u_{con}) = 0.001 kg m^{-3}

Uncertainty due to sample impurity also is present. Let's sample purity is 98% and difference between the density of pure sample and impurity is 10%.

So relative uncertainty due to impurity (u_r) = 0.1*(1-0.98) = 0.002

So uncertainty due to impurity present in pure compound (u_I) = u_r* ρ = 1.98 kg m^{-3}

Now calculate temperature gradient $\left(\frac{\partial \rho}{\partial T}\right)$. We will find different slope at different point so we take average.

$\left(\frac{\partial \rho}{\partial T}\right)$ = 0.405 kg/m^3.K

Similarly we take concentration gradient $\left(\frac{\partial \rho}{\partial con}\right)$ = 0.885 kg/kmol.

Now calculate combined uncertainty (u_c) =

$$\left[\left\{u_T\left(\frac{\partial \rho}{\partial T}\right)\right\}^2+\left\{u_{con}\left(\frac{\partial \rho}{\partial con}\right)\right\}^2+u_I^2\right]^{0.5} = 1.99 \text{ kg/m}^3$$

Finally expended combined uncertainty $U_c = 2*u_c = 3.97$ kg/m^3

Relative uncertainty $U_r = \frac{U_c}{\rho} = 0.004$ kg/m^3

APPENDIX II

Tabulated Representation of Different Physicochemical Properties (Supplementary Information of Chapter 3)

II.1 Summary of the Literature Review

Physicochemical Properties such as the density and viscosity of aqueous single and blended amine solutions as well as the solubility and diffusivity of N_2O in various aqueous amine solutions have been reported in several literature. The studied temperature ranges for the measurement of different physicochemical properties by different researchers and the details concentration ranges for different single and blended alkanolamine solutions are given in Tables II.1- II.7 of Appendix II.

Table II.1
Summary of the literature survey about density of different binary aqueous amine solutions

Solvent	Amine mass%	Temperature (K)	Reference
PZ + H_2O	5.358 – 14.5	293.15 – 323.15	[Derks et al., 2005]
	1.74 – 6.88	298 – 333	[Samanta and Bandyopadhyay, 2006]
	30	298 – 333	[Samanta and Bandyopadhyay, 2006]
	1.978 – 7.912	303 – 313	[Sun et al., 2005]
AEPD + H_2O	4.94 – 25.63	303.15 – 318.15	[Yoon et al., 2002a]
AMPD + H_2O	10 – 30	303 – 343	[Baek et al., 2000]
	4.97 – 31.11	303 – 323	[Yoon et al., 2003]
MEA + H_2O	30	293 – 323	[Mandal et al., 2003]
	20	303 – 333	[Laddha et al., 1981]
DEA + H_2O	10 – 30	293 – 373	[Rinker et al., 1994]
	30	293 – 323	[Mandal et al., 2003]
	20 – 30	313 – 353	[Hsu and Li., 1997a]
MDEA + H_2O	10 – 50	293 – 373	[Rinker et al., 1994]
	30	293 – 323	[Mandal et al., 2003]
	20 – 30	303 – 333	[Laddha et al., 1981]
	10 – 50	288 – 333	[Al-Ghawas et al., 1989]
AMP + H_2O	30	293 – 323	[Mandal et al., 2003]
	20	303 – 333	[Laddha et al., 1981]
	30	303 – 333	[Laddha et al., 1981]
	9.05 – 100	293 – 363.7	[Xu et al., 1991]
2-PE + H_2O	10 – 100	298 – 357.2	[Xu et al., 1992]
	1.38 – 12.9	313	[Shen et al., 1991]

Table II.2a
Summary of the literature survey about density of different ternary aqueous amine solutions

Solvent	Amine mass%	Temperature (K)	Reference
PZ + AMP + H_2O	28 + 2	298 – 333	[Samanta and Bandyopadhyay, 2006]
	25 + 5	298 – 333	[Samanta and Bandyopadhyay, 2006]
	22 + 8	298 – 333	[Samanta and Bandyopadhyay, 2006]
	0.86 + 8.9	303 – 313	[Sun et al., 2005]
	1.72 + 8.9	303 – 313	[Sun et al., 2005]
	2.58 + 8.9	303 – 313	[Sun et al., 2005]
	3.44 + 8.9	303 – 313	[Sun et al., 2005]
DEA + AMP + H_2O	1.5 + 28.5	293 – 323	[Mandal et al., 2003]
	3 + 27	293 – 323	[Mandal et al., 2003]
	4.5+ 25.5	293 – 323	[Mandal et al., 2003]
	6 + 24	293 – 323	[Mandal et al., 2003]
	7.5 + 22.5	293 – 323	[Mandal et al., 2003]
	9 + 21	293 – 323	[Mandal et al., 2003]
	24 + 6	303 - 353	[Hsu and Li., 1997a]
	18 + 12	303 - 353	[Hsu and Li., 1997a]
	12+ 18	303 - 353	[Hsu and Li., 1997a]
	6 + 24	303 - 353	[Hsu and Li., 1997a]
	15 + 5	303 - 353	[Hsu and Li., 1997a]
	10 + 10	303 - 353	[Hsu and Li., 1997a]
	5+ 15	303 - 353	[Hsu and Li., 1997a]

Table II.2b
Summary of the literature survey about density of different ternary aqueous amine solutions

Solvent	Amine mass%	Temperature (K)	Reference
DEA + MDEA + H_2O	2.11 + 47.89	293 – 373	[Rinker et al., 1994]
	9 + 41	293 – 373	[Li and Lie, 1994]
	15.3+ 34.7	293 – 373	[Rinker et al., 1994]
	18.5 + 31.5	293 – 373	[Rinker et al., 1994]
	1.5 + 28.5	293 – 323	[Mandal et al., 2003]
	3 + 27	293 – 323	[Mandal et al., 2003]
	4.5+ 25.5	293 – 323	[Mandal et al., 2003]
	6 + 24	293 – 323	[Mandal et al., 2003]
	7.5 + 22.5	293 – 323	[Mandal et al., 2003]
	9 + 21	293 – 323	[Mandal et al., 2003]
	24 + 6	303 - 353	[Hsu and Li., 1997a]
	18 + 12	303 - 353	[Hsu and Li., 1997a]
	12+ 18	303 - 353	[Hsu and Li., 1997a]
	6 + 24	303 - 353	[Hsu and Li., 1997a]
	15 + 5	303 - 353	[Hsu and Li., 1997a]
	10 + 10	303 - 353	[Hsu and Li., 1997a]
	5+ 15	303 - 353	[Hsu and Li., 1997a]
PZ + MDEA + H_2O	8.6 + 3.225	293.15 – 323.15	[Derks et al., 2008]
	1.0 + 6.45	293.15 – 323.15	[Derks et al., 2008]
	1.0 + 9.675	293.15 – 323.15	[Derks et al., 2008]
	1.0 + 12.9	293.15 – 323.15	[Derks et al., 2008]

Table II.2c
Summary of the literature survey about density of different ternary aqueous amine solutions

Solvent	Amine mass%	Temperature (K)	Reference
MEA + MDEA + H_2O	1.5 + 28.5	293 – 323	[Mandal et al., 2003]
	3 + 27	293 – 323	[Mandal et al., 2003]
	4.5+ 25.5	293 – 323	[Mandal et al., 2003]
	6 + 24	293 – 323	[Mandal et al., 2003]
	7.5 + 22.5	293 – 323	[Mandal et al., 2003]
	9 + 21	293 – 323	[Mandal et al., 2003]
	10 + 10	303 - 353	[Hsu and Li., 1997a]
	6 + 24	303 - 353	[Li and Shen, 1992]
	12 + 18	303 - 353	[Li and Shen, 1992]
	18 + 12	303 - 353	[Li and Shen, 1992]
	24 + 6	303 - 353	[Li and Shen, 1992]
	5+ 15	303 - 333	[Li and Shen, 1992]
	15+ 5	303 - 333	[Li and Shen, 1992]
MEA + TEA + H_2O	0.61 + 7.45	303 – 313	[Horng et al., 2002]
	1.22 + 7.45	303 – 313	[Horng et al., 2002]
	1.83 + 7.45	303 – 313	[Horng et al., 2002]
	2.44 + 7.45	303 – 313	[Horng et al., 2002]
	3.05 + 7.45	303 – 313	[Horng et al., 2002]

Table II.2d
Summary of the literature survey about density of different ternary aqueous amine solutions

Solvent	Amine mass%	Temperature (K)	Reference
MEA + AMP + H_2O	1.5 + 28.5	293 – 323	[Mandal et al., 2003]
	3 + 27	293 – 323	[Mandal et al., 2003]
	4.5+ 25.5	293 – 323	[Mandal et al., 2003]
	6 + 24	293 – 323	[Mandal et al., 2003]
	7.5 + 22.5	293 – 323	[Mandal et al., 2003]
	9 + 21	293 – 323	[Mandal et al., 2003]
	10 + 10	303 - 353	[Hsu and Li., 1997a]
	24 + 6	303 - 353	[Li and Lie, 1994]
	18 + 12	303 - 353	[Li and Lie, 1994]
	12+ 18	303 - 353	[Li and Lie, 1994]
	6 + 24	303 - 353	[Li and Lie, 1994]
	15 + 5	303 - 353	[Li and Lie, 1994]
	5+ 15	303 - 353	[Li and Lie, 1994]
MEA + 2-PE + H_2O	24 + 6	303 - 353	[Hsu and Li., 1997a]
	18 + 12	303 - 353	[Hsu and Li., 1997a]
	12+ 18	303 - 353	[Hsu and Li., 1997a]
	6 + 24	303 - 353	[Hsu and Li., 1997a]
	15 + 5	303 - 353	[Hsu and Li., 1997a]
	10 + 10	303 - 353	[Hsu and Li., 1997a]
	5+ 15	303 - 353	[Hsu and Li., 1997a]

Table II.3
Summary of the literature survey about viscosity of different binary aqueous amine solutions

Solvent	Amine mass%	Temperature (K)	Reference
PZ + H_2O	5.358 – 14.5	293.15 – 323.15	[Derks et al., 2005]
	1.74 – 6.88	298 – 333	[Samanta and Bandyopadhyay, 2006]
	30	298 – 333	[Samanta and Bandyopadhyay, 2006]
	1.978 – 7.912	303 – 313	[Sun et al., 2005]
AEPD + H_2O	4.94 – 25.63	303.15 – 318.15	[Yoon et al., 2002b]
AMPD + H_2O	10 – 30	303 – 343	[Baek et al., 2000]
	4.97 – 31.11	303 – 323	[Yoon et al., 2003]
MEA + H_2O	30	293 – 323	[Mandal et al., 2003]
DEA + H_2O	10 – 30	293 – 373	[Rinker et al., 1994]
	30	293 – 323	[Mandal et al., 2003]
	10 – 20	313 – 353	[Hsu and Li., 1997b]
MDEA + H_2O	10 – 50	293 – 373	[Rinker et al., 1994]
	30	293 – 323	[Mandal et al., 2003]
	20 – 50	303 – 333	[Li and Lie, 1994]
	10 – 50	288 – 333	[Al-Ghawas et al., 1989]
AMP + H_2O	30	293 – 323	[Mandal et al., 2003]
	17.8 – 26.7	296.6 – 318.9	[Xu et al., 1991]
2-PE + H_2O	10 – 100	298 – 358.2	[Xu et al., 1992]
	1.38 – 12.9	313	[Shen et al., 1991]

Table II.4a
Summary of the literature survey about viscosity of different ternary aqueous amine solutions

Solvent	Amine mass%	Temperature (K)	Reference
PZ + AMP + H_2O	28 + 2	298 – 333	[Samanta and Bandyopadhyay, 2006]
	25 + 5	298 – 333	[Samanta and Bandyopadhyay, 2006]
	22 + 8	298 – 333	[Samanta and Bandyopadhyay, 2006]
	0.86 + 8.9	303 – 313	[Sun et al., 2005]
	1.72 + 8.9	303 – 313	[Sun et al., 2005]
	2.58 + 8.9	303 – 313	[Sun et al., 2005]
	3.44 + 8.9	303 – 313	[Sun et al., 2005]
DEA + AMP + H_2O	1.5 + 28.5	293 – 323	[Mandal et al., 2003]
	3 + 27	293 – 323	[Mandal et al., 2003]
	4.5+ 25.5	293 – 323	[Mandal et al., 2003]
	6 + 24	293 – 323	[Mandal et al., 2003]
	7.5 + 22.5	293 – 323	[Mandal et al., 2003]
	9 + 21	293 – 323	[Mandal et al., 2003]
	24 + 6	303 - 353	[Hsu and Li., 1997b]
	18 + 12	303 - 353	[Hsu and Li., 1997b]
	12+ 18	303 - 353	[Hsu and Li., 1997b]
	6 + 24	303 - 353	[Hsu and Li., 1997b]
	15 + 5	303 - 353	[Hsu and Li., 1997b]
	10 + 10	303 - 353	[Hsu and Li., 1997b]
	5+ 15	303 - 353	[Hsu and Li., 1997b]

Table II.4b
Summary of the literature survey about viscosity of different ternary aqueous amine solutions

Solvent	Amine mass%	Temperature (K)	Reference
DEA + MDEA + H_2O	2.11 + 47.89	293 – 373	[Rinker et al., 1994]
	9 + 41	293 – 373	[Rinker et al., 1994]
	15.3+ 34.7	293 – 373	[Rinker et al., 1994]
	18.5 + 31.5	293 – 373	[Rinker et al., 1994]
	1.5 + 28.5	293 – 323	[Mandal et al., 2003]
	3 + 27	293 – 323	[Mandal et al., 2003]
	4.5+ 25.5	293 – 323	[Mandal et al., 2003]
	6 + 24	293 – 323	[Mandal et al., 2003]
	7.5 + 22.5	293 – 323	[Mandal et al., 2003]
	9 + 21	293 – 323	[Mandal et al., 2003]
	24 + 6	303 - 353	[Hsu and Li., 1997b]
	18 + 12	303 - 353	[Hsu and Li., 1997b]
	12+ 18	303 - 353	[Hsu and Li., 1997b]
	6 + 24	303 - 353	[Hsu and Li., 1997b]
	15 + 5	303 - 353	[Hsu and Li., 1997b]
	10 + 10	303 - 353	[Hsu and Li., 1997b]
	5+ 15	303 - 353	[Hsu and Li., 1997b]
PZ + MDEA + H_2O	8.6 + 3.225	293.15 – 323.15	[Derks et al., 2008]
	1.0 + 6.45	293.15 – 323.15	[Derks et al., 2008]
	1.0 + 9.675	293.15 – 323.15	[Derks et al., 2008]
	1.0 + 12.9	293.15 – 323.15	[Derks et al., 2008]

Table II.4c
Summary of the literature survey about viscosity of different ternary aqueous amine solutions

Solvent	Amine mass%	Temperature (K)	Reference
MEA + MDEA + H_2O	1.5 + 28.5	293 – 323	[Mandal et al., 2003]
	3 + 27	293 – 323	[Mandal et al., 2003]
	4.5+ 25.5	293 – 323	[Mandal et al., 2003]
	6 + 24	293 – 323	[Mandal et al., 2003]
	7.5 + 22.5	293 – 323	[Mandal et al., 2003]
	9 + 21	293 – 323	[Mandal et al., 2003]
	10 + 10	303 - 353	[Hsu and Li., 1997b]
	6 + 24	303 - 353	[Li and Lie., 1994]
	12 + 18	303 - 353	[Li and Lie., 1994]
	18 + 12	303 - 353	[Li and Lie., 1994]
	24 + 6	303 - 353	[Li and Lie., 1994]
	5+ 15	303 - 333	[Li and Lie., 1994]
	15+ 5	303 - 333	[Li and Lie., 1994]
MEA + TEA + H_2O	0.61 + 7.45	303 – 313	[Horng et al., 2002]
	1.22 + 7.45	303 – 313	[Horng et al., 2002]
	1.83 + 7.45	303 – 313	[Horng et al., 2002]
	2.44 + 7.45	303 – 313	[Horng et al., 2002]
	3.05 + 7.45	303 – 313	[Horng et al., 2002]

Table II.4d
Summary of the literature survey about viscosity of different ternary aqueous amine solutions

Solvent	Amine mass%	Temperature (K)	Reference
MEA + AMP + H_2O	1.5 + 28.5	293 – 323	[Mandal et al., 2003]
	3 + 27	293 – 323	[Mandal et al., 2003]
	4.5+ 25.5	293 – 323	[Mandal et al., 2003]
	6 + 24	293 – 323	[Mandal et al., 2003]
	7.5 + 22.5	293 – 323	[Mandal et al., 2003]
	9 + 21	293 – 323	[Mandal et al., 2003]
	10 + 10	303 - 353	[Hsu and Li., 1997b]
	24 + 6	303 - 353	[Li and Lie, 1994]
	18 + 12	303 - 353	[Li and Lie, 1994]
	12+ 18	303 - 353	[Li and Lie, 1994]
	6 + 24	303 - 353	[Li and Lie, 1994]
	15 + 5	303 - 353	[Li and Lie, 1994]
	5+ 15	303 - 353	[Li and Lie, 1994]
MEA + 2-PE + H_2O	24 + 6	303 - 353	[Hsu and Li., 1997b]
	18 + 12	303 - 353	[Hsu and Li., 1997b]
	12+ 18	303 - 353	[Hsu and Li., 1997b]
	6 + 24	303 - 353	[Hsu and Li., 1997b]
	15 + 5	303 - 353	[Hsu and Li., 1997b]
	10 + 10	303 - 353	[Hsu and Li., 1997b]
	5+ 15	303 - 353	[Hsu and Li., 1997b]

Table II.5
Summary of the literature survey about solubility of N_2O into different binary aqueous amine solutions

Solvent	Amine mass%	Temperature (K)	Reference
PZ + H_2O	1.883 – 15.471	293.15 – 323.15	[Derks et al., 2005]
	1.978 – 7.912	303 – 313	[Sun et al., 2005]
	1.74 – 12	293 – 313	[Samanta et al., 2007]
AMPD + H_2O	4.97 – 31.11	303 – 323	[Yoon et al., 2003]
MEA + H_2O	12.2 – 18.3	293 – 313	[Mandal et al., 2003]
	6.1 – 36.6	303 – 313	[Tsai et al., 2000]
DEA + H_2O	4.73 – 21.27	298	[Versteeg and van Swaaij 1988]
	21 – 31.5	293 – 313	[Mandal et al., 2005]
	10.5 – 63	303 – 313	[Tsai et al., 2000]
MDEA + H_2O	4.14 – 32.75	293 - 308	[Versteeg and van Swaaij 1988]
	10 – 50	288 – 333	[Al-Ghawas et al., 1989]
	23.8 – 35.7	293 – 313	[Mandal et al., 2004]
AMP + H_2O	17.8 – 26.7	283.2 – 348.2	[Xu et al., 1992]
	17.8 – 26.7	293 – 313	[Mandal et al., 2004]
	4.45 – 26.7	303 – 313	[Tsai et al., 2000]
	4.45 – 17.8	388.5 – 303	[Saha et al., 1993]
2-PE + H_2O	10 – 100	298 – 356.1	[Xu et al., 1992]

Table II.6
Summary of the literature survey about diffusivity of N_2O into different binary aqueous amine solutions

Solvent	Amine mass%	Temperature (K)	Reference
PZ + H_2O	1.978 – 7.912	303 –313	[Sun et al., 2005]
	1.74 – 6.88	298 –313	[Samanta et al., 2007]
AMPD + H_2O	4.97 – 31.11	303 –323	[Yoon et al., 2003]
MEA + H_2O	3.05– 30.5	303 –313	[Ko et al., 2001]
	30	303 –313	[Li and Lai, 1995]
DEA + H_2O	2.49– 26.25	303 –313	[Ko et al. (2001]
	30	303 –313	[Li and Lee, 1996]
MDEA + H_2O	2.82–26.13	293 –298	[Versteeg and van Swaaij 1988]
	10 – 50	288 –323	[Al-Ghawas et al., 1989]
	30	303 –313	[Li and Lai, 1995]
AMP + H_2O	2.11 – 22.25	303 –313	[Ko et al. 2001]
	17.8 – 26.7	294.4 –348.5	[Xu et al., 1991]
	4.45 – 17.8	294 –318	[Saha et al., 1993]
	30	303 – 313	[Li and Lai, 1995]
2-PE + H_2O	5 – 40	293 – 313	[Xu et al., 1993]

Table II.7a
Summary of the literature survey about solubility and diffusivity of N_2O into different ternary aqueous amine solutions

Solvent	Amine mass%	Temperature (K)	Reference
PZ + AMP + H_2O	0.86 + 8.9	303 – 313	[Sun et al., 2005]
	1.72 + 8.9	303 – 313	[Sun et al., 2005]
	2.58 + 8.9	303 – 313	[Sun et al., 2005]
	3.44 + 8.9	303 – 313	[Sun et al., 2005]
DEA + AMP + H_2O	1.5 + 28.5	293 – 313	[Mandal et al., 2005]
	3 + 27	293 – 313	[Mandal et al., 2004]
	4.5+ 25.5	293 – 313	[Mandal et al., 2004]
	6 + 24	293 – 313	[Mandal et al., 2004]
	7.5 + 22.5	293 – 313	[Mandal et al., 2004]
	9 + 21	293 – 313	[Mandal et al., 2004]
	6 + 24	303 – 313	[Li and Lee, 1996]
	12 + 18	303 – 313	[Li and Lee, 1996]
	18 + 12	303 – 313	[Li and Lee, 1996]
	24 + 6	303 – 313	[Li and Lee, 1996]

Table III.7b
Summary of the literature survey about solubility and diffusivity of N_2O into different ternary aqueous amine solutions

Solvent	Amine mass%	Temperature (K)	Reference
DEA + MDEA + H_2O	1.5 + 28.5	293 – 313	[Mandal et al., 2004]
	3 + 27	293 – 313	[Mandal et al., 2004]
	4.5+ 25.5	293 – 313	[Mandal et al., 2004]
	6 + 24	293 – 313	[Mandal et al., 2004]
	7.5 + 22.5	293 – 313	[Mandal et al., 2004]
	9 + 21	293 – 313	[Mandal et al., 2004]
	6 + 24	303 – 313	[Li and Lee, 1996]
	12 + 18	303 – 313	[Li and Lee, 1996]
	18 + 12	303 – 313	[Li and Lee, 1996]
	24 + 6	303 – 313	[Li and Lee, 1996]
PZ + MDEA + H_2O	2 + 28	293 – 313	[Samanta et al., 2007]
	8 + 22	293 – 313	[Samanta et al., 2007]
	12 + 18	293 – 313	[Samanta et al., 2007]

Table III.7c
Summary of the literature survey about solubility and diffusivity of N_2O into different ternary aqueous amine solutions

Solvent	Amine mass%	Temperature (K)	Reference
MEA + MDEA + H_2O	1.5 + 28.5	293 – 313	[Mandal et al., 2005]
	3 + 27	293 – 313	[Mandal et al., 2005]
	4.5+ 25.5	293 – 313	[Mandal et al., 2005]
	6 + 24	293 – 313	[Mandal et al., 2005]
	7.5 + 22.5	293 – 313	[Mandal et al., 2005]
	9 + 21	293 – 313	[Mandal et al., 2005]
	6 + 24	303 – 313	[Li and Lai, 1995]
	12 + 18	303 – 313	[Li and Lai, 1995]
	18 + 12	303 – 313	[Li and Lai, 1995]
	24 + 6	303 – 313	[Li and Lai, 1995]
MEA + TEA + H_2O	0.61 + 7.45	303 – 313	[Horng et al., 2002]
	1.22 + 7.45	303 – 313	[Horng et al., 2002]
	1.83 + 7.45	303 – 313	[Horng et al., 2002]
	2.44 + 7.45	303 – 313	[Horng et al., 2002]
	3.05 + 7.45	303 – 313	[Horng et al., 2002]

Table II.7d
Summary of the literature survey about solubility and diffusivity of N_2O into different ternary aqueous amine solutions

Solvent	Amine mass%	Temperature (K)	Reference
MEA + AMP + H_2O	1.5 + 28.5	293 – 313	[Mandal et al., 2005]
	3 + 27	293 – 313	[Mandal et al., 2005]
	4.5+ 25.5	293 – 313	[Mandal et al., 2005]
	6 + 24	293 – 313	[Mandal et al., 2005]
	7.5 + 22.5	293 – 313	[Mandal et al., 2005]
	9 + 21	293 – 313	[Mandal et al., 2005]
	6 + 24	303 – 313	[Li and Lai, 1995]
	12 + 18	303 – 313	[Li and Lai, 1995]
	18 + 12	303 – 313	[Li and Lai, 1995]
	24 + 6	303 – 313	[Li and Lai, 1995]

APPENDIX III

Sample Calculations

III.1 Absorption of CO_2 into Aqueous AMP Solution (Supplementary Information of Chapter 4)

III.1.1 Determination of specific rate of absorption (N_{CO_2})

. For material balance of CO_2 in the wetted wall absorber the specific rate of absorption can be expressed as

$$N_{CO_2} = \frac{V_L}{\pi(d+2w)h}(C_{CO_2,o} - C_{CO_2,i}) \qquad \text{(III.1)}$$

where

$C_{CO_2,o}$ = total absorbed CO_2 in the liquid phases at the outlet, kmol m^{-3}

and $C_{CO_2,i}$ = total absorbed CO_2 in the liquid phases at the inlet, kmol m^{-3}

The liquid phase CO_2 concentrations have been determined from the volume of CO_2 evolved from the liquid sample by acidification (Section 4.3.4).

$$C_{CO_2} = v_{CO_2} \times \frac{P-f}{P} \times \frac{273}{T} \times \frac{P}{101.3} \times \frac{1}{22.4} \text{ kmol m}^{-3}$$

$$= v_{CO_2} \times \frac{P-f}{101.3} \times \frac{273}{T} \times \frac{1}{22.4} \text{ kmol m}^{-3}$$

Where

v_{CO_2} = Volumne of CO_2 evolved from unit volume of the liquid sample, m^3 m^{-3}

P = Total pressure, kPa

f = Vapour pressure of the liquid, kPa

T = Temperature at which the gas volumne was measured, K

For $T = 313$ K, [AMP] = 3.0 kmol m^{-3}, $h = 0.07$ m, $V_L = 2 \times 10^{-6}$ m^3 s^{-1} and $d = 2.81 \times 10^{-2}$ m,

and according to Tables 3.8a and 3.9a,

for $\rho = 986.55$ kg m^{-3} and $\mu = 1.95 \times 10^{-3}$ kg m^{-1} s^{-1}

The expression for film thickness (w) as

$$w = \left(\frac{3\mu V_L}{\pi g d \rho} \right)^{\frac{1}{3}} \qquad \text{(III.2)}$$

$$w = \left(\frac{3 \times 1.95 \times 10^{-3} \times 2 \times 10^{-6}}{\pi \times 9.81 \times 2.81 \times 10^{-2} \times 986.55} \right)^{\frac{1}{3}} = 2.393 \times 10^{-4} \text{ m}$$

v_{CO_2} = 0.2011 m^3 m^{-3} liquid

P = 101.3 kPa

f = 7.35 kPa

T = 313 K.

$C_{CO_2,i} = 0$ (Since the aqueous amine solutions inlet to the absorber was always free of CO_2)

$$C_{CO_2,o} = 0.2011 \times \frac{101.3 - 7.35}{101.3} \times \frac{273}{313} \times \frac{1}{22.4}$$

$$= 7.26 \times 10^{-3} \text{ kmol } m^{-3}$$

Hence,

$$N_{CO_2} = \frac{2 \times 10^{-6}}{\pi (2.81 \times 10^{-2} + 2 \times 2.393 \times 10^{-4}) \times 0.07} (7.26 \times 10^{-3} - 0) \text{ kmol } m^{-2} s^{-1}$$

$$= 2.31 \times 10^{-6} \text{ kmol } m^{-2} s^{-1}$$

III.1.2 Determination of overall reaction rate constant (k_{ov})

Equation (4.7) gives the expression for overall reaction rate constant (k_{ov}) as

$$k_{ov} = \frac{\left(\frac{N_{CO_2} \times H_{CO_2}}{p_{CO_2}}\right)^2}{D_{CO_2}} \tag{III.3}$$

For the same experiment mentioned in the previous section,

$p_{CO_2} = 4.70$ kPa

$H_{CO_2} = 4751$ kPa m^3 kmol^{-1} (according to Table 3.18b, Chapter 3)

$D_{CO_2} = 1.29 \times 10^{-9}$ m^2 s^{-1} (according to Table 3.24b, Chapter 3)

and $N_{CO_2} = 2.31 \times 10^{-6}$ kmol m^{-2} s^{-1}

$$k_{ov} = \frac{\left(\frac{2.31\times10^{-6}\times4751}{4.7}\right)^2}{1.29\times10^{-9}} = 4226.8 \text{ s}^{-1} \text{ (Table 4.7b, Chapter 4)}$$

III.1.3 Validity of conditions for fast pseudo-first-order reaction regime

The conditions to be satisfied for the fast pseudo-first-order reaction regime are as follows:

$$\sqrt{M}\,(=E_A) > 3 \tag{III.4}$$

$$\text{and } \sqrt{M} << E_\infty \left(= \sqrt{\frac{D_{CO_2}}{D_{Amn}}} + \frac{[\text{B}_o]}{z[\text{A}^*]}\sqrt{\frac{D_{Amn}}{D_{CO_2}}}\right) \tag{III.5}$$

For all measured CO_2 absorption rates, conditions given by equations (III.4) and (III.5) are found to be satisfied.

The values of k_L, D_A and [A*] required for verifying the conditions were determined by utilizing "N_2O-analogy" (Chapter 3).

For example, from Chapter 4,

For T = 313 K, [AMP] = 3.0 kmol m^{-3}, $D_{CO_2} = 1.29\times10^{-9}$ m^2 s^{-1}, $H_{CO_2} = 4751$ kPa m^3 kmol^{-1}, $p_{CO_2} = 4.70$ kPa, $\theta = 0.49$ s, $k_L = 5.77\times10^{-5}$ m s^{-1} and $E_{CO_2} = 40.44$

$$[A^*] = \frac{p_{CO_2}}{H_{CO_2}} = \frac{4.70}{4751} = 0.989\times10^{-3} \text{ kmol m}^{-1}$$

Hence,

$$\sqrt{M} = \frac{\sqrt{D_{CO_2} k_{ov}}}{k_L} = \frac{\sqrt{1.29\times10^{-9}\times4226.77}}{5.77\times10^{-5}} = 40.44$$

$$E_\infty = \sqrt{\frac{D_{CO_2}}{D_{Amn}}} + \frac{[B_o]}{z[A^*]}\sqrt{\frac{D_{Amn}}{D_{CO_2}}} = 1.826 + \frac{3.0}{1\times0.989\times10^{-3}}\times0.548 = 1662.82$$

Therefore the condition $3 < \sqrt{M} << \sqrt{\frac{D_{CO_2}}{D_{Amn}}} + \frac{[B_o]}{z[A^*]}\sqrt{\frac{D_{Amn}}{D_{CO_2}}}$ is valid.

III.2 Solubility and Diffusivity of CO_2 in Aqueous AMP Solution (Chapter 3)

III.2.1 Solubility

Using the volume of N_2O absorbed in amine solution in the liquid flak, the liquid phase N_2O concentration has been determined from the following expression.

$$[N_2O] = v_G \times \frac{P - f}{P} \times \frac{273}{T} \times \frac{P}{101.3} \times \frac{1}{22.4}$$

$$= v_G \times \frac{P - f}{101.3} \times \frac{273}{T} \times \frac{1}{22.4} \text{ kmol m}^{-3} \qquad \text{(III.6)}$$

Hence,

$$H_{N_2O} = \frac{p_{N_2O}}{[N_2O]} = \frac{P - f}{v_G \times \frac{P - f}{101.3} \times \frac{273}{T} \times \frac{1}{22.4}}$$

$$= \frac{T \times 22.4 \times 101.3}{273 \times v_G} \text{ kPa m}^3 \text{ kmol}^{-1} \quad \text{(III.7)}$$

where, v_G = volume of gas absorbed per unit volume of liquid m^{-3} m^{-3}

Table 3.18b and Chapter 3

For, [AMP] = 3.0 kmol/m^3, T = 313K and $v_G = 3.9477 \times 10^{-1}$ m^3 m^{-3} of liquid,

Hence,

$$H_{N_2O} = \frac{313 \times 22.4 \times 101.3}{273 \times 3.9477 \times 10^{-1}} = 6590 \text{ kPa m}^3 \text{ kmol}^{-1} \quad \text{(III.8)}$$

For the solubility of CO_2 in aqueous amine solutions the corresponding H_{CO_2} values have been found out using "N_2O analogy" as follows (discussed in Chapter 3):

$$(H_{CO_2})_{am} = (H_{N_2O})_{am} \times \left(\frac{H_{CO_2}}{H_{N_2O}}\right)_{water} \quad \text{(III.9)}$$

$\left(\frac{H_{CO_2}}{H_{N_2O}}\right)_{water}$ at 313 K was found to be (Table 3.18b)

$$\left(\frac{H_{CO_2}}{H_{N_2O}}\right)_{water} = \frac{4142}{5745} = 7.2097 \times 10^{-1}$$

Hence, the solubility of CO_2 in 3.0 kmol m^{-3} AMP solution at 313 K is,

$$(H_{CO_2})_{AMP} = 6590 \times 7.2097 \times 10^{-1} = 4751 \text{ kPa m}^3 \text{ kmol}^{-1} \text{ (Table 3.18b)}$$

III.2.2 Diffusivity

Table 3.24b and Chapter 3

For, [AMP] = 3.0 kmol m^{-3}, T = 313 K, θ = 0.49 s and h = 0.07 m,

N_{N_2O} for physical absorption of N_2O in amine solution in the wetted wall column was found to be

$$N_{N_2O} = 7.7991\times10^{-7} \text{ kmol m}^{-2} \text{ s}^{-1}$$

Hence, $k_L = \dfrac{N_{N_2O}}{[N_2O]}$

where, $[N_2O] = \dfrac{(P-f)}{(H_{N_2O})_{am}}$

$(H_{N_2O})_{am}$ = 6590 kPa m^3 $kmol^{-1}$ (Table 3.18b, Chapter 3)

Therefore,

$$[N_2O] = \frac{(101.3-7.35)}{6590} = 1.425\times10^{-2} \text{ kmol m}^{-3}$$

Hence,

$$k_L = \frac{7.7991\times10^{-7}}{1.425\times10^{-2}} = 5.4731\times10^{-5} \text{ m s}^{-1}$$

$$(D_{N_2O})_{am} = \frac{k_L^2\times\pi\times\theta}{4} \qquad \text{(III.10)}$$

$$= \frac{(5.4731\times10^{-5})^2\times\pi\times0.493}{4} = 1.16\times10^{-9} \text{ m}^2 \text{ s}^{-1}$$

$(D_{CO_2})_{am}$ has been estimated using 'N_2O analogy' as follows

$$(D_{CO_2})_{am} = 1.16\times10^{-9}\left(\frac{D_{CO_2}}{D_{N_2O}}\right)_{water} \qquad \text{(III.11)}$$

$$\left(\frac{D_{CO_2}}{D_{N_2O}}\right)_{water} = \frac{2.83\times10^{-9}}{2.55\times10^{-9}} = 1.11 \text{ (Table 3.24b)}$$

Hence,

$$(D_{CO_2})_{AMP} = 1.16\times10^{-9}\times1.11 = 1.29\times10^{-9}\ m^2\ s^{-1} \text{ (Table 3.24b, Chapter 3)}$$

APPENDIX IV

Typical M-file and program output

IV.1 Determining Density using Redlich–Kister equation for APA+AMP+Water using nonlinear regression method

```
rho=[927.18, 923.16, 919.14, 915.10, 911.0, 906.79        % density of pure APA
     931.1, 926.9, 922.7, 918.5, 914.2, 910               % density of pure AMP
     997.0, 995.6, 994, 992.2, 990.2, 988];               % density of pure Water
% density of APA+AMP+Water solution
Rhomes  = [ 994.97, 992.54, 989.4, 986.55, 983.22, 979.72
            995.9, 993.58, 990.69, 987.81, 984, 981.09
            997.3 994.87 991.71 988.91 985.2 982.28
            998.86 995.88 992.9 989.63 986.4 982.9
            1000.3 996.9 994.2  991.3 987.7 983.8
            1001.7 998.5 995.5 992.3 989 984.9
            1003.2 1000.1 996.9 993.6 990.3 986.3];
T = [298 303 308 313 318 323];                % Temperature
M = [131.22; 89.13; 18];                      % molar mass
% molar volume of pure component
for j=1:6
V01(j) = M(1)/rho(1,j);
V02(j) = M(2)/rho(2,j);
V03(j) = M(3)/rho(3,j);
end
   V0 = [V01; V02; V03]
```

```
x1=[0 0.1 0.3 0.5 0.7 0.9 1.1 ];                    % mole of APA
x2=[3 2.9 2.7 2.5 2.3 2.1 1.9 ];                    % mole of AMP
x3=[40.42 40.23 39.84 39.46 39.08 38.69 38.3];      % mole of Water
for ii=1:7
xf1(ii)=x1(ii)/(x1(ii)+x2(ii)+x3(ii));              % mole fraction of APA
xf2(ii)=x2(ii)/(x1(ii)+x2(ii)+x3(ii));              % mole fraction of AMP
xf3(ii)=x3(ii)/(x1(ii)+x2(ii)+x3(ii));              % mole fraction of Water
xm(ii)=xf1(ii)*M(1)+xf2(ii)*M(2)+xf3(ii)*M(3);
% Sum of molar volume due to individual component.
for j=1:6
    s1(ii,j)=xf1(ii)*V0(1,j)+xf2(ii)*V0(2,j)+xf3(ii)*V0(3,j);
end
end
% Molar volume of solution
for jj=1:6
VM1(jj)=xm(1)/Rhomes(1,jj);
VM2(jj)=xm(2)/Rhomes(2,jj);
VM3(jj)=xm(3)/Rhomes(3,jj);
VM4(jj)=xm(4)/Rhomes(4,jj);
VM5(jj)=xm(5)/Rhomes(5,jj);
VM6(jj)=xm(6)/Rhomes(6,jj);
VM7(jj)=xm(7)/Rhomes(7,jj);
end
  VM=[VM1;VM2;VM3;VM4;VM5;VM6;VM7]
% Excess molar volume of solution
 VE=VM-s1
% Excess molar volume is a function of Coefficient of mole fraction as shown below
for ii=1:7
```

```
p1(ii)=xf1(ii)*xf2(ii);
p2(ii)=p1(ii)*(xf1(ii)-xf2(ii));
p3(ii)=p1(ii)*(xf1(ii)-xf2(ii))^2;
p11(ii)=xf2(ii)*xf3(ii);
p21(ii)=p11(ii)*(xf2(ii)-xf3(ii));
p31(ii)=p11(ii)*(xf2(ii)-xf3(ii))^2;
p12(ii)=xf1(ii)*xf3(ii);
p22(ii)=p12(ii)*(xf1(ii)-xf3(ii));
p32(ii)=p12(ii)*(xf1(ii)-xf3(ii))^2;
end
    v12=[p1; p2; p3]';
    v23=[p11; p21; p31]';
    v31=[p12; p22; p32]';
    V=[v12 v23 v31]
% Now Redlich–Kister equation is solved by using Matlab built-in routine Isqnonlin
Function density
Format short g
E0=[ 2.4338   -0.10689   0.056249    -3.402   -0.81712   -0.085605    -1.5899
1.5981   -0.36239    1.4403   0.51798   0.35358   -0.13202  1.2175
0.82872    -2.1   0.71508   0.48559   -1.6031   -1.1156   0.2168   -
6.1226   -2.4746   0.44103   -4.7438    -1.368  0.21787];  % Initial guess for
Redlich–Kister equation
options=optimset('Display','iter', 'MaxIter',1000 , 'MaxFunEvals',1000,'TolFun',1e-10)
optnew = optimset(options,'TolX',1e-5);
% optimset creates or edits an optimization options structure
% Display overloads method to display an object
% Maxlter is the maximum number of iterations allowed in the estimation process
% Maxlter specifies the maximum number of objective function evaluations
```

```
% TolFun is the termination tolerance placed on the objective function
[E,resnorm,residual,exitflag,output] = lsqnonlin(@myfun,E0,[],[],options)
% syntax for routine call
% exitflag identifies the reason the algorithm terminated
function f2=myfun(E)
%Value of excess volume of all the concentration and temperature
x= [ -0.000380   -0.000374   -0.000355   -0.000346   -0.000330   -0.000313
   -0.000412   -0.000409   -0.000396   -0.000387   -0.000360   -0.000357
   -0.000466   -0.000461   -0.000442   -0.000436   -0.000412   -0.000410
   -0.000524   -0.000507   -0.000494   -0.000477   -0.000465   -0.000450
   -0.000581   -0.000555   -0.000549   -0.000542   -0.000521   -0.000497
   -0.000638   -0.000617   -0.000605   -0.000592   -0.000579   -0.000551
   -0.000699   -0.000681   -0.000665   -0.000650   -0.000638   -0.000613];
%Value of Coefficients of Redlich–Kister equation
v12 = [0                0                0       0.064318      -0.055430       0.047771
0               0               0
    0.000155   -1.0050e-05    6.5098e-07      0.062427      -0.053907      0.046550
0.002152     -0.001998      0.001855
    0.000441   -2.4725e-05    1.3851e-06      0.058611      -0.050813      0.044052
0.006512     -0.006010      0.005547
    0.000693   -3.2658e-05    1.5383e-06      0.054718      -0.047630      0.041461
0.010943     -0.010041      0.009213
    0.000909   -3.4571e-05    1.3145e-06      0.050761      -0.044367      0.038779
0.015449     -0.014090      0.012851
    0.001087   -3.1300e-05    9.0094e-07      0.046747      -0.041028      0.036009
0.020034     -0.018160      0.016461
    0.001225   -2.3734e-05    4.5975e-07      0.042663      -0.037601      0.033140
0.024699     -0.022247      0.020039];
```

```
T=[298
  303
  308
  313
  318
  323];                                   %Temperature
for j=1:6
for i=1:7
Y(i,j)=((E(1)+(E(2)*T(j))+(E(3)*T(j)*T(j)))*v12(i,1))+((E(4)+(E(5)*T(j))+(E(6)*T(j)
^2))*v12(i,2))+(E(7)+(E(8)*T(j))+(E(9)*T(j)^2))*v12(i,3)+(E(10)+(E(11)*T(j))+(E(1
2)*T(j)^2))*v12(i,4)+(E(13)+(E(14)*T(j))+(E(15)*T(j)^2))*v12(i,5)+(E(16)+(E(17)*
T(j))+(E(18)*T(j)^2))*v12(i,6)+(E(19)+(E(20)*T(j))+(E(21)*T(j)^2))*v12(i,7)+(E(22
)+(E(23)*T(j))+(E(24)*T(j)^2))*v12(i,8)+(E(25)+(E(26)*T(j))+(E(27)*T(j)^2))*v12(
i,9)
end
end
y=(x-Y);                          %Average absolute deviation calculation
P=err./x
b=abs(P);
P1=sum(b);
P2=sum(P1');
aad=(P2*100)/42
f2=[y];
```

Output

```
E =[3.029    -0.304    0.072    -2.114    -0.825    0.256    -3.091    2.134
0.040    1.390    0.556  0.386   -0.029    1.252    0.894    -1.825    0.703
```

0.518 4.856 -1.279 0.449 -1.654 -2.608 0.978 -8.098 -1.3
0.527]

residual =

% signifies the differences between calculated and experimental values of density

[-1.495e-06 -3.033e-06 5.757e-06 1.584e-06 2.525e-06 1.432e-06
6.238e-06 6.315e-07 2.713e-06 -1.030e-06 1.168e-05 -2.516e-06
3.979e-06 -2.877e-06 2.883e-06 -4.443e-06 5.328e-06 -8.430e-06
-5.345e-06 -3.145e-06 -4.741e-06 -3.246e-06 -6.621e-06 -7.419e-06
-1.277e-06 8.675e-06 -1.447e-06 -1.026e-05 -5.640e-06 2.823e-06
5.727e-07 4.537e-06 4.997e-07 -1.974e-06 -5.426e-06 7.348e-06
8.087e-07 2.096e-06 2.470e-06 1.859e-06 -2.378e-06 7.009e-06]

AAD for Excess volume = 2.72%

AAD for Density = 0.12

IV.2 Viscosity using Gruenberg and Nissan model

```
M=[131.22; 89.1; 18];                    % molar masses
x1=[0  0.1  0.3  0.5  0.7  0.9  1.1];    % Moles of APA
x2=[3  2.9  2.7  2.5  2.3  2.1  1.9];    % Moles of AMP
x3=[40.42 40.23 39.84 39.46 39.08 38.69 38.3];  % Moles of Water
T=[298 303 308 313 318 323];             % Temperature
for ii=1:7
xf1(ii)=x1(ii)/(x1(ii)+x2(ii)+x3(ii));  % Mole fraction of APA
xf2(ii)=x2(ii)/(x1(ii)+x2(ii)+x3(ii));  % Mole fraction of AMP
xf3(ii)=x3(ii)/(x1(ii)+x2(ii)+x3(ii));  % Mole fraction of Water
end
% eta1, eta2 and eta3 are the viscosities of the pure components
   eta1=[8.51 7.04 5.92 5.05 4.62 3.99];
```

```
   eta2=[132.3 99.48 69.98 46.92 32.17 24.21];
   eta3=[0.9 0.845 0.8 0.668 0.65 0.559];
% etam is the experimental viscosities
etam=[3.55 2.8  2.32   1.95 1.62  1.4
3.71  2.95 2.42 2.04 1.75  1.5
3.85  3.05 2.56  2.16 1.85   1.6
4.05  3.29  2.72  2.29  1.98  1.72
4.31  3.54 2.94 2.48 2.13  1.85
4.57   3.79 3.16 2.68 2.28 1.98
4.84  4.05 3.38 2.89 2.43 2.13];
% Taking log to pure and solution viscosity
for j=1:6
lneta1(j)=log(eta1(j));
lneta2(j)=log(eta2(j));
lneta3(j)=log(eta3(j));
end
for ii=1:7
for n=1:6
lnetam(ii,n)=log(etam(ii,n));
end
end
   lnetam1=lnetam;
for m=1:7
for k=1:6
          A(m,k)=(xf1(m))*(lneta1(k))+(xf2(m))*(lneta2(k))+(xf3(m))*(lneta3(k));
end
end
   B=lnetam1-A        % Excess viscosity
```

```
% Excess property is function of mole fraction
For kk=1:7
x12(kk)=xf1(kk)*xf2(kk);
x13(kk)=xf1(kk)*xf3(kk);
x23(kk)=xf2(kk)*xf3(kk);
end
x123=[x12;x23;x13];
   C=x123'
Function viscosity
Format short g
% initial guess
E0=[3139.3    -18.436    0.029262    620.62    -3.7124    0.0056583    937.16
-5.8152    0.0091733 ];
options=optimset('Display','iter','MaxIter',1000 , 'MaxFunEvals',1000,'TolFun',1e-10)
optnew = optimset(options,'TolX',1e-5);
% optimset creates or edits an optimization options structure
% Display overloads method to display an object
% Maxlter is the maximum number of iterations allowed in the estimation process
% Maxlter specifies the maximum number of objective function evaluations
% TolFun is the termination tolerance placed on the objective function
[E,resnorm,residual,exitflag,output] = lsqnonlin(@myfun,E0,[],[],options)
% syntax for routine call
% exitflag identifies the reason the algorithm terminated
function f2=myfun(E)
%Value of excess volume of all the concentration and temperature
x= [1.027506  0.868578    0.755773    0.777520    0.643622    0.657711
    1.076422  0.925442    0.802329    0.826506    0.724116    0.729730
    1.123178  0.968186    0.867326    0.891432    0.786321    0.800343
```

```
    1.183790   1.053584    0.936937    0.957850    0.861050    0.878908
    1.256160   1.136649    1.023864    1.045675    0.941016    0.958126
    1.324997   1.214826    1.105277    1.131438    1.016079    1.032454
    1.392854   1.291301    1.182007    1.215237    1.086936    1.112017];
%Value of Coefficients of Grunberg and Nissan model
 v12 = [ 0              0.064318        0
         0.000155       0.062427        0.002152
         0.000441       0.058611        0.006512
         0.000693       0.054718        0.010943
         0.000909       0.050761        0.015449
         0.001087       0.046747        0.020034
         0.001225       0.042663        0.024699];
  T=[298
  303
  308
  313
  318
  323];
for j=1:6
for i=1:7
Y(i,j)=((E(1)+(E(2)*T(j))+(E(3)*T(j)*T(j)))*v12(i,1))+((E(4)+(E(5)*T(j))+(E(6)*T(j)
^2))*v12(i,2))+(E(7)+(E(8)*T(j))+(E(9)*T(j)^2))*v12(i,3)
end
end
y=(x-Y);
err=x-Y;
%average absolute deviation calculation
P=err./x;
```

```
b=abs(P);
P1=sum(b);
P2=sum(P1');
aad=(P2*100)/42
f2=[y];
```

Output

```
E = [43971      -289.8     0.47704      951.42     -5.8358     0.009048      -2146.1
14.421    -0.023888]
residual =
[ 0.00758    -0.02338    -0.03731     0.05422    -0.03900    -0.01332
  0.02563     0.00057    -0.02600     0.06535     0.00076     0.01480
  0.00890    -0.02475    -0.03353     0.05339    -0.01817     0.00014
  0.00415    -0.00999    -0.03880     0.04174    -0.02366    -0.00262
  0.00898    -0.00046    -0.02938     0.05011    -0.02308    -0.00069
  0.00772     0.00091    -0.02844     0.05476    -0.02671     0.00039
  0.00308    -0.00261    -0.03508     0.05594    -0.03358     0.01125]
```

AAD for excess viscosity = 2.41%

AAD for viscosity= 2.23%

IV.3 Solubility using semi-empirical model

```
Clc
Clear all
Format long
T=[298 303 308 313  318 323];                % Temperature
% mole fraction of APA and AMP
x11=[0.0 0.0 0.0 0.0 0.0 0.0];
x21=
```

```
[0.002303   0.002310   0.002319   0.002328   0.002338   0.002348];
x31=
[0.006938   0.006958   0.006984   0.007010   0.007045   0.007072];
x41=
[0.011668   0.011705   0.011753   0.011796   0.011854   0.011900];
x51=
[0.016481   0.016546   0.016611   0.016683   0.016754   0.016833];
x61=
[0.021385   0.021481   0.021558   0.021642   0.021746   0.021861];
x71=
[0.026381   0.026494   0.026600   0.026715   0.026835   0.026985];
x13=
[0.069090   0.069306   0.069586   0.069843   0.070145   0.070465];
x23=
[0.067068   0.067268   0.067520   0.067772   0.068109   0.068369];
x33=
[0.063008   0.063208   0.063468   0.063701   0.064013   0.064260];
x43=
[0.058863   0.059093   0.059325   0.059582   0.059838   0.060118];
x53=
[0.054651   0.054897   0.055094   0.055308   0.055575   0.055868];
x63=
[0.050363   0.050579   0.050783   0.051002   0.051230   0.051517];
x73=
[0.045989   0.046182   0.046382   0.046591   0.046801   0.047059];
% Mole fraction of water
x12=1-x11-x13;
x22=1-x21-x23;
```

```
x32=1-x31-x33;
x42=1-x41-x43;
x52=1-x51-x53;
x62=1-x61-x63;
x72=1-x71-x73;
%Component 1 APA
%Component 2 Water
%Component 3 AMP
% molar volume
v1 =[0.141261  0.141876  0.142497  0.143126  0.14377  0.144437];
v2 =[0.018  0.0181  0.0181  0.0182  0.0182  0.0182];
v3 =[0.09572  0.096159  0.096596  0.097038  0.097495  0.097945];
%Henry constant of solution
H_sol=
[5025  5471  6015  6590  7285  7924
4955  5405  5968  6550  7203  7875
4895  5341  5910  6487  7097  7807
4851  5285  5860  6405  7025  7721
4795  5225  5785  6345  6935  7605
4730  5165  5728  6310  6880  7555
4688  5135  5690  6272  6845  7521];
%henry pure APA
H_apa=[2215 2355 2495 2645 2805 2971;2215 2355 2495 2645 2805 2971;2215
2355 2495 2645 2805 2971;2215 2355 2495 2645 2805 2971;2215 2355 2495 2645
2805 2971;2215 2355 2495 2645 2805 2971;2215 2355 2495 2645 2805 2971];
%henry constatnt Water
```

```
H_water=[4011 4552 5145 5792 6496 7260;4011 4552 5145 5792 6496 7260;4011
4552 5145 5792 6496 7260;4011 4552 5145 5792 6496 7260;4011 4552 5145 5792
6496 7260;4011 4552 5145 5792 6496 7260;4011 4552 5145 5792 6496 7260];
%henry constatnt AMP
H_amp=[1515.3 1619.9 1727.9 1839.4 1954.2 2072.3;1515.3 1619.9 1727.9 1839.4
1954.2 2072.3;1515.3 1619.9 1727.9 1839.4 1954.2 2072.3;1515.3 1619.9 1727.9
1839.4 1954.2 2072.3;1515.3 1619.9 1727.9 1839.4 1954.2 2072.3;1515.3 1619.9
1727.9 1839.4 1954.2 2072.3;1515.3 1619.9 1727.9 1839.4 1954.2 2072.3];
% Calculation of phi
for i=1:6
phi11(i)=x11(i)*v1(i)/(x11(i)*v1(i)+x12(i)*v2(i)+x13(i)*v3(i));
phi21(i)=x21(i)*v1(i)/(x21(i)*v1(i)+x22(i)*v2(i)+x23(i)*v3(i));
phi31(i)=x31(i)*v1(i)/(x31(i)*v1(i)+x32(i)*v2(i)+x33(i)*v3(i));
phi41(i)=x41(i)*v1(i)/(x41(i)*v1(i)+x42(i)*v2(i)+x43(i)*v3(i));
phi51(i)=x51(i)*v1(i)/(x51(i)*v1(i)+x52(i)*v2(i)+x53(i)*v3(i));
phi61(i)=x61(i)*v1(i)/(x61(i)*v1(i)+x62(i)*v2(i)+x63(i)*v3(i));
phi71(i)=x71(i)*v1(i)/(x71(i)*v1(i)+x72(i)*v2(i)+x73(i)*v3(i));
end
phi1(1,:)=phi11;
phi1(2,:)=phi21;
phi1(3,:)=phi31;
phi1(4,:)=phi41;
phi1(5,:)=phi51;
phi1(6,:)=phi61;
phi1(7,:)=phi71;
for i=1:6
phi12(i)=x12(i)*v2(i)/(x11(i)*v1(i)+x12(i)*v2(i)+x13(i)*v3(i));
phi22(i)=x22(i)*v2(i)/(x21(i)*v1(i)+x22(i)*v2(i)+x23(i)*v3(i));
```

```
phi32(i)=x32(i)*v2(i)/(x31(i)*v1(i)+x32(i)*v2(i)+x33(i)*v3(i));
phi42(i)=x42(i)*v2(i)/(x41(i)*v1(i)+x42(i)*v2(i)+x43(i)*v3(i));
phi52(i)=x52(i)*v2(i)/(x51(i)*v1(i)+x52(i)*v2(i)+x53(i)*v3(i));
phi62(i)=x62(i)*v2(i)/(x61(i)*v1(i)+x62(i)*v2(i)+x63(i)*v3(i));
phi72(i)=x72(i)*v2(i)/(x71(i)*v1(i)+x72(i)*v2(i)+x73(i)*v3(i));
end
phi2(1,:)=phi12;
phi2(2,:)=phi22;
phi2(3,:)=phi32;
phi2(4,:)=phi42;
phi2(5,:)=phi52;
phi2(6,:)=phi62;
phi2(7,:)=phi72;
phi13=1-phi11-phi12;
phi23=1-phi21-phi22;
phi33=1-phi31-phi32;
phi43=1-phi41-phi42;
phi53=1-phi51-phi52;
phi63=1-phi61-phi62;
phi73=1-phi71-phi72;
phi3=1-phi1-phi2;
% Excess Henry constant
R(1,:)=log(H_sol(1,:))-phi11.*log(H_amine(1,:))-phi12.*log(H_water(1,:))-
phi13.*log(H_amp(1,:));
R(2,:)=log(H_sol(2,:))-phi21.*log(H_amine(2,:))-phi22.*log(H_water(2,:))-
phi23.*log(H_amp(2,:));
R(3,:)=log(H_sol(3,:))-phi31.*log(H_amine(3,:))-phi32.*log(H_water(3,:))-
phi33.*log(H_amp(3,:));
```

```
R(4,:)=log(H_sol(4,:))-phi41.*log(H_amine(4,:))-phi42.*log(H_water(4,:))-
phi43.*log(H_amp(4,:));
R(5,:)=log(H_sol(5,:))-phi51.*log(H_amine(5,:))-phi52.*log(H_water(5,:))-
phi53.*log(H_amp(5,:));
R(6,:)=log(H_sol(6,:))-phi61.*log(H_amine(6,:))-phi62.*log(H_water(6,:))-
phi63.*log(H_amp(6,:));
R(7,:)=log(H_sol(7,:))-phi71.*log(H_amine(7,:))-phi72.*log(H_water(7,:))-
phi73.*log(H_amp(7,:));
RJ=R
for j=1:6
for i=1:7
    u1=(phi1(i,j)*phi2(i,j))^1;
    u2=(phi2(i,j)*phi3(i,j))^1;
    R(i,j)=R(i,j)-u1*(249.973-1.284*(298+5*(j-1))+0.00184*(298+5*(j-
1))*(298+5*(j-1))-31.347*phi2(i,j))-u2*(-29.760815+0.2362248*(298+5*(j-1))-
0.0004171*(298+5*(j-1))*(298+5*(j-1))-1.577*phi2(i,j));
end
end
RR=R;
O=[T;T;T;T;T;T;T];
phi11=phi1;
phi22=phi2;
phi33=phi3;
for i=1:6
K(7*i-6:7*i,1)=R(1:7,i);
L(7*i-6:7*i,1)=phi1(1:7,i);
M(7*i-6:7*i,1)=phi2(1:7,i);
T(7*i-6:7*i,1)=O(1:7,i);
```

```
end
R=K;
phi1=L;
phi2=M;
phi3=1-phi1-phi2;
%Formation of Z matrix
Z=zeros(42,5);
for i=1:42
Z(i,1)=(phi1(i,1)*phi3(i,1))^1;
Z(i,2)=Z(i,1)*T(i,1);
Z(i,3)=Z(i,1)*(T(i,1))^2;
Z(i,4)=(phi3(i,1)*Z(i,1));
   Z(i,5)=(phi1(i,1)*phi2(i,1)*phi3(i,1));
end
Z;
%Calculation of coefficient
disp('The values of constants are')
coef=(inv(Z'*Z))*(Z'*R)
%Calculation of AAD
cal_R=Z*coef
j=1;
for k=1:42
   i=mod(k,7);
if i==0
      i=7;
end
R1(i,j)=cal_R(k);
if i==7
```

```
    j=j+1;
end
end
% Excess Henry constant
for j=1:6
for i=1:7
    u1=(phi11(i,j)*phi22(i,j))^1;
    u2=(phi22(i,j)*phi33(i,j))^1;
    R1(i,j)=R1(i,j)+u1*(249.973-1.284*(298+5*(j-1))+0.00184*(298+5*(j-
1))*(298+5*(j-1))-31.347*phi22(i,j))+u2*(-29.760815+0.2362248*(298+5*(j-1))-
0.0004171*(298+5*(j-1))*(298+5*(j-1))-1.577*phi22(i,j));
end
end
for i=1:7
for j=1:6
R1(i,j)=R1(i,j)+phi11(i,j)*log(H_apa(i,j))+phi22(i,j)*log(H_water(i,j))+phi33(i,j)*log
(H_amp(i,j));
end
end
tt=exp(R1)
err=0;
for i=1:7
for j=1:6
    t=abs(exp(R1(i,j))-H_sol(i,j))/H_sol(i,j);
err=err+t;
end
end
AAD=err*100/42   % AAD value
```

Output

Calculated Henry constant

1.0e+03 *

[5.01982 5.52064 6.02563 6.52312 7.00795 7.47055
4.99265 5.50504 6.03623 6.56068 7.09345 7.61330
4.90406 5.42416 5.98737 6.54482 7.14627 7.75352
4.80258 5.31638 5.88594 6.45714 7.09198 7.75913
4.72660 5.22269 5.77943 6.34086 6.98872 7.68777
4.71047 5.17774 5.71302 6.25635 6.89462 7.60163
4.78827 5.22128 5.72839 6.24570 6.86364 7.56022]

coef =

1.0e+02 *

[-4.4795
0.02505
-0.00003231
1.8023
-1.1180]

AAD = 0.95%.

IV.4 Solubility using Arrhenious type equation

function Arrhenious_equation

format short g

E0=[7.6867e+07
1.5566e+05
-8.3653e+06
3.4288e+08
-1.226e+08

```
   -1.31e+08
   1809.2];
 options=optimset('Display','iter','MaxIter',5000,'MaxFunEvals',5000,'TolFun',1e-10);
 [E,resnorm,residual,exitflag,output] = lsqnonlin(@myfun,E0,[],[],options)
function f2=myfun(E)
H= [5025    5471    6015    6590    7285    7924
4955    5405    5968    6550    7203    7875
4895    5341    5910    6487    7097    7807
4851    5285    5860    6405    7025    7721
4795    5225    5785    6345    6935    7605
4730    5165    5728    6310    6880    7555
4688    5135    5690    6272    6845    7521];
x=(H);
T=[298
  303
  308
  313
  318
  323];
  Cm1=[0 0.1 0.3 0.5 0.7 0.9 1.1];
  Cm2=[3 2.9 2.7 2.5 2.3 2.1 1.9];
for i=1:6
   Y1(i)=
(E(1)+(E(2)*Cm1(1))+(E(3)*(Cm1(1)^2))+(E(4)*Cm2(1))+(E(5)*(Cm2(1)^2))+(E(6)
*Cm1(1)*Cm2(1)))*(exp(-E(7)/T(i)));
   Y2(i)=
(E(1)+(E(2)*Cm1(2))+(E(3)*(Cm1(2)^2))+(E(4)*Cm2(2))+(E(5)*(Cm2(2)^2))+(E(6)
*Cm1(2)*Cm2(2)))*(exp(-E(7)/T(i)));
```

```
  Y3(i)=(E(1)+(E(2)*Cm1(3))+(E(3)*(Cm1(3)^
2))+(E(4)*Cm2(3))+(E(5)*(Cm2(3)^2))+(E(6)*Cm1(3)*Cm2(3)))*(exp(-E(7)/T(i)));
  Y4(i)=
(E(1)+(E(2)*Cm1(4))+(E(3)*(Cm1(4)^2))+(E(4)*Cm2(4))+(E(5)*(Cm2(4)^2))+(E(6)
*Cm1(4)*Cm2(4)))*(exp(-E(7)/T(i)));
  Y5(i)=
(E(1)+(E(2)*Cm1(5))+(E(3)*(Cm1(5)^2))+(E(4)*Cm2(5))+(E(5)*(Cm2(5)^2))+(E(6)
*Cm1(5)*Cm2(5)))*(exp(-E(7)/T(i)));
  Y6(i)=
(E(1)+(E(2)*Cm1(6))+(E(3)*(Cm1(6)^2))+(E(4)*Cm2(6))+(E(5)*(Cm2(6)^2))+(E(6)
*Cm1(6)*Cm2(6)))*(exp(-E(7)/T(i)));
  Y7(i)=
(E(1)+(E(2)*Cm1(7))+(E(3)*(Cm1(7)^2))+(E(4)*Cm2(7))+(E(5)*(Cm2(7)^2))+(E(6)
*Cm1(7)*Cm2(7)))*(exp(-E(7)/T(i)));
 end
y1=(x(1,:)-Y1);
y2=(x(2,:)-Y2);
y3=(x(3,:)-Y3);
y4=(x(4,:)-Y4);
y5=(x(5,:)-Y5);
y6=(x(6,:)-Y6);
y7=(x(7,:)-Y7);
 % s=std(y1)
plot(T,x(1,:),T,Y1,T,x(2,:),T,Y2,T,x(3,:),T,Y3,T,x(4,:),T,Y4,T,x(5,:),T,Y5,T,x(6,:),T,
Y6,T,x(7,:),T,Y7)
Y=[Y1;Y2;Y3;Y4;Y5;Y6;Y7]
ans=Y';
%standard deviation calculation
```

```
err=x-Y;
err1=err.^2;
err2=sum(err1);
err3=sum(err2');
sd=sqrt(err3/41)
%average absolute deviation calculation
b=abs(err);
P=b./x;
P1=sum(P);
P2=sum(P1');
aad=(P2*100)/42
tt=E
f2=[y1
   y2
   y3
   y4
   y5
   y6
   y7]
```

Output

% coefficient

```
E =
 7.6867e+07
   1.5537e+05
  -8.3652e+06
   3.4288e+08
   -1.226e+08
```

-1.31e+08

1809.2

residual =

[71.092 -4.925 -18.292 -36.837 27.672 -1.4729

35.365 -33.04 -23.551 -30.99 -4.1185 4.3591

38.399 -27.364 -4.783 -9.6692 -17.775 37.204

50.084 -21.812 13.034 -17.18 -8.1995 40.29

42.418 -28.384 -3.1003 -12.524 -27.391 1.6172

18.402 -43.081 -10.186 7.301 -22.35 17.186

10.037 -35.903 -7.2233 14.294 - 8.0769 36.995]

AAD = 0.38%.

IV.5 Diffusivity using Modified Stokes Einstein model

```
Clc
Clear all
Format long
T=[298 303 308 313 318 323];                    % Temperature
% Diffusivity values at different concentration and temperature
diff=[0.68    0.64    0.6    0.56    0.52    0.47    0.43
0.82    0.76    0.72    0.68    0.64    0.61    0.57
0.97    0.91    0.87    0.83    0.79    0.75    0.7
1.16    1.1     1.05    1       0.96    0.92    0.86
1.31    1.25    1.2     1.15    1.1     1.05    1
1.49    1.42    1.38    1.34    1.29    1.24    1.18];
diff=diff'*10^-9;
% Viscosity values of different concentration and temperature
N=[3.55 2.8  2.32   1.95 1.62  1.4
```

```
3.71  2.95 2.42 2.04 1.75  1.5
3.85  3.05 2.56  2.16 1.85   1.6
4.05  3.29  2.72  2.29  1.98  1.72
4.31  3.54 2.94 2.48 2.13  1.85
4.57   3.79 3.16 2.68 2.28 1.98
4.84  4.05 3.38 2.89 2.43 2.13];
diff1=log(diff);  % To change in linear regression take log both side
T1=[T;T;T;T;T;T;T];
 N1=log(N);
%Using regression arrange in a row
B(1:7,1)=diff1(:,1);
B(8:14,1)=diff1(:,2);
B(15:21,1)=diff1(:,3);
B(22:28,1)=diff1(:,4);
B(29:35,1)=diff1(:,5);
B(36:42,1)=diff1(:,6);
Q(1:7,1)=T1(:,1);
Q(8:14,1)=T1(:,2);
Q(15:21,1)=T1(:,3);
Q(22:28,1)=T1(:,4);
Q(29:35,1)=T1(:,5);
Q(36:42,1)=T1(:,6);
C(1:7,1)=N1(:,1);
C(8:14,1)=N1(:,2);
C(15:21,1)=N1(:,3);
C(22:28,1)=N1(:,4);
C(29:35,1)=N1(:,5);
C(36:42,1)=N1(:,6);
```

```
 Z=ones(42,2);
Z(:,2)=C;
P=B;
B=B-log(Q);  % Subtract with temperature
coef=(inv(Z'*Z))*(Z'*B)  % Calculation of the coefficient
constant=exp(coef(1))
nitas_power=-coef(2)
cal_diff=Z*coef;
cal_diff=exp(cal_diff+log(Q));                    % Add with temperature
diff2=exp(P);
%AAD calculation
for i=1:42
      g=cal_diff(i)-diff2(i);
if g>0
err(i)=g;
else
err(i)=-g;
end
end
   AAD=sum(err'./diff2)*100/42
    j=1;
for k=1:42
       i=mod(k,7);
if i==0
          i=7;
end
diff3(i,j)=cal_diff(k);
if i==7
```

```
        j=j+1;
end
end
diff3
for i=1:7
```

Output

```
Calculated diffusivity=
1.0e-08 *
[ 0.06368   0.08030   0.09681   0.11518   0.13845   0.16054
  0.06119  0.07659   0.09318   0.11056   0.12909   0.15080
  0.05916   0.07431   0.08854  0.10497   0.12274   0.14222
  0.05651   0.06938  0.08380   0.09955   0.11541  0.13319
  0.05341   0.06492  0.07810   0.09261   0.10801  0.12467
  0.05064   0.06102 0.07315  0.08632  0.10155   0.11722
  0.04807  0.05745  0.06881   0.08061   0.09584 0.10971]
P = -0.907
C = 1.0e-12 *6.74
AAD=3.05%.
```

IV.6 Diffusivity using polynominal model

```
clc
clear all
format long
T=[298 303 308 313 318 323];
diff=[0.68  0.64    0.6 0.56    0.52    0.47    0.43
0.82    0.76    0.72    0.68    0.64    0.61    0.57
```

```
0.97   0.91   0.87   0.83   0.79   0.75   0.7
1.16   1.1 1.05   1   0.96   0.92   0.86
1.31   1.25   1.2 1.15   1.1 1.05   1
1.49   1.42   1.38   1.34   1.29   1.24   1.18];
diff4=(diff*10^-9)
diff=log(diff4);
x1=[0 .1 0.3 0.5 0.7 0.9 1.1 ];
x2=[3 2.9 2.7 2.5 2.3 2.1 1.9 ];
x3=[40.42 40.23 39.84 39.46 39.08 38.69 38.3];
for ii=1:7
   xf1(ii)=x1(ii)/(x1(ii)+x2(ii)+x3(ii));
   xf2(ii)=x2(ii)/(x1(ii)+x2(ii)+x3(ii));
end
 W1=xf1;
 W2=xf2;
B(1:6,1)=diff(:,1);
B(7:12,1)=diff(:,2);
B(13:18,1)=diff(:,3);
B(19:24,1)=diff(:,4);
B(25:30,1)=diff(:,5);
B(31:36,1)=diff(:,6);
B(37:42,1)=diff(:,7);
diff1=B;
B(1:6,1)  = W1(:,1);
B(7:12,1) = W1(:,2);
B(13:18,1)= W1(:,3);
B(19:24,1)= W1(:,4);
B(25:30,1)= W1(:,5);
```

```
B(31:36,1)= W1(:,6);
B(37:42,1)= W1(:,7);
W1=B;
B(1:6,1)  =W2(:,1);
B(7:12,1) =W2(:,2);
B(13:18,1)=W2(:,3);
B(19:24,1)=W2(:,4);
B(25:30,1)=W2(:,5);
B(31:36,1)=W2(:,6);
B(37:42,1)=W2(:,7);
W2=B;
T1(1:6,1)=T';
T1(7:12,1)=T';
T1(13:18,1)=T';
T1(19:24,1)=T';
T1(25:30,1)=T';
T1(31:36,1)=T';
T1(37:42,1)=T';
Z=ones(42,6);
Z(:,2)=W1;
Z(:,3)=W2.^2;
Z(:,4)=T1;
Z(:,5)=T1.*W1;
Z(:,6)=T1.*W2.^2;
Z;
coef=(inv(Z'*Z))*(Z'*diff1)
cal_diff=Z*coef;
cal_diff1=exp(cal_diff)
```

```
diff5=exp(diff1)
%cal_diff./diff1;
   for i=1:42
      g=cal_diff1(i)-diff5(i);
      if g>0
         err(i)=g;
      else
         err(i)=-g;
      end
   end
  AAD=sum(err'./diff5)*100/42
   j=1;
   for k=1:42
      i=mod(k,6);
      if i==0
         i=6;
      end
      diff2(i,j)=cal_diff(k);
      if i==6
         j=j+1;
      end
   end
   diff2;
  diff3=exp(diff2)
```

Output

Calculated diffusivity=

1.0e-08 *

```
[ 0.06868   0.08043   0.09419   0.11030   0.12917   0.15127
  0.06623  0.07781   0.09142   0.10741   0.12620   0.14828
  0.06156   0.07282   0.08614  0.10190   0.12054   0.14259
  0.05719   0.06813   0.08117   0.09671   0.11521  0.13726
  0.05311   0.06374  0.07651   0.09183   0.11021  0.13228
  0.04929   0.05963  0.07213   0.08724  0.10553   0.12765
  0.04573  0.055775  0.06801  0.08294   0.10115  0.12335]

coefficient =
1.0e+02 *
 [-0.29028
 -1.36921
 -3.10404
  0.00026
  0.00416
  0.01125]
AAD= 2.44%
```

IV.7 Calculation of $k_{1,APA}$ and $k_{2,AMP}$

```
Function secondorder_APA_AMP
Format long g
% initial guess
E0=[  166062.52        1114.55
        287057.51        1411.05
        463447.56        2116.33];
options=optimset('Display','iter','MaxIter',1000,'MaxFunEvals',1000,'TolFun',1e-10);
optnew = optimset(options,'TolX',1e-5);
```

```
lb=[0
    0
    0];
```

[E,resnorm,residual,exitflag,output] = lsqnonlin(@myfun,E0,lb,[],options)

function f2=myfun(E)

% k_{ov} at 303 K

x1=[3238.4

26869

53463

75066

3199.5

27054

52535.6

74336

3347.28

27513

52553.4

74791];

% k_{ov} at 313 K

x2= [4226.8

44453

86166

1.32654e+005

4108.4

45403

86156

1.31863e+005

4129.8

44899

86156

```
    1.30160e+005];
% kov at 323 K
x3=[ 6295.5
    79594.4
    1.4661e+005
    2.07033e+005
    6150
    79860
     1.41954e+005
     2.02742e+005
     6210
    80534
    1.40697e+005
    2.00977e+005];
% Temperature
 T=[303
   313
   323];
%Concentration
APA=[0.0
        0.1
        0.3
        0.5
        0.0
        0.1
        0.3
        0.5
        0.0
```

```
        0.1
        0.3
        0.5];
AMP= [3
        2.9
        2.7
         2.5
        3
        2.9
        2.7
        2.5
        3
        2.9
        2.7
        2.5];
for i=1:12
   Y1(i)=(APA(i,1)*E(1,1)/x1(i,1))+(AMP(i,1)*E(1,2)/x1(i,1));
   Y2(i)=(APA(i,1)*E(2,1)/x2(i,1))+(AMP(i,1)*E(2,2)/x2(i,1));
   Y3(i)=(APA(i,1)*E(3,1)/x3(i,1))+(AMP(i,1)*E(3,2)/x3(i,1));
end
Y1
A=ones(12,1);
y1=(A-Y1');
y2=(A-Y2');
y3=(A-Y3');
A1=[A A A]
Y=[Y1;Y2;Y3]
err=A1-Y'
```

```
b=abs(err);
P=b;
P1=P(1,:);
P2=P(2,:);
P3=P(3,:);
P11=sum(P1);
P21=sum(P11');
P12=sum(P2);
P22=sum(P12');
P13=sum(P3);
P23=sum(P13');
aad1=(P21*100)/12
aad2=(P22*100)/12
aad3=(P23*100)/12
aad=(aad1+aad2+aad3)/3
f2=[y1
   y2
   y3];
```

Output

```
E=[166062.52      1114.55
     287057.51      1411.05
     463447.56       2116.33]
AAD= 2.71%
```

IV.8 Evaluation of Arrhenius parameters

Function Arrhenius

```
Format short g
%initial guess
E0=[8.0729e+11        38695];
options=optimset('Display','iter','MaxIter',1000,'MaxFunEvals',1000,'TolFun',1e-10)
optnew = optimset(options,'TolX',1e-5);
lb=[0,0];

[E,resnorm,residual,exitflag,output] = lsqnonlin(@myfun,E0,  lb,[],options)
function f2=myfun(E)
% k2,APA values
x=[166062.52  287057.51    463447.55 ];
 T=[303
    313
    323];
R=8.314;
for i=1:3
Y(i)=E(1)*(exp(-E(2)/(R*T(i))));
end
y=(x-Y);
err=x-Y;
b=abs(err);
P=b./x;
P1=sum(P);
P2=sum(P1');
aad=(P2*100)/3
f2=[y];
```

Output

E= [2.18e+12   41256]

AAD = 0.87%